Dipl.-Ing. Helmut Niederwieser, BSc.

Unknown Input Observer Design
for Linear Time-Invariant Multivariable Systems

DOCTORAL THESIS

to achieve the university degree of
Doctor of Technical Sciences

submitted to
Graz University of Technology

Supervisor

Univ.-Prof. Dipl.-Ing. Dr.techn. Markus Reichhartinger

Institute of Automation and Control
Faculty of Electrical and Information Engineering

Graz, July 2024

STATUTORY DECLARATION

I declare that I have authored this thesis independently, that I have not used other than the declared sources/resources, and that I have explicitly indicated all material that has been quoted either literally or by content from the sources used.

....
date

....
signature

Abstract

The estimation of state variables of dynamical systems that are excited by unknown inputs, such as unmeasurable external disturbances, is of great interest in various applications in the field of control engineering. The main challenge in the design of so-called unknown input observers is that the unknown inputs cannot be explicitly included in the observer dynamics and, thus, also excite the resulting estimation error dynamics. A detailed literature analysis shows that all existing unknown input observers suffer from at least one of the following drawbacks:

1. The system must fulfil certain structural conditions, which represent a strong restriction of the system class.

2. In order to ensure convergence of the estimation error, the trajectories of the system which is the subject of the state estimation problem must be bounded. The required tuning parameters of the unknown input observer depend on the bounds of the state variables.

3. The number of tuning parameters as well as the order of the observer is at least twice as large as the system order. The main difficulty is the choice of the mutually influencing observer parameters.

Motivated by the aforementioned disadvantages of existing methods, new design methods for unknown input observers for strongly observable, linear time-invariant systems with unknown inputs are developed in this thesis. The key ingredient is given by a new observer normal form which, in contrast to classical normal forms, also takes into account the impact of the unknown inputs on the system. This normal form represents the overall system as coupled subsystems, each with a single output. The couplings are favourably chosen from the perspective of the observer design, as they can either be regarded as an output injection or represent purely serial couplings, i.e., each subsystem is only influenced by the state variables of previous subsystems.

Different observers can be designed for the individual subsystems. For subsystems that are not influenced by an unknown input, the choice of a Luenberger observer, for example, is sufficient to ensure asymptotic convergence of the estimation error. For subsystems with an excitation by unknown inputs, however, suitable estimation methods must be applied. The resulting overall observer does not require restrictive conditions on the considered system class, nor does it rely on bounded trajectories of the underlying system or unnecessarily increase the observer order and the number of tuning parameters. In the case of single-input single-output systems, the observer design can be performed directly in original coordinates. The proposed design formula

can be considered as a non-linear generalization of Ackermann's eigenvalue placement.

Several extensions and generalizations in terms of the considered system class, the class of unknown inputs and the application of the unknown input observer to state-feedback control are presented. In addition to numerical simulations, the proposed unknown input observer concept is also verified by means of a practical application. Thereby, the temperature profile along an aluminium rod is estimated, which is affected by heat flows unknown to the observer.

Danksagung (Acknowledgement)

Am Ende dieser langen und schönen Zeit der Dissertation möchte ich *Danke* sagen. Beginnen möchte ich mit meinem Doktorvater Markus Reichhartinger. Vielen Dank für deine fachlich so wertvolle und menschlich so angenehme Betreuung sowie die thematische Offenheit, welche es mir ermöglicht hat, meine eigene Ideen zu den Inhalten dieser Arbeit einzubringen.

Bedanken möchte ich mich auch bei Martin Horn und Markus Gölles für die guten Rahmenbedingungen, wodurch ich mich sowohl mit theoretischen Betrachtungen zum Beobachterentwurf beschäftigen, wertvolle Erfahrungen in der Hochschullehre sammeln, als auch anwendungsmotivierte Forschung im Bereich der erneuerbaren Energien betreiben konnte.

Ein großer Dank gilt meinen lieben Kolleg*innen am IRT und bei BEST, sei es für den netten, freundschaftlichen Umgang miteinander sowie auch für die bereichernden fachlichen Diskussionen. Insbesondere hervorheben möchte ich an dieser Stelle Stefan Hölzl, Stefan Koch, Markus Tranninger, Richard Seeber, Prof. Nicolaos Dourdoumas, Valentin Kaisermayer, Christopher Zemann und Markus Deutsch sowie meine Bürokolleg*innen Jasmina Muminovic, Tobias Renzler, Katarina Stanojevic, Benedikt Andritsch, Josef Pucher und Marijan Palmisano.

Zum Schluss möchte ich noch meiner Familie danken, ohne deren Rückhalt so vieles in meinem Leben nicht möglich gewesen wäre. Vielen Dank meinen Eltern Rita und Ignaz, die mich auf meinem Weg immer gefördert, unterstützt und an mich geglaubt haben. Danke an meine Brüder Thomas, Johannes und Andreas, mit denen ich in meinem Leben schon so viel erleben durfte. Ein besonderes Dankeschön gilt meiner lieben Frau Caroline, welche stets zu mir gestanden ist, mich aufgemuntert und ausgehalten hat und immer für mich da war.

Graz, Juni 2024

Helmut Niederwieser

Contents

1

Introduction

This introductory chapter explains the background and the motivation for this thesis which contributes to the field of unknown input observer design. Limitations and problems of existing unknown input observers are discussed and the research gap is identified. The main contributions of this work to the field are summarized and an outline of the thesis's structure is given. Finally, the notation used throughout the thesis is introduced.

1.1 Background and Motivation

The behaviour of a wide range of physical, biological, chemical and economic systems can be mathematically described by means of sets of ordinary differential equations, often referred to as dynamical systems. The spectrum ranges from weather and global climate [1, 2] to the combustion of biomass [3], the effects of the suspension system on the driving behaviour of vehicles [4], the growth of bacteria in a bioreactor [5] and the evolution of stock prices [6]. The internal state of dynamical systems is characterized by a set of state variables whose evolution over time in general depends on the system dynamics and external inputs.

Dynamical systems serve as the basis for the field of control engineering, whereby a fundamental distinction can be made between two main disciplines: automatic control and state estimation. The aim of automatic control is to manipulate the system through so-called control inputs in a targeted manner, such that (a function of) the state variables follow a desired trajectory. The algorithms used for this are referred to as controllers. The objective of state estimation is to reconstruct the state variables from measured outputs and available inputs, where the output signals are functions of the state variables and, therefore, contain relevant information about the current system state. For the purpose of state estimation, so-called observers[1] are applied. Observers are dynamical systems which provide estimates of the system's state variables. They usually consist of a copy of the mathematical model of the system and an innovation term that is based on the current error between the actual and estimated output. This way, non-measurable state variables can be estimated, which can then be

---

[1]The observer concept was introduced by David G. Luenberger [7] in 1964.

used, for example, to detect faults in the system [8] or in a model-based state-feedback controller [9].

One of the main challenges in state estimation arises from influences on the system that are unknown to the observer. These include, for example, unknown external disturbances, parameter uncertainties and unmodelled system dynamics. One approach is to regard them as unknown inputs and to subsequently apply robust state estimation methods. Such methods, referred to as unknown input observers[2] (formerly strong observers [10]), estimate the state variables from the outputs without knowledge of the unknown inputs.

Especially for linear time-invariant (LTI) systems, existence conditions for unknown input observers have already been thoroughly researched, see e.g. [10], and a huge variety of different methods has been proposed. However, all available methods either

1. rely on restrictive conditions regarding the system structure,

2. require bounded state variables for convergence of the estimation error

3. or unnecessarily increase the observer order and the number of observer parameters beyond the original system order, which may drastically complicate their tuning.

This gap motivates further research in this direction. This thesis aims to develop new unknown input observers for LTI systems with multiple unknown inputs and multiple outputs which do not exhibit the aforementioned limitations and problems of the state of the art.

1.2 Scientific Contribution

In the following, the main contributions of this thesis to the field of unknown input observer design are summarized:

1. For strongly observable LTI single-input single-ouput (SISO) systems, a non-linear generalization of Ackermann's formula for the design of unknown input observers is proposed, see Theorem 5.4.1. This formula allows for an elegant unknown input observer design in original coordinates. The unknown input observer is able to provide exact estimates of the state variables within finite time despite a bounded unknown input. In addition, a necessary condition on the choice of the observer parameters is provided. It is pointed out that this unknown input observer does not suffer from the limitations and problems of existing unknown input observers.

2. A new observer normal form for strongly observable LTI multiple-input multiple-ouput (MIMO) systems is proposed, see Definition 6.1.1. This normal form turns out highly suitable for the design of unknown input observers. The existence of the required transformations is guaranteed by Theorem 6.1.1 and a transfor-

---

[2]The name may seem misleading in the sense that unknown input observers do not estimate the unknown inputs, but the state variables in the presence of unknown inputs. However, as this is an established nomenclature, this term is also used throughout this thesis.

mation algorithm for the calculation of the transformations is presented, see Section 6.3.1.

3. An unknown input observer for LTI MIMO systems represented in observer normal form is proposed in Theorem 6.2.1. The unknown input observer is able to provide exact estimates of the state variables within finite time in the presence of bounded unknown inputs. As in the SISO case, a necessary condition regarding the choice of the observer parameters is provided and the unknown input observer does not suffer from the limitations and problems of existing methods.

4. The practical application of the proposed unknown input observer for LTI MIMO systems is demonstrated by estimating the temperature profile in a thermal laboratory setup, see Chapter 8.

1.3 List of Publications

The author of this thesis published several articles in journals and proceedings of international conferences during his doctoral studies. The following publications provide the basis for this thesis:

1. **H. Niederwieser**, S. Koch, M. Reichhartinger, A generalization of Ackermann's formula for the design of continuous and discontinuous observers, in: 2019 IEEE 58th Conference on Decision and Control (CDC), IEEE, 2019, pp. 6930–6935. `doi:10.1109/CDC40024.2019.9030192`

2. **H. Niederwieser**, M. Tranninger, R. Seeber, M. Reichhartinger, Unknown input observer design for linear time-invariant multivariable systems based on a new observer normal form, International Journal of Systems Science 53 (10) (2022) 2180–2206. `doi:10.1080/00207721.2022.2046201`

3. **H. Niederwieser**, S. Koch, M. Reichhartinger, Unknown Input Observer for Temperature Profile Estimation in Systems with Unknown Heat Fluxes (Accepted for presentation at European Control Conference 2024).

4. M. Tranninger, **H. Niederwieser**, R. Seeber, M. Horn, Unknown input observer design for linear time-invariant systems—a unifying framework, International Journal of Robust and Nonlinear Control 33 (15) (2023) 8911–8934. `doi:10.1002/rnc.6399`

In addition, the following scientific papers on state estimation and some practical applications were published:

1. **H. Niederwieser**, M. Reichhartinger, On the characteristic polynomial of the dynamic matrix of linear time-invariant multivariable systems in Luenberger's canonical forms, Automatica 162 (2024) 111532. `doi:10.1016/j.automatica.2024.111532`

2. **H. Niederwieser**, C. Zemann, M. Goelles, M. Reichhartinger, Model-based estimation of the flue gas mass flow in biomass boilers, IEEE Transactions on Control Systems Technology 29 (4) (2020) 1609–1622. `doi:10.1109/TCST.2020.3016404`

3. **H. Niederwieser**, C. Zemann, M. Gölles, M. Reichhartinger, Soft-sensor for the on-line estimation of the flue gas mass flow in biomass boilers with additional monitoring of the heat exchanger fouling, in: 28th European Biomass Conference & Exhibition, 2020, pp. 280–284. `doi:10.5071/28thEUBCE2020-2AO.8.3`

4. B. Andritsch, M. Horn, S. Koch, **H. Niederwieser**, M. Wetzlinger, M. Reichhartinger, The robust exact differentiator toolbox revisited: Filtering and discretization features, in: 2021 IEEE International Conference on Mechatronics (ICM), IEEE, 2021, pp. 01–06. `doi:10.1109/ICM46511.2021.9385675`

5. C. Zemann, **H. Niederwieser**, M. Gölles, Operational optimization and error detection in biomass boilers by model based monitoring: methods and practice, in: 7. Mitteleuropäische Biomassekonferenz (CEBC), 2023.

1.4 Structure of the Thesis

This thesis is organised into ten chapters. After this introductory part in Chapter 1, observability properties of LTI systems subject to unknown inputs and existence conditions for unknown input observers are recalled in Chapter 2. In Chapter 3, the relation between unknown input observation and numerical differentiation is discussed, which motivates the application of differentiators in unknown input observation problems. In Chapter 4, the specific unknown input observation problem considered in this thesis is introduced. Moreover, existing approaches are discussed theoretically, compared by means of a numerical example and the main gaps motivating further research into this direction are identified. The limitations and problems of existing methods motivate the development of new unknown input observers, which are presented in Chapter 5 and Chapter 6 for SISO and MIMO systems, respectively. In Chapter 7, several useful extensions of the presented unknown input observers are given, such as generalizations to systems with direct feed-through and to strongly detectable systems and the application to state-feedback control with integrated rejection of unknown disturbance inputs. In Chapter 8, the practical applicability of the proposed methods is demonstrated by means of a thermal laboratory setup. Chapter 9 concludes the thesis and suggests possible directions for further research. Chapter 10, the Appendix, shortly recaps a method for modal model order reduction, which is applied during modelling of the laboratory setup in Chapter 8. Furthermore, the Appendix contains the major part of the mathematical proofs required in Chapter 6.

1.5 Notation

Throughout this thesis, bold lowercase letters refer to vectors and bold uppercase letters refer to matrices. The i-th canonical unit vector is denoted by $\boldsymbol{e}_i$. Furthermore, $\boldsymbol{I}_i$ represents the $i \times i$ identity matrix and $\boldsymbol{0}_{j \times k}$ and $\boldsymbol{1}_{j \times k}$ are the zero matrix and the matrix of ones of dimension $j \times k$, respectively. A block diagonal matrix with the submatrices $\boldsymbol{A}_1, \ldots, \boldsymbol{A}_n$ on the diagonal is denoted by $\mathrm{diag}(\boldsymbol{A}_1, \ldots, \boldsymbol{A_n})$. Moreover, rank $(\cdot)$ describes the rank of a matrix and $\mathrm{spec}\{\cdot\}$ is the spectrum of a matrix, i.e.,

the set of its eigenvalues. The generalized left-inverse and generalized right-inverse of a matrix $\boldsymbol{A}$ are written as $\boldsymbol{A}^{\dagger}$ and $\boldsymbol{A}^{\ddagger}$, respectively.

The notations $\overset{(i)}{=}$ or $\underset{(i)}{=}$ indicate an insertion of equation (i). In order to abbreviate sign preserving power functions, the notation

$$\lfloor\cdot\rceil^{\gamma} = |\cdot|^{\gamma}\text{sign}(\cdot) \quad \text{and particularly} \quad \lfloor\cdot\rceil^{0} = \text{sign}(\cdot)$$

is used. The notation

$$a \leftarrow f(a)$$

refers to an update step for the value of a required in the description of iterative algorithms, i.e., the new value of a is some function $f(\cdot)$ of the old value of a. The ceiling function $\lceil\cdot\rceil$ rounds numbers to their nearest larger integer.

The first derivative $\frac{\mathrm{d}}{\mathrm{d}t}x$ is also denoted by $\dot{x}$, whereas $x^{(i)}$ also allows for representing higher derivatives $\frac{\mathrm{d}^i}{\mathrm{d}t^i}x$ with respect to time t. Estimates of some variable x are indicated by $\hat{x}$. Moreover, the solutions of differential equations with discontinuous right-hand side are understood in the sense of Filippov [11]. All numbers are represented rounded to two decimal places and at least two significant digits.

2

Observability of Linear Time-Invariant Systems with Unknown Inputs

This chapter explains the basic concepts of observability and detectability for linear time-invariant systems that are affected by unknown inputs. The problem of estimating state variables of systems excited by unknown inputs, referred to in the literature as problem of unknown input observation, is introduced and fundamental terms are defined. Subsequently, the system properties observability and detectability are discussed, which provide existence conditions for observers for the case without unknown inputs. Finally, the more general notions of strong observability, strong detectability and strong* detectability for systems with unknown inputs are recalled.

2.1 The Unknown Input Observation Problem

Consider the LTI system

$$
\begin{aligned}
\dot{\boldsymbol{x}}(t) &= \boldsymbol{A}\boldsymbol{x}(t) + \boldsymbol{B}\boldsymbol{u}(t) + \boldsymbol{D}\boldsymbol{w}(t), \\
\boldsymbol{y}(t) &= \boldsymbol{C}\boldsymbol{x}(t) + \boldsymbol{E}\boldsymbol{u}(t) + \boldsymbol{F}\boldsymbol{w}(t),
\end{aligned}
\tag{2.1}
$$

where $\boldsymbol{x} \in \mathbb{R}^n$ is the state vector with initial condition $\boldsymbol{x}(0) = \boldsymbol{x}_0$, $\boldsymbol{u} \in \mathbb{R}^o$ denotes the vector of known inputs[1], $\boldsymbol{w} \in \mathbb{R}^m$ describes the vector of unknown inputs and $\boldsymbol{y} \in \mathbb{R}^p$ is the output vector. Furthermore, $\boldsymbol{A} \in \mathbb{R}^{n \times n}$, $\boldsymbol{B} \in \mathbb{R}^{n \times o}$, $\boldsymbol{D} \in \mathbb{R}^{n \times m}$, $\boldsymbol{C} \in \mathbb{R}^{p \times n}$, $\boldsymbol{E} \in \mathbb{R}^{p \times o}$ and $\boldsymbol{F} \in \mathbb{R}^{p \times m}$ are constant matrices. Without loss of generality, the unknown inputs as well as the outputs are assumed linear independent[2], i.e.,

$$
\operatorname{rank} \begin{bmatrix} \boldsymbol{D} \\ \boldsymbol{F} \end{bmatrix} = m, \quad \operatorname{rank} \begin{bmatrix} \boldsymbol{C} & \boldsymbol{F} \end{bmatrix} = p.
\tag{2.2}
$$

---

[1]The elements of $\boldsymbol{u}$ are not necessarily control inputs, but known functions of time t. This includes control inputs, if the controller communicates the applied signals, as well as measured disturbances.

[2]In the case of linear dependent unknown inputs or outputs, it is always possible to describe them by means of a linear independent basis, see Section 4.1.2.

The goal is to estimate the state vector $\boldsymbol{x}$ from the output $\boldsymbol{y}$ and the known input $\boldsymbol{u}$ in the presence of the unknown input $\boldsymbol{w}$. An algorithm solving this task is referred to as unknown input observer. This term, together with some other fundamental terms related to state estimation in dynamic systems, is defined in the following.

Definition 2.1.1 (observer)**.** Consider system (2.1) without unknown input, i.e., let $\boldsymbol{w} = \boldsymbol{0}$ for all $t \geqslant 0$. An observer is a dynamical system providing an estimate $\hat{\boldsymbol{x}}$ of the state vector $\boldsymbol{x}$ using the system structure $\boldsymbol{A}$, $\boldsymbol{B}$, $\boldsymbol{C}$, $\boldsymbol{E}$, the known input $\boldsymbol{u}$ and (not necessarily) the output $\boldsymbol{y}$.

Definition 2.1.2 (unknown input observer)**.** Consider system (2.1) excited by the unknown input $\boldsymbol{w}(t)$. An unknown input observer is an observer providing an estimate $\hat{\boldsymbol{x}}$ of the state vector $\boldsymbol{x}$ without knowledge of the unknown input $\boldsymbol{w}$.

Definition 2.1.3 (convergence behaviour)**.** An (unknown input) observer is called

  (i) an asymptotic (unknown input) observer if the estimation error $\boldsymbol{\sigma} = \boldsymbol{x} - \hat{\boldsymbol{x}}$ vanishes asymptotically, i.e., $\lim_{t \to \infty} \boldsymbol{\sigma}(t) = \boldsymbol{0}$ for all $\boldsymbol{x}_0$.

  (ii) a finite-time (unknown input) observer if the estimation error vanishes after finite time $\tau > 0$, i.e., $\boldsymbol{\sigma}(t) = \boldsymbol{0}$ for all $t \geqslant \tau(\boldsymbol{\sigma}(0))$, where τ depends on the initial estimation error $\boldsymbol{\sigma}(0)$.

  (iii) a fixed-time (unknown input) observer if the finite convergence time τ is independent of the initial estimation error $\boldsymbol{\sigma}(0)$.

The question arises, of course, which conditions system (2.1) must fulfil such that there exists an (unknown input) observer with desired convergence behaviour. This question is directly related to the different notions of observability and detectability, which are discussed in the next sections.

2.2 Classical Observability and Detectability

For the classical notion of observability and detectability, consider system (2.1) without unknown input, i.e., $\boldsymbol{w} = \boldsymbol{0}$ for all $t \geqslant 0$, which yields

$$
\begin{aligned}
\dot{\boldsymbol{x}} &= \boldsymbol{A}\boldsymbol{x} + \boldsymbol{B}\boldsymbol{u}, \\
\boldsymbol{y} &= \boldsymbol{C}\boldsymbol{x} + \boldsymbol{E}\boldsymbol{u}.
\end{aligned}
\tag{2.3}
$$

Definition 2.2.1 (observability/detectability[3] [12])**.** Consider solutions $\boldsymbol{x}_a(t)$ and $\boldsymbol{x}_b(t)$ of system (2.3) for a given input $\boldsymbol{u}(t)$ and the respective outputs $\boldsymbol{y}_a(t)$ and $\boldsymbol{y}_b(t)$. System (2.3) is said to be

  (i) observable[4], if $\boldsymbol{y}_a(t) = \boldsymbol{y}_b(t)$ $\forall t \geqslant 0$ implies $\boldsymbol{x}_a(t) = \boldsymbol{x}_b(t)$.

  (ii) detectable, if $\boldsymbol{y}_a(t) = \boldsymbol{y}_b(t)$ $\forall t \geqslant 0$ implies $\lim_{t \to \infty}(\boldsymbol{x}_a(t) - \boldsymbol{x}_b(t)) = \boldsymbol{0}$.

Obviously, observability is the stronger property and implies detectability. If a system is observable, any two different solutions can be distinguished from each other by means of their output signals only. An observer can specify the convergence behaviour of the estimation error independent from the system itself. Observability is necessary and sufficient for the existence of a finite-time observer for the considered system class which is shown e.g. in [13]. If system (2.3) is detectable only, the state vector $\boldsymbol{x}$ can be reconstructed asymptotically only, i.e., for $t \to \infty$, as different solutions producing the same output converge asymptotically to each other. The convergence behaviour of the estimation error depends on the system itself and cannot be specified arbitrarily by an observer. In the following, two well-known criteria for testing the observability/detectability of LTI systems of the form (2.3) are recalled.

2.2.1 Kalman Criterion for Observability

Assuming the input $\boldsymbol{u}$ sufficiently often differentiable[5], differentiation of the output yields

$$
\begin{aligned}
\boldsymbol{y} &= \boldsymbol{C}\boldsymbol{x} + \boldsymbol{E}\boldsymbol{u}, \\
\dot{\boldsymbol{y}} &= \boldsymbol{C}\boldsymbol{A}\boldsymbol{x} + \boldsymbol{C}\boldsymbol{B}\boldsymbol{u} + \boldsymbol{E}\dot{\boldsymbol{u}}, \\
\boldsymbol{y}^{(2)} &= \boldsymbol{C}\boldsymbol{A}^2\boldsymbol{x} + \boldsymbol{C}\boldsymbol{A}\boldsymbol{B}\boldsymbol{u} + \boldsymbol{C}\boldsymbol{B}\dot{\boldsymbol{u}} + \boldsymbol{E}\boldsymbol{u}^{(2)}, \\
&\;\vdots \\
\boldsymbol{y}^{(n-1)} &= \boldsymbol{C}\boldsymbol{A}^{(n-1)}\boldsymbol{x} + \sum_{i=0}^{n-2} \boldsymbol{C}\boldsymbol{A}^{(n-2-i)}\boldsymbol{B}\boldsymbol{u}^{(i)} + \boldsymbol{E}\boldsymbol{u}^{(n-1)},
\end{aligned}
\tag{2.4}
$$

or, equivalently,

$$
\begin{bmatrix} \boldsymbol{y} \\ \dot{\boldsymbol{y}} \\ \boldsymbol{y}^{(2)} \\ \vdots \\ \boldsymbol{y}^{(n-1)} \end{bmatrix} = \begin{bmatrix} \boldsymbol{C} \\ \boldsymbol{C}\boldsymbol{A} \\ \boldsymbol{C}\boldsymbol{A}^2 \\ \vdots \\ \boldsymbol{C}\boldsymbol{A}^{n-1} \end{bmatrix} \boldsymbol{x} + \begin{bmatrix} \boldsymbol{E} & \boldsymbol{0} & \dots & \dots & \boldsymbol{0} \\ \boldsymbol{C}\boldsymbol{B} & \boldsymbol{E} & \ddots & & \vdots \\ \boldsymbol{C}\boldsymbol{A}\boldsymbol{B} & \ddots & \ddots & \ddots & \vdots \\ \vdots & & \ddots & \ddots & \boldsymbol{0} \\ \boldsymbol{C}\boldsymbol{A}^{n-2}\boldsymbol{B} & \dots & \boldsymbol{C}\boldsymbol{A}\boldsymbol{B} & \boldsymbol{C}\boldsymbol{B} & \boldsymbol{E} \end{bmatrix} \begin{bmatrix} \boldsymbol{u} \\ \dot{\boldsymbol{u}} \\ \boldsymbol{u}^{(2)} \\ \vdots \\ \boldsymbol{u}^{(n-1)} \end{bmatrix}.
\tag{2.5}
$$

It can be shown that in the LTI case there can not appear additional information from taking the n-th and further derivatives into account[6], see [16, Lemma 4.26]. From

---

[3]In the given reference [12, Definition 5] detectability is referred to as asymptotic observability.

[4]Often, see e.g. [13, 14], a different definition of observability is used: System (2.3) is said to be observable, if every initial state $\boldsymbol{x}_0$ can be uniquely determined from the measurement $\boldsymbol{y}(t)$ and the input $\boldsymbol{u}(t)$ on a finite time interval $t \in [0, \tau]$, $\tau > 0$ for every $\boldsymbol{u}(t)$. Note that this definition is equivalent to Definition 2.2.1(i). From this definition it is clear that the observability of the system is decisive for the existence of finite-time observers.

[5]Note that the differentiability assumption of $\boldsymbol{u}$ can be avoided by considering derivatives of linear combinations of $\boldsymbol{y}$ and $\boldsymbol{u}$ instead. For example, the derivative $\frac{\mathrm{d}}{\mathrm{d}t}(\boldsymbol{y} - \boldsymbol{E}\boldsymbol{u})$, which exists for sure, could be considered rather than $\dot{\boldsymbol{y}}$. However, for the sake of convenience, the derivatives of $\boldsymbol{y}$ are considered which require the assumption made.

[6]This follows directly from the theorem of Caley-Hamilton which states that a square matrix $\boldsymbol{A} \in \mathbb{R}^{n \times n}$ satisfies its own characteristic equation $\Delta(s) = s^n + \alpha_{n-1}s^{n-1} + \dots + \alpha_1 s + \alpha_0 = 0$.

(2.5) it can be seen that $\boldsymbol{x}$ can be determined from $\boldsymbol{y}$, $\boldsymbol{u}$ and their derivatives if and only if the so-called observability matrix

$$
\boldsymbol{\mathcal{O}} = \begin{bmatrix} \boldsymbol{C} \\ \boldsymbol{CA} \\ \boldsymbol{CA}^2 \\ \vdots \\ \boldsymbol{CA}^{n-1} \end{bmatrix} \tag{2.6}
$$

is left-invertible, which finally yields

> **Proposition 2.2.1** (Kalman observability criterion)**.** *System* (2.3) *is observable if and only if the observability matrix* (2.6) *has full column rank, i.e.,*
>
> $$ rank\ \boldsymbol{\mathcal{O}} = n. \tag{2.7} $$

2.2.2 Hautus Criteria for Observability and Detectability

In contrast to the Kalman criterion, the Hautus criteria additionally allow for investigation of the detectability. The criteria are recalled in

> **Proposition 2.2.2** (Hautus observability/detectability criterion)**.** *System* (2.3) *is*
> *(i) observable, if and only if*
>
> $$ rank\ \begin{bmatrix} s\boldsymbol{I} - \boldsymbol{A} \\ \boldsymbol{C} \end{bmatrix} = n \quad \forall s \in \mathbb{C}. \tag{2.8a} $$
>
> *(ii) detectable, if and only if*
>
> $$ rank\ \begin{bmatrix} s\boldsymbol{I} - \boldsymbol{A} \\ \boldsymbol{C} \end{bmatrix} = n \quad \forall s \in \mathbb{C}\ with\ Re\{s\} \geqslant 0. \tag{2.8b} $$

Note that it is sufficient to check the observability rank condition (2.8a) for the eigenvalues $s_i \in \mathrm{spec}\{\boldsymbol{A}\}$, $i = 1, \dots, n$, as rank $(s\boldsymbol{I} - \boldsymbol{A}) = n$ for all $s \notin \mathrm{spec}\{\boldsymbol{A}\}$ anyway. Following the same reasoning, it is sufficient to check the detectability rank condition (2.8b) only for the eigenvalues $s_i \in \mathrm{spec}\{\boldsymbol{A}\}$ with $\mathrm{Re}\{s_i\} \geqslant 0$. The loss of rank when inserting the respective eigenvalues has to be compensated by the rows of $\boldsymbol{C}$. It follows that the respective right-eigenvectors $\boldsymbol{p}_i$ of $\boldsymbol{A}$ must not be in the kernel of $\boldsymbol{C}$, which leads to the alternative formulation of the Hautus criterion in

---

Hence, $\boldsymbol{A}^n = -\sum_{i=1}^{n} \alpha_{n-i}\boldsymbol{A}^{n-i}$ can always be represented as a linear combination of lower powers of $\boldsymbol{A}$, see e.g. [15]. The same is true for all further powers $\boldsymbol{A}^k$ with exponent $k > n$, $k \in \mathbb{N}$, which can be shown by induction.

> **Corollary 2.2.3** (Hautus observability/detectability criterion)**.** *System* (2.3) *is*
>
> *(i) observable, if and only if all solutions $\boldsymbol{p}_i$ of the eigenvalue problem $\boldsymbol{A}\boldsymbol{p}_i = s_i\boldsymbol{p}_i$ satisfy $\boldsymbol{C}\boldsymbol{p}_i \neq \boldsymbol{0}$.*
>
> *(ii) detectable, if and only if all solutions $\boldsymbol{p}_i$ of the eigenvalue problem $\boldsymbol{A}\boldsymbol{p}_i = s_i\boldsymbol{p}_i$ corresponding to eigenvalues s_i with $\mathrm{Re}\{s_i\} \geqslant 0$ satisfy $\boldsymbol{C}\boldsymbol{p}_i \neq \boldsymbol{0}$.*

It is pointed out that the relations stated in Corollary 2.2.3 must be satisfied for all eigenvectors $\boldsymbol{p}_i$ in the eigenspace associated with the particular eigenvalue s_i. This is especially important in the case of higher dimensional eigenspaces which can occur for eigenvalues with multiplicity greater than one.

For an intuitive explanation of Corollary 2.2.3, let $\boldsymbol{A}$ have n linear independent eigenvectors. Then, the system (2.3) can be transformed into diagonal form[7] using the state transformation $\boldsymbol{z} = \boldsymbol{P}^{-1}\boldsymbol{x}$ with $\boldsymbol{P} = \begin{bmatrix} \boldsymbol{p}_1 & \dots & \boldsymbol{p}_n \end{bmatrix}$, see e.g. [17, Section 7.4], which yields

$$
\begin{aligned}
\dot{\boldsymbol{z}} &= \begin{bmatrix} s_1 & & \\ & \ddots & \\ & & s_n \end{bmatrix} \boldsymbol{z} + \boldsymbol{P}^{-1}\boldsymbol{B}\boldsymbol{u}, \\
\boldsymbol{y} &= \begin{bmatrix} \boldsymbol{C}\boldsymbol{p}_1 & \dots & \boldsymbol{C}\boldsymbol{p}_n \end{bmatrix} \boldsymbol{z} + \boldsymbol{E}\boldsymbol{u}.
\end{aligned}
\tag{2.9}
$$

This system consists of n decoupled first-order dynamics. If $\boldsymbol{C}\boldsymbol{p}_i = \boldsymbol{0}$ for some i, then the output does not provide any information about the state variable associated with the eigenvalue s_i and, thus, the system is not observable. The system is detectable if all unobservable eigenvalues satisfy $\mathrm{Re}\{s_i\} < 0$, i.e., the related first-order dynamics are asymptotically stable which allows for asymptotically determining the respective solutions.

2.2.3 Concluding Remarks on Classical Observability/Detectability

From the Kalman criterium as well as from the Hautus criteria it becomes evident that the observability/detectability of the LTI system (2.3) depends on the dynamic matrix $\boldsymbol{A}$ and the output matrix $\boldsymbol{C}$ only, i.e., it does not depend on $\boldsymbol{B}$ and $\boldsymbol{E}$. This fact is not surprising, since the input $\boldsymbol{u}$ is assumed to be known, and therefore can be considered easily by a potential observer. For this reason, it is also said that the pair $(\boldsymbol{A}, \boldsymbol{C})$ is observable/detectable.

Obviously, the classical concepts of observability and detectability need to be adapted for the unknown input case. In addition to the matrices $\boldsymbol{A}$ and $\boldsymbol{C}$, also the way the input affects the system matters. The associated notions recalled in the next section are referred to as strong observability, strong detectability and strong* detectability.

---

[7]The following reasoning can be extended in the case there do not exist n linearly independent eigenvectors. Then, the system can be transformed to Jordan block form, in which the same conclusions can be drawn.

2.3 Strong Observability, Strong Detectability and Strong* Detectability

Consider system (2.1) with possibly time-varying unknown input $\boldsymbol{w}$. As discussed in the previous section, known inputs do not affect the observability/detectability properties in the LTI case. Hence, $\boldsymbol{u} = \boldsymbol{0}$ is assumed without loss of generality which reduces the considered system to

$$
\begin{aligned}
\dot{\boldsymbol{x}} &= \boldsymbol{A}\boldsymbol{x} + \boldsymbol{D}\boldsymbol{w}, \\
\boldsymbol{y} &= \boldsymbol{C}\boldsymbol{x} + \boldsymbol{F}\boldsymbol{w}.
\end{aligned}
\tag{2.10}
$$

In contrast to the classical notions of observability/detectability, the related notions for systems with unknown input are referred to as *strong* observability/detectability, which are given in

Definition 2.3.1 (strong observability/detectability, strong* detectability [10]). System (2.10) is called

(i) strongly observable, if $\boldsymbol{y}(t) = \boldsymbol{0}$ for all $t \geqslant 0$ implies $\boldsymbol{x}(t) = \boldsymbol{0}$ for all $t \geqslant 0$, all inputs $\boldsymbol{w}(t)$ and all initial conditions $\boldsymbol{x}_0$.

(ii) strongly detectable, if $\boldsymbol{y}(t) = \boldsymbol{0}$ for all $t \geqslant 0$ implies $\boldsymbol{x}(t) \to \boldsymbol{0}$ for $t \to \infty$, all inputs $\boldsymbol{w}(t)$ and all initial conditions $\boldsymbol{x}_0$.

(iii) strong* detectable, if $\boldsymbol{y}(t) \to \boldsymbol{0}$ for $t \to \infty$ implies $\boldsymbol{x}(t) \to \boldsymbol{0}$ for $t \to \infty$, all inputs $\boldsymbol{w}(t)$ and all initial conditions $\boldsymbol{x}_0$.

In the case of strong observability there exists no input $\boldsymbol{w}$ that renders the output $\boldsymbol{y} = \boldsymbol{0}$ although $\boldsymbol{x} \neq \boldsymbol{0}$. As the considered system is linear, it follows that two identical output signals $\boldsymbol{y}_a(t) = \boldsymbol{y}_b(t)$ for all $t \geqslant 0$ imply identical state vectors $\boldsymbol{x}_a(t) = \boldsymbol{x}_b(t)$ independent of the unknown input $\boldsymbol{w}$. Then, it is possible to exactly reconstruct $\boldsymbol{x}$ within some arbitrary small time interval, i.e., strong observability ensures the existence of finite-time and fixed-time observers, see e.g. [18–20].

If system (2.10) is strongly detectable, two identical output signals $\boldsymbol{y}_a(t) = \boldsymbol{y}_b(t)$ for all $t \geqslant 0$ do not necessarily imply identical state vectors, but at least asymptotic convergence of the respective solutions to each other, i.e., $\lim_{t \to \infty}(\boldsymbol{x}_a(t) - \boldsymbol{x}_b(t)) = \boldsymbol{0}$. Hence, if the system is strongly detectable but not strongly observable, it is not possible to reconstruct the state vector within finite-time or fixed-time but asymptotically only, see e.g. [19].

In the case of strong* detectable systems, two output signals converging asymptotically to each other, i.e., $\lim_{t \to \infty}(\boldsymbol{y}_a(t) - \boldsymbol{y}_b(t)) = \boldsymbol{0}$, imply that also the respective state vectors converge asymptotically to each other, i.e., $\lim_{t \to \infty}(\boldsymbol{x}_a(t) - \boldsymbol{x}_b(t)) = \boldsymbol{0}$. Strong* detectability is the minimum requirement for the existence of a linear unknown input observer [10] allowing for asymptotic convergence of the estimation error.

It is pointed out that strong observability as well as strong* detectability imply strong detectability which becomes evident directly from the definitions. However, strong ob-

servability does not imply strong* detectability. This is demonstrated by the insightful example given in [10, pp. 356–357].

As this thesis mainly focuses on strongly observable systems, the properties of such systems are discussed in more detail in the following sections.

2.3.1 Important Properties of Strongly Observable Systems

In order to identify some important system properties, let system (2.10) be strongly observable and the unknown input $\boldsymbol{w}$ sufficiently often differentiable. Similar to the case with known inputs, see (2.5), differentiation of the output yields

$$\underbrace{\begin{bmatrix} \boldsymbol{y} \\ \dot{\boldsymbol{y}} \\ \boldsymbol{y}^{(2)} \\ \vdots \\ \boldsymbol{y}^{(n-1)} \end{bmatrix}}_{\tilde{\boldsymbol{y}}} = \underbrace{\begin{bmatrix} \boldsymbol{C} \\ \boldsymbol{CA} \\ \boldsymbol{CA}^2 \\ \vdots \\ \boldsymbol{CA}^{n-1} \end{bmatrix}}_{\boldsymbol{\mathcal{O}}} \boldsymbol{x} + \underbrace{\begin{bmatrix} \boldsymbol{F} & \boldsymbol{0} & \cdots & \cdots & \boldsymbol{0} \\ \boldsymbol{CD} & \boldsymbol{F} & \ddots & & \vdots \\ \boldsymbol{CAD} & \ddots & \ddots & \ddots & \vdots \\ \vdots & & \ddots & \ddots & \boldsymbol{0} \\ \boldsymbol{CA}^{n-2}\boldsymbol{D} & \cdots & \boldsymbol{CAD} & \boldsymbol{CD} & \boldsymbol{F} \end{bmatrix}}_{\boldsymbol{\mathcal{J}}} \underbrace{\begin{bmatrix} \boldsymbol{w} \\ \dot{\boldsymbol{w}} \\ \boldsymbol{w}^{(2)} \\ \vdots \\ \boldsymbol{w}^{(n-1)} \end{bmatrix}}_{\tilde{\boldsymbol{w}}}.$$

(2.11)

Again, the n-th and all further derivatives do not carry additional information, see e.g. [16, Lemma 4.26]. Hence, differentiation is stopped after the $(n-1)$-st derivative. As in Definition 2.3.1 of strong observability, assume $\boldsymbol{y} \equiv \boldsymbol{0}$, which consequently also implies $\dot{\boldsymbol{y}} \equiv \boldsymbol{y}^{(2)} \equiv \ldots \equiv \boldsymbol{y}^{(n-1)} \equiv \boldsymbol{0}$. Insertion into (2.11) yields

$$\boldsymbol{0} = \boldsymbol{\mathcal{O}}\boldsymbol{x} + \boldsymbol{\mathcal{J}}\tilde{\boldsymbol{w}}. \tag{2.12}$$

As the system is strongly observable, $\boldsymbol{y} \equiv \boldsymbol{0}$ implies $\boldsymbol{x} \equiv \boldsymbol{0}$ independent of the unknown input $\boldsymbol{w}$. Equation (2.12) implies $\boldsymbol{x} \equiv \boldsymbol{0}$ independent of $\boldsymbol{w}$ (and its derivatives contained in $\tilde{\boldsymbol{w}}$) if and only if there exists a generalized left-inverse $\boldsymbol{\mathcal{O}}^{\dagger}$ of the observability matrix such that

$$\boldsymbol{\mathcal{O}}^{\dagger}\boldsymbol{\mathcal{J}} = \boldsymbol{0}, \tag{2.13}$$

see [21]. The construction of such a left-inverse can be found e.g. in [20].

From the ensured existence of the left-inverse $\boldsymbol{\mathcal{O}}^{\dagger}$ satisfying (2.13), the following conclusions are drawn:

- The observability matrix is left-invertible, i.e., rank $\boldsymbol{\mathcal{O}} = n$. Hence, strong observability implies classical observability, see the Kalman criterion given in Proposition 2.2.1.

- The state vector $\boldsymbol{x}$ of a strongly observable system can be represented as a linear combination of the output $\boldsymbol{y}$ and finitely many of its derivatives $\dot{\boldsymbol{y}}, \boldsymbol{y}^{(2)}, \ldots, \boldsymbol{y}^{(n-1)}$ (if they exist[8]) only, without requiring $\boldsymbol{w}$. This can be shown by multiply-

---

[8]If $\boldsymbol{y}$ is not sufficiently often differentiable (because $\boldsymbol{w}$ is not sufficiently often differentiable), derivatives of linear combinations of $\boldsymbol{y}$, $\boldsymbol{w}$ and consequent derivatives can be considered instead. For example, the derivative $\frac{\mathrm{d}}{\mathrm{d}t}(\boldsymbol{y} - \boldsymbol{F}\boldsymbol{w})$, which exists for sure, could be considered rather than $\dot{\boldsymbol{y}}$.

ing (2.11) with $\boldsymbol{\mathcal{O}}^\dagger$ from the left-hand side, which yields

$$\boldsymbol{\mathcal{O}}^\dagger \tilde{\boldsymbol{y}} = \underbrace{\boldsymbol{\mathcal{O}}^\dagger \boldsymbol{\mathcal{O}}}_{\boldsymbol{I}} \, \boldsymbol{x} + \underbrace{\boldsymbol{\mathcal{O}}^\dagger \boldsymbol{\mathcal{J}}}_{\boldsymbol{0}} \, \tilde{\boldsymbol{w}} \quad \Leftrightarrow \quad \boldsymbol{x} = \boldsymbol{\mathcal{O}}^\dagger \tilde{\boldsymbol{y}}. \tag{2.14}$$

2.3.2 Strong Observability in the Single-Input Single-Output Case

In the special case of a system with a single unknown input w and a single output y, further noteworthy system properties arise. Consider the strongly observable SISO system

$$\begin{aligned} \dot{\boldsymbol{x}} &= \boldsymbol{A}\boldsymbol{x} + \boldsymbol{d}w, \\ y &= \boldsymbol{c}^\mathrm{T}\boldsymbol{x} + fw, \end{aligned} \tag{2.15}$$

where $\boldsymbol{d} \in \mathbb{R}^{n \times 1}$, $\boldsymbol{c} \in \mathbb{R}^{n \times 1}$ and $f \in \mathbb{R}$. The observability matrix $\boldsymbol{\mathcal{O}}$ is an $n \times n$ square matrix and, because of the strong observability assumption, has full rank. As a consequence, its generalized left-inverse $\boldsymbol{\mathcal{O}}^\dagger$ is uniquely determined and given by its inverse $\boldsymbol{\mathcal{O}}^{-1}$, i.e.,

$$\boldsymbol{\mathcal{O}}^\dagger = \boldsymbol{\mathcal{O}}^{-1}. \tag{2.16}$$

Furthermore,

$$\boldsymbol{\mathcal{J}} = \begin{bmatrix} f & 0 & \dots & \dots & 0 \\ \boldsymbol{c}^\mathrm{T}\boldsymbol{d} & f & \ddots & & \vdots \\ \boldsymbol{c}^\mathrm{T}\boldsymbol{A}\boldsymbol{d} & \ddots & \ddots & \ddots & \vdots \\ \vdots & & \ddots & \ddots & 0 \\ \boldsymbol{c}^\mathrm{T}\boldsymbol{A}^{n-2}\boldsymbol{d} & \dots & \boldsymbol{c}^\mathrm{T}\boldsymbol{A}\boldsymbol{d} & \boldsymbol{c}^\mathrm{T}\boldsymbol{d} & f \end{bmatrix} \tag{2.17}$$

is also an $n \times n$ square matrix. Since $\boldsymbol{\mathcal{O}}^{-1}$ has full rank, $\boldsymbol{\mathcal{O}}^{-1}\boldsymbol{\mathcal{J}} = \boldsymbol{0}$ (see (2.13)) can be satisfied if and only if $\boldsymbol{\mathcal{J}} = \boldsymbol{0}$ holds, or equivalently[9]

$$f = \boldsymbol{c}^\mathrm{T}\boldsymbol{d} = \boldsymbol{c}^\mathrm{T}\boldsymbol{A}\boldsymbol{d} = \dots = \boldsymbol{c}^\mathrm{T}\boldsymbol{A}^{n-2}\boldsymbol{d} = 0. \tag{2.18}$$

Consequently, the unknown input does not directly act on the output y nor on its first $(n-1)$ derivatives. Hence, strong observability implies the relative degree $\delta = n$ of y with respect to w, i.e.,

$$y^{(n)} = \boldsymbol{c}^\mathrm{T}\boldsymbol{A}^n \boldsymbol{x} + \boldsymbol{c}^\mathrm{T}\boldsymbol{A}^{n-1}\boldsymbol{d}w \qquad \text{with} \quad \boldsymbol{c}^\mathrm{T}\boldsymbol{A}^{n-1}\boldsymbol{d} \neq 0 \tag{2.19}$$

is the first derivative with a direct impact[10] of w. Furthermore, due to this relative degree condition, the differentiability of w is not required for the existence of the first $(n-1)$ derivatives of y, i.e., $\dot{y}, \dots, y^{(n-1)}$ exist for sure independent of w. For the

---

[9]The parameters $\boldsymbol{c}^\mathrm{T}\boldsymbol{A}^k\boldsymbol{d}$, $k \in \mathbb{N}_0$ are often referred to as the Markov parameters of system (2.15).

[10]For non-trivial unknown-input vector $\boldsymbol{d} \neq \boldsymbol{0}$. Otherwise, the unknown input does not act on the system at all, the relative degree is not defined and the classical notion of observability applies.

later observer design it is beneficial to represent this relative degree condition (2.18) by means of the observability matrix which yields

$$f = 0 \quad \text{and} \quad \boldsymbol{\mathcal{O}d} = \begin{bmatrix} 0 \\ \vdots \\ 0 \\ \boldsymbol{c}^{\mathrm{T}} \boldsymbol{A}^{n-1} \boldsymbol{d} \end{bmatrix}. \tag{2.20}$$

Based on the above discussion, it is evident that observability and the relative degree condition (2.20) are necessary for strong observability in the SISO case. Indeed, these two conditions are also sufficient which can be verified easily by the criterion for strong observability recapped in the next section.

2.3.3 Characterization of Strong Observability/Detectability

The criteria for strong observability/detectability considered in the following are based on the so-called Rosenbrock matrix[11]

$$\boldsymbol{P}(s) = \begin{bmatrix} s\boldsymbol{I}_n - \boldsymbol{A} & -\boldsymbol{D} \\ \boldsymbol{C} & \boldsymbol{F} \end{bmatrix}. \tag{2.21}$$

The criteria are recalled in

Proposition 2.3.1 (criteria for strong observability/detectability). *System* (2.10) *is*

(i) *strongly observable, if and only if rank* $\boldsymbol{P}(s) = n + m$ *for all* $s \in \mathbb{C}$.

(ii) *strongly detectable, if and only if rank* $\boldsymbol{P}(s) = n + m$ *for all* $s \in \mathbb{C}$ *with* $Re\{s\} \geqslant 0$.

(iii) *strong* detectable, if and only if it is strongly detectable and satisfies*

$$rank \begin{bmatrix} \boldsymbol{CD} & \boldsymbol{F} \\ \boldsymbol{F} & \boldsymbol{0} \end{bmatrix} = rank \, \boldsymbol{F} + m. \tag{2.22}$$

It becomes apparent that the required rank conditions for $\boldsymbol{P}(s)$ can only be fulfilled if there are at least as many linearly independent outputs as inputs, i.e., $p \geqslant m$. Furthermore, these criteria for strong observability and strong detectability can be regarded as a generalization of the Hautus criteria for classical observability and detectability given in Proposition 2.2.2. The matrix considered in the Hautus criteria is augmented

---

[11]Originally, the Rosenbrock matrix was called the system matrix in [22, Sec. 1, p. 43], as it contains all the mathematical information relevant for discussing the system properties. Note that in the given reference the input matrix and the output matrix appear with reversed sign, i.e.,

$$\boldsymbol{P}(s) = \begin{bmatrix} s\boldsymbol{I}_n - \boldsymbol{A} & \boldsymbol{D} \\ -\boldsymbol{C} & \boldsymbol{F} \end{bmatrix},$$

whereas e.g. in [10] uses the convention given in (2.21). In any case, the rank of $\boldsymbol{P}(s)$ is not changed by swapping this sign.

with the unknown-input matrix $\boldsymbol{D}$ and the related direct feed-through matrix $\boldsymbol{F}$ to account for the impact of the unknown input. The criteria are consistent in the sense, that the criteria for strong observability and strong detectability reduce to the Hautus criteria for classical observability and detectability in the special case without unknown input.

The rank condition (2.22) required for strong* detectability, which is also referred to as observer matching condition [23], demands a relative degree of all components of $\boldsymbol{w}$ of either 0 or 1. This means that all unknown inputs act either directly on the output $\boldsymbol{y}$ or its first derivative $\dot{\boldsymbol{y}}$.

Other criteria in the literature characterize strong observability/detectability by means of the invariant zeros of the system [10], weakly unobservable subspaces, see [24, Ch. 7] or [25], or different rank conditions [21]. In the context of this work, it is sufficient to consider the criteria given in Proposition 2.3.1.

2.3.4 Concluding Remarks on Strong Observability/Detectability

A potential unknown input observer requires the output to contain all relevant information for estimating the system state, independent of the unknown input. Therefore, in contrast to classical observability/detectability, the concepts of strong observability/detectability additionally consider the way the unknown input affects the system, i.e., the matrices $\boldsymbol{D}$ and $\boldsymbol{F}$. For this reason, it is also said that the quadruple $(\boldsymbol{A}, \boldsymbol{D}, \boldsymbol{C}, \boldsymbol{F})$ is strongly observable/detectable.

In the case of strong observability the state vector can be represented by means of the output and output derivatives (if they exist) only (independent of the unknown input), see (2.14). This relation already indicates that differentiation of $\boldsymbol{y}$ might be useful in order to estimate $\boldsymbol{x}$ in the presence of $\boldsymbol{w}$ and, therefore, motivates to deal with numerical differentiation in the next chapter.

<div style="text-align: right; font-size: 5em;">3</div>

Numerical Differentiation and Unknown Input Observation

This chapter deals with the relation of numerical differentiation and unknown input observation. It is shown that the differentiation problem can be regarded as a special case of the state observation problem of LTI systems, namely for a chain of integrators. Furthermore, one prominent solution to the differentiation problem, namely a family of homogeneous differentiators including the Robust Exact Differentiator (RED), is recalled. The application of these differentiators for the construction of unknown input observers for strongly observable systems is motivated.

3.1 The Differentiation Problem

Consider the noisy signal $\tilde{f}(t) = f(t) + v(t)$, where $f(t) = f^{(0)}(t)$ is a (sufficiently often differentiable) signal to be differentiated and $v(t)$ represents the measurement noise. The goal is to estimate the first $(n-1)$ derivatives $f^{(1)}(t), f^{(2)}(t), \ldots, f^{(n-1)}(t)$ from $\tilde{f}(t)$.

The numerical differentiation problem can be transferred into a state estimation problem by considering the signal model depicted in Figure 3.1.

Therein, the signal to be differentiated is generated by n times integration of the n-th derivative $f^{(n)}$. The signal model is therefore a chain of n integrators, which is
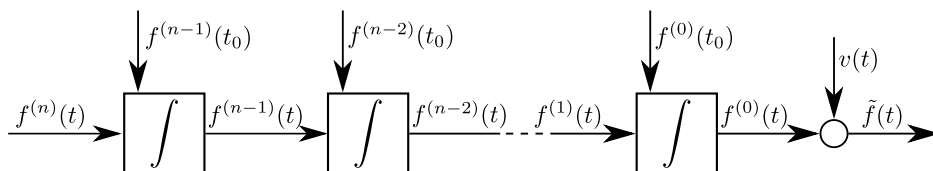
Figure 3.1: *The signal model considered for differentiation. The signal $f(t) = f^{(0)}(t)$ to be differentiated is generated by n times integrating its n-th derivative $f^{(n)}$. In practice, $f(t)$ is typically corrupted by some measurement noise $v(t)$.*

described by the state-space model

$$\frac{\mathrm{d}f^{(0)}}{\mathrm{d}t} = f^{(1)},$$

$$\vdots$$

$$\frac{\mathrm{d}f^{(n-2)}}{\mathrm{d}t} = f^{(n-1)},$$

$$\frac{\mathrm{d}f^{(n-1)}}{\mathrm{d}t} = f^{(n)},$$

(3.1a)

with the noisy output

$$\tilde{f}(t) = f^{(0)}(t) + v(t).$$

(3.1b)

As the n-th derivative is unknown in general, $f^{(n)}(t)$ acts as an unknown input to system (3.1). It is pointed out that in the absence of measurement noise, i.e., $v(t) \equiv 0$, system (3.1) is strongly observable as the state variables correspond directly to the output derivatives and, thus, $f(t) = 0 \ \forall t \geqslant 0$ implies $f^{(0)} = f^{(1)} = \cdots = f^{(n-1)} = 0$ $\forall t \geqslant 0$, see Definition 2.3.1(i).

It can be concluded that the estimation of the first $n-1$ signal derivates of $f(t)$ is equivalent to the estimation of the state variables of a chain of integrators affected by the unknown input $f^{(n)}$. Hence, an unknown input observer for (3.1) can be regarded as a differentiator.

3.2 Homogeneous Differentiators and the Robust Exact Differentiator

In the following, a family of homogeneous differentiators proposed in [26] is recalled. The differentiator is given by the observer

$$\frac{\mathrm{d}\hat{f}_0}{\mathrm{d}t} = \hat{f}_1 + \kappa_{n-1}\lfloor \tilde{f} - \hat{f}_0 \rceil^{\frac{r_2}{r_1}},$$

$$\vdots$$

$$\frac{\mathrm{d}\hat{f}_{n-2}}{\mathrm{d}t} = \hat{f}_{n-1} + \kappa_1\lfloor \tilde{f} - \hat{f}_0 \rceil^{\frac{r_n}{r_1}},$$

$$\frac{\mathrm{d}\hat{f}_{n-1}}{\mathrm{d}t} = \kappa_0\lfloor \tilde{f} - \hat{f}_0 \rceil^{\frac{r_{n+1}}{r_1}},$$

(3.2a)

which consists of a copy of the system dynamics (3.1a) and some (probably) nonlinear output error injection. The observer's state variables $\hat{f}_0, \ldots, \hat{f}_{n-1}$ are the respective derivative estimates, $\kappa_0, \ldots, \kappa_{n-1}$ are constant positive parameters and $r_1, \ldots, r_n$ are the so-called homogeneity weights. The constant r_{n+1} is not a weight but is introduced for the sake of simplicity. The homogeneity weights are defined as

$$r_i = 1 - (n-i)q, \qquad i = 1, \ldots, n,$$

(3.2b)

where $q \in [-1, 0]$ is the so-called homogeneity degree to be chosen:

- For $q = 0$ one obtains a linear differentiator which is a classical linear observer for the chain of integrators. In this case, the parameters $\kappa_0, \ldots, \kappa_{n-1}$ are the coefficients of the characteristic polynomial of the estimation error dynamics.

- The choice $q = -1$ yields Levant's RED [27, 28][1]. It is pointed out that $q = -1$ yields a discontinuous right-hand side of system (3.2a) which is a so-called sliding mode differentiator. Here and hereafter, solutions of such systems are understood in the sense of Filippov [11].

- For $-1 < q < 0$ the differentiator is nonlinear, but with a continuous right-hand side.

The convergence behaviour of the differentiator is summarized in

Proposition 3.2.1 (convergence of homogeneous differentiator [26]). *Consider the unknown input observer* (3.2) *for the estimation of the state variables of system* (3.1). *Moreover, suppose $v \equiv 0$.*

(i) If $f^{(n)}(t) = 0 \ \forall t \geqslant 0$, then for each $q \in [-1, 0]$ there exist parameters $\kappa_0, \kappa_1, \ldots, \kappa_{n-1}$ such that the estimation error variables $\sigma_i = f^{(i-1)} - \hat{f}_{i-1}$ with $i = 1, \ldots, n$ converge to zero globally. In the case $q = 0$ the convergence is exponential, i.e., for all initial states there exist constants $K > 0$ and $\gamma > 0$ such that $|\sigma_i| < K e^{-\gamma t} \ \forall t$. In the case $-1 \leqslant q < 0$ the estimation error variables σ_i vanish within a finite time, i.e., for all initial states there exists a finite time $T \geqslant 0$ such that $\sigma_i(t) = 0 \ \forall i \ \forall t \geqslant T$.

(ii) If $q = -1$ and $f^{(n)}$ is bounded, i.e., there exists a constant $L = \sup_t \left| f^{(n)}(t) \right|$, then there exist parameters $\kappa_0, \kappa_1, \ldots, \kappa_{n-1}$ such that the estimation error variables converge to zero within finite time despite $f^{(n)}$, i.e., for all initial states there exists a finite time $T > 0$ such that $\sigma_i(t) = 0 \ \forall i \ \forall t \geqslant T$. Moreover, a necessary condition for the choice of κ_0 is given by $\kappa_0 > L$.

It is pointed out that in the case of uniformly bounded measurement noise, i.e., $|v| \leqslant v_{\max}$, $v_{\max} \geqslant 0$, the estimation error variables $\sigma_i = f^{(i-1)} - \hat{f}_{i-1}$, $i = 1, \ldots, n$ stay bounded with bounds discussed e.g. in [26]. The estimation error dynamics are given by

$$\frac{\mathrm{d}\sigma_1}{\mathrm{d}t} = \sigma_2 - \kappa_{n-1} \lfloor \sigma_1 + v \rceil^{\frac{r_2}{r_1}},$$

$$\vdots$$

$$\frac{\mathrm{d}\sigma_{n-1}}{\mathrm{d}t} = \sigma_n - \kappa_1 \lfloor \sigma_1 + v \rceil^{\frac{r_{n-1}}{r_1}},$$

$$\frac{\mathrm{d}\sigma_n}{\mathrm{d}t} = f^{(n)} - \kappa_0 \lfloor \sigma_1 + v \rceil^{\frac{r_n}{r_1}}.$$

(3.3)

---

[1] In contrast to the notation used in this thesis, the given references [27, 28] denote n as the numbers of derivatives to be estimated, i.e., the system order of the differentiator is $n + 1$.

In the case of the RED, i.e., $q = -1$, and in the absence of measurement noise, i.e., $v \equiv 0$, the last differential equation in (3.3) becomes

$$\frac{\mathrm{d}\sigma_n}{\mathrm{d}t} = f^{(n)} - \kappa_0 \mathrm{sign}(\sigma_1), \tag{3.4}$$

where $\mathrm{sign}(\sigma_1) = \lfloor \sigma_1 \rceil^0$ is discontinuous in $\sigma_1 = 0$. The necessary condition $\kappa_0 > L$ for convergence of the RED stated in Proposition 3.2.1(ii) arises from the fact that the discontinuous function $\kappa_0 \mathrm{sign}(\sigma_1)$ must be able to dominate the n-th derivative $f^{(n)}$. A parameter setting for $n \leqslant 6$ is proposed in [29, Section 6.7], where the parameters are given by

$$\kappa_{n-i} = \tilde{\lambda}_{n-i} L^{\frac{i}{n}}, \qquad i = 1, \ldots, n \tag{3.5}$$

with $\tilde{\lambda}_{n-1} = \lambda_{n-1}$ and $\tilde{\lambda}_j = \lambda_j \tilde{\lambda}_{j+1}^{\frac{j}{j+1}}$, $j = 0, \ldots, n-2$, where $\lambda_0 = 1.1$, $\lambda_1 = 1.5$, $\lambda_2 = 3$, $\lambda_3 = 5$, $\lambda_4 = 8$ and $\lambda_5 = 12$. Another reasonable parameter tuning strategy can be found e.g. in [30].

It is noted that the discussed differentiator is called homogeneous, because, if $v \equiv 0$ and $f^{(n)} \equiv 0$, its estimation error dynamics (3.3) are $\boldsymbol{r}$-homogeneous[2] of homogeneity degree q with the weights $\boldsymbol{r} = \begin{bmatrix} r_1 & \ldots & r_n \end{bmatrix}^{\mathrm{T}}$.

3.3 Motivation for the Construction of Unknown Input Observers

In the absence of measurement noise, the RED is able to provide exact estimates of the first $n - 1$ derivatives of $f(t)$ within finite time if $f^{(n)}$ is bounded. The stability proofs exist for arbitrary order [26, 28, 33], there are well-established parameter settings available in the literature, see e.g. [29, Section 6.7] or [30], and a large variety of discretization methods has been proposed [34–44]. The RED can be interpreted as an unknown input observer for a special LTI system, namely a chain of integrators with a single unknown input and a single output. The central research question deals with the generalization to a larger class of systems:

How can numerical differentiation methods such as the RED be applied to construct unknown input observers for the general class of strongly observable LTI systems with multiple unknown inputs and multiple outputs?

Note that, beside the RED, there exist other established differentiators such as the high gain differentiator [45, 46], which is exact when its gains tend to infinity, or Moreno's

---

[2]The notion of weighted homogeneity [31] generalizes the classical homogeneity in the following way: Consider the vector field $\boldsymbol{g} : \mathbb{R}^n \to \mathbb{R}^n$ and the autonomous system $\frac{\mathrm{d}\boldsymbol{x}}{\mathrm{d}t} = \boldsymbol{g}(\boldsymbol{x})$. The vector field is said to be $\boldsymbol{r}$-homogeneous of degree $q \in \mathbb{R}$ if $q \geqslant - \min\limits_{0 \leqslant i \leqslant n} r_i$ and $\boldsymbol{g}(\boldsymbol{K_r x}) = k^q \boldsymbol{K_r g}(\boldsymbol{x})$ hold $\forall \boldsymbol{x} \in \mathbb{R}^n$ and $\forall k > 0$, where $\boldsymbol{K_r} = \mathrm{diag}\{k^{r_i}\}_{i=1}^n$ is the so-called dilation matrix. The positive constants $r_i > 0$ denote the so-called homogeneity weights (also called dilation coefficients), which are summarized in the dilation coefficient vector $\boldsymbol{r} = \begin{bmatrix} r_1 & r_2 & \ldots & r_n \end{bmatrix}$. The autonomous system is said to be $\boldsymbol{r}$-homogeneous of degree q if its right hand side is $\boldsymbol{r}$-homogeneous of degree q. For more details see e.g. [32].

bi-homogeneous differentiator [47, 48] which provides exact estimates in fixed time, i.e., there exists an upper limit for the finite convergence time. However, those are not explicitly considered in this thesis. It will turn out that the key in constructing the unknown input observer is to find a suitable representation of the system under consideration, rather than using a particular differentiator. Once the system is represented in an appropriate form, the unknown input observer design is simple and straightforward regardless of the applied differentiator. This thesis focuses on RED-based observer design only, as it does not require infinite gains for exactness as the high gain differentiator, and its structure is simpler compared to the bi-homogeneous differentiator.

4

Problem Statement and Existing Unknown Input Observers for Linear Time-Invariant Systems

Motivated by the previous chapter on numerical differentiation, the goal is to find a suitable way to apply the RED as an unknown input observer to arbitrary strongly observable LTI systems. For this purpose, a detailed problem statement is provided in order to clarify the considered system class. Subsequently, existing unknown input observers are recalled and analyzed. Their advantages and disadvantages are discussed by means of a numerical example. Finally, the research gap that serves as motivation is explained.

4.1 Problem Statement

A detailed description of the problem statement considered in this thesis is provided in the following. Furthermore, the assumptions made in the problem statement are discussed in order to show that they are either non-restrictive or reasonable from a practical point of view.

4.1.1 Formulation of the Unknown Input Observation Problem

Consider the LTI system[1]

$$\begin{aligned}
\dot{\boldsymbol{x}} &= \boldsymbol{A}\boldsymbol{x} + \boldsymbol{D}\boldsymbol{w}, \\
\boldsymbol{y} &= \boldsymbol{C}\boldsymbol{x},
\end{aligned} \tag{4.1}$$

where $\boldsymbol{x} = \begin{bmatrix} x_1 & x_2 & \ldots & x_n \end{bmatrix}^{\mathrm{T}}$ is the n-dimensional state vector with initial value $\boldsymbol{x}(0) = \boldsymbol{x}_0$, $\boldsymbol{w} = \begin{bmatrix} w_1 & w_2 & \ldots & w_m \end{bmatrix}^{\mathrm{T}}$ denotes the vector of possibly time-varying, un-

---

[1]Note that no direct feed-trough term is considered, i.e., $\boldsymbol{F} = \boldsymbol{0}$, compare to system (2.1). This is non-restrictive since one can always get rid of the direct feed-through term for the purpose of state estimation, which is shown later on in Section 7.1.

known inputs and $\boldsymbol{y} = \begin{bmatrix} y_1 & y_2 & \dots & y_p \end{bmatrix}^{\mathrm{T}}$ is the output vector. Furthermore, the dynamic matrix $\boldsymbol{A} \in \mathbb{R}^{n \times n}$, the unknown-input matrix $\boldsymbol{D} \in \mathbb{R}^{n \times m}$ and the output matrix $\boldsymbol{C} \in \mathbb{R}^{p \times n}$ are constant matrices. The unknown-input matrix and the output matrix are partitioned into column and row vectors, respectively, i.e.,

$$\boldsymbol{D} = \begin{bmatrix} \boldsymbol{d}_1 & \boldsymbol{d}_2 & \dots & \boldsymbol{d}_m \end{bmatrix}, \qquad \boldsymbol{C} = \begin{bmatrix} \boldsymbol{c}_1^{\mathrm{T}} \\ \boldsymbol{c}_2^{\mathrm{T}} \\ \vdots \\ \boldsymbol{c}_p^{\mathrm{T}} \end{bmatrix}. \tag{4.2}$$

Assumption 4.1.1. System (4.1) is strongly observable.

Assumption 4.1.2. The unknown inputs are bounded, i.e.,

$$|w_i(t)| \leqslant L_i \quad \forall t, \qquad \text{with} \quad 0 \leqslant L_i < \infty, \quad i = 1, \dots, m. \tag{4.3}$$

Assumption 4.1.3. The columns of $\boldsymbol{D}$ as well as the rows of $\boldsymbol{C}$ are linearly independent, i.e., rank $\boldsymbol{D} = m$ and rank $\boldsymbol{C} = p$.

The goal is to design an unknown input observer for the exact estimation of the state vector $\boldsymbol{x}$ of system (4.1) from the measured output $\boldsymbol{y}$ despite the unknown input $\boldsymbol{w}$.

4.1.2 Discussion of the Problem Statement

Assumption 4.1.2 on the boundedness of the input arises from the boundedness assumption of the RED, i.e., it requires the n-th derivative to be bounded. Many physical systems will naturally satisfy this boundedness assumption. For example, mass and energy flows entering a physical system as inputs are finite.

Assumption 4.1.3 is non-restrictive, as linear dependent inputs and outputs can always be summarized by means of a linear independent basis. Consider e.g. linear dependent unknown inputs $\boldsymbol{w}$, i.e., rank $\boldsymbol{D} = \tilde{m} < m$. Then, one can introduce the new unknown input vector

$$\tilde{\boldsymbol{w}} = \boldsymbol{M}\boldsymbol{w}, \qquad \text{with} \quad \boldsymbol{M} \in \mathbb{R}^{\tilde{m} \times m}, \quad \text{rank } \boldsymbol{M} = \tilde{m}, \tag{4.4}$$

such that the new unknown-input matrix

$$\tilde{\boldsymbol{D}} = \boldsymbol{D}\boldsymbol{M}^{\ddagger} \tag{4.5}$$

satisfies rank $\tilde{\boldsymbol{D}} = \tilde{m}$, where $\boldsymbol{M}^{\ddagger}$ denotes a generalized right-inverse of $\boldsymbol{M}$.

It is pointed out that the problem statement does not consider a direct feed-through term. This is non-restrictive since one can always get rid of the direct feed-through term for the purpose of state estimation, which is shown later on in Section 7.1. Furthermore, known inputs are not explicitly taken into account as they can always be easily considered by an observer, see Section 2.2.

4.2 Existing Unknown Input Observers for Strongly Observable Linear Time-Invariant Systems

In this section, different existing unknown input observers for the considered problem statement are analyzed. Beside a general discussion of each method, the respective benefits and drawbacks are demonstrated by means of the numerical

Example 4.2.1. Consider the linearized model of the lateral motion of a light aircraft taken from [49] which has been already used by the unknown input observers proposed in [50, 51]. The matrices of the system of order $n = 7$ with $m = 1$ unknown input and $p = 2$ outputs are given by

$$
\boldsymbol{A} = \begin{bmatrix}
-0.3 & 0 & -33 & 9.81 & 0 & -5.4 & 0 \\
-0.1 & -8.3 & 3.75 & 0 & 0 & 0 & -28.6 \\
0.37 & 0 & -0.64 & 0 & 0 & -9.5 & 0 \\
0 & 1 & 0 & 0 & 0 & 0 & 0 \\
0 & 0 & 1 & 0 & 0 & 0 & 0 \\
0 & 0 & 0 & 0 & 0 & -10 & 0 \\
0 & 0 & 0 & 0 & 0 & 0 & -5
\end{bmatrix},
$$

$$
\boldsymbol{D} = \begin{bmatrix} 0 \\ 0 \\ 0 \\ 0 \\ 0 \\ 20 \\ 0 \end{bmatrix}, \quad
\boldsymbol{C} = \begin{bmatrix} 0 & 1 & 0 & 0 & 0 & 0 & 0 \\ 0 & 0 & 0 & 0 & 1 & 0 & 0 \end{bmatrix}.
\tag{4.6}
$$

The state vector $\boldsymbol{x} = \begin{bmatrix} v & z & r & \phi & \psi & \zeta & \xi \end{bmatrix}^{\mathrm{T}}$ consists of the sideslip velocity v, the roll rate z, the yaw rate r, the roll angle ϕ, the yaw angle ψ, the rudder angle ζ and the aileron angle ξ. The unknown input w models a fault in the rudder. The output $\boldsymbol{y} = \begin{bmatrix} y_1 & y_2 \end{bmatrix}^{\mathrm{T}}$ provides measurements of the roll rate z and the yaw angle ψ. In the simulation studies presented in this thesis, the initial state vector of the system is chosen as

$$
\boldsymbol{x}_0 = \begin{bmatrix} -0.5 & 0.1 & 0.02 & 0.2 & -0.1 & -0.3 & 0.2 \end{bmatrix}^{\mathrm{T}},
\tag{4.7}
$$

and the unknown input is selected as

$$
w = 0.008 + 0.01\sin(2t) + 0.002\cos(13t).
\tag{4.8}
$$

Note that the unknown input is bounded[2] by $L = 0.02$. Furthermore, the considered system is strongly observable which can be e.g. shown by means of the Rosenbrock matrix according to Proposition 2.3.1. The system is unstable since $\boldsymbol{A}$ has two eigenvalues with non-negative real part located at $s_1 = 0$ and $s_2 = 0.1219$. Because

of these unstable eigenvalues and the lack of a stabilizing control, the system trajectories diverge which results in unbounded state variables. The goal is to estimate the state vector $\boldsymbol{x}$ from the output $\boldsymbol{y}$ despite the unknown input w.

4.2.1 Design of a Linear Luenberger Observer

As a first approach the standard linear Luenberger observer [7]

$$
\begin{aligned}
\dot{\hat{\boldsymbol{x}}} &= \boldsymbol{A}\hat{\boldsymbol{x}} + \boldsymbol{L}(\boldsymbol{y} - \hat{\boldsymbol{y}}), \\
\hat{\boldsymbol{y}} &= \boldsymbol{C}\hat{\boldsymbol{x}},
\end{aligned}
\tag{4.9}
$$

which ignores the unknown input is investigated. It consists of a copy of the known parts of the system dynamics and a linear injection of the output estimation error with the output-injection matrix $\boldsymbol{L} \in \mathbb{R}^{n \times p}$. The dynamics of the estimation error $\boldsymbol{\eta} = \boldsymbol{x} - \hat{\boldsymbol{x}}$ are given by

$$
\dot{\boldsymbol{\eta}} = (\boldsymbol{A} - \boldsymbol{L}\boldsymbol{C})\boldsymbol{\eta} + \boldsymbol{D}w.
\tag{4.10}
$$

The considered system is strongly observable and, thus, also observable, which allows for assigning any desired eigenvalues to the dynamic matrix $\boldsymbol{A} - \boldsymbol{L}\boldsymbol{C}$ of the estimation error dynamics.

Example 4.2.2. Consider the task provided in Example 4.2.1. Assignment of the desired eigenvalues

$$
\begin{aligned}
\tilde{s}_1 &= -1, \quad \tilde{s}_2 = -2, \quad \tilde{s}_3 = -3, \quad \tilde{s}_4 = -4, \\
\tilde{s}_5 &= -5, \quad \tilde{s}_6 = -6, \quad \tilde{s}_7 = -7,
\end{aligned}
\tag{4.11}
$$

using the method proposed in [52] yields the output-injection matrix

$$
\boldsymbol{L} = \begin{bmatrix}
-9.82 & -105.14 \\
-2.95 & 13.06 \\
1.38 & 19.51 \\
2.01 & 5.45 \\
0.57 & 6.71 \\
-0.77 & 8.81 \\
0.03 & -0.08
\end{bmatrix}.
\tag{4.12}
$$

Figure 4.1 shows the resulting estimation error variables for the initial state (4.7), the unknown input (4.8) and the initial observer state $\hat{\boldsymbol{x}}(0) = \boldsymbol{0}$.

---

[2]The bound $L = 0.02$ is probably not the smallest bound for w. However, for the purpose of observer design, the existence of a certain bound is sufficient.
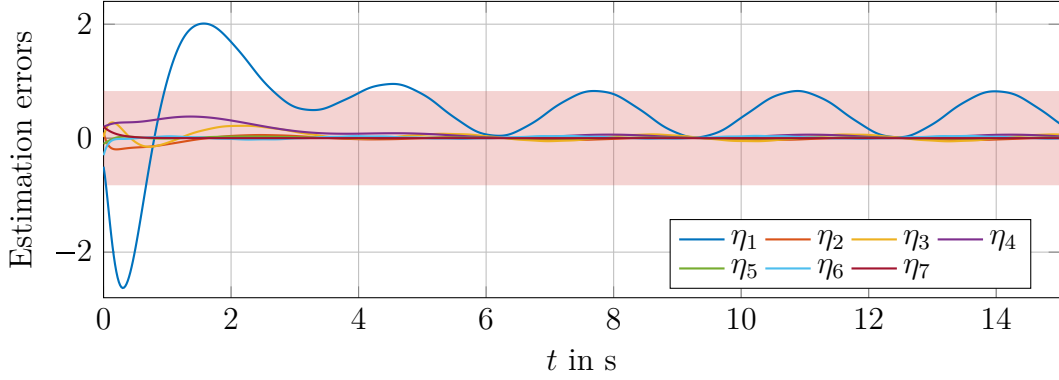
Figure 4.1: *Estimation error variables $\boldsymbol{\eta}_i = \boldsymbol{x}_i - \hat{\boldsymbol{x}}_i$, $i = 1, \ldots, 7$ of the linear Lu-enberger observer (4.9) with eigenvalues $\tilde{s}_i = -1, -2, \ldots, -7$. The esti-mation error variables converge into a band of approximately ± 0.8.*

It becomes apparent that the estimation errors converge within a certain band around zero, but do not vanish as the unknown input still excites the estimation error dynamics. The more aggressive choice of the desired observer eigenvalues

$$
\begin{aligned}
&\tilde{s}_1 = -6, \quad \tilde{s}_2 = -7, \quad \tilde{s}_3 = -8, \quad \tilde{s}_4 = -9, \\
&\tilde{s}_5 = -10, \quad \tilde{s}_6 = -11, \quad \tilde{s}_7 = -12,
\end{aligned}
\tag{4.13}
$$

and assignment using again the method proposed in [52] results in the output-injection matrix

$$
\boldsymbol{L} = \begin{bmatrix}
-2459.62 & 6584.86 \\
2.72 & 423.81 \\
-117.14 & 460.08 \\
-735.14 & 1819.02 \\
-4.73 & 36.04 \\
0.002 & -0.006 \\
0.14 & -0.57
\end{bmatrix} .
\tag{4.14}
$$

Figure 4.2 shows the resulting estimation errors.
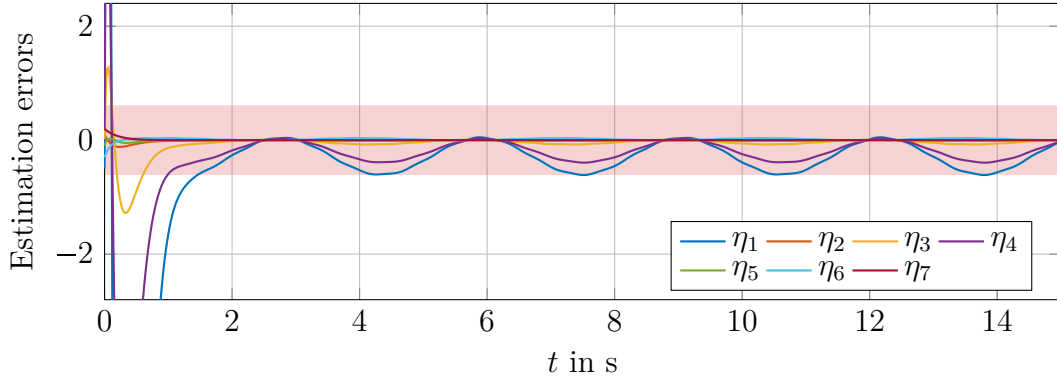
Figure 4.2: *Estimation error variables $\boldsymbol{\eta}_i = \boldsymbol{x}_i - \hat{\boldsymbol{x}}_i$, $i = 1, \ldots, 7$ of the linear Luenberger observer (4.9) with eigenvalues $\tilde{s}_i = -6, -7, \ldots, -12$. The estimation error variables converge into a band of approximately ± 0.6.*

Again, the estimation error converges within a bound around zero. Due to the more aggressive eigenvalue setting, the transients are stronger and the resulting steady-state error band is smaller.

Since $\boldsymbol{A} - \boldsymbol{LC}$ is a Hurwitz matrix, the estimation error dynamics are input-to-state stable (ISS), i.e., the estimation error stays bounded as long as the unknown input is bounded. The error band can be made arbitrarily small by appropriately selecting the observer eigenvalues, i.e., with a sufficiently small real part[3]. However, the observer gain $\boldsymbol{L}$ and, in consequence, also the amplification of potential measurement noise increase, which limits the suitable region for the choice of the eigenvalues in practical applications. Anyway, this linear observer (4.9) (with finite gain $\boldsymbol{L}$) can not provide exact estimates of the state even in the theoretical case without measurement noise.

4.2.2 Unknown Input Observers Requiring the Observer Matching Condition

Classical linear unknown input observers [10, 56–62], conventional first-order sliding mode observers [63–65] as well as the observer proposed in [66] require the so-called observer matching condition

$$\text{rank} \left(\boldsymbol{CD} \right) = \text{rank } \boldsymbol{D} \tag{4.15}$$

to be fulfilled, i.e., all unknown inputs have a direct impact on the first output derivative. Note that (4.15) is a special case of the general observer matching condition (2.22) required for strong* detectability. Both conditions coincide in the case without direct feed-through, i.e., $\boldsymbol{F} = \boldsymbol{0}$. These types of unknown input observers therefore require that the system is not strongly observable, but strong* detectable. Obviously, this strongly restricts the system class under consideration. This is emphasized by means of the numerical example.

---

[3]This behaviour is exploited in the design of so-called high-gain observers, see e.g. [53–55], which provide exact estimates as the observer gains tend to infinity.

Example 4.2.3. For the system provided in Example 4.2.1

$$\boldsymbol{CD} = \begin{bmatrix} 0 \\ 0 \end{bmatrix} \tag{4.16}$$

holds and, therefore, the observer matching condition

$$\text{rank}\,(\boldsymbol{CD}) = 0 \neq 1 = \text{rank}\,\boldsymbol{D} \tag{4.17}$$

is not fulfilled. In consequence, the considered system is not strong* detectable although it is strongly observable. Thus, classical linear unknown input observers as well as conventional first-order sliding mode method can not be applied.

4.2.3 Unknown Input Observation via Direct Differentiation of the Output

As shown Section 2.3.1 the state vector of a strongly observable system can be represented by means of the output and finitely many of its derivatives (if they exist) without requiring the unknown input, i.e.,

$$\boldsymbol{x} = \boldsymbol{\mathcal{O}}^{\dagger} \begin{bmatrix} \boldsymbol{y} \\ \dot{\boldsymbol{y}} \\ \boldsymbol{y}^{(2)} \\ \vdots \\ \boldsymbol{y}^{(n-1)} \end{bmatrix}, \tag{4.18}$$

where $\boldsymbol{\mathcal{O}}^{\dagger}$ is a generalized left-inverse of the observability matrix. This relation naturally suggests the idea of using the RED to estimate the required derivatives of the output in order to calculate an estimated value for the state. Multiple methods work in exactly this way, such as [67, 68] for nonlinear SISO systems and [69] for nonlinear MIMO systems under a restrictive relative degree condition. In [70] differentiation of the output is applied in order to generate auxiliary outputs used for the design of a linear observer. In order to successfully apply the RED for output differentiation, the respective output derivatives acting as unknown input to its estimation error dynamics are required to be bounded. As shown in Section 2.3.1, the r-th output derivative is given by

$$\boldsymbol{y}^{(r)} = \boldsymbol{CA}^r\boldsymbol{x} + \sum_{i=0}^{r-1} \boldsymbol{CA}^{r-1-i}\boldsymbol{Dw}^{(i)}. \tag{4.19}$$

It is apparent that, beside of the unknown input, the output derivatives also depend on input derivatives and the state variables. Hence, boundedness of a certain output derivative, which is a prerequisite for the application of the RED, requires sufficiently many input derivatives and the state vector $\boldsymbol{x}$ to be bounded. However, the system trajectories may be unbounded, e.g. for unstable systems, where state variables can grow arbitrarily large. Furthermore, in order to keep the differentiator gains as small as possible, it would be desirable to have the bound independent of $\boldsymbol{x}$.

Example 4.2.4. For the system given in Example 4.2.1, the algorithm in [20] provides

$$\mathcal{O}^\dagger = \begin{bmatrix} -82.56 & 0 & -8.11 & 37.5 & 3.92 & -2.3 & 0.45 & -1.65 & 0 & \dots & 0 \\ 1 & 0 & 0 & 0 & 0 & 0 & 0 & 0 & \vdots & & \vdots \\ 0 & 0 & 0 & 1 & 0 & 0 & 0 & 0 & \vdots & & \vdots \\ -4.52 & 0 & -9.85 & 5.28 & -2.82 & 4.82 & -0.2 & 0.75 & \vdots & & \vdots \\ 0 & 1 & 0 & 0 & 0 & 0 & 0 & 0 & \vdots & & \vdots \\ -3.22 & 0 & -0.32 & 1.39 & 0.15 & -0.2 & 0.017 & -0.064 & \vdots & & \vdots \\ -0.0015 & 0 & -0.0066 & 0 & -0.014 & 0.0081 & -0.0016 & 0.0058 & 0 & \dots & 0 \end{bmatrix} \quad (4.20)$$

for the left-inverse of the observability matrix The algorithm in [20] minimizes the number of required derivatives, i.e., it maximizes the number of **0**-columns at the end of $\mathcal{O}^\dagger$. In this case there are eight nonzero columns, i.e., the outputs $\boldsymbol{y} = \begin{bmatrix} y_1 & y_2 \end{bmatrix}^\mathrm{T}$ and the first three respective derivatives $\dot{\boldsymbol{y}}, \boldsymbol{y}^{(2)}, \boldsymbol{y}^{(3)}$ are required to represent $\boldsymbol{x}$ by means of (4.18). For this reason, two REDs are applied, one for each output to estimate the first three derivatives. The differentiator parameters are chosen as $\kappa_{1,3} = 5.8$, $\kappa_{1,2} = 15.57$, $\kappa_{1,1} = 22.14$ and $\kappa_{1,0} = 15.4$ for the differentiation of y_1 and $\kappa_{2,3} = 4.7$, $\kappa_{2,2} = 10.2$, $\kappa_{2,1} = 11.73$ and $\kappa_{2,0} = 6.6$ for the differentiation of y_2, based on the setting provided in [29, Section 6.7]. Figure 4.3 depicts evolution of the state variables and the estimation errors.
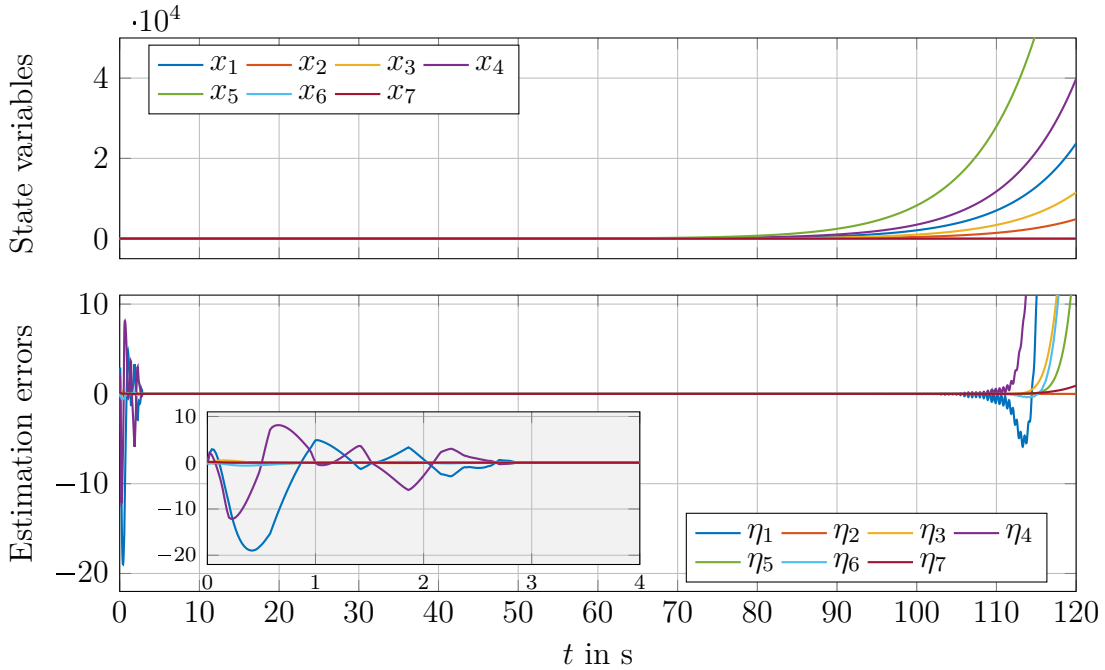
Figure 4.3: *State variables x_i and estimation errors $\eta_i = x_i - \hat{x}_i$, $i = 1, \dots, 7$ when applying two REDs directly as an unknown input observer by estimating the derivatives of the output. After initial convergence, the observer later diverges due to the unbounded state variables.*

> The estimation errors vanish within a finite time of approximately 2.9 s in the presence of the unknown input. However, the system is unstable and the state variables do not stay bounded. As a consequence of (4.19) for $r = 4$, the fourth derivatives of the outputs grow arbitrarily large. After 100 s the REDs are not capable of compensating for the growing fourth derivatives any more which finally leads to divergence of the estimation errors.

There exists a workaround for the problem of unbounded trajectories, see e.g. [71] where output differentiation is applied to a certain fourth order LTI system with two outputs. Therein, the observer additionally includes estimates $\hat{\boldsymbol{x}}$ of the state vector in the last differential equation, which for r times differentiation of the j-th output results in

$$
\begin{aligned}
\frac{\mathrm{d}\hat{y}_j}{\mathrm{d}t} &= \hat{\dot{y}}_j + \kappa_{j,r-1}\lfloor\sigma_{j,1}\rceil^{\frac{r-1}{r}}, \\
&\ \ \vdots \\
\frac{\mathrm{d}\hat{y}_j^{(r-2)}}{\mathrm{d}t} &= \hat{y}_j^{(r-1)} + \kappa_{j,1}\lfloor\sigma_{j,1}\rceil^{\frac{1}{r}}, \\
\frac{\mathrm{d}\hat{y}_j^{(r-1)}}{\mathrm{d}t} &= \boldsymbol{c}_j^{\mathrm{T}}\boldsymbol{A}^r\hat{\boldsymbol{x}} + \kappa_{j,0}\lfloor\sigma_{j,1}\rceil^{0},
\end{aligned}
\tag{4.21}
$$

where $\sigma_{j,i} = y_j^{(i-1)} - \hat{y}_j^{(i-1)}$, $i = 1,\dots,r$ are the estimation errors of the respective output derivatives. The error dynamics are given by

$$
\begin{aligned}
\frac{\mathrm{d}\sigma_{j,1}}{\mathrm{d}t} &= \sigma_{j,2} - \kappa_{j,r-1}\lfloor\sigma_{j,1}\rceil^{\frac{r-1}{r}}, \\
&\ \ \vdots \\
\frac{\mathrm{d}\sigma_{j,r-1}}{\mathrm{d}t} &= \sigma_{j,r} + \kappa_{j,1}\lfloor\sigma_{j,1}\rceil^{\frac{1}{r}}, \\
\frac{\mathrm{d}\sigma_{j,r}}{\mathrm{d}t} &= \boldsymbol{c}_j^{\mathrm{T}}\boldsymbol{A}^r\boldsymbol{\eta} + \sum_{i=0}^{r-1}\boldsymbol{c}_j^{\mathrm{T}}\boldsymbol{A}^{r-1-i}\boldsymbol{D}\boldsymbol{w}^{(i)} - \kappa_{j,0}\lfloor\sigma_{j,1}\rceil^{0}.
\end{aligned}
\tag{4.22}
$$

According to Proposition 3.2.1(ii) on page 19 the errors vanish only if

$$
\kappa_{j,0} > \left| \boldsymbol{c}_j^{\mathrm{T}}\boldsymbol{A}^r\boldsymbol{\eta} + \sum_{i=0}^{r-1}\boldsymbol{c}_j^{\mathrm{T}}\boldsymbol{A}^{r-1-i}\boldsymbol{D}\boldsymbol{w}^{(i)} \right| \qquad \forall t \geqslant 0.
\tag{4.23}
$$

Note that the lower bound for $\kappa_{j,0}$ in (4.23) depends on the error $\boldsymbol{\eta} = \boldsymbol{x} - \hat{\boldsymbol{x}}$ instead of the state vector $\boldsymbol{x}$ itself. Hence, this approach is able to handle unbounded trajectories as long as the estimation error is bounded. However, in the case of an unstable system and if the initial estimation error $\boldsymbol{\eta}(0)$ is not sufficiently small, such an observer will still diverge.

In conclusion, unknown input observers that estimate the system state by directly differentiating the output allow only for semi-global stabilization of the estimation error. Tuning of such an unknown input observer may be cumbersome as the expected system trajectories influence the required observer gain. Furthermore, these approaches

are not applicable in the case when output is not sufficiently often differentiable. In this case, the output can be additionally filtered to ensure existence of the required derivatives, see [20], which unnecessarily increases the observer order and the number of tuning parameters.

4.2.4 Step-by-Step Sliding Mode Observers

In contrast to the direct differentiation of the output, so-called step-by-step sliding mode observers relax the differentiability assumption on $\boldsymbol{y}$ by differentiating linear combinations of the outputs and their existing derivatives. In the absence of measurement noise, exact estimates are obtained after finite time, which are then again used as auxiliary outputs for further differentiation. This procedure is continued until the complete state space is recovered.

The different methods vary with respect to the applied method of differentiation. The first approaches [72, 73] apply classical first-order sliding mode techniques for successive differentiation. In [74, 75] the concept is extended to the use of second-order sliding mode which doubles the required observer order to $2n$. The method proposed in [50] provides a normal form for LTI MIMO systems, where the successive application of higher-order sliding mode differentiators, e.g. the RED, is straightforward.

However, step-by-step sliding mode observers require bounded state variables. Similar to the previously presented unknown input observers based on direct output differentiation, the applied differentiators require the derivative acting as unknown input to be bounded. As this derivative is a function of $\boldsymbol{x}$, step-by-step sliding mode observers also only provide semi-global stabilization of the estimation error.

4.2.5 Cascaded Unknown Input Observers

The assumption on the boundedness of the state vector required by the aforementioned methods is very restrictive as it excludes their application to unstable systems. Cascaded unknown input observers solve this problem and guarantee global convergence. These observers basically consist of two parts:

1. A stabilizing observer, for instance a linear Luenberger observers as shown in Section 4.2.1, provides state estimates with a bounded estimation error.

2. An RED based observer determines exact estimates of the bounded estimation error of the stabilization observer following the ideas of direct differentiation of the output, see Section 4.2.3.

Since the resulting estimation error of the stabilizing observer convergences into an error band, the derivatives acting as unknown input on the RED based observer are bounded. Hence, boundedness of the system trajectories is not required any more. Different cascaded unknown input observers exist for LTI SISO systems [76], LTI MIMO systems [18–20, 77], linear time-varying systems [78] and nonlinear systems [79].

Example 4.2.5. The cascaded observer proposed in [20] is designed for the system provided in Example 4.2.1. In this design scheme, a linear Luenberger observer as shown in Section 4.2.1 is applied as a stabilizing observer. The eigenvalues of its estimation error dynamics are chosen as

$$\tilde{s}_1 = -1, \quad \tilde{s}_2 = -1.5, \quad \tilde{s}_3 = -2, \quad \tilde{s}_4 = -2.5,$$
$$\tilde{s}_5 = -3, \quad \tilde{s}_6 = -3.5, \quad \tilde{s}_7 = -4,$$

(4.24)

which results in yields the output-injection matrix

$$\boldsymbol{L} = \begin{bmatrix} 97.82 & -291.79 \\ -20.35 & 43.32 \\ 3.84 & 9.66 \\ -1.57 & 9.43 \\ -4 & 13.61 \\ 13.46 & -15.3 \\ -0.092 & 0.33 \end{bmatrix}$$

(4.25)

using the eigenvalue assignment proposed in [52]. As the original system is strongly observable, also the estimation error dynamics

$$\dot{\tilde{\boldsymbol{\eta}}} = (\boldsymbol{A} - \boldsymbol{LC})\tilde{\boldsymbol{\eta}} + \boldsymbol{Dw},$$
$$\tilde{\boldsymbol{\eta}}_y = \boldsymbol{C}\tilde{\boldsymbol{\eta}},$$

(4.26)

are strongly observable, see [20, Equation (31)]. In consequence, the estimation error $\tilde{\boldsymbol{\eta}}$ of the Luenberger observer can be represented by means of the output error $\tilde{\boldsymbol{\eta}}_y$ and its derivatives (if they exist), i.e.,

$$\tilde{\boldsymbol{\eta}} = \tilde{\mathcal{O}}^\dagger \begin{bmatrix} \tilde{\boldsymbol{\eta}}_y \\ \dot{\tilde{\boldsymbol{\eta}}}_y \\ \vdots \\ \tilde{\boldsymbol{\eta}}_y^{(n-1)} \end{bmatrix},$$

(4.27)

where

$$\tilde{\mathcal{O}} = \begin{bmatrix} \boldsymbol{C} \\ \boldsymbol{C}(\boldsymbol{A} - \boldsymbol{LC}) \\ \vdots \\ \boldsymbol{C}(\boldsymbol{A} - \boldsymbol{LC})^{n-1} \end{bmatrix},$$

(4.28)

see Section 2.3.1. In this example, the required left-inverse is given by

$$
\tilde{\mathcal{O}}^{\dagger} =
\begin{bmatrix}
-33.79 & 92.06 & -6.59 & 24.96 & 1.45 & -5.4 & 0.45 & -1.65 & 0 & \dots & 0 \\
1 & 0 & 0 & 0 & 0 & 0 & 0 & 0 & \vdots & & \vdots \\
-4 & 13.61 & 0 & 1 & 0 & 0 & 0 & 0 & \vdots & & \vdots \\
-5.9 & 21.86 & -4.87 & 18.09 & -1.68 & 6.23 & -0.2 & 0.75 & \vdots & & \vdots \\
0 & 1 & 0 & 0 & 0 & 0 & 0 & 0 & \vdots & & \vdots \\
-1.45 & 1.65 & 0.16 & -0.53 & 0.056 & -0.32 & 0.017 & -0.064 & \vdots & & \vdots \\
0.015 & -0.052 & -0.012 & 0.044 & -0.0051 & 0.019 & -0.0016 & 0.0058 & 0 & \dots & 0
\end{bmatrix}.
$$

$$(4.29)$$

Since only the first eight columns are nonzero, only the two outputs themselves and their first three derivatives are required. The calculation of $\tilde{\boldsymbol{\eta}}$ according to (4.27) works only if $\tilde{\boldsymbol{\eta}}_y$ (or rather $\boldsymbol{w}$) is sufficiently often differentiable. To deal also with non-differentiable unknown inputs, the considered method applies linear filtering instead of differentiation in order to get rid of the non-differentiable parts of the signal. The filtered version of (4.27) in Laplace domain in given by

$$
\boldsymbol{\psi}(s) = \frac{1}{\mu(s)} \tilde{\boldsymbol{\eta}}(s) = \tilde{\mathcal{O}}^{\dagger}
\begin{bmatrix}
\frac{1}{\mu(s)} \tilde{\boldsymbol{\eta}}_y(s) \\
\frac{s}{\mu(s)} \tilde{\boldsymbol{\eta}}_y(s) \\
\vdots \\
\frac{s^{n-1}}{\mu(s)} \tilde{\boldsymbol{\eta}}_y(s)
\end{bmatrix},
\tag{4.30}
$$

where $\mu(s)$ is a Hurwitz polynomial of sufficiently high order. Note that $\tilde{\boldsymbol{\eta}}(s)$ and $\tilde{\boldsymbol{\eta}}_y(s)$ denote the Laplace transforms of $\tilde{\boldsymbol{\eta}}(t)$ and $\tilde{\boldsymbol{\eta}}_y(t)$, respectively. Due to the zero columns in $\tilde{\mathcal{O}}^{\dagger}$, only three derivatives need to be estimated in this numerical example and, thus, the third-order choice

$$
\mu(s) = (s + 0.5)^3 = s^3 + 1.5s^2 + 0.75s + 0.125
\tag{4.31}
$$

is sufficient. The resulting third-order filters, one for each component of $\tilde{\boldsymbol{\eta}}_y$, can be efficiently implemented in controllability canonical form, where the state variables correspond to the four outputs of the filter. According to (4.30), $\tilde{\boldsymbol{\eta}}$ is given by

$$
\tilde{\boldsymbol{\eta}}(s) = \mu(s)\boldsymbol{\psi}(s) \overset{(4.31)}{=} s^3\boldsymbol{\psi}(s) + 1.5s^2\boldsymbol{\psi}(s) + 0.75s\boldsymbol{\psi}(s) + 0.125\boldsymbol{\psi}(s).
\tag{4.32}
$$

It becomes apparent that $\tilde{\boldsymbol{\eta}}(t)$ is a linear combination of $\boldsymbol{\psi}(t)$ and its first three derivatives. Hence, $n = 7$ REDs are applied, one for each component of $\boldsymbol{\psi}(t)$ and $\tilde{\boldsymbol{\eta}}$ is calculated according to (4.32). The REDs are tuned according to [29, Section 6.7]. The resulting parameter set is given in Table 4.1.

i	1	2	3	4	5	6	7
$\kappa_{i,3}$	7.35	3.57	2.39	5.58	3.14	3.57	2.39
$\kappa_{i,2}$	24.96	5.88	2.63	14.41	4.56	5.88	2.63
$\kappa_{i,1}$	44.96	5.15	1.54	19.73	3.51	5.15	1.54
$\kappa_{i,0}$	39.6	2.2	0.44	13.2	1.32	2.2	0.44

Table 4.1: *Parameters set for the 7 REDs for the differentiation of $\boldsymbol{\psi}$. The number $i = 1, \ldots, 7$ refers to the respective RED for the differentiation of the i-th component of $\boldsymbol{\psi}$.*

Finally, the estimation error of the Luenberger observer can be corrected by the obtained error estimate. The estimation error $\boldsymbol{\eta}$ of the overall observer is depicted in Figure 4.4.
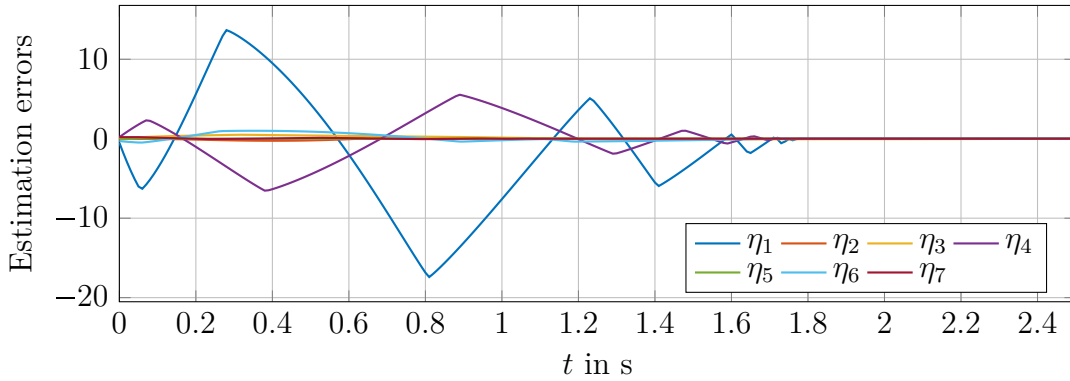
Figure 4.4: *Estimation error variables $\eta_i = x_i - \hat{x}_i$, $i = 1, \ldots, 7$ of the cascaded observer proposed in [20]. The estimation error variables vanish within finite-time despite the unknown input w.*

The estimation error vanishes within approximately 1.8 s despite the unknown input w. The unknown input observer does not diverge in the case of unbounded state variables, and does not require the unknown input to be differentiable at all.

It is pointed out that the overall observer has order 41, as it consists of a Luenberger observer of order 7, the two linear filters each of order 3 and seven REDs each of order 4. Thus, the observer has a substantially higher order than the original system of order $n = 7$. The number of tuning parameters is 45, when considering the components of the matrix $\boldsymbol{L}$ as independent tuning parameters.

The example demonstrates that cascaded unknown input observers require an extensive design procedure. For all previously mentioned cascaded unknown input observers the order and the number of tuning parameters are at least twice the order of the original system. Especially the tuning of these unknown input observers can be cumbersome, since the parameters of the applied REDs depend on the parameters of the stabilizing observer and on the bounds of the unknown inputs.

4.2.6 Unknown Input Observers based on Luenberger's Observability Canonical Form

The main disadvantages of cascaded unknown input observers, i.e., the high system order and the large number of tuning parameters, are avoided by unknown input observers relying on Luenberger's observability canonical form [80, 81]. These methods apply a state transformation $\bar{\boldsymbol{x}} = \boldsymbol{T}\boldsymbol{x}$ and an output transformation $\bar{\boldsymbol{y}} = \boldsymbol{\Gamma}\boldsymbol{y}$ to represent the system in the form

$$
\begin{aligned}
\dot{\bar{\boldsymbol{x}}} &= \bar{\boldsymbol{A}}\bar{\boldsymbol{x}} + \bar{\boldsymbol{D}}\boldsymbol{w}, \\
\bar{\boldsymbol{y}} &= \bar{\boldsymbol{C}}\bar{\boldsymbol{x}},
\end{aligned}
\tag{4.33a}
$$

with the dynamic matrix

$$
\bar{\boldsymbol{A}} =
\left[
\begin{array}{ccccc|c|cccc}
\alpha_{1,1} & 1 & 0 & \cdots & 0 & & \alpha_{p,1} & 0 & \cdots & \cdots & 0 \\
\alpha_{1,2} & 0 & 1 & \ddots & \vdots & & \alpha_{p,2} & \vdots & & & \vdots \\
\vdots & \vdots & \ddots & \ddots & 0 & & \vdots & \vdots & & & \vdots \\
\vdots & \vdots & & \ddots & 1 & & \vdots & \vdots & & & \vdots \\
\alpha_{1,\mu_1} & 0 & \cdots & \cdots & 0 & & \alpha_{p,\mu_1} & 0 & \cdots & \cdots & 0 \\ \hline
\vdots & & & & & \ddots & \vdots & & & & \\ \hline
\alpha_{1,\mu_1+\cdots+\mu_{p-1}+1} & 0 & \cdots & \cdots & 0 & & \alpha_{p,\mu_1+\cdots+\mu_{p-1}+1} & 1 & 0 & \cdots & 0 \\
\alpha_{1,\mu_1+\cdots+\mu_{p-1}+2} & \vdots & & & \vdots & & \vdots & 0 & 1 & \ddots & \vdots \\
\vdots & \vdots & & & \vdots & & \vdots & \vdots & \ddots & \ddots & 0 \\
\vdots & \vdots & & & \vdots & & \vdots & \vdots & & \ddots & 1 \\
\alpha_{1,n} & 0 & \cdots & \cdots & 0 & & \alpha_{p,n} & 0 & \cdots & \cdots & 0
\end{array}
\right]
\tag{4.33b}
$$

$$
\underbrace{\qquad}_{\mu_1} \qquad\qquad \underbrace{\qquad}_{\mu_p}
$$

and the output matrix

$$
\bar{\boldsymbol{C}} =
\left[
\begin{array}{cccc|cccc|c|cccc}
1 & 0 & \cdots & 0 & 0 & \cdots & \cdots & 0 & \cdots & 0 & \cdots & \cdots & 0 \\
0 & \cdots & \cdots & 0 & 1 & 0 & \cdots & 0 & \cdots & 0 & \cdots & \cdots & 0 \\
\vdots & & & & & & & & \ddots & & & & \vdots \\
0 & \cdots & \cdots & 0 & 0 & \cdots & \cdots & 0 & \cdots & 1 & 0 & \cdots & 0
\end{array}
\right].
\tag{4.33c}
$$

$$
\underbrace{\qquad}_{\mu_1} \quad \underbrace{\qquad}_{\mu_2} \quad\quad \underbrace{\qquad}_{\mu_p}
$$

In observability canonical form, the system is decomposed into p coupled single-output systems. The orders μ_j, $j = 1, \ldots, p$, of these subsystems denote the so-called observability indices which satisfy

$$
\sum_{j=1}^{p} \mu_j = n.
\tag{4.33d}
$$

Due to the structure of $\bar{\boldsymbol{C}}$, the coupling coefficients $\alpha_{j,i}$ can be regarded as a linear injection of the output, which makes this form highly convenient for the design of classical observers. It is well-known that an LTI system can be transformed into Luenberger's observability canonical form (4.33) if and only if the system is observable. The

systems under consideration are certainly observable, since the already assumed property of strong observability implies observability. However, the observability canonical form (4.33) does not account for unknown inputs. Hence, $\bar{D}$ will not show a specific structure in general, which would be desirable for the design of unknown input observers. Hence, the unknown input observer proposed in [82, Section 4.5] additionally requires

$$\bar{D} = \begin{bmatrix} \mathbf{0} & \cdots & \mathbf{0} & \bar{d}_1 & \cdots & \mathbf{0} & \cdots & \mathbf{0} & \bar{d}_p \end{bmatrix}^{\mathrm{T}} \tag{4.34a}$$

in order to provide exact estimates of the state vector. Accordingly, the relative degree δ_j of each output $\bar{y}_j$ of $\bar{y} = \begin{bmatrix} \bar{y}_1 & \ldots & \bar{y}_p \end{bmatrix}^{\mathrm{T}}$, if it exists, must be greater than or equal to the respective observability index μ_j, i.e.,

$$\delta_j \geqslant \mu_j \qquad \forall j = 1, \ldots, p. \tag{4.34b}$$

It is pointed out that this assumption strongly restricts the system class, as strongly observable systems in general do not satisfy this condition on the output relative degree. The same holds for the unknown input observer for linear time-varying systems presented in [83] which coincides with the one proposed in [82] in the LTI case.

The unknown input observer in observability canonical form is given by

$$\dot{\hat{\bar{x}}} = \bar{A}\hat{\bar{x}} + \bar{\Pi}\sigma_{\bar{y}} + \bar{l}(\sigma_{\bar{y}}), \tag{4.35a}$$

where

$$\sigma_{\bar{y}} = \bar{y} - \bar{C}\hat{\bar{x}} = \begin{bmatrix} \sigma_1 & \sigma_{\mu_1+1} & \ldots & \sigma_{\mu_1+\cdots+\mu_{p-1}+1} \end{bmatrix}^{\mathrm{T}} \tag{4.35b}$$

denotes the error of the estimated output,

$$\bar{\Pi} = \begin{bmatrix} \alpha_{1,1} & \cdots & \alpha_{p,1} \\ \vdots & & \vdots \\ \alpha_{1,n} & \cdots & \alpha_{p,n} \end{bmatrix} \tag{4.35c}$$

is the linear output-injection matrix accounting for the coupling coefficients and

$$\bar{l}(\sigma_{\bar{y}}) = \begin{bmatrix} \kappa_{1,\mu_1-1}\lfloor\sigma_1\rceil^{\frac{\mu_1-1}{\mu_1}} \\ \vdots \\ \kappa_{1,1}\lfloor\sigma_1\rceil^{\frac{1}{\mu_1}} \\ \kappa_{1,0}\lfloor\sigma_1\rceil^0 \\ \hline \vdots \\ \hline \kappa_{p,\mu_p-1}\lfloor\sigma_{\mu_1+\cdots+\mu_{p-1}+1}\rceil^{\frac{\mu_p-1}{\mu_p}} \\ \vdots \\ \kappa_{p,0}\lfloor\sigma_{\mu_1+\cdots+\mu_{p-1}+1}\rceil^0 \end{bmatrix} \tag{4.35d}$$

is the nonlinear output injection applying an RED to each subsystem. The dynamics of the estimation error

$$\sigma = \bar{x} - \hat{\bar{x}} = \begin{bmatrix} \sigma_1 & \ldots & \sigma_n \end{bmatrix}^{\mathrm{T}} \tag{4.36}$$

of the j-th subsystem under the relative degree assumption (4.34) are given by

$$
\begin{aligned}
\dot{\sigma}_{\mu_1+\cdots+\mu_{j-1}+1} &= \sigma_{\mu_1+\cdots+\mu_{j-1}+2} - \kappa_{j,\mu_j-1}\lfloor\sigma_{\mu_1+\cdots+\mu_{j-1}+1}\rceil^{\frac{\mu_j-1}{\mu_j}}, \\
&\vdots \\
\dot{\sigma}_{\mu_1+\cdots+\mu_j-1} &= \sigma_{\mu_1+\cdots+\mu_j} - \kappa_{j,1}\lfloor\sigma_{\mu_1+\cdots+\mu_{j-1}+1}\rceil^{\frac{1}{\mu_j}}, \\
\dot{\sigma}_{\mu_1+\cdots+\mu_j} &= \bar{\boldsymbol{d}}_j^{\mathrm{T}}\boldsymbol{w} - \kappa_{j,0}\lfloor\sigma_{\mu_1+\cdots+\mu_{j-1}+1}\rceil^0.
\end{aligned}
\tag{4.37}
$$

It becomes apparent that (4.37) coincides with the estimation error dynamics of an RED with unknown input $\bar{\boldsymbol{d}}_j^{\mathrm{T}}\boldsymbol{w}$, see Section 3.2. Since the single components of $\boldsymbol{w}$ are bounded, also their linear combination $\bar{\boldsymbol{d}}_j^{\mathrm{T}}\boldsymbol{w}$ is bounded. Hence, there exist parameters $\kappa_{j,0}, \kappa_{j,1}, \ldots, \kappa_{j,\mu_j-1}$ such that the errors converge to zero in finite time. This holds for all subsystems and, thus, the overall observer converges within finite time despite the unknown input $\boldsymbol{w}$.

Example 4.2.6. For the system given in Example 4.2.1, the transformation into Luenberger's observability canonical form yields the matrices

$$
\bar{\boldsymbol{A}} = \left[\begin{array}{cccc|ccc}
-23.98 & 1 & 0 & 0 & 0 & 0 & 0 \\
-235.42 & 0 & 1 & 0 & 570.04 & 0 & 0 \\
-2066.29 & 0 & 0 & 1 & 3004.45 & 0 & 0 \\
-6972.9 & 0 & 0 & 0 & 0 & 0 & 0 \\
\hline
0.83 & 0 & 0 & 0 & -0.26 & 1 & 0 \\
-9.21 & 0 & 0 & 0 & 32.73 & 0 & 1 \\
-75.75 & 0 & 0 & 0 & 0 & 0 & 0
\end{array}\right], \bar{\boldsymbol{D}} = \left[\begin{array}{c}
0 \\
0 \\
\colorbox{red}{-701.7} \\
-4313.16 \\
\hline
0 \\
0 \\
-46.99
\end{array}\right], \bar{\boldsymbol{C}} = \left[\begin{array}{cc}
1 & 0 \\
0 & 0 \\
0 & 0 \\
0 & 0 \\
0 & 1 \\
0 & 0 \\
0 & 0
\end{array}\right]^{\mathrm{T}}.
\tag{4.38}
$$

The system is decomposed into $p = 2$ coupled single-output systems. The observability indices are $\mu_1 = 4$ and $\mu_2 = 3$, whereas the output relative degrees are $\delta_1 = \delta_2 = 3$. Since $\delta_1 \ngeq \mu_1$, the relative degree condition (4.34) is violated. The unknown input directly affects the third differential equation of the first subsystem, which is indicated by the highlighted element of $\bar{\boldsymbol{D}}$. This impact can not be compensated for by the respective RED and, thus, the unknown input observer will not able to exactly reconstruct the states.

In order to demonstrate this behaviour, an unknown input observer of the form (4.35) is constructed. The output-injection matrix is given by

$$
\bar{\boldsymbol{\Pi}} = \left[\begin{array}{cc}
-23.98 & 0 \\
-235.42 & 570.04 \\
-2066.29 & 3004.45 \\
-6972.9 & 0 \\
0.83 & -0.26 \\
-9.21 & 32.73 \\
-75.75 & 0
\end{array}\right].
\tag{4.39}
$$

The parameters of the nonlinear output injection

$$\kappa_{1,3} = 17.84, \quad \kappa_{1,2} = 147.14, \quad \kappa_{1,1} = 643.56, \quad \kappa_{1,0} = 1376.1,$$
$$\kappa_{2,2} = 6.7, \quad \kappa_{2,1} = 23.81, \quad \kappa_{2,0} = 41.36, \tag{4.40}$$

are chosen according to [29, Section 6.7]. The estimation error variables are shown in Figure 4.5.
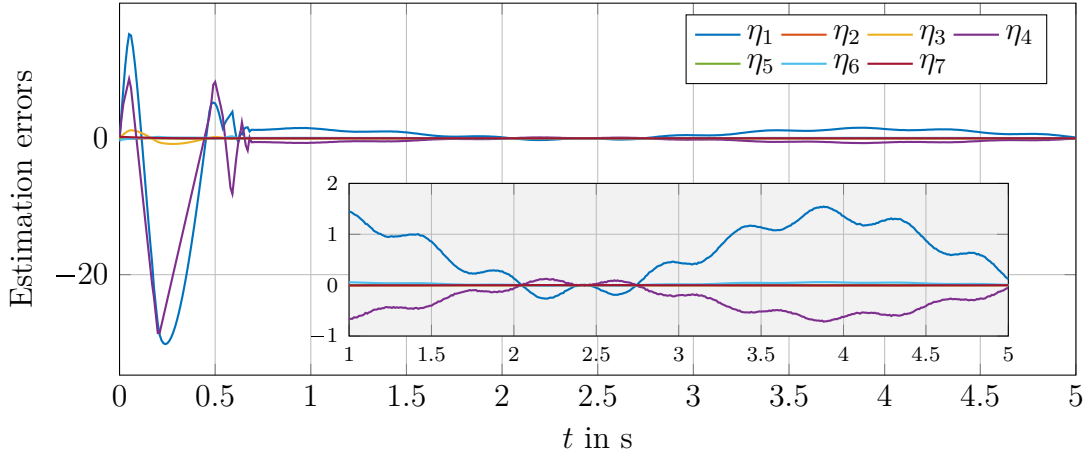
Figure 4.5: *Estimation error variables $\eta_i = x_i - \hat{x}_i$, $i = 1, \ldots, 7$ of the unknown input observer designed in Luenberger's observability canonical form. The method is not able to provide exact estimates, since the consiered system does not satisfy the relative degree condition (4.34).*

The estimation error converges into a vicinity around the origin. However, as the relative degree condition (4.34) is violated, the observer is not capable of providing exact estimates of the state variables in the presence of w.

Unlike the cascaded unknown input observer, the unknown input observer based on Luenberger's canonical form does neither increase the observer order nor the number of tuning parameters beyond the order of the original system. Once the system is in canonical form, the unknown input observer design is straightforward. Furthermore, neither the observer matching condition nor the differentiability of the unknown input nor the boundedness of some certain output derivatives are required. However, exact estimates of the state vector are provided only if the system satisfies an additional restrictive condition.

4.3 Conclusions on the presented State Of The Art

Table 4.2 summarizes the advantages and disadvantages of the previously discussed classes of unknown input observers. In addition to those, there exist a few other approaches such as the adaptive sliding mode observer proposed in [84] that requires bounded state variables. The unknown input observer [85] exhibits some zero dynamics

which might be unstable and also requires bounded state variables. It can be concluded that all available unknown input observers suffer from at least one of the following drawbacks:

(a) The system must satisfy the restrictive observer matching condition (4.15), i.e., the strongly observable system has to be strong* detectable additionally.

(b) Bounded state variables are required for convergence of the observer.

(c) The unknown input must be sufficiently often differentiable.

(d) The choice of the observer parameters depends also on the system trajectory and not on the unknown input only.

(e) The observer order and the number of tuning parameters are at least twice the system order which significantly complicates the design and the tuning.

(f) Exact estimates are obtained only if the system satisfies a restrictive condition (4.34) on the output relative degree.

This research gap motivates for the design of a new unknown input observer presented in the next chapters.

Class	Literature	Providing exact estimates	Observer matching condition (4.15) not required	Bounded state variables not required	Unknown input not required differentiable	Observer parameters independent of system trajectory	Not increasing observer order and number of observer parameters	Restrictive relative degree condition (4.34) not required
Luenberger observer (Section 4.2.1)	[7]	✗	✓	✓	✓	✓	✓	✓
Linear unknown input observers (Section 4.2.2)	[10, 56–61]	✓	✗	✓	✓	✓	✓	✓
First-order sliding mode observers (Section 4.2.2)	[63–65]	✓	✗	✓	✓	✓	✓	✓
Direct output differentiation (Section 4.2.3)	[67–71]	✓	✓	✗	✗	✗	✓	✓/✗
Step-by-step sliding mode observers (Section 4.2.4)	[50, 72–75]	✓	✓	✗	✓	✗	✓/✗	✓
Cascaded unknown input observers (Section 4.2.5)	[18–20, 77–79]	✓	✓	✓	✓	✓	✗	✓
Unknown input observers based on Luenberger's observability canonical form (Section 4.2.6)	[82, 83]	✓	✓	✓	✓	✓	✓	✗

Table 4.2: Advantages (✓) and disadvantages (✗) of classes of existing unknown input observers. In the case both marks (✓/✗) are present the particular property is satisfied for some and not satisfied for some other unknown input observers within the considered class.

5

Unknown Input Observer Design for Linear Time-Invariant Systems – The Single-Input Single-Output Case

The aim of this thesis is to overcome all the disadvantages of existing unknown input observers which are summarized in Section 4.3. In this chapter, the SISO case is considered in order to obtain useful insights and ideas for the more complex MIMO case. A new unknown input observer is proposed that relies on the classical observability canonical form. The observer's output injection can be calculated by means of an elegant formula, the main contribution, which can be regarded as a nonlinear generalization of Ackermann's formula. A numerical example demonstrates the simplicity of the design procedure as well as the effectiveness of the unknown input observer.

This chapter is essentially based on:

H. Niederwieser, S. Koch, M. Reichhartinger, A generalization of Ackermann's formula for the design of continuous and discontinuous observers, in: 2019 IEEE 58th Conference on Decision and Control (CDC), IEEE, 2019, pp. 6930–6935. `doi:10.1109/CDC40024.2019.9030192`

5.1 Basic Structure of the Unknown Input Observer

Consider the LTI SISO system

$$\dot{\boldsymbol{x}} = \boldsymbol{A}\boldsymbol{x} + \boldsymbol{d}w,$$
$$y = \boldsymbol{c}^{\mathrm{T}}\boldsymbol{x}, \tag{5.1}$$

where the unknown input $w \in \mathbb{R}$ as well as the output $y \in \mathbb{R}$ are scalar, i.e., $m = p = 1$ and $\boldsymbol{c} \in \mathbb{R}^{n \times 1}$, $\boldsymbol{d} \in \mathbb{R}^{n \times 1}$. The aim is to design an unknown input observer according to the problem statement provided in Section 4.1. Therein, the system is assumed strongly observable and the unknown input is assumed to be bounded by a constant

L, i.e.,

$$|w(t)| \leqslant L \quad \forall t, \qquad \text{with} \quad 0 \leqslant L < \infty. \tag{5.2}$$

The unknown input observer proposed in this chapter has the structure

$$\dot{\hat{x}} = A\hat{x} + l(\sigma_1),$$
$$\hat{y} = c^{\mathrm{T}}\hat{x}. \tag{5.3a}$$

It consists of a copy of the known parts of the plant dynamics (5.1) and the output error injection

$$l(\sigma_1) = \begin{bmatrix} l_1(\sigma_1) & l_2(\sigma_1) & \dots & l_n(\sigma_1) \end{bmatrix}^{\mathrm{T}}, \tag{5.3b}$$

where $\sigma_1 = y - \hat{y}$ denotes the output error. The question remains how $l(\sigma_1)$ should be selected.

5.2 Representation of Strongly Observable Systems in Observability Canonical Form

For the SISO case the classical observability canonical form, see e.g. [87, 88], will prove to be a suitable system representation for the design of an unknown input observer. For this purpose, a regular state transformation

$$\bar{x} = T^{-1}x \tag{5.4a}$$

is applied, where the transformation matrix is given by

$$T = \begin{bmatrix} A^{n-1}t_n & A^{n-2}t_n & \dots & At_n & t_n \end{bmatrix}, \tag{5.4b}$$

where

$$t_n = \mathcal{O}^{-1}e_n \tag{5.4c}$$

is the last column of the inverse observability matrix. It is pointed out that the existence and the invertibility of T is ensured, as strong observability implies classical observability. The dynamics of system (5.1) in observability canonical form are given by

$$\dot{\bar{x}} = \bar{A}\bar{x} + \bar{d}w,$$
$$y = \bar{c}^{\mathrm{T}}\bar{x}, \tag{5.5a}$$

where the dynamic matrix

$$\bar{A} = T^{-1}AT = \begin{bmatrix} -\alpha_{n-1} & 1 & 0 & \dots & 0 \\ -\alpha_{n-2} & 0 & 1 & \ddots & \vdots \\ \vdots & \vdots & \ddots & \ddots & 0 \\ -\alpha_1 & 0 & & \ddots & 1 \\ -\alpha_0 & 0 & \dots & \dots & 0 \end{bmatrix} \tag{5.5b}$$

contains the coefficients $\alpha_0, \alpha_1, \ldots, \alpha_{n-1}$ of the characteristic polynomial of $\boldsymbol{A}$,

$$\bar{\boldsymbol{c}}^{\mathrm{T}} = \boldsymbol{c}^{\mathrm{T}}\boldsymbol{T} = \boldsymbol{e}_1^{\mathrm{T}} = \begin{bmatrix} 1 & 0 & \ldots & 0 \end{bmatrix} \tag{5.5c}$$

and

$$\bar{\boldsymbol{d}} = \boldsymbol{T}^{-1}\boldsymbol{d}. \tag{5.5d}$$

The unknown-input vector $\bar{\boldsymbol{d}}$ determines how the unknown input affects the system and, hence, its particular structure is examined in

Lemma 5.2.1. *Consider system (5.1) and the transformation (5.4) into observability canonical form (5.5). If system (5.1) is strongly observable, then the unknown-input vector in observability canonical form is given by*

$$\bar{\boldsymbol{d}} = \begin{bmatrix} 0 \\ \vdots \\ 0 \\ \boldsymbol{c}^{\mathrm{T}}\boldsymbol{A}^{n-1}\boldsymbol{d} \end{bmatrix}. \tag{5.6}$$

Proof. Insertion of the identity matrix $\boldsymbol{\mathcal{O}}^{-1}\boldsymbol{\mathcal{O}}$ into (5.5d) yields

$$\bar{\boldsymbol{d}} = \boldsymbol{T}^{-1}\boldsymbol{\mathcal{O}}^{-1}\boldsymbol{\mathcal{O}}\boldsymbol{d}. \tag{5.7}$$

Since the system is strongly observable, it satisfies the relative degree condition

$$\boldsymbol{\mathcal{O}}\boldsymbol{d} = \begin{bmatrix} 0 \\ \vdots \\ 0 \\ \boldsymbol{c}^{\mathrm{T}}\boldsymbol{A}^{n-1}\boldsymbol{d} \end{bmatrix} = \boldsymbol{e}_n\boldsymbol{c}^{\mathrm{T}}\boldsymbol{A}^{n-1}\boldsymbol{d} \tag{5.8}$$

as demonstrated in Section 2.3.2. Insertion into (5.7) yields

$$\bar{\boldsymbol{d}} = \boldsymbol{T}^{-1}\boldsymbol{\mathcal{O}}^{-1}\boldsymbol{e}_n\boldsymbol{c}^{\mathrm{T}}\boldsymbol{A}^{n-1}\boldsymbol{d}. \tag{5.9}$$

Substituting $\boldsymbol{\mathcal{O}}^{-1}\boldsymbol{e}_n$ according to (5.4c) leads to

$$\bar{\boldsymbol{d}} = \boldsymbol{T}^{-1}\boldsymbol{t}_n\boldsymbol{c}^{\mathrm{T}}\boldsymbol{A}^{n-1}\boldsymbol{d}. \tag{5.10}$$

The vector $\boldsymbol{t}_n$ is the last column of the transformation matrix (5.4b), i.e.,

$$\boldsymbol{t}_n = \boldsymbol{T}\boldsymbol{e}_n, \tag{5.11}$$

which simplifies (5.10) to the relation

$$\bar{\boldsymbol{d}} = \boldsymbol{e}_n\boldsymbol{c}^{\mathrm{T}}\boldsymbol{A}^{n-1}\boldsymbol{d} = \begin{bmatrix} 0 \\ \vdots \\ 0 \\ \boldsymbol{c}^{\mathrm{T}}\boldsymbol{A}^{n-1}\boldsymbol{d} \end{bmatrix} \tag{5.12}$$

which was to be proven. $\square$

From Lemma 5.2.1 it follows that the unknown input has a direct impact only on the last differential equation of the system represented in observability canonical form. Moreover, (5.12) provides a useful representation of the nonzero coefficient of $\bar{\boldsymbol{d}}$ by means of the dynamic matrix, the input vector and output vector of the system in original coordinates.

Due to the structure of $\bar{\boldsymbol{c}}$, the coefficients $\alpha_0, \ldots, \alpha_{n-1}$ of $\bar{\boldsymbol{A}}$ can be regarded as an output injection. The remaining part of the system is a chain of n integrators with unknown input $\boldsymbol{c}^{\mathrm{T}} \boldsymbol{A}^{n-1} \boldsymbol{d} w$ and output y, i.e., exactly the structure suitable for the application of differentiators as unknown input observers.

5.3 Unknown Input Observer Design in Observability Canonical Form

The previously discussed representation of the system in observability canonical form is exploited in the design of the unknown input observer. For this purpose, the unknown input observer (5.3) is also considered in observability canonical form, i.e., the state transformation

$$\hat{\bar{\boldsymbol{x}}} = \boldsymbol{T}^{-1}\hat{\boldsymbol{x}} \tag{5.13}$$

is applied which yields

$$\begin{aligned} \dot{\hat{\bar{\boldsymbol{x}}}} &= \bar{\boldsymbol{A}}\hat{\bar{\boldsymbol{x}}} + \bar{\boldsymbol{l}}(\sigma_1), \\ \hat{y} &= \bar{\boldsymbol{c}}^{\mathrm{T}}\hat{\bar{\boldsymbol{x}}}, \end{aligned} \tag{5.14}$$

with the output error injection

$$\bar{\boldsymbol{l}}(\sigma_1) = \boldsymbol{T}^{-1}\boldsymbol{l}(\sigma_1). \tag{5.15}$$

A particular choice of $\bar{\boldsymbol{l}}(\sigma_1)$ is provided in

Lemma 5.3.1. *Consider the unknown input observer* (5.14) *with the choice*

$$\bar{\boldsymbol{l}}(\sigma_1) = \begin{bmatrix} -\alpha_{n-1} \\ -\alpha_{n-2} \\ \vdots \\ -\alpha_0 \end{bmatrix} \sigma_1 + \begin{bmatrix} \kappa_{n-1}\lfloor\sigma_1\rceil^{\frac{r_2}{r_1}} \\ \kappa_{n-2}\lfloor\sigma_1\rceil^{\frac{r_3}{r_1}} \\ \vdots \\ \kappa_0\lfloor\sigma_1\rceil^{\frac{r_{n+1}}{r_1}} \end{bmatrix} \tag{5.16}$$

and constants

$$r_i = 1 - (n-i)q, \qquad i = 1, \ldots, n, \tag{5.17}$$

for the estimation of the state vector $\bar{\boldsymbol{x}}$ of the strongly observable system (5.5) *represented in observability canonical form.*

(i) If $w = 0 \quad \forall t \geqslant 0$, then for each $q \in [-1, 0]$ there exist parameters $\kappa_0, \kappa_1, \ldots, \kappa_{n-1}$ such that the estimation error variables $\sigma_i = \bar{x}_i - \hat{\bar{x}}_i$ with

$i = 1, \ldots, n$ *converge to zero globally. In the case $q = 0$ the convergence is exponential, i.e., for all initial states $\sigma_i(0)$ there exist constants $K > 0$ and $\gamma > 0$ such that $|\sigma_i| < Ke^{-\gamma t}$ $\forall t$. In the case $-1 \leqslant q < 0$ the estimation error variables σ_i vanish within a finite time, i.e., for all initial states there exists a finite time $T \geqslant 0$ such that $\sigma_i(t) = 0$ $\forall t \geqslant T$.*

(ii) If $q = -1$ and w is bounded, i.e., $|w(t)| \leqslant L$ $\forall t \geqslant 0$ with $0 \leqslant L < \infty$, then there exist parameters $\kappa_0, \kappa_1, \ldots, \kappa_{n-1}$ such that the estimation error variables converge to zero within finite time despite w, i.e., for all initial states there exists a finite time $T \geqslant 0$ such that $\sigma_i(t) = 0$ $\forall t \geqslant T$. Moreover, convergence for all admissible unknown inputs $w(t)$ is achieved only if $\kappa_0 > L\left|\boldsymbol{c}^{\mathrm{T}}\boldsymbol{A}^{n-1}\boldsymbol{d}\right|$.

Proof. Definition of the estimation error

$$\boldsymbol{\sigma} = \bar{\boldsymbol{x}} - \hat{\boldsymbol{x}} = \begin{bmatrix} \sigma_1 & \ldots & \sigma_n \end{bmatrix}^{\mathrm{T}} \tag{5.18}$$

and the application of Lemma 5.2.1 yields the estimation error dynamics

$$
\begin{aligned}
\dot{\sigma}_1 &= \sigma_2 - \kappa_{n-1}\lfloor\sigma_1\rceil^{\frac{r_2}{r_1}}, \\
\dot{\sigma}_2 &= \sigma_3 - \kappa_{n-2}\lfloor\sigma_1\rceil^{\frac{r_3}{r_1}}, \\
&\;\;\vdots \\
\dot{\sigma}_n &= -\kappa_0\lfloor\sigma_1\rceil^{\frac{r_{n+1}}{r_1}} + \boldsymbol{c}^{\mathrm{T}}\boldsymbol{A}^{n-1}\boldsymbol{d}w.
\end{aligned}
\tag{5.19}
$$

These dynamics coincide with the estimation error dynamics of the homogeneous differentiators, where $\boldsymbol{c}^{\mathrm{T}}\boldsymbol{A}^{n-1}\boldsymbol{d}w$ acts as unknown input, see Section 3.2. Hence, the results of Proposition 3.2.1 apply which completes the proof. $\square$

At this point, the unknown input observer (5.14) with the choice of $\bar{\boldsymbol{l}}(\sigma_1)$ given in (5.16) can already be implemented. Estimates of the original state vector $\boldsymbol{x}$ can be obtained by inverting the state transformation (5.13). It may be desirable, however, to directly implement the observer in original coordinates which is shown in the next section.

5.4 A Nonlinear Generalization of Ackermann's Formula

In order to express the unknown input observer in original coordinates, see e.g. (5.3), $\boldsymbol{l}(\sigma_1)$ is calculated by using (5.15). The resulting formula, which constitutes the main contribution of this thesis to the SISO case, is presented in

Theorem 5.4.1. *Consider the unknown input observer (5.3) for the estimation of the state vector $\boldsymbol{x}$ of the strongly observable system (5.1). Suppose the output error injection*

$$\boldsymbol{l}(\sigma_1) = \sigma_1\chi(\boldsymbol{A}, \sigma_1)\boldsymbol{t}_n \tag{5.20a}$$

with the output error dependent matrix polynomial

$$\chi(\boldsymbol{A}, \sigma_1) = \boldsymbol{A}^n + \sum_{i=1}^{n} \kappa_{n-i} |\sigma_1|^{\frac{i \cdot q}{1-(n-1)q}} \boldsymbol{A}^{n-i} \tag{5.20b}$$

and $\boldsymbol{t}_n$ denoting the last column of the inverse observability matrix, see (5.4c).

(i) If $w = 0$ $\forall t \geqslant 0$, then for each $q \in [-1, 0]$ there exist parameters $\kappa_0, \kappa_1, \ldots, \kappa_{n-1}$ such that the estimation error variables $\eta_i = x_i - \hat{x}_i$ with $i = 1, \ldots, n$ converge to zero globally. In the case $q = 0$ the convergence is exponential, i.e., for all initial states $\eta_i(0)$ there exist constants $K > 0$ and $\gamma > 0$ such that $|\eta_i| < K e^{-\gamma t}$ $\forall t$. In the case $-1 \leqslant q < 0$ the estimation error variables η_i vanish within a finite time, i.e., for all initial states there exists a finite time $T \geqslant 0$ such that $\eta_i(t) = 0$ $\forall t \geqslant T$.

(ii) If $q = -1$ and w is bounded, i.e., $|w(t)| \leqslant L$ $\forall t \geqslant 0$ with $0 \leqslant 0 < \infty$, then there exist parameters $\kappa_0, \kappa_1, \ldots, \kappa_{n-1}$ such that the estimation error variables converge to zero within finite time despite w, i.e., for all initial states there exists a finite time $T \geqslant 0$ such that $\eta_i(t) = 0$ $\forall t \geqslant T$. Moreover, convergence for all admissible unknown inputs $w(t)$ is achieved only if $\kappa_0 > L |\boldsymbol{c}^{\mathrm{T}} \boldsymbol{A}^{n-1} \boldsymbol{d}|$.

Proof. As the considered system is strongly observable, the existence of an invertible transformation into observability canonical form is guaranteed. Since the estimation error $\boldsymbol{\eta} = \boldsymbol{x} - \hat{\boldsymbol{x}} = \begin{bmatrix} \eta_1 & \ldots & \eta_n \end{bmatrix}^{\mathrm{T}}$ is related to the estimation error $\boldsymbol{\sigma}$ by

$$\boldsymbol{\eta} = \boldsymbol{T} \boldsymbol{\sigma}, \tag{5.21}$$

and $\boldsymbol{T}$ is invertible, $\boldsymbol{\sigma} = \boldsymbol{0}$ implies $\boldsymbol{\eta} = \boldsymbol{0}$ and vice versa, i.e., the estimation error $\boldsymbol{\eta}$ vanishes if and only if $\boldsymbol{\sigma}$ vanishes. Therefore, it is sufficient to prove that $\boldsymbol{l}(\sigma_1) \overset{(5.15)}{=} \boldsymbol{T} \bar{\boldsymbol{l}}(\sigma_1)$ is satisfied in order to show that the results of Lemma 5.3.1 also apply to the observer in original coordinates $\boldsymbol{x}$. According to (5.15) and (5.16), $\boldsymbol{l}(\sigma_1)$ is given by

$$\boldsymbol{l}(\sigma_1) = \boldsymbol{T} \bar{\boldsymbol{l}}(\sigma_1) = \boldsymbol{T} \left(\begin{bmatrix} -\alpha_{n-1} \\ -\alpha_{n-2} \\ \vdots \\ -\alpha_0 \end{bmatrix} \sigma_1 + \begin{bmatrix} \kappa_{n-1} \lfloor \sigma_1 \rceil^{\frac{r_2}{r_1}} \\ \kappa_{n-2} \lfloor \sigma_1 \rceil^{\frac{r_3}{r_1}} \\ \vdots \\ \kappa_0 \lfloor \sigma_1 \rceil^{\frac{r_n+1}{r_1}} \end{bmatrix} \right). \tag{5.22}$$

Insertion of the definition of $\boldsymbol{T}$ yields

$$\boldsymbol{l}(\sigma_1) \overset{(5.4b)}{=} \begin{bmatrix} \boldsymbol{A}^{n-1} \boldsymbol{t}_n & \ldots & \boldsymbol{A} \boldsymbol{t}_n & \boldsymbol{t}_n \end{bmatrix} \left(\begin{bmatrix} -\alpha_{n-1} \\ -\alpha_{n-2} \\ \vdots \\ -\alpha_0 \end{bmatrix} \sigma_1 + \begin{bmatrix} \kappa_{n-1} \lfloor \sigma_1 \rceil^{\frac{r_2}{r_1}} \\ \kappa_{n-2} \lfloor \sigma_1 \rceil^{\frac{r_3}{r_1}} \\ \vdots \\ \kappa_0 \lfloor \sigma_1 \rceil^{\frac{r_n+1}{r_1}} \end{bmatrix} \right) = \tag{5.23}$$

$$= -\sigma_1 \sum_{i=1}^{n} \alpha_{n-i} \boldsymbol{A}^{n-i} \boldsymbol{t}_n + \sum_{i=1}^{n} \kappa_{n-i} \lfloor \sigma_1 \rceil^{\frac{r_{i+1}}{r_1}} \boldsymbol{A}^{n-i} \boldsymbol{t}_n.$$

Exploiting the theorem of Caley-Hamilton[1]

$$\boldsymbol{A}^n = -\sum_{i=1}^{n} \alpha_{n-i} \boldsymbol{A}^{n-i},$$ (5.24)

see e.g. [15], and substitution of the constants r_i according to (5.17) finally yields the desired relation

$$\boldsymbol{l}(\sigma_1) = \sigma_1 \boldsymbol{A}^n \boldsymbol{t}_n + \sum_{i=1}^{n} \kappa_{n-i} \lceil \sigma_1 \rceil^{\frac{1-(n-i-1)q}{1-(n-1)q}} \boldsymbol{A}^{n-i} \boldsymbol{t}_n =$$

$$= \sigma_1 \underbrace{\left(\boldsymbol{A}^n + \sum_{i=1}^{n} \kappa_{n-i} |\sigma_1|^{\frac{iq}{1-(n-1)q}} \boldsymbol{A}^{n-i} \right)}_{\chi(\boldsymbol{A},\sigma_1)} \boldsymbol{t}_n,$$ (5.25)

which completes the proof. $\qquad\qquad\qquad\qquad\qquad\qquad\qquad\qquad\qquad$ $\square$

The "one-step" design procedure represented in (5.20) in Theorem 5.4.1 can be regarded as a nonlinear generalization of Ackermann's formula [89], where the well-known linear case is obtained for $q = 0$. The estimation error dynamics are transformable into a particular representation which coincides with the estimation error dynamics of a family of homogenous differentiators, see Section 3.2. For $q = 0$ the approach matches with the construction of a linear Luenberger observer using Ackermann's eigenvalue assignment, where $\kappa_0, \kappa_1, \ldots, \kappa_{n-1}$ are the coefficients of the desired characteristic polynomial of the estimation error dynamics, i.e.,

$$w(s) = s^n + \kappa_{n-1} s^{n-1} + \cdots + \kappa_1 s + \kappa_0.$$ (5.26)

For $q = -1$ a nonlinear discontinuous observer is obtained, where the parameters $\kappa_0, \kappa_1, \ldots, \kappa_{n-1}$ correspond to the gains of an RED. The choice $-1 < q < 0$ yields a nonlinear but continuous observer.

In the nonlinear case the proposed formula can be understood as the assignment of state-dependent eigenvalues $s_i(\sigma_1) = p_i |\sigma_1|^{\frac{q}{1-(n-1)q}}$ with $p_i \in \mathbb{C}$ to the estimation error dynamics. The related concept of homogeneous eigenvalues [90–92] provides necessary stability criteria for $w = 0$ which are also sufficient for $n \leqslant 2$.

5.5 Application to a Numerical Example

The application of the proposed unknown input observer is demonstrated with the help of a numerical example.

---

[1]The theorem of Caley-Hamilton states that a square matrix $\boldsymbol{A} \in \mathbb{R}^{n \times n}$ satisfies its own characteristic equation $\Delta(s) = s^n + \alpha_{n-1} s^{n-1} + \cdots + \alpha_1 s + \alpha_0 = 0$, i.e., $\Delta(\boldsymbol{A}) = \boldsymbol{0}_{n \times n}$.

Example 5.5.1. Consider system (5.1) with

$$
\boldsymbol{A} = \begin{bmatrix} 0 & 1 & 0 & 0 \\ 0 & 0 & 1 & 0 \\ 0 & 0 & 0 & 1 \\ 6 & 5 & -5 & -5 \end{bmatrix}, \quad \boldsymbol{d} = \begin{bmatrix} 0 \\ 0 \\ 0 \\ 1 \end{bmatrix},
$$
$$
\boldsymbol{c}^{\mathrm{T}} = \begin{bmatrix} 1 & 0 & 0 & 0 \end{bmatrix}
$$

(5.27)

and the unknown input

$$
w(t) = \cos(0.5t) + 0.5\sin(t) + 0.5.
$$

(5.28)

This example is taken from [29, Section 7.2.3], where the application of a cascaded unknown input observer is demonstrated. Note that this system does not fulfill the observer matching condition as $\boldsymbol{c}^{\mathrm{T}}\boldsymbol{d} = 0$. The system is strongly observable and is represented in controllable canonical form, where the output corresponds to the first state variable. In this case, the state variables correspond directly to the output and its derivatives. Since the matrix $\boldsymbol{A}$ has one positive eigenvalue located at $s_i = 1$, the state variables are unbounded and, consequently, the RED cannot be used to directly differentiate the output. In contrast, and as stated in Theorem 5.4.1, the proposed observer with $q = -1$ is expected to achieve global finite-time convergence of the estimation errors despite the unbounded state variables and the unknown input. In this particular example the unknown input is bounded by $L = 2$ and $\boldsymbol{c}^{\mathrm{T}}\boldsymbol{A}^{n-1}\boldsymbol{d} = 1$. Calculating the parameters according to [29, Section 6.7] yields $\kappa_0 = 2.2$, $\kappa_1 = 7.5$, $\kappa_2 = 12.5$ and $\kappa_3 = 6$ and, thus, the necessary condition

$$
\kappa_0 = 2.2 > L\left|\boldsymbol{c}^{\mathrm{T}}\boldsymbol{A}^{n-1}\boldsymbol{d}\right| = 2
$$

(5.29)

given in Theorem 5.4.1(ii) is satisfied. The output error injection

$$
\boldsymbol{l}(\sigma_1) = \begin{bmatrix} -5 \\ 20 \\ -70 \\ 231 \end{bmatrix} \sigma_1 + \begin{bmatrix} 6 \\ -30 \\ 120 \\ -420 \end{bmatrix} \lfloor\sigma_1\rceil^{\frac{3}{4}} + \begin{bmatrix} 0 \\ 12.5 \\ 62.5 \\ 250 \end{bmatrix} \lfloor\sigma_1\rceil^{\frac{1}{2}}
$$
$$
+ \begin{bmatrix} 0 \\ 0 \\ 15 \\ -75 \end{bmatrix} \lfloor\sigma_1\rceil^{\frac{1}{4}} + \begin{bmatrix} 0 \\ 0 \\ 0 \\ 2.2 \end{bmatrix} \lfloor\sigma_1\rceil^{0}
$$

(5.30)

calculated according to (5.20) consists of linear combinations of some nonlinear functions of the output error σ_1. In the following simulation, the initial state vectors are selected as $\boldsymbol{x}(0) = \begin{bmatrix} 1 & 0 & 1 & 1 \end{bmatrix}^{\mathrm{T}}$ for the system and $\hat{\boldsymbol{x}}(0) = \boldsymbol{0}$ for the unknown input observer. The resulting estimation error variables are depicted in Figure 5.1.
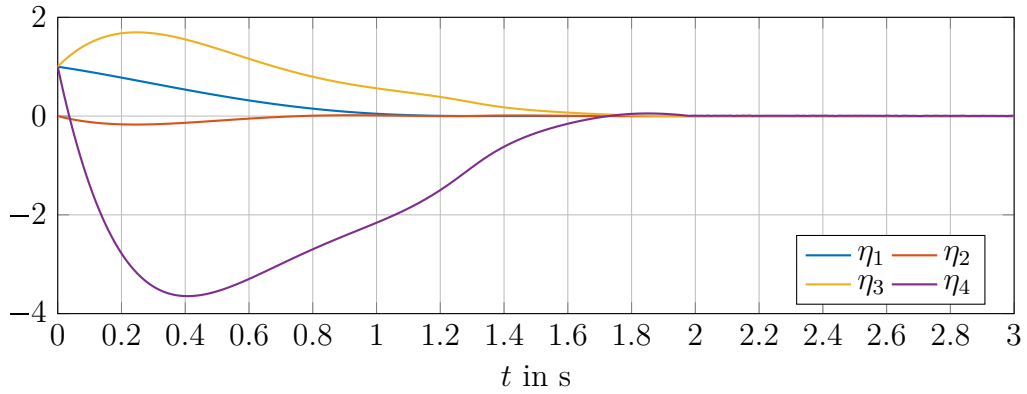
Figure 5.1: *Estimation error variables $\eta_i = x_i - \hat{x}_i$, $i = 1,\ldots,4$ of the proposed unknown input observer. The estimation errors converge to zero in finite time despite the unknown input.*

The estimation error variables vanish within a finite time of approximately 2 s despite the unknown input w.

5.6 Conclusions on the Single-Input Single-Output Case

In this chapter, a new unknown input observer for LTI SISO systems has been proposed. The main result, a nonlinear generalization of Ackermann's formula, allows for a compact calculation of the output error injection without explicitly transforming the system. If the parameter q is chosen as 0, a classical Luenberger observer is obtained. For $-1 < q < 0$ the resulting nonlinear continuous observer offers finite time convergence of the estimation error in the absence of the unknown input. For a bounded unknown input the choice $q = -1$ yields of a RED based unknown input observer that is capable of providing exact estimates of the state variables in finite time. In this case the tuning procedure is supported by means of a necessary stability condition. Therein, the involved quantities are the bound L of the unknown input as well as the vectors $\boldsymbol{c}$, $\boldsymbol{d}$ and the matrix $\boldsymbol{A}$ of the system represented in original coordinates. For this reason, the observer tuning is straightforward even in original coordinates.

In the following, the proposed unknown input observer, which is obtained for $q = -1$, is evaluated with respect to the disadvantages of existing methods discussed in Section 4.3:

(a) The unknown input observer does not require the restrictive observer matching condition (4.15). For instance, the system considered in Example 5.5.1 does not satisfy the observer matching condition.

(b) Bounded state variables are not required for convergence of the estimation error dynamics, as the necessary condition for the choice of κ_0 is independent of the state variables and the estimation errors. This is confirmed by Example 5.5.1

which deals with an unstable system and, thus, has unbounded trajectories.

(c) The unknown input does not have to be differentiable at all. During the derivations made, no derivatives of w occur.

(d) The necessary condition $\kappa_0 > L\left|\boldsymbol{c}^{\mathrm{T}}\boldsymbol{A}^{n-1}\boldsymbol{d}\right|$ does not involve the state variables. Hence, the choice of the observer parameters does not depend on the particular system trajectories, but only on the bound of the unknown input.

(e) The observer order as well as the number of tuning parameters are equal to the order n of the original system and, thus, not unnecessarily increased.

(f) In order to provide exact estimates, the unknown input requires a full output relative degree, i.e., $\delta = n$. This condition is the special case of the restrictive relative degree condition (4.34) of the MIMO case. However, in the SISO case this condition is intrinsically satisfied due to the strong observability assumption which has been shown in Section 2.3.2. Hence, it does not restrict the considered system class.

It can be concluded that the proposed unknown input observer avoids all the drawbacks of existing approaches. Moreover, the observer's effectiveness and especially the simplicity regarding the design and the tuning have been demonstrated by means of the numerical example.

6

Unknown Input Observer Design for Linear Time-Invariant Systems – The Multiple-Input Multiple-Output Case

In the SISO case the classical observability canonical form has proven to be the key for the unknown input observer design. As strong observability implies a full output relative degree of the SISO system, the unknown input need not be explicitly taken into account by the normal form. In the MIMO case, however, no such simple and useful property is satisfied in general. Existing observability canonical forms and observer normal forms[1] do not properly account for the unknown input and, hence, are not suitable for the unknown input observer design. For this reason, a new observer normal form for strongly observable LTI MIMO systems with unknown inputs is proposed. Therein, the unknown input observer design is straightforward and without any further restrictions regarding the system class. A tutorial example and numerical simulations demonstrate the functionality and the effectiveness of the proposed method.

6.1 An Observer Normal Form for LTI MIMO Systems with Unknown Inputs

In the following the main contributions to the MIMO case, a new observer normal form for strongly observable LTI MIMO systems and a theorem ensuring its existence, are presented.

---

[1]Such as Luenberger's observability canonical form, see the discussion in Section 4.2.6.

6.1.1 A New Observer Normal Form

The new observer normal form is proposed in

Definition 6.1.1. A strongly observable system

$$
\begin{aligned}
\dot{\bar{x}} &= \bar{A}\bar{x} + \bar{D}w, \\
\bar{y} &= \bar{C}\bar{x},
\end{aligned}
\tag{6.1a}
$$

is said to be in observer normal form if its dynamic matrix takes the structure

$$
\bar{A} = \left[
\begin{array}{ccccc|ccccc|c|ccccc}
\alpha_{1,1} & 1 & 0 & \cdots & 0 & \alpha_{2,1} & 0 & \cdots & \cdots & 0 & & \alpha_{p,1} & 0 & \cdots & \cdots & 0 \\
\alpha_{1,2} & 0 & 1 & \ddots & \vdots & \alpha_{2,2} & \vdots & & & \vdots & & \alpha_{p,2} & \vdots & & & \vdots \\
\vdots & \vdots & \ddots & \ddots & 0 & \vdots & \vdots & & & \vdots & \cdots & \vdots & \vdots & & & \vdots \\
\vdots & \vdots & & \ddots & 1 & \vdots & \vdots & & & \vdots & & \vdots & \vdots & & & \vdots \\
\vdots & 0 & \cdots & \cdots & 0 & \vdots & 0 & \cdots & \cdots & 0 & & \vdots & 0 & \cdots & \cdots & 0 \\
\hline
\vdots & 0 & \cdots & \cdots & 0 & \vdots & 1 & 0 & \cdots & 0 & & \vdots & 0 & \cdots & \cdots & 0 \\
\vdots & \vdots & & & \vdots & \vdots & 0 & 1 & \ddots & \vdots & & \vdots & \vdots & & & \vdots \\
\vdots & \vdots & & & \vdots & \vdots & \vdots & \ddots & \ddots & 0 & & \vdots & \vdots & & & \vdots \\
\vdots & 0 & \cdots & \cdots & 0 & \vdots & \vdots & & \ddots & 1 & & \vdots & \vdots & & & \vdots \\
\vdots & \beta_{1,2,1} & \cdots & \cdots & \beta_{1,2,\mu_1-1} & \vdots & 0 & \cdots & \cdots & 0 & & \vdots & 0 & \cdots & \cdots & 0 \\
\hline
\vdots & & & & & \vdots & & & & & \ddots & \vdots \\
\hline
\vdots & 0 & \cdots & \cdots & 0 & \vdots & 0 & \cdots & \cdots & 0 & & \vdots & 1 & 0 & \cdots & 0 \\
\vdots & \vdots & & & \vdots & \vdots & \vdots & & & \vdots & & \vdots & 0 & 1 & \ddots & \vdots \\
\vdots & \vdots & & & \vdots & \vdots & \vdots & & & \vdots & \cdots & \vdots & \vdots & \ddots & \ddots & 0 \\
\vdots & 0 & \cdots & \cdots & 0 & \vdots & 0 & \cdots & \cdots & 0 & & \vdots & \vdots & & \ddots & 1 \\
\alpha_{1,n} & \beta_{1,p,1} & \cdots & \cdots & \beta_{1,p,\mu_1-1} & \alpha_{2,n} & \beta_{2,p,1} & \cdots & \cdots & \beta_{2,p,\mu_2-1} & & \alpha_{p,n} & 0 & \cdots & \cdots & 0
\end{array}
\right],
\tag{6.1b}
$$

the unknown-input matrix is given by

$$
\bar{D} = \left[
\begin{array}{ccc}
0 & \cdots & 0 \\
\vdots & & \vdots \\
0 & \cdots & 0 \\
\hline
\bar{d}_{\mu_1,1} & \cdots & \bar{d}_{\mu_1,m} \\
0 & \cdots & 0 \\
\vdots & & \vdots \\
0 & \cdots & 0 \\
\hline
\bar{d}_{\mu_1+\mu_2,1} & \cdots & \bar{d}_{\mu_1+\mu_2,m} \\
\vdots & & \vdots \\
\hline
0 & \cdots & 0 \\
\vdots & & \vdots \\
0 & \cdots & 0 \\
\hline
\bar{d}_{n,1} & \cdots & \bar{d}_{n,m}
\end{array}
\right]
\tag{6.1c}
$$

and the output matrix has the form

$$
\bar{\boldsymbol{C}} = \left[
\begin{array}{ccccc|ccccc|c|ccccc}
1 & 0 & \cdots & \cdots & 0 & 0 & \cdots & \cdots & \cdots & 0 & \cdots & 0 & \cdots & \cdots & \cdots & 0 \\
0 & \cdots & \cdots & \cdots & 0 & 1 & 0 & \cdots & \cdots & 0 & \cdots & 0 & \cdots & \cdots & \cdots & 0 \\
\vdots & & & & & & & & & & \ddots & & & & & \vdots \\
0 & \cdots & \cdots & \cdots & 0 & 0 & \cdots & \cdots & \cdots & 0 & \cdots & 1 & 0 & \cdots & \cdots & 0
\end{array}
\right] .
\tag{6.1d}
$$

$$\underbrace{}_{\mu_1} \quad \underbrace{}_{\mu_2} \quad \underbrace{}_{\mu_p}$$

The system in observer normal form (6.1) consists of p coupled single-output systems of orders $\mu_1, \ldots, \mu_p$. Each subsystem contains a chain of integrators like structure which serves as the basis for the application of the RED as a state observer. The couplings between the subsystems can be partitioned into two parts:

(a) The coupling coefficients $\alpha_{j,i}$ with $j = 1, \ldots, p$ and $i = 1, \ldots, n$ directly correspond to the outputs due to the structure of $\bar{\boldsymbol{C}}$. Thus, they can be regarded as an output injection by a potential unknown input observer.

(b) The coupling coefficients $\beta_{j,k,l}$ with $j = 1, \ldots, p - 1$, $k = j + 1, \ldots, p$ and $l = 1, \ldots, \mu_{j-1}$ can not be considered as an output injection. However, they only appear in the blocks below the main diagonal of $\bar{\boldsymbol{A}}$.

In contrast to Luenberger's observability canonical form [80] which has been discussed in Section 4.2.6, the proposed observer normal form also accounts for the unknown input $\boldsymbol{w}$ by means of the specific structure of $\bar{\boldsymbol{D}}$. By permitting additional coupling coefficients $\beta_{j,k,l}$ to be present, this typical structure of the unknown-input matrix is achieved. This way, the orders of the subsystems $\mu_1, \ldots, \mu_p$ do not necessarily need to coincide with the observability indices of the system or the output relative degrees any more and the restrictive condition (4.34) is no longer required. In the special case when the considered system satisfies condition (4.34), the proposed observer normal form coincides with Luenberger's observability canonical form, i.e., $\beta_{j,k,l} = 0$ $\forall j$, $\forall k$ and $\forall l$.

Note that for SISO systems, i.e., $p = 1$, the proposed observer normal form (6.1) coincides with the classical observability canonical form for linear single-output systems, see Section 5.2. Thus, it is consistent with the approach for the SISO case presented in Chapter 5.

6.1.2 Existence of Transformations into Observer Normal Form

Consider the system

$$
\begin{aligned}
\dot{\boldsymbol{x}} &= \boldsymbol{A}\boldsymbol{x} + \boldsymbol{D}\boldsymbol{w}, \\
\boldsymbol{y} &= \boldsymbol{C}\boldsymbol{x},
\end{aligned}
\tag{6.2}
$$

under the assumptions provided in the problem statement in Section 4.1. Every strongly observable system (6.2) of order n with p linear independent outputs and m unknown inputs can be transformed into observer normal form (6.1) which is guaranteed by

Theorem 6.1.1. *Let the LTI system* (6.2) *be strongly observable. Then, there exist non-singular matrices* $\boldsymbol{T} \in \mathbb{R}^{n \times n}$ *and* $\boldsymbol{\Gamma} \in \mathbb{R}^{p \times p}$ *such that the state transformation* $\bar{\boldsymbol{x}} = \boldsymbol{T}^{-1}\boldsymbol{x}$ *and the output transformation* $\bar{\boldsymbol{y}} = \boldsymbol{\Gamma}\boldsymbol{y}$ *yield a system description in observer normal form* (6.1), *where the orders of the subsystems given by the integers* $\mu_j,\ j = 1, \ldots, p,$ *are sorted in descending order, i.e.,*

$$\mu_1 \geqslant \mu_2 \geqslant \cdots \geqslant \mu_p > 0, \qquad \sum_{j=1}^{p} \mu_j = n. \tag{6.3}$$

The proof of Theorem 6.1.1 and an algorithm which allows for determining suitable transformation matrices are given in Section 6.3.

6.2 Unknown Input Observer Design in Observer Normal Form

In order to reconstruct the state vector $\bar{\boldsymbol{x}}$ of system (6.1) in observer normal form, a finite-time convergent unknown input observer relying on the RED is designed. Convergence of the estimation error in the presence of the unknown input $\boldsymbol{w}$ is proven and the observer's properties are discussed.

6.2.1 Proposed Unknown Input Observer Design

The proposed unknown input observer takes the form

$$
\begin{aligned}
\dot{\hat{\bar{\boldsymbol{x}}}} &= \bar{\boldsymbol{A}}\hat{\bar{\boldsymbol{x}}} + \bar{\boldsymbol{\Pi}}\boldsymbol{\sigma}_{\bar{\boldsymbol{y}}} + \bar{\boldsymbol{l}}(\boldsymbol{\sigma}_{\bar{\boldsymbol{y}}}), \\
\hat{\bar{\boldsymbol{y}}} &= \bar{\boldsymbol{C}}\hat{\bar{\boldsymbol{x}}} = \begin{bmatrix} \hat{\bar{y}}_1 & \hat{\bar{y}}_2 & \ldots & \hat{\bar{y}}_p \end{bmatrix}^{\mathrm{T}} = \\
&= \begin{bmatrix} \hat{\bar{x}}_1 & \hat{\bar{x}}_{\mu_1+1} & \ldots & \hat{\bar{x}}_{\mu_1+\cdots+\mu_{p-1}+1} \end{bmatrix}^{\mathrm{T}},
\end{aligned} \tag{6.4a}
$$

where

$$\boldsymbol{\sigma}_{\bar{\boldsymbol{y}}} = \bar{\boldsymbol{y}} - \hat{\bar{\boldsymbol{y}}} = \begin{bmatrix} \sigma_1 & \sigma_{\mu_1+1} & \ldots & \sigma_{\mu_1+\cdots+\mu_{p-1}+1} \end{bmatrix}^{\mathrm{T}} \tag{6.4b}$$

is the output error,

$$\bar{\boldsymbol{\Pi}} = \begin{bmatrix} \alpha_{1,1} & \ldots & \alpha_{p,1} \\ \vdots & & \vdots \\ \alpha_{1,n} & \ldots & \alpha_{p,n} \end{bmatrix} \tag{6.4c}$$

provides for a linear output injection in order to compensate for the output related couplings between the single-output subsystems and $\bar{\boldsymbol{l}}(\boldsymbol{\sigma}_{\bar{\boldsymbol{y}}})$ is the nonlinear output injection. A suitable choice of $\bar{\boldsymbol{l}}(\boldsymbol{\sigma}_{\bar{\boldsymbol{y}}})$ relying on the RED is proposed in

Theorem 6.2.1. *Consider the observer* (6.4) *for the estimation of the state vector* $\bar{\boldsymbol{x}}$ *of system* (6.1), *the choice*

$$
\bar{\boldsymbol{l}}(\boldsymbol{\sigma}_{\bar{y}}) =
\begin{bmatrix}
\kappa_{1,\mu_1-1} \lfloor \sigma_1 \rceil^{\frac{\mu_1-1}{\mu_1}} \\
\vdots \\
\kappa_{1,1} \lfloor \sigma_1 \rceil^{\frac{1}{\mu_1}} \\
\kappa_{1,0} \lfloor \sigma_1 \rceil^{0} \\
\hline
\vdots \\
\kappa_{p,\mu_p-1} \lfloor \sigma_{\mu_1+\cdots+\mu_{p-1}+1} \rceil^{\frac{\mu_p-1}{\mu_p}} \\
\vdots \\
\kappa_{p,0} \lfloor \sigma_{\mu_1+\cdots+\mu_{p-1}+1} \rceil^{0}
\end{bmatrix}
\tag{6.5}
$$

for the nonlinear output injection[2] and the bounds L_i for the unknown inputs given in Assumption 4.1.2. Then, there exist parameters $\kappa_{j,k}$, $j = 1,\ldots,p$, $k = 0,\ldots,\mu_j-1$, such that the estimation error $\boldsymbol{\sigma} = \bar{\boldsymbol{x}} - \hat{\bar{\boldsymbol{x}}}$ converges to zero within finite time despite the unknown inputs for any initial states. Moreover, convergence of the observer for all admissible unknown input signals in terms of Assumption 4.1.2 is achieved only if $\kappa_{j,0} > \sum_{i=1}^{m} L_i \left| \bar{d}_{\mu_1+\cdots+\mu_j,i} \right|$.

Proof of Theorem 6.2.1. Definition of the estimation error

$$
\boldsymbol{\sigma} = \bar{\boldsymbol{x}} - \hat{\bar{\boldsymbol{x}}} = \begin{bmatrix} \sigma_1 & \sigma_2 & \ldots & \sigma_n \end{bmatrix}^{\mathrm{T}}
\tag{6.6}
$$

yields the estimation error dynamics

$$
\begin{aligned}
\dot{\boldsymbol{\sigma}} &= \bar{\boldsymbol{A}}\boldsymbol{\sigma} - \bar{\boldsymbol{\Pi}}\boldsymbol{\sigma}_{\bar{y}} - \bar{\boldsymbol{l}}(\boldsymbol{\sigma}_{\bar{y}}) + \bar{\boldsymbol{D}}\boldsymbol{w}, \\
\boldsymbol{\sigma}_{\bar{y}} &= \bar{\boldsymbol{C}}\boldsymbol{\sigma}.
\end{aligned}
\tag{6.7}
$$

Taking into account the structure of the involved matrices allows to rewrite the esti-

---

[2]Note that in terms of structure the proposed unknown input observer coincides with the unknown input observer for systems in Luenberger's observability canonical form, see Section 4.2.6. The additional coupling terms $\beta_{j,k,l}$ in the dynamic matrix do not impair the convergence properties of the estimation error dynamics which is shown subsequently in the proof of Theorem 6.2.1.

mation error dynamics (6.7) as p coupled subsystems Σ_j of order μ_j, i.e.,

$$
\begin{aligned}
\Sigma_1 &\begin{cases}
\dot{\sigma}_1 = \sigma_2 - \kappa_{1,\mu_1-1}\lfloor\sigma_1\rceil^{\frac{\mu_1-1}{\mu_1}} \\
\vdots \\
\dot{\sigma}_{\mu_1-1} = \sigma_{\mu_1} - \kappa_{1,1}\lfloor\sigma_1\rceil^{\frac{1}{\mu_1}} \\
\dot{\sigma}_{\mu_1} = -\kappa_{1,0}\lfloor\sigma_1\rceil^0 + \sum_{i=1}^{m}\bar{d}_{\mu_1,i}w_i
\end{cases} \\[2mm]
\Sigma_2 &\begin{cases}
\dot{\sigma}_{\mu_1+1} = \sigma_{\mu_1+2} - \kappa_{2,\mu_2-1}\lfloor\sigma_{\mu_1+1}\rceil^{\frac{\mu_2-1}{\mu_2}} \\
\vdots \\
\dot{\sigma}_{\mu_1+\mu_2-1} = \sigma_{\mu_1+\mu_2} - \kappa_{2,1}\lfloor\sigma_{\mu_1+1}\rceil^{\frac{1}{\mu_2}} \\
\dot{\sigma}_{\mu_1+\mu_2} = \sum_{l=1}^{\mu_1-1}\beta_{1,2,l}\sigma_{l+1} - \kappa_{2,0}\lfloor\sigma_{\mu_1+1}\rceil^0 + \sum_{i=1}^{m}\bar{d}_{\mu_1+\mu_2,i}w_i
\end{cases} \\[2mm]
&\quad\vdots \\[2mm]
\Sigma_p &\begin{cases}
\dot{\sigma}_{\mu_1+\cdots+\mu_{p-1}+1} = \sigma_{\mu_1+\cdots+\mu_{p-1}+2} - \kappa_{p,\mu_p-1}\lfloor\sigma_{\mu_1+\cdots+\mu_{p-1}+1}\rceil^{\frac{\mu_p-1}{\mu_p}} \\
\vdots \\
\dot{\sigma}_{n-1} = \sigma_n - \kappa_{p,1}\lfloor\sigma_{\mu_1+\cdots+\mu_{p-1}+1}\rceil^{\frac{1}{\mu_p}} \\
\dot{\sigma}_n = \sum_{i=1}^{p-1}\sum_{l=1}^{\mu_i-1}\beta_{i,p,l}\sigma_{\mu_1+\cdots+\mu_{i-1}+l+1} - \kappa_{p,0}\lfloor\sigma_{\mu_1+\cdots+\mu_{p-1}+1}\rceil^0 + \sum_{i=1}^{m}\bar{d}_{n,i}w_i,
\end{cases}
\end{aligned}
\tag{6.8}
$$

where each subsystem Σ_j, in terms of structure coincides with the estimation error dynamics of an RED with unknown input $\sum_{i=1}^{j-1}\sum_{l=1}^{\mu_i-1}\beta_{i,j,l}\sigma_{\mu_1+\cdots+\mu_{i-1}+l+1} + \sum_{i=1}^{m}\bar{d}_{\mu_1+\cdots+\mu_j,i}w_i$ in the last differential equation. According to Proposition 3.2.1(ii) there exist parameters $\kappa_{j,k}$, $k = 0,\ldots,\mu_j-1$ such that the state variables $\sigma_{\mu_1+\cdots+\mu_{j-1}+1},\ldots,\sigma_{\mu_1+\cdots+\mu_j}$ of the respective subsystem Σ_j converge to zero in finite time if the right-hand side of the last differential equation is bounded. Therefore, since all the unknown inputs w_i are bounded, the estimation error variables $\sigma_1,\ldots,\sigma_{\mu_1}$ of subsystem Σ_1 converge to zero within finite time for properly chosen parameters $\kappa_{1,k}$. During the convergence of the state variables of Σ_1, the state variables of the other subsystems remain bounded as the subsystems do not offer a finite escape time. After finite-time convergence of the state variables of Σ_1, the coupling terms of Σ_1 and Σ_2 through the last differential equation of Σ_2 vanishes and the estimation error variables $\sigma_{\mu_1+1},\ldots,\sigma_{\mu_1+\mu_2}$ of system Σ_2 converge to zero within finite time for properly chosen parameters $\kappa_{2,k}$. This further decouples Σ_3 from Σ_2. By induction, it can be shown, that this step-wise finite-time convergence is achieved for all further subsystems $\Sigma_3,\ldots,\Sigma_p$. Thus, it can be concluded that the estimation error $\boldsymbol{\sigma}$ vanishes in finite time despite the unknown inputs for properly chosen parameters $\kappa_{j,k}$, $j = 1,\ldots,p$, $k = 0,\ldots,\mu_j-1$.

Furthermore, the exactness of (6.8) requires that the discontinuity in the last differential equation of each subsystem Σ_j is capable of dominating the respective right-hand side, see Proposition 3.2.1(ii). Since the linear coupling terms in Σ_j vanish when all

the previous subsystems $\Sigma_1, \ldots, \Sigma_{j-1}$ have converged, the necessary condition

$$\kappa_{j,0} > \sum_{i=1}^{m} L_i \left| \bar{d}_{\mu_1 + \cdots + \mu_j, i} \right| \qquad \text{for } j = 1, \ldots, p \tag{6.9}$$

is required. $\qquad\qquad\qquad\qquad\qquad\qquad\qquad\qquad\qquad\qquad\qquad\qquad\qquad$ $\square$

6.2.2 Discussion of the Proposed Unknown Input Observer

The necessary condition (6.9) on the choice of the observer parameters $\kappa_{j,0}$ depends on the bounds L_i of the unknown inputs only and, thus, is independent of the coupling terms. Since the subsystems are decoupled of each other after some finite time, the parameters of each subsystem can be selected independently from the parameters of the other subsystems.

If there acts no unknown input on the j-th subsystem Σ_j at all, i.e., $\bar{d}_{\mu_1 + \cdots + \mu_j, 1} = \bar{d}_{\mu_1 + \cdots + \mu_j, 2} = \cdots = \bar{d}_{\mu_1 + \cdots + \mu_j, m} = 0$, the output injection $\bar{l}(\sigma_{\bar{y}})$ can be modified such that the corresponding subsystem Σ_j coincides with the estimation error dynamics of any other finite-time differentiator, e.g. one of the continuous differentiators considered in [26, 47, 93].

It is pointed out that, in contrast to the existing unknown input observers discussed in Section 4.2, the proposed unknown input observer does neither require bounded state variables, differentiability of the unknown input nor exhibits any restrictions regarding the system class. Furthermore, the observer order and the number of tuning parameters is n and, thus, not unnecessarily increased beyond the system order.

For SISO systems, i.e., $p = m = 1$, the proposed unknown input observer (6.4) with the output injection (6.5) coincides with the unknown input observer for the SISO case with homogeneity degree $q = -1$ proposed in Chapter 5.

If the output is corrupted by additive, uniformly bounded measurement noise $\boldsymbol{v} = \begin{bmatrix} v_1 & \cdots & v_p \end{bmatrix}^{\mathrm{T}}$, i.e., $\bar{\boldsymbol{y}} = \bar{\boldsymbol{C}}\bar{\boldsymbol{x}} + \boldsymbol{v}$, $|v_j| \leqslant v_{j,\max}$, $v_{j,\max} \geqslant 0$, $j = 1, \ldots, p$, the estimation error $\boldsymbol{\sigma}$ stays bounded with bounds discussed e.g. in [26].

6.3 Transformation into Observer Normal Form

The transformation of system (6.2) into the proposed observer normal form (6.1) is achieved by a regular state transformation of the form

$$\bar{\boldsymbol{x}} = \boldsymbol{T}^{-1}\boldsymbol{x} \quad \text{with} \quad \boldsymbol{T} \in \mathbb{R}^{n \times n}, \tag{6.10}$$

and a regular output transformation

$$\bar{\boldsymbol{y}} = \boldsymbol{\Gamma}\boldsymbol{y} \quad \text{with} \quad \boldsymbol{\Gamma} \in \mathbb{R}^{p \times p}, \tag{6.11}$$

which yield the matrices

$$\bar{\boldsymbol{A}} = \boldsymbol{T}^{-1}\boldsymbol{A}\boldsymbol{T}, \tag{6.12a}$$

$$\bar{\boldsymbol{D}} = \boldsymbol{T}^{-1}\boldsymbol{D}, \tag{6.12b}$$

$$\bar{\boldsymbol{C}} = \boldsymbol{\Gamma}\boldsymbol{C}\boldsymbol{T}, \tag{6.12c}$$

of the transformed system. An algorithm for the construction of the transformation matrices $\boldsymbol{T}$ and $\boldsymbol{\Gamma}$ is presented in the following. Afterwards, the theoretical basis including the proof of Theorem 6.1.1 is provided.

6.3.1 Description of the Transformation Algorithm

In order to construct the state transformation matrix $\boldsymbol{T}$ and the output transformation matrix $\boldsymbol{\Gamma}$, apply the following four-step algorithm:

Step 1: Output transformation and output-feedback based decomposition of the dynamic matrix

The first step aims for maximizing the relative degrees of the outputs with respect to $\boldsymbol{w}$ by means of an output transformation and some linear output-feedback $\boldsymbol{\Xi}$. To be more specific, the goal is to find an output transformation (6.11) and a decomposition of the dynamic matrix into

$$\boldsymbol{A} = \check{\boldsymbol{A}} - \boldsymbol{\Xi}\boldsymbol{C} \quad \text{with} \quad \boldsymbol{\Xi} \in \mathbb{R}^{n \times p}, \tag{6.13}$$

such that the auxiliary system

$$\begin{aligned} \dot{\check{\boldsymbol{x}}} &= \check{\boldsymbol{A}}\check{\boldsymbol{x}} + \boldsymbol{D}\boldsymbol{w}, \\ \check{\boldsymbol{y}} &= \begin{bmatrix} \check{y}_1 & \check{y}_2 & \dots & \check{y}_p \end{bmatrix}^{\mathrm{T}} = \check{\boldsymbol{C}}\check{\boldsymbol{x}}, \end{aligned} \tag{6.14}$$

with

$$\check{\boldsymbol{C}} = \begin{bmatrix} \check{\boldsymbol{c}}_1 & \check{\boldsymbol{c}}_2 & \dots & \check{\boldsymbol{c}}_p \end{bmatrix}^{\mathrm{T}} = \boldsymbol{\Gamma}\boldsymbol{C} \tag{6.15}$$

has the following properties:

(i) There exist integers $\mu_1 \geqslant \mu_2 \geqslant \dots \geqslant \mu_p > 0$ satisfying $\sum_{j=1}^{p} \mu_j = n$ such that the $n \times n$ matrix

$$\mathcal{O}_{\mathrm{R}} = \begin{bmatrix} \check{\boldsymbol{c}}_1^{\mathrm{T}} \\ \vdots \\ \check{\boldsymbol{c}}_1^{\mathrm{T}} \check{\boldsymbol{A}}^{\mu_1-1} \\ \check{\boldsymbol{c}}_2^{\mathrm{T}} \\ \vdots \\ \check{\boldsymbol{c}}_2^{\mathrm{T}} \check{\boldsymbol{A}}^{\mu_2-1} \\ \vdots \\ \check{\boldsymbol{c}}_p^{\mathrm{T}} \\ \vdots \\ \check{\boldsymbol{c}}_p^{\mathrm{T}} \check{\boldsymbol{A}}^{\mu_p-1} \end{bmatrix} \tag{6.16}$$

is invertible, i.e.,

$$\operatorname{rank} \mathcal{O}_{\mathrm{R}} = n. \tag{6.17}$$

(ii) If the relative degree $\check{\delta}_j$ of the output $\check{y}_j$ with respect to the unknown input $\boldsymbol{w}$ exists, it satisfies $\check{\delta}_j \geqslant \mu_j$, i.e.,

$$\check{\boldsymbol{c}}_j^{\mathrm{T}} \check{\boldsymbol{A}}^i \boldsymbol{D} = \boldsymbol{0}^{\mathrm{T}} \qquad \text{for } j = 1, \ldots, p, \ i = 0, \ldots, \mu_j - 2. \tag{6.18}$$

For this purpose, parts[3] of the iterative decomposition algorithm proposed in [25, Section 5.3, pages 119-127] are applied in a slightly modified way in the following. First of all, initialize

$$\boldsymbol{Z} = \boldsymbol{C}, \quad \boldsymbol{Z}_j = \boldsymbol{c}_j^{\mathrm{T}}, \quad \boldsymbol{\Psi}_j = \boldsymbol{e}_j^{\mathrm{T}} \in \mathbb{R}^{1 \times p}, \quad \boldsymbol{\Omega} = \begin{bmatrix} \boldsymbol{\omega}_1^{\mathrm{T}} \\ \boldsymbol{\omega}_2^{\mathrm{T}} \\ \vdots \\ \boldsymbol{\omega}_p^{\mathrm{T}} \end{bmatrix} = \begin{bmatrix} \boldsymbol{0}_{1 \times m} \\ \boldsymbol{0}_{1 \times m} \\ \vdots \\ \boldsymbol{0}_{1 \times m} \end{bmatrix}, \quad \nu_j = 1, \tag{6.19}$$

for all $j = 1, \ldots, p$ and the flag vector

$$\boldsymbol{f} = \begin{bmatrix} f_1 \\ f_2 \\ \vdots \\ f_p \end{bmatrix} = \begin{bmatrix} 1 \\ 1 \\ \vdots \\ 1 \end{bmatrix}. \tag{6.20}$$

Note that these quantities are modified from iteration to iteration and $\boldsymbol{Z}$, $\boldsymbol{Z}_j$ and $\boldsymbol{\Psi}_j$ will be augmented by further rows. Repeat until all elements of $\boldsymbol{f}$ have become zero:

For each non-zero element f_j consider the last row $\boldsymbol{z}_{j,\nu_j}^{\mathrm{T}}$ of the corresponding matrix

$$\boldsymbol{Z}_j = \begin{bmatrix} \boldsymbol{z}_{j,1}^{\mathrm{T}} \\ \vdots \\ \boldsymbol{z}_{j,\nu_j}^{\mathrm{T}} \end{bmatrix}. \tag{6.21}$$

Case 1: If

$$\operatorname{rank} \begin{bmatrix} \boldsymbol{\Omega} \\ \boldsymbol{z}_{j,\nu_j}^{\mathrm{T}} \boldsymbol{D} \end{bmatrix} > \operatorname{rank} \boldsymbol{\Omega} \tag{6.22}$$

set $f_j \leftarrow 0$ and $\boldsymbol{\omega}_j^{\mathrm{T}} \leftarrow \boldsymbol{z}_{j,\nu_j}^{\mathrm{T}} \boldsymbol{D}$. Then, continue with the next non-zero f_j.
Case 2: If

$$\operatorname{rank} \begin{bmatrix} \boldsymbol{\Omega} \\ \boldsymbol{z}_{j,\nu_j}^{\mathrm{T}} \boldsymbol{D} \end{bmatrix} = \operatorname{rank} \boldsymbol{\Omega} \tag{6.23}$$

calculate coefficients $\zeta_{j,\nu_j,k}$, $k = 1, \ldots, p$ which allow to represent $\boldsymbol{z}_{j,\nu_j}^{\mathrm{T}} \boldsymbol{D}$ as a linear combination of the rows $\boldsymbol{\omega}_j^{\mathrm{T}}$ of $\boldsymbol{\Omega}$, i.e.,

$$\boldsymbol{z}_{j,\nu_j}^{\mathrm{T}} \boldsymbol{D} = \begin{bmatrix} \zeta_{j,\nu_j,1} & \cdots & \zeta_{j,\nu_j,p} \end{bmatrix} \boldsymbol{\Omega}. \tag{6.24}$$

---

[3]Namely the steps SCB.1, SCB.2 and SCB.3.

Note that (6.24) may have infinitely many solutions. A reasonable choice is given by the solution with the minimum Euclidean norm. Update the rows of $\boldsymbol{Z}_j$ according to

$$
\begin{aligned}
\boldsymbol{z}_{j,1}^{\mathrm{T}} &\leftarrow \boldsymbol{z}_{j,1}^{\mathrm{T}} - \sum_{k=1}^{p} \zeta_{j,\nu_j,k} \boldsymbol{z}_{k,\nu_k-\nu_j+1}^{\mathrm{T}} \\
\boldsymbol{z}_{j,2}^{\mathrm{T}} &\leftarrow \boldsymbol{z}_{j,2}^{\mathrm{T}} - \sum_{k=1}^{p} \zeta_{j,\nu_j,k} \boldsymbol{z}_{k,\nu_k-\nu_j+2}^{\mathrm{T}} \\
&\vdots \\
\boldsymbol{z}_{j,\nu_j}^{\mathrm{T}} &\leftarrow \boldsymbol{z}_{j,\nu_j}^{\mathrm{T}} - \sum_{k=1}^{p} \zeta_{j,\nu_j,k} \boldsymbol{z}_{k,\nu_k}^{\mathrm{T}},
\end{aligned}
\tag{6.25}
$$

where $\boldsymbol{z}_{k,l} = \boldsymbol{0}^{\mathrm{T}}$ if $l < 1$. Thus, $\boldsymbol{Z}_j^{\mathrm{T}} \boldsymbol{D} = \boldsymbol{0}$ is satisfied. Furthermore, update

$$
\boldsymbol{\Psi}_j \leftarrow \boldsymbol{\Psi}_j - \sum_{k=1}^{p} \zeta_{j,\nu_j,k} \begin{bmatrix} \boldsymbol{0}_{(\nu_j-\nu_k)\times p} \\ \boldsymbol{\Psi}_k \end{bmatrix}, \quad \boldsymbol{Z} \leftarrow \begin{bmatrix} \boldsymbol{Z}_1 \\ \vdots \\ \boldsymbol{Z}_p \end{bmatrix}.
\tag{6.26}
$$

Sub-case 2.1: If

$$
\operatorname{rank} \begin{bmatrix} \boldsymbol{Z} \\ \boldsymbol{z}_{j,\nu_j}^{\mathrm{T}} \boldsymbol{A} \end{bmatrix} = \operatorname{rank} \boldsymbol{Z}
\tag{6.27}
$$

set the corresponding flag $f_j \leftarrow 0$.
Sub-case 2.2: If

$$
\operatorname{rank} \begin{bmatrix} \boldsymbol{Z} \\ \boldsymbol{z}_{j,\nu_j}^{\mathrm{T}} \boldsymbol{A} \end{bmatrix} > \operatorname{rank} \boldsymbol{Z}
\tag{6.28}
$$

augment the matrices

$$
\boldsymbol{Z}_j \leftarrow \begin{bmatrix} \boldsymbol{Z}_j \\ \boldsymbol{z}_{j,\nu_j}^{\mathrm{T}} \boldsymbol{A} \end{bmatrix}, \quad \boldsymbol{\Psi}_j \leftarrow \begin{bmatrix} \boldsymbol{\Psi}_j \\ \boldsymbol{0}_{1\times p} \end{bmatrix},
\tag{6.29}
$$

update

$$
\boldsymbol{Z} \leftarrow \begin{bmatrix} \boldsymbol{Z}_1 \\ \vdots \\ \boldsymbol{Z}_p \end{bmatrix},
\tag{6.30}
$$

and increase

$$
\nu_j \leftarrow \nu_j + 1.
\tag{6.31}
$$

This procedure is repeated with the next non-zero element f_j until $\boldsymbol{f} = \boldsymbol{0}$. Note that, once all elements in the flag vector $\boldsymbol{f}$ have become zero, $\boldsymbol{Z}$ is an invertible $n \times n$ matrix and $\sum_{j=1}^{p} \nu_j = n$ is ensured, which is shown later on. Assign the integers $1, 2, \ldots, p$ to $j_1, j_2, \ldots, j_p$ such that

$$\nu_{j_1} \geqslant \nu_{j_2} \geqslant \cdots \geqslant \nu_{j_p} \tag{6.32}$$

are sorted in descending order and assign the orders μ_j of the subsystems as

$$\mu_1 = \nu_{j_1}, \quad \mu_2 = \nu_{j_2}, \quad \ldots, \quad \mu_p = \nu_{j_p}. \tag{6.33}$$

Consider the matrices $\boldsymbol{\Psi}_j$ partitioned into their rows

$$\boldsymbol{\Psi}_j = \begin{bmatrix} \boldsymbol{\psi}_{j,1}^{\mathrm{T}} \\ \vdots \\ \boldsymbol{\psi}_{j,\nu_j}^{\mathrm{T}} \end{bmatrix}. \tag{6.34}$$

and construct the output transformation matrix

$$\boldsymbol{\Gamma} = \begin{bmatrix} \boldsymbol{\psi}_{j_1,1}^{\mathrm{T}} \\ \boldsymbol{\psi}_{j_2,1}^{\mathrm{T}} \\ \vdots \\ \boldsymbol{\psi}_{j_p,1}^{\mathrm{T}} \end{bmatrix}. \tag{6.35}$$

Finally, construct the matrix $\boldsymbol{\Xi}$ introduced in (6.13) according to

$$\boldsymbol{\Xi} = \boldsymbol{Z}^{-1} \begin{bmatrix} \boldsymbol{\psi}_{1,2}^{\mathrm{T}} \\ \vdots \\ \boldsymbol{\psi}_{1,\nu_1}^{\mathrm{T}} \\ \boldsymbol{0}^{\mathrm{T}} \\ \hline \vdots \\ \hline \boldsymbol{\psi}_{p,2}^{\mathrm{T}} \\ \vdots \\ \boldsymbol{\psi}_{p,\nu_p}^{\mathrm{T}} \\ \boldsymbol{0}^{\mathrm{T}} \end{bmatrix}, \tag{6.36}$$

and calculate the matrices $\check{\boldsymbol{A}}$ and $\check{\boldsymbol{C}}$ of the auxiliary system (6.14) from (6.13) and (6.15), respectively.

Step 2: Calculation of p columns of the state transformation matrix

The construction of the state transformation (6.10) is based on the auxiliary system (6.14). Consider the transformation matrix $\boldsymbol{T}$ to be expressed by its column vectors $\boldsymbol{t}_i$ i.e.,

$$\boldsymbol{T} = \begin{bmatrix} \boldsymbol{t}_1 & \boldsymbol{t}_2 & \ldots & \boldsymbol{t}_{\mu_1} & \boldsymbol{t}_{\mu_1+1} & \ldots & \boldsymbol{t}_{\mu_1+\mu_2} & \ldots & \boldsymbol{t}_{\mu_1+\cdots+\mu_{p-1}+1} & \ldots & \boldsymbol{t}_n \end{bmatrix}. \tag{6.37}$$

Calculate the column vectors $\boldsymbol{t}_{\mu_1}$, $\boldsymbol{t}_{\mu_1+\mu_2}$, ..., $\boldsymbol{t}_n$ of the transformation matrix $\boldsymbol{T}$ from

$$\begin{bmatrix} \boldsymbol{t}_{\mu_1} & \boldsymbol{t}_{\mu_1+\mu_2} & \cdots & \boldsymbol{t}_n \end{bmatrix} = \boldsymbol{\mathcal{O}}_{\mathrm{R}}^{-1} \begin{bmatrix} \boldsymbol{e}_{\mu_1} & \boldsymbol{e}_{\mu_1+\mu_2} & \cdots & \boldsymbol{e}_n \end{bmatrix}, \tag{6.38}$$

where $\boldsymbol{\mathcal{O}}_{\mathrm{R}}$ is the observability matrix like matrix of the auxiliary system given in (6.16).

Step 3: Calculation of the coefficients $\beta_{j,k,l}$

For each $j = 1, 2, \ldots, p-1$ calculate the coefficients $\beta_{j,k,l}$ of the matrix $\bar{\boldsymbol{A}}$ for $k = j+1, j+2, \ldots, p$ and $l = 1, 2 \ldots, \mu_j - 1$ in the following way:

(a) Construct the invertible matrix

$$\boldsymbol{H}^{(j)} = \begin{bmatrix} \boldsymbol{H}_{j+1,j+1}^{(j)} & \cdots & \boldsymbol{H}_{j+1,p}^{(j)} \\ \vdots & \ddots & \vdots \\ \boldsymbol{H}_{p,j+1}^{(j)} & \cdots & \boldsymbol{H}_{p,p}^{(j)} \end{bmatrix}, \tag{6.39}$$

where the submatrices $\boldsymbol{H}_{r,s}^{(j)} \in \mathbb{R}^{(\mu_j - \mu_r) \times (\mu_j - \mu_s)}$ have the Toeplitz structure

$$\boldsymbol{H}_{r,s}^{(j)} = \begin{cases} \begin{bmatrix} \check{\boldsymbol{c}}_r^{\mathrm{T}} \check{\boldsymbol{A}}^{\mu_s-1} \boldsymbol{t}_{\mu_1+\cdots+\mu_s} & \check{\boldsymbol{c}}_r^{\mathrm{T}} \check{\boldsymbol{A}}^{\mu_s} \boldsymbol{t}_{\mu_1+\cdots+\mu_s} & \cdots & \check{\boldsymbol{c}}_r^{\mathrm{T}} \check{\boldsymbol{A}}^{\mu_j-2} \boldsymbol{t}_{\mu_1+\cdots+\mu_s} \\ \check{\boldsymbol{c}}_r^{\mathrm{T}} \check{\boldsymbol{A}}^{\mu_s-2} \boldsymbol{t}_{\mu_1+\cdots+\mu_s} & \check{\boldsymbol{c}}_r^{\mathrm{T}} \check{\boldsymbol{A}}^{\mu_s-1} \boldsymbol{t}_{\mu_1+\cdots+\mu_s} & \ddots & \check{\boldsymbol{c}}_r^{\mathrm{T}} \check{\boldsymbol{A}}^{\mu_j-3} \boldsymbol{t}_{\mu_1+\cdots+\mu_s} \\ \vdots & \ddots & \ddots & \vdots \\ \check{\boldsymbol{c}}_r^{\mathrm{T}} \check{\boldsymbol{A}}^{\mu_r} \boldsymbol{t}_{\mu_1+\cdots+\mu_s} & \ddots & \ddots & \vdots \\ 0 & \ddots & \ddots & \vdots \\ \vdots & \ddots & \ddots & \vdots \\ \vdots & & \ddots & \check{\boldsymbol{c}}_r^{\mathrm{T}} \check{\boldsymbol{A}}^{\mu_r} \boldsymbol{t}_{\mu_1+\cdots+\mu_s} \\ 0 & \cdots & \cdots & 0 \end{bmatrix} & \begin{array}{l} \text{if } r > s \\ (\Rightarrow \mu_r \leqslant \mu_s), \end{array} \\[2ex] \begin{bmatrix} 1 & \check{\boldsymbol{c}}_r^{\mathrm{T}} \check{\boldsymbol{A}}^{\mu_r} \boldsymbol{t}_{\mu_1+\cdots+\mu_r} & \cdots & \check{\boldsymbol{c}}_r^{\mathrm{T}} \check{\boldsymbol{A}}^{\mu_j-2} \boldsymbol{t}_{\mu_1+\cdots+\mu_r} \\ 0 & \ddots & \ddots & \vdots \\ \vdots & \ddots & \ddots & \check{\boldsymbol{c}}_r^{\mathrm{T}} \check{\boldsymbol{A}}^{\mu_r} \boldsymbol{t}_{\mu_1+\cdots+\mu_r} \\ 0 & \cdots & 0 & 1 \end{bmatrix} & \begin{array}{l} \text{if } r = s \\ (\Rightarrow \mu_r = \mu_s), \end{array} \\[2ex] \begin{bmatrix} 0 & \cdots & 0 & \check{\boldsymbol{c}}_r^{\mathrm{T}} \check{\boldsymbol{A}}^{\mu_r} \boldsymbol{t}_{\mu_1+\cdots+\mu_s} & \cdots & \check{\boldsymbol{c}}_r^{\mathrm{T}} \check{\boldsymbol{A}}^{\mu_j-2} \boldsymbol{t}_{\mu_1+\cdots+\mu_s} \\ \vdots & \vdots & \ddots & \ddots & \vdots \\ \vdots & \vdots & & \ddots & \check{\boldsymbol{c}}_r^{\mathrm{T}} \check{\boldsymbol{A}}^{\mu_r} \boldsymbol{t}_{\mu_1+\cdots+\mu_s} \\ 0 & \cdots & 0 & \cdots & \cdots & 0 \end{bmatrix} & \begin{array}{l} \text{if } r < s \\ (\Rightarrow \mu_r \geqslant \mu_s). \end{array} \end{cases} \tag{6.40}$$

(b) Build up the vector

$$\boldsymbol{\rho}^{(j)} = \begin{bmatrix} \boldsymbol{\rho}_{j+1}^{(j)} \\ \boldsymbol{\rho}_{j+2}^{(j)} \\ \vdots \\ \boldsymbol{\rho}_p^{(j)} \end{bmatrix}, \quad \text{where} \quad \boldsymbol{\rho}_r^{(j)} = \begin{bmatrix} \check{\boldsymbol{c}}_r^{\mathrm{T}} \check{\boldsymbol{A}}^{\mu_j-1} \boldsymbol{t}_{\mu_1+\cdots+\mu_j} \\ \check{\boldsymbol{c}}_r^{\mathrm{T}} \check{\boldsymbol{A}}^{\mu_j-2} \boldsymbol{t}_{\mu_1+\cdots+\mu_j} \\ \vdots \\ \check{\boldsymbol{c}}_r^{\mathrm{T}} \check{\boldsymbol{A}}^{\mu_r} \boldsymbol{t}_{\mu_1+\cdots+\mu_j} \end{bmatrix}. \tag{6.41}$$

(c) Solve the linear system of equations

$$\boldsymbol{H}^{(j)}\boldsymbol{\beta}^{(j)} = \boldsymbol{\rho}^{(j)} \tag{6.42}$$

for the vector $\boldsymbol{\beta}^{(j)}$ which holds the coefficients $\beta_{j,k,l}$ for $l \geqslant \mu_k$, i.e.,

$$\boldsymbol{\beta}^{(j)} = \begin{bmatrix} \boldsymbol{\beta}^{(j)}_{j+1} \\ \boldsymbol{\beta}^{(j)}_{j+2} \\ \vdots \\ \boldsymbol{\beta}^{(j)}_{p} \end{bmatrix}, \qquad \text{with} \quad \boldsymbol{\beta}^{(j)}_{r} = \begin{bmatrix} \beta_{j,r,\mu_r} \\ \vdots \\ \beta_{j,r,\mu_j-1} \end{bmatrix}. \tag{6.43}$$

Set the remaining coefficients to zero, i.e.,

$$\beta_{j,k,l} = 0 \qquad \text{for} \quad l < \mu_k. \tag{6.44}$$

Step 4: Construction of the state transformation matrix

Calculate the remaining columns of the transformation matrix $\boldsymbol{T}$ given in (6.37) according to

$$\boldsymbol{t}_{\mu_1+\cdots+\mu_j-i} = \check{\boldsymbol{A}}^i \boldsymbol{t}_{\mu_1+\cdots+\mu_j} - \sum_{r=j+1}^{p} \sum_{q=1}^{i} \beta_{j,r,\mu_j-q} \check{\boldsymbol{A}}^{i-q} \boldsymbol{t}_{\mu_1+\cdots+\mu_r}, \tag{6.45}$$

where $j = 1, 2, \ldots, p$ and $i = 0, 1, \ldots, \mu_j - 1$. Note that (6.45) is also consistent in the case $i = 0$ which is exploited in the proofs in the appendix.

The presented algorithm yields non-singular transformation matrices $\boldsymbol{T}$ and $\boldsymbol{\Gamma}$ whenever the original system (6.2) is strongly observable, which is shown in the the next section.

6.3.2 Existence of the Proposed Transformations

In this section, the theoretical basis for the previously presented state and output transformation is established. It is shown that the algorithm proposed in Section 6.3.1 yields a description of the system in the proposed observer normal form (6.1) which finally proves Theorem 6.1.1.

Proof of Theorem 6.1.1. In order to prove Theorem 6.1.1, the following lemma is useful:

Lemma 6.3.1. *Under the conditions given in Theorem 6.1.1, the following statements are true:*

(a) *The auxiliary system* (6.14) *generated by Step 1 of the algorithm proposed in Section 6.3.1 satisfies the conditions* (6.17) *and* (6.18).

(b) *The transformation matrix $\boldsymbol{T}$ constructed by the proposed algorithm in Section 6.3.1 is guaranteed to be non-singular, regardless of the specific values of $\beta_{j,k,l}$.*

(c) *There exists a unique solution of the system of equations* (6.42) *in Step 3 of*

the algorithm proposed in Section 6.3.1.

(d) If the transformation matrices $\boldsymbol{T}$ and $\boldsymbol{\Gamma}$ are constructed according to the algorithm in Section 6.3.1, then the dynamic matrix $\bar{\boldsymbol{A}}$ of the transformed system (6.1a) given in (6.12a) takes the proposed form (6.1b).

(e) If the transformation matrices $\boldsymbol{T}$ and $\boldsymbol{\Gamma}$ are constructed according to the algorithm in Section 6.3.1, then the unknown-input matrix $\bar{\boldsymbol{D}}$ of the transformed system (6.1a) given in (6.12b) takes the proposed form (6.1c).

(f) If the transformation matrices $\boldsymbol{T}$ and $\boldsymbol{\Gamma}$ are constructed according to the algorithm in Section 6.3.1, then the output matrix $\bar{\boldsymbol{C}}$ of the transformed system (6.1a) given in (6.12c) takes the proposed form (6.1d).

The proof of Lemma 6.3.1 is provided in the appendix in Section 10.2. Note that Lemma 6.3.1(a) is a prerequisite for the proofs of Lemma 6.3.1(b) to 6.3.1(f). Lemma 6.3.1(b) ensures $\boldsymbol{T}$ to be non-singular. Moreover, $\boldsymbol{\Gamma}$ is ensured to be non-singular which follows directly from the results presented in [25, Section 5.3, pages 119-127]. Lemma 6.3.1(c) states that a unique solution of the system of equations (6.42) exists, which ensures the existence of the coefficients $\beta_{j,k,l}$ of the dynamic matrix $\bar{\boldsymbol{A}}$ of the transformed system. Finally, from Lemma 6.3.1(d), 6.3.1(e) and 6.3.1(f) it follows directly that the transformed system takes the proposed observer normal form, which completes the proof of Theorem 6.1.1. $\qquad\square$

6.4 A Tutorial Example

In order to demonstrate the effectiveness of the proposed unknown input observer, it is applied to a linearized model of the lateral motion of a light aircraft taken from [49] which has already been given in Example 4.2.1. The algorithm proposed in Section 6.3.1 is applied in order to provide a system description in the presented observer normal form. An unknown input observer is designed according to Section 6.2 in order to provide exact estimates of the state vector in the presence of an unknown input w. The effectiveness of this observer is confirmed by numerical simulations.

6.4.1 Transformation into the Proposed Observer Normal Form

In the following, the construction of the state transformation matrix $\boldsymbol{T}$ and the output transformation matrix $\boldsymbol{\Gamma}$ based on the algorithm presented in Section 6.3.1 is illustrated step by step.

Step 1: Output transformation and output-feedback based decomposition of the dynamic matrix

First of all, the initialization of the required quantities yields

$$\boldsymbol{Z} = \boldsymbol{C} = \begin{bmatrix} 0 & 1 & 0 & 0 & 0 & 0 & 0 \\ 0 & 0 & 0 & 0 & 1 & 0 & 0 \end{bmatrix}, \quad \boldsymbol{Z}_1 = \boldsymbol{c}_1^{\mathrm{T}} = \begin{bmatrix} 0 & 1 & 0 & 0 & 0 & 0 & 0 \end{bmatrix},$$

$$\boldsymbol{Z}_2 = \boldsymbol{c}_2^{\mathrm{T}} = \begin{bmatrix} 0 & 0 & 0 & 0 & 1 & 0 & 0 \end{bmatrix}, \quad \boldsymbol{\Psi}_1 = \boldsymbol{e}_1^{\mathrm{T}} = \begin{bmatrix} 1 & 0 \end{bmatrix}, \quad \boldsymbol{\Psi}_2 = \boldsymbol{e}_2^{\mathrm{T}} = \begin{bmatrix} 0 & 1 \end{bmatrix},$$

$$\boldsymbol{\Omega} = \begin{bmatrix} \omega_1 \\ \omega_2 \end{bmatrix} = \begin{bmatrix} 0 \\ 0 \end{bmatrix}, \quad \nu_1 = 1, \quad \nu_2 = 1, \quad \boldsymbol{f} = \begin{bmatrix} f_1 \\ f_2 \end{bmatrix} = \begin{bmatrix} 1 \\ 1 \end{bmatrix}.$$

$$(6.46)$$

Iteration 1: Starting with the first non-zero flag $f_1 = 1$ leads to Case 2 since $\boldsymbol{z}_{1,1}^{\mathrm{T}} \boldsymbol{D} = 0$. Thus, $\zeta_{1,1,1} = \zeta_{1,1,2} = 0$ and $\boldsymbol{z}_{1,1}$ and $\boldsymbol{\Psi}_1$ remain unchanged. Then, Sub-case 2.2 is entered and the updates

$$\boldsymbol{Z}_1 \leftarrow \begin{bmatrix} \boldsymbol{Z}_1 \\ \boldsymbol{z}_{1,1}^{\mathrm{T}} \boldsymbol{A} \end{bmatrix} = \begin{bmatrix} 0 & 1 & 0 & 0 & 0 & 0 & 0 \\ -0.1 & -8.3 & 3.75 & 0 & 0 & 0 & -28.6 \end{bmatrix},$$

$$\boldsymbol{\Psi}_1 \leftarrow \begin{bmatrix} \boldsymbol{\Psi}_1 \\ \boldsymbol{0}^{\mathrm{T}} \end{bmatrix} = \begin{bmatrix} 1 & 0 \\ 0 & 0 \end{bmatrix},$$

$$\boldsymbol{Z} \leftarrow \begin{bmatrix} \boldsymbol{Z}_1 \\ \boldsymbol{Z}_2 \end{bmatrix} = \begin{bmatrix} 0 & 1 & 0 & 0 & 0 & 0 & 0 \\ -0.1 & -8.3 & 3.75 & 0 & 0 & 0 & -28.6 \\ 0 & 0 & 0 & 0 & 1 & 0 & 0 \end{bmatrix}, \quad \nu_1 \leftarrow \nu_1 + 1 = 2,$$

$$(6.47)$$

are carried out.

Iteration 2: Continue with the non-zero flag $f_2 = 1$. Again, $\boldsymbol{z}_{2,1}^{\mathrm{T}} \boldsymbol{D} = 0$ leads to Case 2, where $\zeta_{2,1,1} = \zeta_{2,1,2} = 0$ and $\boldsymbol{z}_{2,1}$ and $\boldsymbol{\Psi}_2$ remain unchanged. Sub-case 2.2 occurs and the updates

$$\boldsymbol{Z}_2 \leftarrow \begin{bmatrix} \boldsymbol{Z}_2 \\ \boldsymbol{z}_{2,1}^{\mathrm{T}} \boldsymbol{A} \end{bmatrix} = \begin{bmatrix} 0 & 0 & 0 & 0 & 1 & 0 & 0 \\ 0 & 0 & 1 & 0 & 0 & 0 & 0 \end{bmatrix}, \quad \boldsymbol{\Psi}_2 \leftarrow \begin{bmatrix} \boldsymbol{\Psi}_2 \\ \boldsymbol{0}^{\mathrm{T}} \end{bmatrix} = \begin{bmatrix} 0 & 1 \\ 0 & 0 \end{bmatrix},$$

$$\boldsymbol{Z} \leftarrow \begin{bmatrix} \boldsymbol{Z}_1 \\ \boldsymbol{Z}_2 \end{bmatrix} = \begin{bmatrix} 0 & 1 & 0 & 0 & 0 & 0 & 0 \\ -0.1 & -8.3 & 3.75 & 0 & 0 & 0 & -28.6 \\ 0 & 0 & 0 & 0 & 1 & 0 & 0 \\ 0 & 0 & 1 & 0 & 0 & 0 & 0 \end{bmatrix}, \quad \nu_2 \leftarrow \nu_2 + 1 = 2,$$

$$(6.48)$$

are performed.

Iterations 3 & 4: Both, $\boldsymbol{z}_{1,2}^{\mathrm{T}} \boldsymbol{D} = 0$ and $\boldsymbol{z}_{2,2}^{\mathrm{T}} \boldsymbol{D} = 0$ and, again, Case 2 and Sub-

case 2.2 are entered which yield the updates

$$\boldsymbol{Z}_1 \leftarrow \begin{bmatrix} \boldsymbol{Z}_1 \\ \boldsymbol{z}_{1,2}^{\mathrm{T}} \boldsymbol{A} \end{bmatrix} = \begin{bmatrix} 0 & 1 & 0 & 0 & 0 & 0 & 0 \\ -0.1 & -8.3 & 3.75 & 0 & 0 & 0 & -28.6 \\ 2.25 & 68.89 & -30.23 & -0.98 & 0 & -35.09 & 380.38 \end{bmatrix},$$

$$\boldsymbol{\Psi}_1 \leftarrow \begin{bmatrix} \boldsymbol{\Psi}_1 \\ \boldsymbol{0}^{\mathrm{T}} \end{bmatrix} = \begin{bmatrix} 1 & 0 \\ 0 & 0 \\ 0 & 0 \end{bmatrix},$$

$$\boldsymbol{Z}_2 \leftarrow \begin{bmatrix} \boldsymbol{Z}_2 \\ \boldsymbol{z}_{2,2}^{\mathrm{T}} \boldsymbol{A} \end{bmatrix} = \begin{bmatrix} 0 & 0 & 0 & 0 & 1 & 0 & 0 \\ 0 & 0 & 1 & 0 & 0 & 0 & 0 \\ 0.37 & 0 & -0.64 & 0 & 0 & -9.5 & 0 \end{bmatrix},$$

$$\boldsymbol{\Psi}_2 \leftarrow \begin{bmatrix} \boldsymbol{\Psi}_2 \\ \boldsymbol{0}^{\mathrm{T}} \end{bmatrix} = \begin{bmatrix} 0 & 1 \\ 0 & 0 \\ 0 & 0 \end{bmatrix},$$

$$\tag{6.49}$$

and

$$\boldsymbol{Z} \leftarrow \begin{bmatrix} \boldsymbol{Z}_1 \\ \boldsymbol{Z}_2 \end{bmatrix} = \begin{bmatrix} 0 & 1 & 0 & 0 & 0 & 0 & 0 \\ -0.1 & -8.3 & 3.75 & 0 & 0 & 0 & -28.6 \\ 2.25 & 68.89 & -30.23 & -0.98 & 0 & -35.09 & 380.38 \\ 0 & 0 & 0 & 0 & 1 & 0 & 0 \\ 0 & 0 & 1 & 0 & 0 & 0 & 0 \\ 0.37 & 0 & -0.64 & 0 & 0 & -9.5 & 0 \end{bmatrix}, \tag{6.50}$$

$$\nu_1 \leftarrow \nu_1 + 1 = 3, \quad \nu_2 \leftarrow \nu_2 + 1 = 3.$$

Iteration 5: Again, the non-zero flag $f_1 = 1$ is considered. Since $\boldsymbol{z}_{1,3}^{\mathrm{T}} \boldsymbol{D} = -701.7$ increases the rank of $\boldsymbol{\Omega}$, Case 1 is applied, i.e.,

$$f_1 \leftarrow 0, \quad \boldsymbol{\Omega} \leftarrow \begin{bmatrix} \omega_1 \\ \omega_2 \end{bmatrix} = \begin{bmatrix} -701.7 \\ 0 \end{bmatrix}. \tag{6.51}$$

Iteration 6: The flag $f_2 = 1$ is the only remaining non-zero flag. Considering $\boldsymbol{z}_{2,3}^{\mathrm{T}} \boldsymbol{D} = -190$ leads to Case 2, since $\boldsymbol{z}_{2,3}^{\mathrm{T}} \boldsymbol{D}$ can be expressed in terms of the rows of $\boldsymbol{\Omega}$, i.e., $\boldsymbol{z}_{2,3}^{\mathrm{T}} \boldsymbol{D} = \zeta_{2,3,1} \omega_1 + \zeta_{2,3,2} \omega_2$, where

$$\zeta_{2,3,1} = 0.27, \quad \zeta_{2,3,2} = 0. \tag{6.52}$$

Updating the rows of $\boldsymbol{Z}_2$ yields

$$\begin{aligned} \boldsymbol{z}_{2,1}^{\mathrm{T}} &\leftarrow \boldsymbol{z}_{2,1}^{\mathrm{T}} - \zeta_{2,3,1} \boldsymbol{z}_{1,1}^{\mathrm{T}} = \begin{bmatrix} 0 & -0.27 & 0 & 0 & 1 & 0 & 0 \end{bmatrix} \\ \boldsymbol{z}_{2,2}^{\mathrm{T}} &\leftarrow \boldsymbol{z}_{2,2}^{\mathrm{T}} - \zeta_{2,3,1} \boldsymbol{z}_{1,2}^{\mathrm{T}} = \begin{bmatrix} 0.027 & 2.25 & -0.015 & 0 & 0 & 0 & 7.74 \end{bmatrix} \\ \boldsymbol{z}_{2,3}^{\mathrm{T}} &\leftarrow \boldsymbol{z}_{2,3}^{\mathrm{T}} - \zeta_{2,3,1} \boldsymbol{z}_{1,3}^{\mathrm{T}} = \begin{bmatrix} -0.24 & -18.65 & 7.54 & 0.27 & 0 & 0 & -103 \end{bmatrix}. \end{aligned} \tag{6.53}$$

Furthermore,

$$\boldsymbol{\Psi}_2 \leftarrow \boldsymbol{\Psi}_2 - \zeta_{2,3,1} \boldsymbol{\Psi}_1 = \begin{bmatrix} -0.27 & 1 \\ 0 & 0 \\ 0 & 0 \end{bmatrix} \tag{6.54}$$

is updated. Then, Sub-case 2.2 occurs, i.e.,

$$
\boldsymbol{Z}_2 \leftarrow \begin{bmatrix} \boldsymbol{Z}_2 \\ \boldsymbol{z}_{2,3}^{\mathrm{T}}\boldsymbol{A} \end{bmatrix} = \begin{bmatrix} 0 & -0.27 & 0 & 0 & 1 & 0 & 0 \\ 0.027 & 2.25 & -0.015 & 0 & 0 & 0 & 7.74 \\ -0.24 & -18.65 & 7.54 & 0.27 & 0 & 0 & -103 \\ 4.73 & 155.09 & -66.91 & -2.34 & 0 & -70.38 & 1048.47 \end{bmatrix},
$$

$$
\boldsymbol{\Psi}_2 \leftarrow \begin{bmatrix} \boldsymbol{\Psi}_2 \\ \boldsymbol{0}^{\mathrm{T}} \end{bmatrix} = \begin{bmatrix} -0.27 & 1 \\ 0 & 0 \\ 0 & 0 \\ 0 & 0 \end{bmatrix},
$$

$$
\boldsymbol{Z} \leftarrow \begin{bmatrix} \boldsymbol{Z}_1 \\ \boldsymbol{Z}_2 \end{bmatrix} = \begin{bmatrix} 0 & 1 & 0 & 0 & 0 & 0 & 0 \\ -0.1 & -8.3 & 3.75 & 0 & 0 & 0 & -28.6 \\ 2.25 & 68.89 & -30.23 & -0.98 & 0 & -35.09 & 380.38 \\ 0 & -0.27 & 0 & 0 & 1 & 0 & 0 \\ 0.027 & 2.25 & -0.015 & 0 & 0 & 0 & 7.74 \\ -0.24 & -18.65 & 7.54 & 0.27 & 0 & 0 & -103 \\ 4.73 & 155.09 & -66.91 & -2.34 & 0 & -70.38 & 1048.47 \end{bmatrix},
$$

$$
\nu_2 \leftarrow \nu_2 + 1 = 4,
$$
(6.55)

Iteration 7: The flag $f_2 = 1$ is still non-zero. Hence, $\boldsymbol{z}_{2,4}^{\mathrm{T}}\boldsymbol{D} = -1407.61$ is examined which results in Case 2 since $\boldsymbol{z}_{2,4}^{\mathrm{T}}\boldsymbol{D} = \zeta_{2,4,1}\omega_1 + \zeta_{2,4,2}\omega_2$ with

$$
\zeta_{2,4,1} = 2.01, \quad \zeta_{2,4,2} = 0.
$$
(6.56)

The rows of $\boldsymbol{Z}_2$ are updated as

$$
\boldsymbol{z}_{2,2}^{\mathrm{T}} \leftarrow \boldsymbol{z}_{2,2}^{\mathrm{T}} - \zeta_{2,4,1}\boldsymbol{z}_{1,1}^{\mathrm{T}} = \begin{bmatrix} 0.027 & 0.24 & -0.015 & 0 & 0 & 0 & 7.74 \end{bmatrix}
$$
$$
\boldsymbol{z}_{2,3}^{\mathrm{T}} \leftarrow \boldsymbol{z}_{2,3}^{\mathrm{T}} - \zeta_{2,4,1}\boldsymbol{z}_{1,2}^{\mathrm{T}} = \begin{bmatrix} -0.038 & -2 & 0.022 & 0.27 & 0 & 0 & -45.62 \end{bmatrix}
$$
(6.57)
$$
\boldsymbol{z}_{2,4}^{\mathrm{T}} \leftarrow \boldsymbol{z}_{2,4}^{\mathrm{T}} - \zeta_{2,4,1}\boldsymbol{z}_{1,3}^{\mathrm{T}} = \begin{bmatrix} 0.22 & 16.9 & -6.27 & -0.37 & 0 & 0 & 285.43 \end{bmatrix}
$$

and

$$
\boldsymbol{\Psi}_2 \leftarrow \boldsymbol{\Psi}_2 - \zeta_{2,4,1}\begin{bmatrix} \boldsymbol{0}^{\mathrm{T}} \\ \boldsymbol{\Psi}_1 \end{bmatrix} = \begin{bmatrix} -0.27 & 1 \\ -2.01 & 0 \\ 0 & 0 \\ 0 & 0 \end{bmatrix}.
$$
(6.58)

Then, Sub-case 2.1 is entered and, hence,

$$
\boldsymbol{Z} \leftarrow \begin{bmatrix} \boldsymbol{Z}_1 \\ \boldsymbol{Z}_2 \end{bmatrix} = \begin{bmatrix} 0 & 1 & 0 & 0 & 0 & 0 & 0 \\ -0.1 & -8.3 & 3.75 & 0 & 0 & 0 & -28.6 \\ 2.25 & 68.89 & -30.23 & -0.98 & 0 & -35.09 & 380.38 \\ 0 & -0.27 & 0 & 0 & 1 & 0 & 0 \\ 0.027 & 0.24 & -0.015 & 0 & 0 & 0 & 7.74 \\ -0.038 & -2 & 0.022 & 0.27 & 0 & 0 & -45.62 \\ 0.22 & 16.9 & -6.27 & -0.37 & 0 & 0 & 285.42 \end{bmatrix}
$$
(6.59)

is updated and the corresponding flag is set to zero, i.e.,

$$f_2 \leftarrow 0. \tag{6.60}$$

It is noted that now $\boldsymbol{f} = \boldsymbol{0}$ and, thus, the iterative procedure is stopped. Furthermore, $\boldsymbol{Z}$ given in (6.59) has become an invertible $n \times n$ matrix and $\nu_1 + \nu_2 = n$. From $\nu_2 = 4 > \nu_1 = 3$ it follows that $j_1 = 2$ and $j_2 = 1$ and, thus,

$$\mu_1 = \nu_2 = 4, \quad \mu_2 = \nu_1 = 3, \quad \boldsymbol{\Gamma} = \begin{bmatrix} \boldsymbol{\psi}_{2,1}^{\mathrm{T}} \\ \boldsymbol{\psi}_{1,1}^{\mathrm{T}} \end{bmatrix} = \begin{bmatrix} -0.27 & 1 \\ 1 & 0 \end{bmatrix},$$

$$\boldsymbol{\Xi} = \boldsymbol{Z}^{-1} \begin{bmatrix} \boldsymbol{\psi}_{1,2}^{\mathrm{T}} \\ \boldsymbol{\psi}_{1,3}^{\mathrm{T}} \\ \boldsymbol{0}^{\mathrm{T}} \\ \boldsymbol{\psi}_{2,2}^{\mathrm{T}} \\ \boldsymbol{\psi}_{2,3}^{\mathrm{T}} \\ \boldsymbol{\psi}_{2,4}^{\mathrm{T}} \\ \boldsymbol{0}^{\mathrm{T}} \end{bmatrix} = \begin{bmatrix} 0 & 0 \\ 0 & 0 \\ 0 & 0 \\ 0 & 0 \\ -2.01 & 0 \\ 0 & 0 \\ 0 & 0 \end{bmatrix}. \tag{6.61}$$

Finally, the matrices of the auxiliary system are given by

$$\check{\boldsymbol{A}} = \boldsymbol{A} + \boldsymbol{\Xi}\boldsymbol{C} = \begin{bmatrix} -0.3 & 0 & -33 & 9.81 & 0 & -5.4 & 0 \\ -0.1 & -8.3 & 3.75 & 0 & 0 & 0 & -28.6 \\ 0.37 & 0 & -0.64 & 0 & 0 & -9.5 & 0 \\ 0 & 1 & 0 & 0 & 0 & 0 & 0 \\ 0 & -2.01 & 1 & 0 & 0 & 0 & 0 \\ 0 & 0 & 0 & 0 & 0 & -10 & 0 \\ 0 & 0 & 0 & 0 & 0 & 0 & -5 \end{bmatrix},$$

$$\check{\boldsymbol{C}} = \boldsymbol{\Gamma}\boldsymbol{C} = \begin{bmatrix} 0 & 0 \\ -0.27 & 1 \\ 0 & 0 \\ 0 & 0 \\ 1 & 0 \\ 0 & 0 \\ 0 & 0 \end{bmatrix}^{\mathrm{T}}. \tag{6.62}$$

Step 2: Calculation of p columns of the state transformation matrix

Calculation of the matrix

$$\mathcal{O}_{\mathrm{R}} = \begin{bmatrix} \check{\boldsymbol{c}}_1^{\mathrm{T}} \\ \check{\boldsymbol{c}}_1^{\mathrm{T}}\check{\boldsymbol{A}} \\ \check{\boldsymbol{c}}_1^{\mathrm{T}}\check{\boldsymbol{A}}^2 \\ \check{\boldsymbol{c}}_1^{\mathrm{T}}\check{\boldsymbol{A}}^3 \\ \check{\boldsymbol{c}}_2^{\mathrm{T}} \\ \check{\boldsymbol{c}}_2^{\mathrm{T}}\check{\boldsymbol{A}} \\ \check{\boldsymbol{c}}_2^{\mathrm{T}}\check{\boldsymbol{A}}^2 \end{bmatrix} = \begin{bmatrix} 0 & -0.27 & 0 & 0 & 1 & 0 & 0 \\ 0.027 & 0.24 & -0.015 & 0 & 0 & 0 & 7.74 \\ -0.038 & -2 & 0.022 & 0.27 & 0 & 0 & -45.62 \\ 0.22 & 16.9 & -6.27 & -0.37 & 0 & 0 & 285.43 \\ 0 & 1 & 0 & 0 & 0 & 0 & 0 \\ -0.1 & -8.3 & 3.75 & 0 & 0 & 0 & -28.6 \\ 2.25 & 68.89 & -30.23 & -0.98 & 0 & -35.09 & 380.38 \end{bmatrix} \tag{6.63}$$

allows for determining the columns $\boldsymbol{t}_4$ and $\boldsymbol{t}_7$ of the state transformation matrix $\boldsymbol{T}$ according to

$$
\begin{bmatrix} \boldsymbol{t}_4 & \boldsymbol{t}_7 \end{bmatrix} = \boldsymbol{\mathcal{O}}_{\mathrm{R}}^{-1} \begin{bmatrix} \boldsymbol{e}_4 & \boldsymbol{e}_7 \end{bmatrix} = \begin{bmatrix} -1.65 & 0 \\ 0 & 0 \\ 0 & 0 \\ 0.75 & 0 \\ 0 & 0 \\ -0.064 & -0.029 \\ 0.0058 & 0 \end{bmatrix}.
\tag{6.64}
$$

Step 3: Calculation of the coefficients $\beta_{j,k,l}$

The coefficients $b_{1,2,l}$ are calculated in the following way:

(a) In the given example, the matrix $\boldsymbol{H}^{(1)}$ consists of one single submatrix which actually is a scalar and equal to one, i.e.,

$$
\boldsymbol{H}^{(1)} = \begin{bmatrix} \boldsymbol{H}_{2,2}^{(1)} \end{bmatrix} = 1.
\tag{6.65}
$$

(b) The corresponding vector $\boldsymbol{\rho}^{(1)}$ is also scalar in this case and is given by

$$
\boldsymbol{\rho}^{(1)} = \begin{bmatrix} \rho_2^{(1)} \end{bmatrix} = \check{\boldsymbol{c}}_2^{\mathrm{T}} \check{\boldsymbol{A}}^3 \boldsymbol{t}_4 = -14.93.
\tag{6.66}
$$

(c) The coefficient $\beta_{1,2,3}$ is given by

$$
\boldsymbol{\beta}^{(1)} = \beta_{1,2,3} = \left(\boldsymbol{H}^{(1)} \right)^{-1} \boldsymbol{\rho}^{(1)} = -14.93.
\tag{6.67}
$$

The remaining coefficients are set to zero, i.e., $\beta_{1,2,1} = \beta_{1,2,2} = 0$.

Step 4: Construction of the state transformation matrix

The remaining columns of $\boldsymbol{T}$ are given by

$$
\begin{aligned}
\boldsymbol{t}_1 &= \check{\boldsymbol{A}}^3 \boldsymbol{t}_4 - \beta_{1,2,3} \check{\boldsymbol{A}}^2 \boldsymbol{t}_7, \\
\boldsymbol{t}_2 &= \check{\boldsymbol{A}}^2 \boldsymbol{t}_4 - \beta_{1,2,3} \check{\boldsymbol{A}} \boldsymbol{t}_7, \\
\boldsymbol{t}_3 &= \check{\boldsymbol{A}} \boldsymbol{t}_4 - \beta_{1,2,3} \boldsymbol{t}_7, \\
\boldsymbol{t}_5 &= \check{\boldsymbol{A}}^2 \boldsymbol{t}_7, \\
\boldsymbol{t}_6 &= \check{\boldsymbol{A}} \boldsymbol{t}_7,
\end{aligned}
\tag{6.68}
$$

which finally yields the state transformation matrix

$$
\boldsymbol{T} = \begin{bmatrix}
-20.30 & -3.63 & 8.23 & -1.64 & -10.52 & 0.15 & 0 \\
0 & 0 & 0 & 0 & 1 & 0 & 0 \\
18.45 & 1 & 0 & 0 & -2.82 & 0.27 & 0 \\
0 & 0 & 0 & 0.75 & 0 & 0 & 0 \\
1 & 0 & 0 & 0 & 0.27 & 0 & 0 \\
21.51 & -2.15 & 0.22 & -0.064 & -2.85 & 0.29 & -0.029 \\
-0.72 & 0.14 & -0.029 & 0.0058 & 0 & 0 & 0
\end{bmatrix}.
\tag{6.69}
$$

Applying the state transformation $\bar{\boldsymbol{x}} = \boldsymbol{T}^{-1}\boldsymbol{x}$ and the output transformation $\bar{\boldsymbol{y}} = \boldsymbol{\Gamma}\boldsymbol{y}$ yields the system

$$
\begin{aligned}
\dot{\bar{\boldsymbol{x}}} &= \bar{\boldsymbol{A}}\bar{\boldsymbol{x}} + \bar{\boldsymbol{D}}w, \\
\bar{\boldsymbol{y}} &= \bar{\boldsymbol{C}}\bar{\boldsymbol{x}},
\end{aligned}
\tag{6.70}
$$

in the proposed observer normal form, where the matrices

$$
\bar{\boldsymbol{A}} =
\left[
\begin{array}{cccc|ccc}
-6.4 & 1 & 0 & 0 & 2.01 & 0 & 0 \\
-7.01 & 0 & 1 & 0 & 11.18 & 0 & 0 \\
0 & 0 & 0 & 1 & 6 & 0 & 0 \\
0 & 0 & 0 & 0 & 1.33 & 0 & 0 \\
\hline
91.79 & 0 & 0 & 0 & -17.89 & 1 & 0 \\
593.46 & 0 & 0 & 0 & -271.73 & 0 & 1 \\
0 & 0 & 0 & -14.93 & -1220.79 & 0 & 0
\end{array}
\right], \quad
\bar{\boldsymbol{D}} =
\left[
\begin{array}{c}
0 \\
0 \\
0 \\
0 \\
\hline
0 \\
0 \\
-701.7
\end{array}
\right],
\tag{6.71}
$$

$$
\bar{\boldsymbol{C}} =
\left[
\begin{array}{cccc|ccc}
1 & 0 & 0 & 0 & 0 & 0 & 0 \\
0 & 0 & 0 & 0 & 1 & 0 & 0
\end{array}
\right],
$$

are calculated according to (6.12).

6.4.2 Design of the Unknown Input Observer

In order to reconstruct the state vector $\bar{\boldsymbol{x}}$ despite the unknown input w, an unknown input observer is designed according to Section 6.2 which yields

$$
\begin{aligned}
\dot{\hat{\bar{\boldsymbol{x}}}} &= \bar{\boldsymbol{A}}\hat{\bar{\boldsymbol{x}}} + \bar{\boldsymbol{\Pi}}\boldsymbol{\sigma}_{\bar{\boldsymbol{y}}} + \bar{\boldsymbol{l}}(\boldsymbol{\sigma}_{\bar{\boldsymbol{y}}}), \\
\hat{\bar{\boldsymbol{y}}} &= \bar{\boldsymbol{C}}\hat{\bar{\boldsymbol{x}}},
\end{aligned}
\tag{6.72}
$$

where

$$
\boldsymbol{\sigma}_{\bar{\boldsymbol{y}}} = \bar{\boldsymbol{y}} - \hat{\bar{\boldsymbol{y}}} = \begin{bmatrix} \sigma_1 & \sigma_5 \end{bmatrix}^{\mathrm{T}}
\tag{6.73}
$$

is the output error,

$$
\bar{\boldsymbol{\Pi}} =
\left[
\begin{array}{cc}
-6.4 & 2.01 \\
-7.01 & 11.18 \\
0 & 6 \\
0 & 1.33 \\
\hline
91.79 & -17.84 \\
593.46 & -271.73 \\
0 & -1220.79
\end{array}
\right]
\tag{6.74}
$$

is the linear output-injection matrix and

$$
\bar{\boldsymbol{l}}(\boldsymbol{\sigma}_{\bar{\boldsymbol{y}}}) =
\Big[
\begin{array}{cccc}
\kappa_{1,3}\lfloor\sigma_1\rceil^{\frac{3}{4}} & \kappa_{1,2}\lfloor\sigma_1\rceil^{\frac{1}{2}} & \kappa_{1,1}\lfloor\sigma_1\rceil^{\frac{1}{4}} & \kappa_{1,0}\lfloor\sigma_1\rceil^{0}
\end{array}
\Big|
$$
$$
\begin{array}{ccc}
\kappa_{2,2}\lfloor\sigma_5\rceil^{\frac{2}{3}} & \kappa_{2,1}\lfloor\sigma_5\rceil^{\frac{1}{3}} & \kappa_{2,0}\lfloor\sigma_5\rceil^{0}
\end{array}
\Big]^{\mathrm{T}}
\tag{6.75}
$$
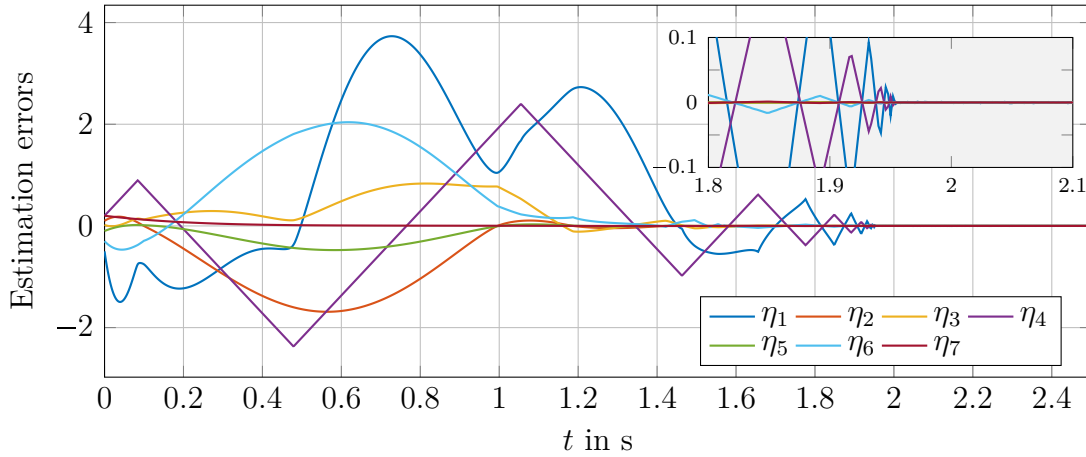
Figure 6.1: *Estimation error variables $\eta_i = x_i - \hat{x}_i$, $i = 1, \ldots, 7$ in original coordinates. The estimation error variables vanish within finite-time despite the unknown input w.*

is the nonlinear output injection vector.

It is pointed out that, since the unknown input w does not directly act on the first subsystem, it is also possible to choose the nonlinear output injection of the first subsystem according to e.g. a continuous finite-time differentiator [26], i.e.,

$$\bar{l}(\boldsymbol{\sigma}_{\bar{y}}) \rightsquigarrow \bar{l}'(\boldsymbol{\sigma}_{\bar{y}}) = \left[\begin{array}{cccc} \kappa'_{1,3}\lfloor\sigma_1\rceil^{\frac{r_2}{r_1}} & \kappa'_{1,2}\lfloor\sigma_1\rceil^{\frac{r_3}{r_1}} & \kappa'_{1,1}\lfloor\sigma_1\rceil^{\frac{r_4}{r_1}} & \kappa'_{1,0}\lfloor\sigma_1\rceil^{\frac{r_5}{r_1}} \end{array} \right| \quad \kappa_{2,2}\lfloor\sigma_5\rceil^{\frac{2}{3}} \quad \kappa_{2,1}\lfloor\sigma_5\rceil^{\frac{1}{3}} \quad \kappa_{2,0}\lfloor\sigma_5\rceil^0 \left. \right]^{\mathrm{T}},$$

(6.76)

where $r_i = 1 - (n-i)q$, $i = 1, \ldots, n+1$ are the homogeneity weights and $q \in (-1, 0)$ is the homogeneity degree to be chosen.

6.4.3 Simulation Results

The observer parameters

$$\begin{aligned} \kappa_{1,3} &= 5.33, \quad \kappa_{1,2} = 13.16, \quad \kappa_{1,1} = 17.20, \quad \kappa_{1,0} = 11, \\ \kappa_{2,2} &= 9.65, \quad \kappa_{2,1} = 49.37, \quad \kappa_{2,0} = 123.5, \end{aligned}$$

(6.77)

of the nonlinear output injection (6.75) are chosen according to [29, Section 6.7]. Note that the necessary condition $\kappa_{2,0} > L|\bar{d}_{7,1}| = 14.03$ given in Theorem 6.2.1 is satisfied. The initial observer state vector is selected as $\hat{\bar{\boldsymbol{x}}}(0) = \boldsymbol{0}$ and the unknown input is taken from Example 4.2.1. The estimation error variables $\eta_i = x_i - \hat{x}_i$, $i = 1, \ldots, 7$ obtained by a numerical simulation are shown in Figure 6.1. After a finite convergence time of approximately 2 s, the error variables vanish despite the unknown input w and, thus, exact estimates of the unbounded[4] state variables are obtained.

---

[4]Due to the unstable eigenvalues of $\boldsymbol{A}$, see Example 4.2.1.

6.5 Conclusions on the Multiple-Input Multiple-Output Case

In this chapter, a new unknown input observer for LTI MIMO systems has been proposed. The main contribution is given by a new observer normal form for strongly observable LTI systems with unknown inputs. In contrast to existing observer normal forms, the proposed observer normal form additionally accounts for the unknown input by enforcing a specific structure of the unknown-input matrix $\bar{D}$. Once the system is represented in observer normal form, the design of a differentiator based unknown input observer is straightforward, which is exemplarily demonstrated by applying multiple REDs in Theorem 6.2.1. The proposed unknown input observer is consistent with the SISO case proposed in Chapter 5 and coincides with the existing approaches based on Luenberger's observability canonical form, if the system satisfies the restrictive relative degree condition (4.34).

In the following, the proposed unknown input observer is evaluated with respect to the disadvantages of existing methods discussed in Section 4.3:

(a) The restrictive observer matching condition (4.15) is not required. For example, the system considered in the tutorial example in Section 6.4 does not satisfy the observer matching condition.

(b) The unknown input observer does not require bounded state variables to ensure convergence of the estimation error dynamics, as the necessary condition for the choice of $\kappa_{j,0}$ is independent of the state variables and the estimation errors. This is confirmed by the unstable example system in Section 6.4 whose trajectories are unbounded.

(c) The unknown input does not have to be differentiable. During the derivations made, no derivatives of w occur.

(d) The necessary condition $\kappa_{j,0} > \sum\limits_{i=1}^{m} L_i \left| \bar{d}_{\mu_1 + \cdots + \mu_j, i} \right|$ for the choice of the observer parameters does not involve any state variables. Hence, the required parameters depends on the unknown input only, but not on the particular system trajectories.

(e) The observer order as well as the number of tuning parameters are equal to the order n of the original system and, thus, not unnecessarily increased. For the system considered in the tutorial example an unknown input observer of order 7 with 7 parameters is obtained, see Section 6.4, whereas the cascaded unknown input observer in Example 4.2.5 has order 41 and 45 parameters to tune.

(f) The restrictive relative degree condition (4.34) is not required. In contrast to the unknown input observer based on Luenberger's observability canonical form, the proposed unknown input observer achieves exact reconstruction of the state variables for the considered example.

It can be concluded that the proposed unknown input observer avoids all the drawbacks of existing approaches. The effectiveness of the unknown input observer and especially the simplicity of its design in observer normal form have been demonstrated by means of the tutorial example.

7

Extensions and Generalizations

This chapter demonstrates the versatility and usability of the previously presented unknown input observer. Several extensions and generalizations are discussed. The unknown input observer concept is extended to systems with direct feed-through term, to strongly detectable systems and to systems with unbounded unknown inputs with bounded time-derivative. Moreover, The applicability to state-feedback control for systems with matched disturbance inputs is shown. For the case of asymmetric bounds of the the unknown input, a method is provided which allows for decreasing the required observer parameters and, thus, helps to reduce the impact of measurement noise and chattering effects.

7.1 Extension to Systems with Direct Feed-Through Term

The unknown input observer design proposed in Chapter 6 can also be applied to systems with direct feed-through in a straightforward manner which is shown in this section. For this purpose, consider the class of LTI systems of the form

$$\begin{aligned}
\dot{\boldsymbol{x}} &= \boldsymbol{A}\boldsymbol{x} + \boldsymbol{D}\boldsymbol{w}, \\
\boldsymbol{y} &= \boldsymbol{C}\boldsymbol{x} + \boldsymbol{F}\boldsymbol{w},
\end{aligned} \tag{7.1}$$

where $\boldsymbol{F} \in \mathbb{R}^{p \times m}$. First, the state estimation problem is reformulated by introducing an equivalent system without direct feed-through term. Then, it is shown that the equivalent system preserves the property of strong observability and, hence, the methods proposed in Chapter 6 can be applied to this equivalent system.

The content of this section is adopted from Appendix 1 of:

7.1.1 Reformulation as System without Direct Feed-Through

In order to obtain an equivalent representation of system (7.1) without direct feed-through, the algorithm proposed in [25, Section 5.4, page 155] is applied. Regular transformation matrices $\boldsymbol{U} \in \mathbb{R}^{p \times p}$ for the output and $\boldsymbol{V} \in \mathbb{R}^{m \times m}$ for the input are chosen[1] such that

$$\boldsymbol{U}\boldsymbol{F}\boldsymbol{V} = \begin{bmatrix} \boldsymbol{I}_{m_{\mathrm{F}}} & \boldsymbol{0} \\ \boldsymbol{0} & \boldsymbol{0} \end{bmatrix}, \tag{7.2}$$

where $m_{\mathrm{F}} = \operatorname{rank} \boldsymbol{F}$. The application of the output and input transformation

$$\tilde{\boldsymbol{y}} = \boldsymbol{U}\boldsymbol{y} = \begin{bmatrix} \tilde{\boldsymbol{y}}_0 \\ \tilde{\boldsymbol{y}}_1 \end{bmatrix}, \qquad \tilde{\boldsymbol{w}} = \boldsymbol{V}^{-1}\boldsymbol{w} = \begin{bmatrix} \tilde{\boldsymbol{w}}_0 \\ \tilde{\boldsymbol{w}}_1 \end{bmatrix}, \tag{7.3}$$

allows for an equivalent representation of system (7.1) with the new output $\tilde{\boldsymbol{y}}$ and the new input $\tilde{\boldsymbol{w}}$, i.e.,

$$\dot{\boldsymbol{x}} = \boldsymbol{A}\boldsymbol{x} + \begin{bmatrix} \tilde{\boldsymbol{D}}_0 & \tilde{\boldsymbol{D}}_1 \end{bmatrix} \begin{bmatrix} \tilde{\boldsymbol{w}}_0 \\ \tilde{\boldsymbol{w}}_1 \end{bmatrix}, \tag{7.4a}$$

$$\begin{bmatrix} \tilde{\boldsymbol{y}}_0 \\ \tilde{\boldsymbol{y}}_1 \end{bmatrix} = \begin{bmatrix} \tilde{\boldsymbol{C}}_0 \\ \tilde{\boldsymbol{C}}_1 \end{bmatrix} \boldsymbol{x} + \begin{bmatrix} \boldsymbol{I}_{m_{\mathrm{F}}} & \boldsymbol{0} \\ \boldsymbol{0} & \boldsymbol{0} \end{bmatrix} \begin{bmatrix} \tilde{\boldsymbol{w}}_0 \\ \tilde{\boldsymbol{w}}_1 \end{bmatrix}, \tag{7.4b}$$

where $\tilde{\boldsymbol{D}}_0 \in \mathbb{R}^{n \times m_{\mathrm{F}}}$, $\tilde{\boldsymbol{D}}_1 \in \mathbb{R}^{n \times (m-m_{\mathrm{F}})}$, $\tilde{\boldsymbol{C}}_0 \in \mathbb{R}^{m_{\mathrm{F}} \times n}$ and $\tilde{\boldsymbol{C}}_1 \in \mathbb{R}^{(p-m_{\mathrm{F}}) \times n}$. The output equation (7.4b) is solved for

$$\tilde{\boldsymbol{w}}_0 = \tilde{\boldsymbol{y}}_0 - \tilde{\boldsymbol{C}}_0 \boldsymbol{x} \tag{7.5}$$

and substituted into (7.4a) which yields

$$\dot{\boldsymbol{x}} = \boldsymbol{A}\boldsymbol{x} + \tilde{\boldsymbol{D}}_0 \left(\tilde{\boldsymbol{y}}_0 - \tilde{\boldsymbol{C}}_0 \boldsymbol{x} \right) + \tilde{\boldsymbol{D}}_1 \tilde{\boldsymbol{w}}_1. \tag{7.6}$$

Combining (7.6) and the remaining outputs $\tilde{\boldsymbol{y}}_1$ given in (7.4b) finally results the equivalent system without direct feed-through

$$\begin{aligned} \dot{\boldsymbol{x}} &= \tilde{\boldsymbol{A}}\boldsymbol{x} + \tilde{\boldsymbol{D}}_1 \tilde{\boldsymbol{w}}_1 + \tilde{\boldsymbol{D}}_0 \tilde{\boldsymbol{y}}_0, \\ \tilde{\boldsymbol{y}}_1 &= \tilde{\boldsymbol{C}}_1 \boldsymbol{x}, \end{aligned} \tag{7.7}$$

where $\tilde{\boldsymbol{A}} = \boldsymbol{A} - \tilde{\boldsymbol{D}}_0 \tilde{\boldsymbol{C}}_0$.

Instead of the original system (7.1) the equivalent system (7.7) without direct feed-through can be considered for the estimation of $\boldsymbol{x}$. Since the property of strong observability is preserved as shown later, the unknown input observer design procedure proposed in Chapter 6 can be applied to system (7.7). In addition to the unknown input $\tilde{\boldsymbol{w}}_1$, $\tilde{\boldsymbol{y}}_0$ acts as an input to the system. However, as $\tilde{\boldsymbol{y}}_0$ is known it can be easily considered by an observer, see Section 2.2.3.

---

[1]For instance by applying singular value decomposition.

7.1.2 Preservation of Strong observability

In the following, it is shown that strong observability of the original system (7.1) with direct feed-through implies strong observability of the equivalent system (7.7) without direct feed-through.

Since the strong observability property is invariant with respect to to regular transformations of the output and the input, strong observability of system (7.4) directly follows from the strong observability of the original system (7.1). According to Proposition 2.3.1, the Rosenbrock matrix of system (7.4) satisfies

$$
\operatorname{rank}
\begin{bmatrix}
s\boldsymbol{I}_n - \boldsymbol{A} & -\tilde{\boldsymbol{D}}_0 & -\tilde{\boldsymbol{D}}_1 \\
\tilde{\boldsymbol{C}}_0 & \boldsymbol{I}_{m_\mathrm{F}} & \boldsymbol{0} \\
\tilde{\boldsymbol{C}}_1 & \boldsymbol{0} & \boldsymbol{0}
\end{bmatrix}
= n + m \qquad \forall s \in \mathbb{C}.
\tag{7.8}
$$

Furthermore, consider the Rosenbrock matrix[2]

$$
\tilde{\boldsymbol{P}}(s) =
\begin{bmatrix}
s\boldsymbol{I}_n - (\boldsymbol{A} - \tilde{\boldsymbol{D}}_0\tilde{\boldsymbol{C}}_0) & -\tilde{\boldsymbol{D}}_1 \\
\tilde{\boldsymbol{C}}_1 & \boldsymbol{0}
\end{bmatrix}
\tag{7.9}
$$

of the equivalent system (7.7). It follows that

$$
\begin{aligned}
\operatorname{rank} \tilde{\boldsymbol{P}}(s) = \operatorname{rank}
&\begin{bmatrix}
s\boldsymbol{I}_n - (\boldsymbol{A} - \tilde{\boldsymbol{D}}_0\tilde{\boldsymbol{C}}_0) & -\tilde{\boldsymbol{D}}_1 \\
\boldsymbol{0} & \boldsymbol{0} \\
\tilde{\boldsymbol{C}}_1 & \boldsymbol{0}
\end{bmatrix} = \\
= \operatorname{rank}
&\begin{bmatrix}
s\boldsymbol{I}_n - \boldsymbol{A} & -\tilde{\boldsymbol{D}}_0 & -\tilde{\boldsymbol{D}}_1 \\
\tilde{\boldsymbol{C}}_0 & \boldsymbol{I}_{m_\mathrm{F}} & \boldsymbol{0} \\
\tilde{\boldsymbol{C}}_1 & \boldsymbol{0} & \boldsymbol{0}
\end{bmatrix}
\begin{bmatrix}
\boldsymbol{I}_n & \boldsymbol{0} \\
-\tilde{\boldsymbol{C}}_0 & \boldsymbol{0} \\
\boldsymbol{0} & \boldsymbol{I}_{m-m_\mathrm{F}}
\end{bmatrix} = \\
\overset{(7.8)}{=} \operatorname{rank}
&\begin{bmatrix}
\boldsymbol{I}_n & \boldsymbol{0} \\
-\tilde{\boldsymbol{C}}_0 & \boldsymbol{0} \\
\boldsymbol{0} & \boldsymbol{I}_{m-m_\mathrm{F}}
\end{bmatrix} = n + m - m_\mathrm{F} = n + \operatorname{rank} \tilde{\boldsymbol{D}}_1 \quad \forall s \in \mathbb{C},
\end{aligned}
\tag{7.10}
$$

and, thus, system (7.7) is strongly observable according to Proposition 2.3.1. In conclusion, strong observability of the original system (7.1) implies strong observability of the equivalent system (7.7). Thus, the unknown input observer design procedure proposed in Chapter 6 can be applied to the equivalent system (7.7) if the original system (7.1) is strongly observable.

---

[2]Note that the input matrix $\tilde{\boldsymbol{D}}_0$ is not considered in the Rosenbrock matrix (7.9) since the input $\tilde{\boldsymbol{y}}_0$ is known and, thus, does not affect the property of strong observability.

7.2 Extension to Strongly Detectable Systems

In this section, the presented unknown input observer for strongly observable systems is generalized to the strongly detectable case. The content of this section shortly summarizes one main idea of the content presented in:

M. Tranninger, H. Niederwieser, R. Seeber, M. Horn, Unknown input observer design for linear time-invariant systems—a unifying framework, International Journal of Robust and Nonlinear Control 33 (15) (2023) 8911–8934. `doi:10.1002/rnc.6399`

7.2.1 Structural System Decomposition

In the case the system is not strongly observable but at least strongly detectable, the system can be transformed into the representation

$$\begin{bmatrix} \dot{z}_1 \\ \dot{z}_2 \end{bmatrix} = \begin{bmatrix} \breve{A}_1 & \breve{L}\breve{C}_2 \\ \breve{D}_2\breve{K} & \breve{A}_2 \end{bmatrix} \begin{bmatrix} z_1 \\ z_2 \end{bmatrix} + \begin{bmatrix} 0 \\ \breve{D}_2 \end{bmatrix} w,$$

$$y = \begin{bmatrix} 0 & \breve{C}_2 \end{bmatrix} \begin{bmatrix} z_1 \\ z_2 \end{bmatrix}, \tag{7.11}$$

or, equivalently,

$$\dot{z}_1 = \breve{A}_1 z_1 + \breve{L} y, \tag{7.12a}$$

$$\dot{z}_2 = \breve{A}_2 z_2 + \breve{D}_2(\breve{K} z_1 + w), \tag{7.12b}$$

$$y = \breve{C}_2 z_2, \tag{7.12c}$$

by means of the state transformation $\begin{bmatrix} z_1 & z_2 \end{bmatrix}^{\mathrm{T}} = \breve{T} x$ proposed in [25, Chapter 5.4]. In this representation, the system is decomposed into two subsystems:

1. Subsystem (7.12a) with the state vector z_1 constitutes the part of the system which is strongly detectable only. This part of the system is not explicitly influenced by the unknown input w and its state vector z_1 does not appear in the system output y. Due to the strong detectability property, its dynamic matrix $\breve{A}_1$ is a Hurwitz matrix. Furthermore, the system output y acts as a known input via the input matrix $\breve{L}$.

2. Subsystem (7.12b) with the state vector z_2 represents the strongly observable part of the system, i.e., the triple $(\breve{A}_2, \breve{C}_2, \breve{D}_2)$ is strongly observable. In addition, this subsystem is coupled via $\breve{K} z_1$ to the part of the system that is strongly detectable only. It is pointed out that the coupling term acts in the same channels as the unknown input and, hence, can not be distinguished from the unknown input by means of the output.

7.2.2 Unknown Input Observer Design

An observer is now designed for each of the two subsystems individually. For subsystem (7.12a) a trivial observer

$$\dot{\hat{z}}_1 = \breve{A}_1 \hat{z}_1 + \breve{L} y, \tag{7.13}$$

is designed. The dynamics of its estimation error $\boldsymbol{\zeta}_1 = \boldsymbol{z}_1 - \hat{\boldsymbol{z}}_1$ are given by

$$\dot{\boldsymbol{\zeta}}_1 = \breve{\boldsymbol{A}}_1 \boldsymbol{\zeta}_1. \tag{7.14}$$

Since $\breve{\boldsymbol{A}}_1$ is a Hurwitz matrix, the estimation error dynamics are asymptotically stable, i.e., $\lim_{t \to \infty} \boldsymbol{\zeta}_1 = \boldsymbol{0}$. Furthermore, $\boldsymbol{\zeta}_1$ converges within an arbitrarily small vicinity around the origin within some finite time $\tau_1(\boldsymbol{\zeta}_1(0)) > 0$, which is exploited by the observer for the second subsystem later on.

Subsystem (7.12b) is strongly observable and, hence, can be transformed in observer normal form

$$\begin{aligned}
\dot{\bar{\boldsymbol{z}}}_2 &= \bar{\boldsymbol{A}}_2 \bar{\boldsymbol{z}}_2 + \bar{\boldsymbol{D}}_2 (\breve{\boldsymbol{K}} \boldsymbol{z}_1 + \boldsymbol{w}), \\
\bar{\boldsymbol{y}} &= \bar{\boldsymbol{C}}_2 \bar{\boldsymbol{z}}_2,
\end{aligned} \tag{7.15}$$

by applying suitable transformations $\bar{\boldsymbol{z}}_2 = \boldsymbol{T}^{-1} \boldsymbol{z}_2$ and $\bar{\boldsymbol{y}} = \boldsymbol{\Gamma} \boldsymbol{y}$, see Section 6.3. Therein, the unknown input observer

$$\begin{aligned}
\dot{\hat{\bar{\boldsymbol{z}}}}_2 &= \bar{\boldsymbol{A}}_2 \hat{\bar{\boldsymbol{z}}}_2 + \bar{\boldsymbol{D}}_2 \breve{\boldsymbol{K}} \hat{\boldsymbol{z}}_1 + \bar{\boldsymbol{\Pi}} \boldsymbol{\sigma}_{\bar{\boldsymbol{y}}} + \bar{\boldsymbol{l}}(\boldsymbol{\sigma}_{\bar{\boldsymbol{y}}}), \\
\hat{\bar{\boldsymbol{y}}} &= \bar{\boldsymbol{C}}_2 \hat{\bar{\boldsymbol{z}}}_2,
\end{aligned} \tag{7.16}$$

with the output estimation error $\boldsymbol{\sigma}_{\bar{\boldsymbol{y}}} = \boldsymbol{y} - \hat{\bar{\boldsymbol{y}}}$ is applied, which additionally considers estimates $\hat{\boldsymbol{z}}_1$ of the first subsystem. The dynamics of the estimation error $\boldsymbol{\sigma}_2 = \bar{\boldsymbol{z}}_2 - \hat{\bar{\boldsymbol{z}}}_2$ are given by

$$\dot{\boldsymbol{\sigma}}_2 = \bar{\boldsymbol{A}}_2 \boldsymbol{\sigma}_2 - \bar{\boldsymbol{\Pi}} \boldsymbol{\sigma}_{\bar{\boldsymbol{y}}} - \bar{\boldsymbol{l}}(\boldsymbol{\sigma}_{\bar{\boldsymbol{y}}}) + \bar{\boldsymbol{D}}_2 (\breve{\boldsymbol{K}} \boldsymbol{\zeta}_1 + \boldsymbol{w}), \tag{7.17}$$

which coincide with the estimation error dynamics (6.7) of the proposed unknown input observer, where $\breve{\boldsymbol{K}} \boldsymbol{\zeta}_1$ additionally acts in the channel of the unknown input. As the error $\boldsymbol{\zeta}_1$ convergences into an arbitrarily small vicinity around the origin within finite time τ_1, boundedness of $\breve{\boldsymbol{K}} \boldsymbol{\zeta}_1$ for all $t \geqslant \tau_1$ can be guaranteed. Thus, all the terms acting in the channel of the unknown input[3] are bounded and $\boldsymbol{\sigma}_2$ vanishes within finite time for appropriately chosen observer parameters.

---

[3]The coupling term error $\breve{\boldsymbol{K}} \boldsymbol{\zeta}_1$ and the unknown input $\boldsymbol{w}$ itself.

7.3 Extension to Unbounded Inputs with Bounded Derivatives

It may happen that some of the unknown inputs w_i, are not bounded[4], but their γ_i-th derivative $w_i^{(\gamma_i)}$ is bounded instead, i.e.,

$$\left| w_i^{(\gamma_i)}(t) \right| \leqslant \tilde{L}_i \quad \forall t, \qquad \text{with} \quad 0 \leqslant \tilde{L}_i < \infty, \quad i = 1, \dots, m. \tag{7.18}$$

In this case, the system can be extended and the unknown input observer proposed in Chapter 6 can still be applied by using the following procedure which regards $w_i^{(\gamma_i)}$ as unknown inputs rather than w_i, see e.g. in [95–97].

7.3.1 Augmentation of the State Vector

Without loss of generality assume that the unknown inputs are ordered such that $\gamma_i > 0$ for $i = 1, \dots, \tilde{m}$ and $\gamma_i = 0$ for $i = \tilde{m} + 1, \dots, m$. The state vector is augmented with the unbounded unknown inputs $w_1, \dots, w_{\tilde{m}}$ and their first $(\gamma_i - 1)$-st derivatives accordingly, i.e.,

$$\boldsymbol{\chi} = \left[\begin{array}{c|ccccc|c|cccc} \boldsymbol{x}^\mathrm{T} & w_1 & \dot{w}_1 & \dots & w_1^{(\gamma_1 - 1)} & \dots & w_{\tilde{m}} & \dot{w}_{\tilde{m}} & \dots & w_{\tilde{m}}^{(\gamma_{\tilde{m}} - 1)} \end{array} \right]^\mathrm{T}. \tag{7.19}$$

System (6.2) given on page 55 in combination with the dynamics of the unknown inputs is captured by

$$\dot{\boldsymbol{\chi}} = \boldsymbol{A}_\chi \boldsymbol{\chi} + \boldsymbol{D}_\chi \tilde{\boldsymbol{w}}, \tag{7.20a}$$
$$\boldsymbol{y} = \boldsymbol{C}_\chi \boldsymbol{\chi},$$

with the matrices

$$\boldsymbol{A}_\chi = \left[\begin{array}{c|cc|c|cc} \boldsymbol{A} & \boldsymbol{d}_1 & \boldsymbol{0} & \dots & \boldsymbol{d}_{\tilde{m}} & \boldsymbol{0} \\ \hline \boldsymbol{0} & 0 & \boldsymbol{I}_{\gamma_1 - 1} & & \boldsymbol{0} & \boldsymbol{0} \\ \boldsymbol{0}^\mathrm{T} & 0 & \boldsymbol{0}^\mathrm{T} & & 0 & \boldsymbol{0}^\mathrm{T} \\ \hline \vdots & & & \ddots & & \\ \hline \boldsymbol{0} & \boldsymbol{0} & \boldsymbol{0} & & 0 & \boldsymbol{I}_{\gamma_{\tilde{m}} - 1} \\ \boldsymbol{0}^\mathrm{T} & 0 & \boldsymbol{0}^\mathrm{T} & & 0 & \boldsymbol{0}^\mathrm{T} \end{array} \right], \tag{7.20b}$$

$$\boldsymbol{D}_\chi = \left[\begin{array}{ccc|ccc} \boldsymbol{0} & \dots & \boldsymbol{0} & \boldsymbol{d}_{\tilde{m}+1} & \dots & \boldsymbol{d}_m \\ \hline \boldsymbol{e}_{\gamma_1} & & \boldsymbol{0} & \boldsymbol{0} & \dots & \boldsymbol{0} \\ & \ddots & & \vdots & & \vdots \\ \boldsymbol{0} & & \boldsymbol{e}_{\gamma_{\tilde{m}}} & \boldsymbol{0} & \dots & \boldsymbol{0} \end{array} \right], \quad \boldsymbol{C}_\chi = \left[\begin{array}{cc} \boldsymbol{C} & \boldsymbol{0}_{p \times (\gamma_1 + \dots + \gamma_{\tilde{m}})} \end{array} \right],$$

and the new unknown input

$$\tilde{\boldsymbol{w}} = \left[\begin{array}{ccc|ccc} w_1^{(\gamma_1)} & \dots & w_{\tilde{m}}^{(\gamma_{\tilde{m}})} & w_{\tilde{m}+1} & \dots & w_m \end{array} \right]^\mathrm{T}. \tag{7.20c}$$

---

[4]This means a violation of Assumption 4.1.2.

The extended system (7.20) preserves the strong observability property, which is shown in the next section, and the single components of the unknown input vector $\tilde{\boldsymbol{w}}$ are bounded by assumption (7.18). Thus, an unknown input observer for the extended system (7.20) can be designed according to Chapter 6. It is pointed out that the resulting unknown input observer, in addition to the system state $\boldsymbol{x}$, also estimates the unknown inputs and their derivatives contained in $\boldsymbol{\chi}$.

7.3.2 Preservation of Strong Observability

It is shown that the extended system (7.20) is strongly observable, if the original system is strongly observable. For this purpose, the augmentation of the state vector with just one single unknown input is considered first. Then, the general result is obtained by induction.

Consider the original state vector $\boldsymbol{x}$ augmented by the first unknown input w_1 which yields the extended system

$$
\begin{bmatrix} \dot{\boldsymbol{x}} \\ \dot{w}_1 \end{bmatrix} = \begin{bmatrix} \boldsymbol{A} & \boldsymbol{d}_1 \\ \boldsymbol{0}^\mathrm{T} & 0 \end{bmatrix} \begin{bmatrix} \boldsymbol{x} \\ w_1 \end{bmatrix} + \begin{bmatrix} \boldsymbol{0} & \boldsymbol{d}_2 & \dots & \boldsymbol{d}_m \\ 1 & 0 & \dots & 0 \end{bmatrix} \begin{bmatrix} \dot{w}_1 \\ w_2 \\ \vdots \\ w_m \end{bmatrix},
$$

$$
\boldsymbol{y} = \begin{bmatrix} \boldsymbol{C} & \boldsymbol{0} \end{bmatrix} \begin{bmatrix} \boldsymbol{x} \\ w_1 \end{bmatrix}.
$$

(7.21)

The rank of its Rosenbrock matrix $\tilde{\boldsymbol{P}}(s)$ is given by

$$
\begin{aligned}
\mathrm{rank}\,\tilde{\boldsymbol{P}}(s) &= \mathrm{rank} \begin{bmatrix} s\boldsymbol{I}_n - \boldsymbol{A} & -\boldsymbol{d}_1 & \boldsymbol{0} & -\boldsymbol{d}_2 & \dots & -\boldsymbol{d}_m \\ \boldsymbol{0}^\mathrm{T} & s & -1 & 0 & \dots & 0 \\ \boldsymbol{C} & \boldsymbol{0} & \boldsymbol{0} & \dots & \dots & \boldsymbol{0} \end{bmatrix} = \\
&= \mathrm{rank} \begin{bmatrix} s\boldsymbol{I}_n - \boldsymbol{A} & -\boldsymbol{d}_1 & -\boldsymbol{d}_2 & \dots & -\boldsymbol{d}_m \\ \boldsymbol{C} & \boldsymbol{0} & \dots & \dots & \boldsymbol{0} \end{bmatrix} + 1 = \\
&= \mathrm{rank} \begin{bmatrix} s\boldsymbol{I}_n - \boldsymbol{A} & -\boldsymbol{D} \\ \boldsymbol{C} & \boldsymbol{0} \end{bmatrix} + 1 = \mathrm{rank}\,\boldsymbol{P}(s) + 1,
\end{aligned}
$$

(7.22)

where $\boldsymbol{P}(s)$ is the Rosenbrock matrix of the original system, i.e., without the state augmentation. Any further augmentation of the state vector with either another unknown input or one further derivative of an already included unknown input increases the rank of the respective Rosenbrock matrix by one, which can be shown by following the same line of reasoning. Thus, it is concluded that the Rosenbrock matrix $\boldsymbol{P}_{\boldsymbol{\chi}}(s)$ of the extended system (7.20) satisfies

$$
\begin{aligned}
\mathrm{rank}\,\boldsymbol{P}_{\boldsymbol{\chi}}(s) &= \mathrm{rank} \begin{bmatrix} s\boldsymbol{I}_{n+\gamma_1+\dots+\gamma_{\tilde{m}}} - \boldsymbol{A}_{\boldsymbol{\chi}} & -\boldsymbol{D}_{\boldsymbol{\chi}} \\ \boldsymbol{C}_{\boldsymbol{\chi}} & \boldsymbol{0} \end{bmatrix} = \\
&= \mathrm{rank}\,\boldsymbol{P}(s) + \gamma_1 + \dots + \gamma_{\tilde{m}}.
\end{aligned}
$$

(7.23)

It becomes apparent that the extended system (7.20) is strongly observable, i.e., $\mathrm{rank}\,\tilde{\boldsymbol{P}}(s) = n + \gamma_1 + \dots + \gamma_{\tilde{m}} \ \forall s \in \mathbb{C}$, if and only if the original system is strongly observable, i.e., $\mathrm{rank}\,\boldsymbol{P}(s) = n \ \forall s \in \mathbb{C}$.

7.4 Application to State-Feedback Control for Systems with Matched Disturbance Inputs

The unknown input observer proposed in Chapter 6 can be utilized in the construction of state-feedback controllers for system with matched disturbance inputs which is shown in the following. The content of this section is partially adopted from Section 5.4 of:

H. Niederwieser, M. Tranninger, R. Seeber, M. Reichhartinger, Unknown input observer design for linear time-invariant multivariable systems based on a new observer normal form, International Journal of Systems Science 53 (10) (2022) 2180–2206. `doi:10.1080/00207721.2022.2046201`

7.4.1 Formulation of the Control Problem

Consider the strongly observable and stabilizable[5] system

$$
\begin{aligned}
\dot{\boldsymbol{x}} &= \boldsymbol{A}\boldsymbol{x} + \boldsymbol{B}\boldsymbol{u} + \boldsymbol{D}\boldsymbol{w}, \\
\boldsymbol{y} &= \boldsymbol{C}\boldsymbol{x},
\end{aligned}
\tag{7.24}
$$

where the unknown input $\boldsymbol{w}$ acts as a matched disturbance with respect to the control input $\boldsymbol{u} \in \mathbb{R}^o$, i.e.,

$$
\boldsymbol{D} = \boldsymbol{B}\boldsymbol{M}
\tag{7.25}
$$

with a constant matrix $\boldsymbol{M} \in \mathbb{R}^{o \times m}$. Furthermore, assume the first derivative $\dot{\boldsymbol{w}}$ of the unknown input to be bounded, i.e.,

$$
|\dot{w}_i(t)| \leqslant \tilde{L}_i \quad \forall t, \qquad \text{with} \quad 0 \leqslant \tilde{L}_i < \infty, \quad i = 1, \dots, m.
\tag{7.26}
$$

The goal is to stabilize system (7.24) at $\boldsymbol{x} = \boldsymbol{0}$ by means of a controller despite the unknown input $\boldsymbol{w}$.

7.4.2 Disturbance Rejection via Unknown Input Observation and State-Feedback Control

This task can be achieved by a linear state-feedback controller with additional disturbance feed-forward. However, the state vector as well as the unknown input are unknown and must be estimated. For this purpose, the method presented in Section 7.3 is applied. The state vector is augmented by $\boldsymbol{w}$, i.e.,

$$
\boldsymbol{\chi} = \begin{bmatrix} \boldsymbol{x} \\ \boldsymbol{w} \end{bmatrix}.
\tag{7.27a}
$$

---

[5]Stabilizability is the dual property to detectability, see e.g. [98–100]. If system (7.24) is stabilizable, then there exists a linear state-feedback controller $\boldsymbol{u} = -\boldsymbol{K}\boldsymbol{x}$ such that the closed-loop dynamic matrix $\boldsymbol{A} - \boldsymbol{B}\boldsymbol{K}$ is a Hurwitz matrix.

Rewriting system (7.24) in terms of the augmented state vector $\boldsymbol{\chi}$ yields

$$
\begin{aligned}
\dot{\boldsymbol{\chi}} &= \boldsymbol{A}_\chi \boldsymbol{\chi} + \boldsymbol{B}_\chi \boldsymbol{u} + \boldsymbol{D}_\chi \dot{\boldsymbol{w}}, \\
\boldsymbol{y} &= \boldsymbol{C}_\chi \boldsymbol{\chi},
\end{aligned}
\tag{7.27b}
$$

where

$$
\boldsymbol{A}_\chi = \begin{bmatrix} \boldsymbol{A} & \boldsymbol{D} \\ \boldsymbol{0} & \boldsymbol{0} \end{bmatrix}, \quad
\boldsymbol{B}_\chi = \begin{bmatrix} \boldsymbol{B} \\ \boldsymbol{0} \end{bmatrix}, \quad
\boldsymbol{D}_\chi = \begin{bmatrix} \boldsymbol{0} \\ \boldsymbol{I}_m \end{bmatrix}, \quad
\boldsymbol{C}_\chi = \begin{bmatrix} \boldsymbol{C} & \boldsymbol{0} \end{bmatrix}.
\tag{7.27c}
$$

Since the original system (7.24) is strongly observable, also the augmented system (7.27c) with the unknown input $\dot{\boldsymbol{w}}$ is strongly observable as shown in Section 7.3.2. Thus, the augmented system (7.27b) can be transformed into the observer normal form. Furthermore, since the unknown input $\dot{\boldsymbol{w}}$ is bounded, the unknown input observer presented in Chapter 6.2 can be used to obtain exact estimates of $\hat{\boldsymbol{\chi}} = \begin{bmatrix} \hat{\boldsymbol{x}}^{\mathrm{T}} & \hat{\boldsymbol{w}}^{\mathrm{T}} \end{bmatrix}^{\mathrm{T}}$ in finite time[6]. A linear state-feedback controller

$$
\boldsymbol{u} = -\begin{bmatrix} \boldsymbol{K} & \boldsymbol{M} \end{bmatrix} \hat{\boldsymbol{\chi}}
\tag{7.28}
$$

is designed, where $\boldsymbol{M}$ yields the disturbance feed-forward and the state-feedback matrix $\boldsymbol{K}$ is designed for the nominal system with $\boldsymbol{w} \equiv \boldsymbol{0}$, i.e., such that the dynamic matrix $\boldsymbol{A} - \boldsymbol{B}\boldsymbol{K}$ of the nominal closed-loop system is a Hurwitz matrix.

Example 7.4.1. Consider the tutorial system of the lateral motion of an aircraft given in Example 4.2.1 extended by $o = 2$ control inputs $\boldsymbol{u} = \begin{bmatrix} \zeta_c & \xi_c \end{bmatrix}^{\mathrm{T}}$, namely the rudder angle demand ζ_c and the aileron angle demand ξ_c. The corresponding input matrix of the control input $\boldsymbol{u}$ is given by

$$
\boldsymbol{B} = \begin{bmatrix}
0 & 0 \\
0 & 0 \\
0 & 0 \\
0 & 0 \\
0 & 0 \\
20 & 0 \\
0 & 10
\end{bmatrix}.
\tag{7.29}
$$

Augmentation of system (7.24) according to (7.27) and transformation into observer

---

[6]The control input $\boldsymbol{u}$ is expected to be known to the unknown input observer and, hence, can be easily taken into account by the observer.

normal form yields

$$\bar{A}_\chi = \left[\begin{array}{cccc|cccc} -17.84 & 1 & 0 & 0 & 91.79 & 0 & 0 & 0 \\ -271.73 & 0 & 1 & 0 & 593.46 & 0 & 0 & 0 \\ -1220.79 & 0 & 0 & 1 & 0 & 0 & 0 & 0 \\ -19.83 & 0 & 0 & 0 & 0 & 0 & 0 & 0 \\ \hline 2.01 & 0 & 0 & 0 & -6.4 & 1 & 0 & 0 \\ 11.18 & 0 & 0 & 0 & -7.01 & 0 & 1 & 0 \\ 6 & 0 & 0 & 0 & 0 & 0 & 0 & 1 \\ 1.33 & 0 & 0 & 0 & 0 & 0 & 0 & 0 \end{array}\right], \quad \bar{D}_\chi = \left[\begin{array}{c} 0 \\ 0 \\ 0 \\ -701.7 \\ 0 \\ 0 \\ 0 \\ 0 \end{array}\right],$$

$$\bar{B}_\chi = \left[\begin{array}{cc} 0 & 0 \\ 0 & -286 \\ -701.7 & -8406.36 \\ 0 & 0 \\ \hline 0 & 0 \\ 0 & 77.44 \\ 0 & 39.52 \\ 0 & 0 \end{array}\right], \quad \bar{C}_\chi = \left[\begin{array}{cccc|cccc} 1 & 0 & 0 & 0 & 0 & 0 & 0 & 0 \\ 0 & 0 & 0 & 0 & 1 & 0 & 0 & 0 \end{array}\right]. \tag{7.30}$$

Furthermore, the first derivative $\dot{w}$ of the unknown input is bounded by $\tilde{L} = 0.046$ which allows for applying an RED-based unknown input observer according to Section 6.2. The observer parameters

$$\begin{aligned} \kappa_{1,3} &= 9.98, \quad \kappa_{1,2} = 46.07, \quad \kappa_{1,1} = 112.76, \quad \kappa_{1,0} = 134.92, \\ \kappa_{2,3} &= 5.33, \quad \kappa_{2,2} = 13.16, \quad \kappa_{2,1} = 17.2, \quad \kappa_{2,0} = 11, \end{aligned} \tag{7.31}$$

are chosen according to [29, Section 6.7]. Note that the necessary condition $\kappa_{1,0} > \tilde{L}|\bar{d}_{\chi,4,1}| = 32.28$ stated in Theorem 6.2.1 is satisfied.

The unknown input w acts as a matched disturbance input, i.e., $\boldsymbol{D} = \boldsymbol{BM}$ with $\boldsymbol{M} = \begin{bmatrix} 1 & 0 \end{bmatrix}^\mathrm{T}$. Hence, its estimate $\hat{w}$ can be incorporated in the control law (7.28) in order to compensate for the effects of the unknown input and achieve asymptotically exact stabilization of the state variables. The particular choice

$$\boldsymbol{K} = \begin{bmatrix} -0.024 & 0.0036 & -0.2 & 0.036 & -0.14 & 0.25 & -0.069 \\ -0.026 & -0.075 & 0.9 & -0.67 & -0.92 & -0.8 & -0.18 \end{bmatrix}, \tag{7.32}$$

for the state-feedback matrix keeps the stable plant eigenvalues and transfers the unstable plant eigenvalues $s_1 = 0$ and $s_2 = 0.1219$ of $\boldsymbol{A}$ to $s_1' = -1$ and $s_2' = -2$ in the nominal closed-loop system with the dynamic matrix $\boldsymbol{A} - \boldsymbol{BK}$. The initial state vector of the plant is again selected as $\boldsymbol{x}(0) = \begin{bmatrix} -0.5 & 0.1 & 0.02 & 0.2 & -0.1 & -0.3 & 0.2 \end{bmatrix}^\mathrm{T}$ and the initial observer state vector is set to $\hat{\boldsymbol{\chi}}(0) = \boldsymbol{0}$. Figure 7.1 shows the state variables, the estimation error variables and the estimate of the unknown input w obtained from numerical simulations of the system with the presented state-feedback controller.
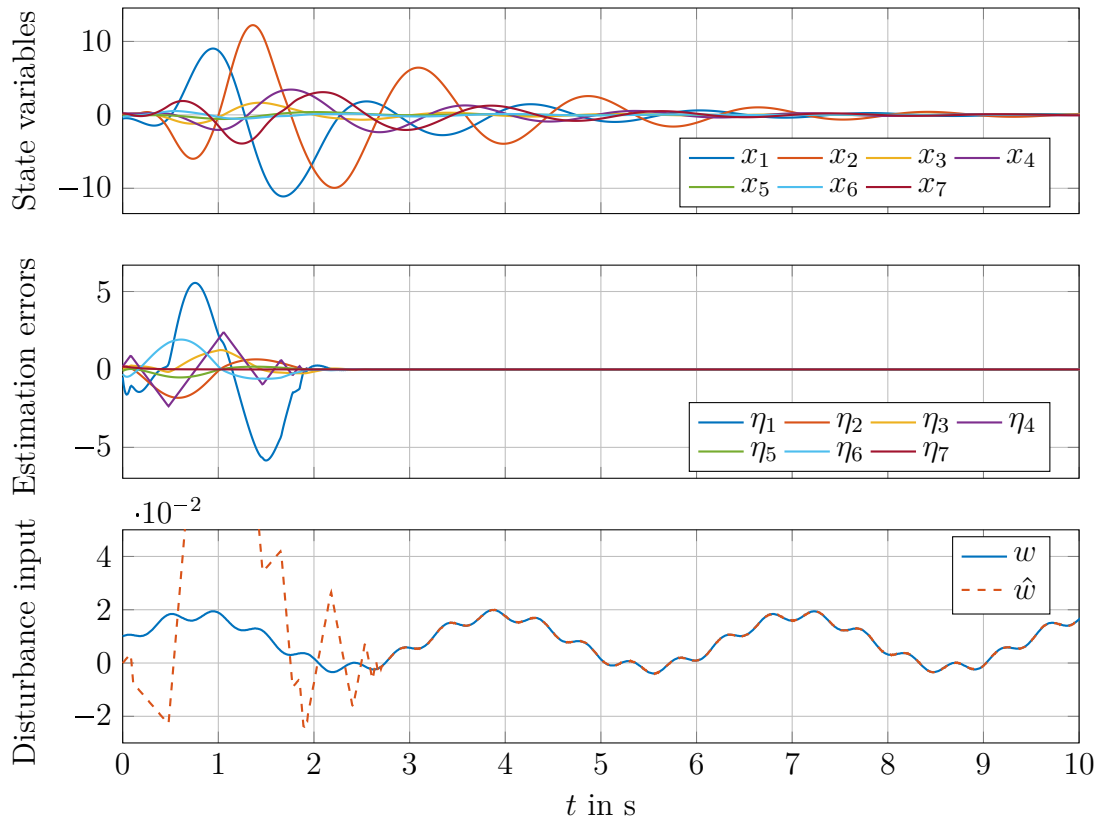
Figure 7.1: *State variables x_i, estimation errors $\eta_i = x_i - \hat{x}_i$ and estimate $\hat{w}$ of the unknown input w. The unknown input observer provides exact estimates of the plant states and the unknown input within a finite time and the states variables of the plant converge to zero asymptotically despite the unknown input.*

After a finite convergence time of approximately 2.7 s the estimation errors vanish despite the unknown input w and, thus, exact estimates of the state variables and the unknown input are obtained. Once the estimation error has converged, the state variables converge to zero asymptotically despite the unknown input.

7.4.3 Discussion of the presented State-Feedback Controller

The unknown input observer for the estimation of the augmented state vector $\boldsymbol{\chi}$ and the state-feedback matrix $\boldsymbol{K}$ for the nominal system can be designed separately from each other. Within the finite convergence time of the estimation error, the state variables of system (7.24) remain bounded, since the estimation error stays bounded and the LTI system does not allow for a finite escape time. After convergence of the estimation error, the closed-loop system is insensitive to the unknown disturbance input. The system dynamics reduce to the nominal closed-loop system

$$\dot{\boldsymbol{x}} = (\boldsymbol{A} - \boldsymbol{B}\boldsymbol{K})\boldsymbol{x}, \tag{7.33}$$

whose convergence behaviour only depends on the chosen eigenvalues of the dynamic matrix $\boldsymbol{A} - \boldsymbol{BK}$.

A major advantage of this observer based state-feedback controller becomes relevant in the case of saturated control inputs, i.e.,

$$u_{i,\text{sat}} = \begin{cases} u_{i,\text{max}} & \text{if } u_i > u_{i,\text{max}}, \\ u_{i,\text{min}} & \text{if } u_i < u_{i,\text{min}}, \\ u_i & \text{else}, \end{cases} \qquad \text{for} \quad i = 1, \dots, o. \tag{7.34}$$

Then, the unknown input observer can be supplied with the saturated control input $\boldsymbol{u}_{\text{sat}} = \begin{bmatrix} u_{1,\text{sat}} & \dots & u_{o,\text{sat}} \end{bmatrix}^{\text{T}}$ instead of $\boldsymbol{u}$, which naturally prevents the controller from wind-up. Other comparable controllers may require complex anti-windup measures, see e.g. [101–103] and the references therein.

7.5 Unknown Inputs with Asymmetric Bounds

The proposed unknown input observer requires the necessary condition

$$\kappa_{j,0} > \sum_{i=1}^{m} L_i \left| \bar{d}_{\mu_1 + \dots + \mu_j, i} \right|, \qquad j = 1, \dots, p, \tag{7.35}$$

for convergence of the estimation error for all admissible unknown inputs

$$w_i(t) \in [-L_i, L_i] \ \forall t, \qquad i = 1, \dots, m, \tag{7.36}$$

see Theorem 6.2.1. However, in many practical applications the unknown inputs do not show such a symmetric characteristic as indicated by (7.36), but rather stay within asymmetric bounds, i.e.,

$$w_i(t) \in [w_{i,\text{min}}, w_{i,\text{max}}] \ \forall t, \qquad i = 1, \dots, m. \tag{7.37}$$

For example, when w_i corresponds to an unknown mass or heat flow with known flow direction, either $w_{i,\text{min}} = 0$ or $w_{i,\text{max}} = 0$ holds.

One approach to deal with this is by simply ignoring the asymmetric nature of the unknown inputs in the design of the unknown input observer and considering the necessary condition (7.35) with $L_i = \max\{|w_{i,\text{min}}|, |w_{i,\text{max}}|\}$ in the choice of the observer parameters. However, in practice it may be desirable to have smaller observer parameters in order to keep the amplification of measurement noise and chattering effects [104, 105] small. The approach described hereafter makes it possible to decrease the observer parameters required for convergence of the estimation error.

Consider unknown inputs w_i with lower bound $w_{i,\text{min}}$ and upper bound $w_{i,\text{max}}$ as indicated in (7.37). Then, the unknown inputs can be expressed as

$$w_i(t) = \frac{w_{i,\text{min}} + w_{i,\text{max}}}{2} + \tilde{w}_i(t), \tag{7.38}$$

which decomposes w_i into a constant offset $\frac{w_{i,\min}+w_{i,\max}}{2}$ and a part with symmetric bounds

$$\tilde{w}_i(t) \in \left[-\frac{w_{i,\max}-w_{i,\min}}{2}, \frac{w_{i,\max}-w_{i,\min}}{2}\right] \quad \forall t. \tag{7.39}$$

If $w_{i,\min}$ and $w_{i,\max}$ are known[7], the constant offset can be additionally considered as a known input by the observer (6.4) which yields

$$\begin{aligned}
\dot{\hat{\bar{x}}} &= \bar{A}\hat{\bar{x}} + \bar{\Pi}\sigma_{\bar{y}} + \bar{l}(\sigma_{\bar{y}}) + \bar{D}w_{\mathrm{off}}, \\
\hat{\bar{y}} &= \bar{C}\hat{\bar{x}},
\end{aligned} \tag{7.40}$$

with

$$\boldsymbol{w}_{\mathrm{off}} = \begin{bmatrix} \frac{w_{1,\min}+w_{1,\max}}{2} \\ \vdots \\ \frac{w_{m,\min}+w_{m,\max}}{2} \end{bmatrix}. \tag{7.41}$$

Then, the offset of the unknown input cancels in the estimation error dynamics of the observer. In consequence, the part $\tilde{w}_i(t)$ given in (7.39) with symmetric bounds remains the only unknown input for the observer. Thus, the necessary condition (7.35) for the choice of the observer parameters relaxes to

$$\kappa_{j,0} > \sum_{i=1}^m \frac{w_{i,\max}-w_{i,\min}}{2}\left|\bar{d}_{\mu_1+\cdots+\mu_j,i}\right|, \qquad j = 1,\ldots,p. \tag{7.42}$$

In the case of symmetric bounds, i.e., $w_{i,\max} = -w_{i,\min}$, the necessary condition (7.42) is consistent with the original one given in (7.35). If the bounds are not symmetric, the observer parameters required by condition (7.42) are guaranteed to be smaller than in the original (7.35). In conclusion, the amplification of measurement noise can be reduced and chattering effects can be diminished by decreasing the observer parameters.

---

[7]Or if one has at least a rough guess of the offset.

Practical Application: Temperature Profile Estimation of an Aluminium Rod subject to Unknown Excitation

In this chapter, the practical application of the proposed observer concept for LTI multivariable systems with unknown inputs is demonstrated using a thermal laboratory setup. The goal is to estimate the temperature profile along an aluminium rod, which is excited with heat fluxes unknown to the observer. The plant is modelled as a distributed parameter system which, furthermore, is spatially discretized and put into a form suitable for the observer design. As discussed in this thesis, a continuous-time observer is designed accordingly. Moreover, an equivalent discrete-time observer is developed to deal with sampled measurement data and to implement the observer in a discrete-time operated environment. Finally, exemplary estimation results are shown to demonstrate the effectiveness of the observer.

In this chapter, the content of the following article is adopted, whereby the individual steps are described in much more detail:

H. Niederwieser, S. Koch, M. Reichhartinger, Unknown Input Observer for Temperature Profile Estimation in Systems with Unknown Heat Fluxes, in: 2024 22nd European Control Conference (ECC), IEEE, 2024

8.1 Problem Statement

At first, the used laboratory setup [107, 108] is described and the estimation problem is formulated.

8.1.1 Description of the Laboratory Setup

The considered laboratory setup allows for an application of a wide variety of control and estimation algorithms to heat conduction problems. A photo of the main components of the setup is given in Figure 8.1.
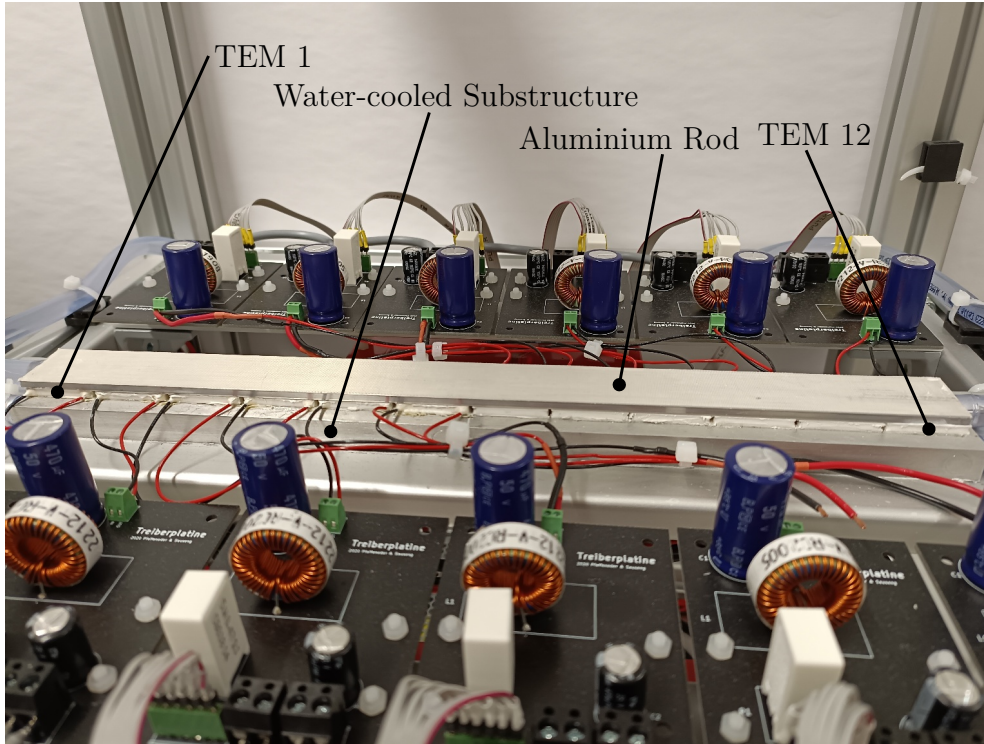
Figure 8.1: *The laboratory setup. Twelve thermoelectric modules (TEMs) are mounted along an aluminium rod. The lower surface of the TEMs is kept at ambient temperature.*

The centrepiece is a uniformly shaped rod made of aluminium alloy `EN AW-6060` with length $l = 315$ mm, width $b = 25$ mm and thickness $d = 3$ mm. Along the rod, different thermal phenomena can be observed, such as heat conduction, convective heat loss and heat loss due to radiation.

In order to thermally excite the rod, $N_{\mathrm{TEM}} = 12$ so-called thermoelectric modules (TEMs) [109] are mounted at the bottom of the rod. Each TEM houses several thermocouples which, with the help of the Peltier effect [110, 111], allow to introduce a heat flux into the rod at the mounting location. Depending on the direction of the applied electric current, the rod is either heated or cooled. A water-cooled substructure keeps the lower surface of the TEMs at ambient temperature T_{amb}, which enlarges the achievable temperature range of the TEMs.

An overview of the entire setup is given in Figure 8.2. Beneath the rod, a water tank is located, which supplies the installed water-cooling system attached to the bottom side of the TEMs. On the top of the setup, a thermal imaging camera with a resolutions of 120×160 pixels is installed. It allows to measure the temperature at any desired position along the rod at a rate of 10 frames per second.

8.1.2 Formulation of the Estimation Problem

The estimation problem is sketched in Figure 8.3. The objective is to estimate the rod's temperature profile along the z-axis from three punctual temperature measurements
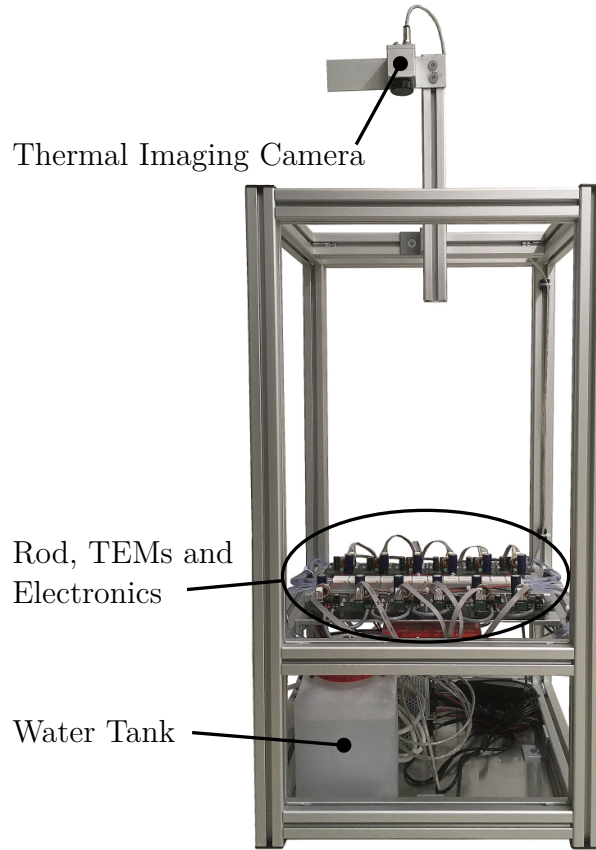
Figure 8.2: *Photo of the entire thermal laboratory setup. A thermal imaging camera is mounted on the top in order to measure the temperature distribution of the rod. The water tank contains the water for the cooling of the bottom side of the TEMs. The image is taken from [107, p. 10] and slightly modified with the authors' permission.*
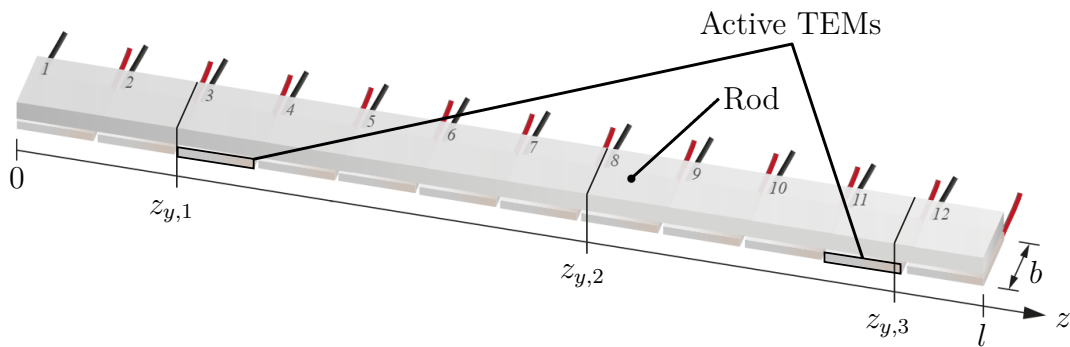
Figure 8.3: *The goal is to estimate the temperature profile of the rod along the z-axis based on the temperature measurements at the positions $z_{y,1}$, $z_{y,2}$ and $z_{y,3}$ in the presence of unknown heat fluxes caused by TEM 3 and TEM 11. The figure is taken from [108, p. 11] and slightly modified with the author's permission.*

located at

$$z_{y,1} = 53.5 \text{ mm}, \quad z_{y,2} = 186.8 \text{ mm} \quad \text{and} \quad z_{y,3} = 285.7 \text{ mm}. \tag{8.1}$$

These measurements correspond to three single pixels of the thermal imaging camera.

Furthermore, only TEM 3 and TEM 11 are actuated. The actuation, i.e., the supplied electric currents and the resulting generated heat fluxes, are considered unknown for the estimation algorithm to be designed. All other TEMs are disabled.

To sum up, the goal is to design an observer that estimates the temperature profile from $p = 3$ available measurements in the presence of $m = 2$ unknown inputs corresponding to the heat fluxes of both actuated TEMs.

8.2 Physical Modelling and Spatial Discretization

In order to describe the thermal behaviour of the aluminium rod, the physical effects of heat conduction, heat losses and the external heat input generated by the TEMs are considered. The resulting model takes the form of a partial differential equation (PDE), which is then spatially discretized on a regular grid and, thus, is transferred into a finite-dimensional state-space model suitable for the subsequent observer design.

8.2.1 Modelling of the Aluminium Rod

Assuming constant material parameters, the temperature T of the aluminium rod can be described by the heat equation [112, eqn. (2.9)]

$$\frac{\partial T}{\partial t} = \frac{k}{c\rho} \nabla^2 T + \frac{1}{c\rho} \dot{q}, \tag{8.2}$$

where k is the thermal conductivity, c is the specific heat capacity, ρ is the density of the rod material, ∇^2 represents the Laplace operator and $\dot{q}$ denotes the volumetric heat flux used for modelling external heat sources given by the TEMs and ambient heat losses. Due to the symmetry in transverse direction and because the rod is narrow compared to its length, i.e., $l \gg b$ and $l \gg d$, the heat transfer mainly takes place along the longitudinal direction (the z-axis introduced in Figure 8.3) of the rod. Hence, the temperature is assumed to be constant over the cross-sectional area and the heat equation (8.2) reduces to the one-dimensional case

$$\frac{\partial T(z,t)}{\partial t} = \frac{k}{c\rho} \frac{\partial^2 T(z,t)}{\partial z^2} + \frac{1}{c\rho} \dot{q}(z,t). \tag{8.3}$$

The volumetric heat flux

$$\dot{q}(z,t) = \dot{q}_{\text{loss}}(z,t) + \sum_{j=1}^{N_{\text{TEM}}} \dot{q}_{\text{TEM},j}(z,t) \tag{8.4}$$

consists of ambient heat losses $\dot{q}_{\text{loss}}$ and volumetric heat fluxes $\dot{q}_{\text{TEM},j}$ generated by the TEMs. Since radiation losses play a negligible role at the temperatures considered, a purely convective heat transfer is assumed for the ambient losses, i.e.,

$$\dot{q}_{\text{loss}}(z,t) = -h\frac{A}{V}\Big(T(z,t) - T_{\text{amb}}\Big), \tag{8.5}$$

where h describes the average heat transfer coefficient[1], A is the rod's surface area[2], V denotes the volume of the rod and T_{amb} is the ambient temperature. The heat generated by the TEMs is assumed to be uniformly distributed over the entire contact area. Thus, the volumetric heat flux of the j-th TEM is given by

$$\dot{q}_{\text{TEM},j}(z,t) = \dot{\bar{q}}_{\text{TEM},j}(t)f_j(z), \tag{8.6}$$

where $\dot{\bar{q}}_{\text{TEM},j}(t)$ is a time-dependent volumetric heat flux and

$$f_j(z) = \begin{cases} 1 & \text{if } (j-1)\frac{l}{N_{\text{TEM}}} < z < j\frac{l}{N_{\text{TEM}}} \\ 0 & \text{else} \end{cases} \tag{8.7}$$

defines the position of the contact surface. It is noted that $\dot{\bar{q}}_{\text{TEM},j}(t)$ could be considered as a function of the applied electric current, the rod temperature at the contact surface and the bottom temperature of the respective TEM. However, these dependencies are not modelled here. Both the volumetric heat flux and the electric current are unknown to the observer being designed. Therefore, modelling this relation would not add any further value for observer design purposes.

Combining the equations (8.3)–(8.7) finally yields the parabolic PDE

$$\frac{\partial T(z,t)}{\partial t} = \frac{k}{c\rho}\frac{\partial^2 T(z,t)}{\partial z^2} - h\frac{A}{c\rho V}\Big(T(z,t) - T_{\text{amb}}\Big) + \frac{1}{c\rho}\sum_{j=1}^{N_{\text{TEM}}}\dot{\bar{q}}_{\text{TEM},j}(t)f_j(z). \tag{8.8}$$

For a complete description of the temperature $T(z,t)$, suitable boundary conditions at $z = 0$ and $z = l$ must be specified. This is done by considering convective heat transfer at the rod's boundaries to the ambient air according to [112, eqn. (2.23)], which yields

$$\left.\frac{\partial T(z,t)}{\partial z}\right|_{z=0} = \frac{\tilde{h}}{k}\Big(T(0,t) - T_{\text{amb}}\Big), \tag{8.9a}$$

$$\left.\frac{\partial T(z,t)}{\partial z}\right|_{z=l} = -\frac{\tilde{h}}{k}\Big(T(l,t) - T_{\text{amb}}\Big), \tag{8.9b}$$

---

[1]The average heat transfer coefficient h can be considered as the weighted average of the heat transfer coefficient to the ambient air and the heat transfer coefficient to the TEMs. The weights correspond to the respective ratios of the contact surface. In the subsequent considerations h is considered to be constant.

[2]The surface area $A = 2bl + 2dl$ includes the bottom area, the top area and the two lateral side areas. The surfaces at the boundary areas are considered later on in the boundary conditions of the heat equation.
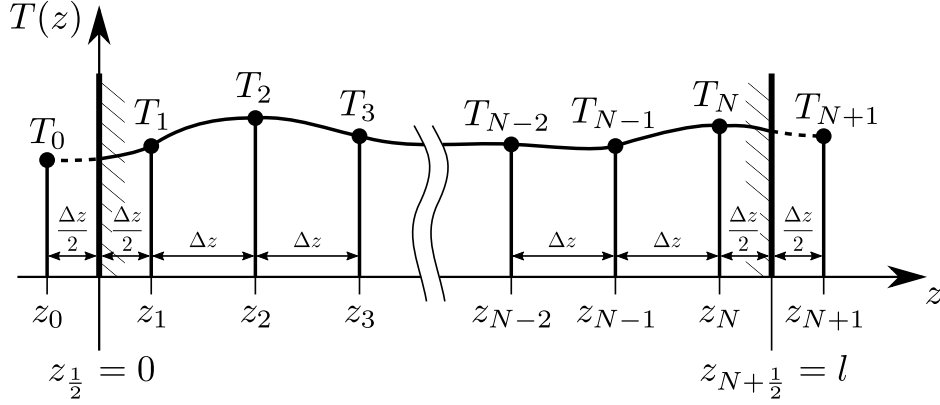
Figure 8.4: *Partitioning of the rod into a grid of N nodes inside of the rod for the spatial discretization of the PDE (8.8). Two additional auxiliary nodes are introduced at positions z_0 and z_{N+1} outside the rod to account for the boundary conditions.*

where $\tilde{h}$ is the corresponding heat transfer coefficient. Note that the heat transfer coefficients h and $\tilde{h}$ do not coincide. On the one hand, h additionally takes into account the rod's bottom side with the heat transfer to the TEMs. On the other hand, the orientation of the surface also plays a significant role in the heat transfer. In contrast to the top surface of the rod, the heated air can rise along the side surfaces. This behaviour leads to an increased heat transfer at the side surfaces.

8.2.2 Spatial Discretization of the Partial Differential Equation

In the following, the PDE (8.8) and its boundary conditions (8.9) are spatially discretized following [112, Chapter 2.4.1][3]. Thereby, the z-domain is divided into a regular grid of nodes at discrete positions in which the spatial derivatives are substituted by difference quotients. This discretization scheme is sufficiently accurate because the grid will be chosen fine enough later. The result of the spatial discretization is given by a system of first-order ordinary differential equations (ODEs), which is a finite-dimensional approximation of the considered PDE.

Partitioning of the Rod into a Regular Grid of Nodes

The z-domain of the aluminium rod is divided into a regular grid of $N+2$ nodes with a discretization width of

$$\Delta z = \frac{l}{N}, \tag{8.10}$$

as depicted in Figure 8.4. Instead of the continuous temperature profile $T(z,t)$ along the rod, only temperatures $T_i(t) = T(z_i, t)$ at the discrete positions

$$z_i = -\frac{\Delta z}{2} + i \cdot \Delta z, \qquad i = 0, \dots, N+1, \tag{8.11}$$

---

[3]In contrast to [112, Chapter 2.4.1], no discretization in time but only spatial discretization is considered here.

are considered, such that N nodes at $z_1, \ldots, z_N$ are located inside the rod and two auxiliary nodes at z_0 and z_{N+1} are located outside. The auxiliary nodes are required to account for the boundary conditions. The boundaries are located centrally between the respective auxiliary node and the first/last inner node[4], i.e., at $z_{\frac{1}{2}} = 0$ and $z_{N+\frac{1}{2}} = 0$.

Approximation of the Second Spatial Derivative

The second spatial derivative of $T(z, t)$ at position z_i is approximated by the second central difference quotient

$$\left. \frac{\partial T(z, t)}{\partial z} \right|_{z=z_i} = \frac{T_{i-1} - 2T_i + T_{i+1}}{\Delta z^2} + O(\Delta z^2), \tag{8.12}$$

where the notation $O(\Delta z^2)$ indicates that the approximation error tends to zero quadratically as the discretization width Δz tends to zero. In this way, PDE (8.8) is approximated by the ODE

$$\frac{\mathrm{d}T_i}{\mathrm{d}t} = \frac{k}{c\rho} \cdot \frac{T_{i-1} - 2T_i + T_{i+1}}{\Delta z^2} - h\frac{A}{c\rho V}\left(T_i - T_{\mathrm{amb}}\right) + \frac{1}{c\rho}\sum_{j=1}^{N_{\mathrm{TEM}}} \dot{q}_{\mathrm{TEM},j}(t)f_{j,i} \tag{8.13}$$

in each node $i = 1, \ldots, N$ inside the rod, where $f_{j,i} = f_j(z_i)$. It is noted that for $N \bmod N_{\mathrm{TEM}} \neq 0$, the energy balance of the TEMs is violated as a result of the discretization[5] of $f_j(z_i)$. For this reason, it is beneficial to restrict the number of nodes N to integer multiples of N_{TEM}, i.e.,

$$N \bmod N_{\mathrm{TEM}} = 0. \tag{8.14}$$

should be satisfied. Note that for $i = 1$ and $i = N$, the ODE (8.13) requires the temperatures T_0 and T_{N+1} of the auxiliary nodes, respectively. These dependencies are resolved next by considering the boundary conditions.

Discretization of the Boundary Conditions

The spatial discretization is exemplarily performed for the left boundary condition (8.9a) as the result can be transferred directly to the right boundary condition (8.9b) for symmetry reasons.

The temperature $T_{\frac{1}{2}} = T(0, t)$ at the left boundary is approximated by a parabola through the points z_0, z_1 and z_2, see [112, eqn. (2.264)], which yields

$$T_{\frac{1}{2}} = \frac{1}{8}(3T_0 + 6T_1 - T_2). \tag{8.15}$$

---

[4]It is also possible to design the grid in a different way, e.g. to place the first and the last node directly on the boundary of the rod. For this application, however, the chosen grid (8.11) is beneficial for consistency with the measurement data later on. For a proper choice of N, each discretization node is located in the centre of a pixel of the thermal imaging camera, which allows for a direct comparison of the observer estimates and the temperature measurements.

[5]In the case $N \bmod N_{\mathrm{TEM}} \neq 0$, nodes close to the border of two neighboured TEMs do not correspond to one TEM only but should be shared proportionally between the TEMs. However, this effect is not covered by the discretization of $f_j(z_i)$.

The spatial derivative at the boundary is approximated by the central finite difference quotient

$$\left.\frac{\partial T(z,t)}{\partial z}\right|_{z=z_{\frac{1}{2}}=0} = \frac{T_1 - T_0}{\Delta z} + O(\Delta z^2).$$ (8.16)

By substituting (8.15) and (8.16) into the boundary condition (8.9a) and solving for T_0, one gets

$$T_0 = \frac{8-6B}{8+3B}T_1 + \frac{B}{8+3B}T_2 + \frac{8B}{8+3B}T_{\mathrm{amb}} \quad \text{with} \quad B = \frac{\tilde{h}\Delta z}{k}.$$ (8.17a)

The representation (8.17a) for T_0 is finally substituted into the ODE (8.13) for $i = 1$ in order to eliminate the dependency on the auxiliary node temperature T_0. The same way,

$$T_{N+1} = \frac{8-6B}{8+3B}T_N + \frac{B}{8+3B}T_{N-1} + \frac{8B}{8+3B}T_{\mathrm{amb}}$$ (8.17b)

can be obtained by exploiting the right boundary condition (8.9b), which allows to eliminate the dependency of (8.13) for $i = N$ on the auxiliary node temperature T_{N+1}.

Temperature Measurements

As already discussed in Section 8.1.2, the rod temperature is measured at the positions $z_{y,j}$ with $j = 1, \ldots, p$. Hence, each measurement is approximated by the temperature of the respective closest node, i.e.,

$$T(z_{y,j}, t) \cong T_{\left\lceil \frac{z_{y,j}}{\Delta z} \right\rceil} \quad \text{with} \quad j = 1, \ldots, p.$$ (8.18)

8.2.3 Representation as Continuous-Time State-Space Model and Parametrization

As a next step, the spatially discretized PDE model is summarized in the form of a LTI continuous-time state-space model, which serves as the basis for the later observer design. The required model parameters are identified and a reasonable spatial discretization width is chosen.

Continuous-Time State-Space Model

To get rid of the unpleasant dependency of the model on the ambient temperature T_{amb}, henceforth T_{amb} is assumed constant and the rod temperatures are referred to T_{amb}, i.e.,

$$\theta_i = T_i - T_{\mathrm{amb}}.$$ (8.19)

Furthermore, the state vector

$$\boldsymbol{\theta} = \begin{bmatrix} \theta_1 & \dots & \theta_N \end{bmatrix}^{\mathrm{T}}, \tag{8.20}$$

the vector of inputs

$$\boldsymbol{u} = \begin{bmatrix} u_1 & \dots & u_{N_{\mathrm{TEM}}} \end{bmatrix}^{\mathrm{T}} = \begin{bmatrix} \dot{q}_{\mathrm{TEM},1} & \dots & \dot{q}_{\mathrm{TEM},N_{\mathrm{TEM}}} \end{bmatrix}^{\mathrm{T}} \tag{8.21}$$

and the vector of measured outputs

$$\boldsymbol{y} = \begin{bmatrix} y_1 & \dots & y_p \end{bmatrix}^{\mathrm{T}} = \begin{bmatrix} \theta_{\left\lceil \frac{z_{y,1}}{\Delta z} \right\rceil} & \dots & \theta_{\left\lceil \frac{z_{y,p}}{\Delta z} \right\rceil} \end{bmatrix}^{\mathrm{T}} \tag{8.22}$$

are introduced. By combining the ODEs (8.13), the auxiliary node temperatures (8.17) and the temperature measurements (8.18), a model in state-space representation

$$\frac{\mathrm{d}\boldsymbol{\theta}}{\mathrm{d}t} = \boldsymbol{A}_\theta \boldsymbol{\theta} + \boldsymbol{B}_\theta \boldsymbol{u}, \tag{8.23a}$$
$$\boldsymbol{y} = \boldsymbol{C}_\theta \boldsymbol{\theta},$$

with the dynamic matrix

$$\boldsymbol{A}_\theta = \frac{k}{c\rho\Delta z^2} \begin{bmatrix} \frac{8-6B}{8+3B} - 2 & \frac{B}{8+3B} + 1 & 0 & \dots & \dots & 0 \\ 1 & -2 & 1 & \ddots & & \vdots \\ 0 & 1 & -2 & 1 & \ddots & \vdots \\ \vdots & \ddots & \ddots & \ddots & \ddots & 0 \\ \vdots & & & \ddots & 1 & -2 & 1 \\ 0 & \dots & \dots & 0 & \frac{B}{8+3B} + 1 & \frac{8-6B}{8+3B} - 2 \end{bmatrix} - \frac{hA}{c\rho V} \boldsymbol{I}_N, \tag{8.23b}$$

the input matrix[6]

$$\boldsymbol{B}_\theta = \frac{1}{c\rho} \begin{bmatrix} \mathbf{1}_{\frac{N}{N_{\mathrm{TEM}}} \times 1} & \mathbf{0}_{\frac{N}{N_{\mathrm{TEM}}} \times 1} & \dots & \mathbf{0}_{\frac{N}{N_{\mathrm{TEM}}} \times 1} \\ \mathbf{0}_{\frac{N}{N_{\mathrm{TEM}}} \times 1} & \mathbf{1}_{\frac{N}{N_{\mathrm{TEM}}} \times 1} & \ddots & \vdots \\ \vdots & \ddots & \ddots & \mathbf{0}_{\frac{N}{N_{\mathrm{TEM}}} \times 1} \\ \mathbf{0}_{\frac{N}{N_{\mathrm{TEM}}} \times 1} & \dots & \mathbf{0}_{\frac{N}{N_{\mathrm{TEM}}} \times 1} & \mathbf{1}_{\frac{N}{N_{\mathrm{TEM}}} \times 1} \end{bmatrix} \tag{8.23c}$$

and the output matrix

$$\boldsymbol{C}_\theta = \begin{bmatrix} \boldsymbol{e}^{\mathrm{T}}_{\left\lceil \frac{z_{y,1}}{\Delta z} \right\rceil} \\ \vdots \\ \boldsymbol{e}^{\mathrm{T}}_{\left\lceil \frac{z_{y,p}}{\Delta z} \right\rceil} \end{bmatrix} \tag{8.23d}$$

is obtained.

ρ in kg/m^3	k in W/(m $\cdot$ K)	c in J/(kg $\cdot$ K)	h in W/(m^2 $\cdot$ K)	$\tilde{h}$ in W/(m^2 $\cdot$ K)
2700	209	898	48.2	1982

Table 8.1: *Density ρ, thermal conductivity k, specific heat capacity c and heat transfer coefficients h and $\tilde{h}$.*

Determination of the Model Parameters

The parameters required by the model are depicted in Table 8.1 and 8.2. The density ρ, the thermal conductivity k and the specific heat capacity c of the rod material[7] were taken from tables in the literature [113, pp. 634 and 637] and a data sheet [114][8]. The heat transfer coefficients h and $\tilde{h}$ were determined from a cool-down experiment by minimizing a quadratic cost function.

l in mm	b in mm	d in mm	T_{amb} in °C	N -
315	25	3	25	156

Table 8.2: *Length l, width b, and thickness d of the rod, ambient temperature T_{amb} and chosen number of nodes N for the spatial discretization of the PDE.*

For the sake of completeness, the dimensions of the rod are given once more, since they are required for the calculation of the surface-to-volume ratio of the rod. The ambient temperature T_{amb} was measured at the beginning of the experiment and is assumed constant hereafter. The number of nodes for the spatial discretization $N = 156$ is beneficial due to the following reasons:

1. The grid has a discretization width of $\Delta z \approx 2$ mm. This is sufficiently small with respect to the resulting discretization error, which is confirmed by the experimental results later on.

2. Since condition (8.14) is satisfied, the energy balances of the TEMs are not violated by the spatial discretization.

3. Due to the position and the resolution of the thermal imaging camera, the distance between two adjacent pixels corresponds exactly to the discretization width Δz. In other words, each node can be assigned to one pixel in the thermal image, allowing for a straightforward validation of the node temperatures estimated by the observer to be designed.

---

[6]Assuming $\frac{N}{N_{\mathrm{TEM}}}$ yields an integer number, i.e., condition (8.14) is satisfied.
[7]Aluminium alloy with material number `EN AW-6060`.
[8]Due to an obviously wrong value, the specific heat capacity could not be taken from [113, p. 639].

Unknown Inputs and Measured Outputs

In the following, the state-space model (8.23) is tailored with respect to the actually active inputs and the actually available outputs. As mentioned, only two TEMs (u_3 and u_{11}) are actuated and, thus, need to be considered by the model for the observer. Furthermore, u_3 and u_{11} are considered to be unknown to the observer and, hence, are considered as unknown input

$$\boldsymbol{w} = \begin{bmatrix} w_1 & w_2 \end{bmatrix}^{\mathrm{T}} = \begin{bmatrix} u_3 & u_{11} \end{bmatrix}^{\mathrm{T}} = \begin{bmatrix} \dot{q}_{\mathrm{TEM},3} & \dot{q}_{\mathrm{TEM},11} \end{bmatrix}^{\mathrm{T}}. \tag{8.24}$$

The temperature measurements given in (8.1) yield the output

$$\boldsymbol{y} = \begin{bmatrix} y_1 & y_2 & y_3 \end{bmatrix}^{\mathrm{T}} \overset{(8.18)}{=} \begin{bmatrix} \theta_{27} & \theta_{93} & \theta_{142} \end{bmatrix}^{\mathrm{T}}. \tag{8.25}$$

Summary of the Model

Inserting the model parameters in coherent SI-units into (8.23), one finally ends up with

$$\frac{\mathrm{d}\boldsymbol{\theta}}{\mathrm{d}t} = \boldsymbol{A}_\theta \boldsymbol{\theta} + \boldsymbol{D}_\theta \boldsymbol{w}, \tag{8.26a}$$
$$\boldsymbol{y} = \boldsymbol{C}_\theta \boldsymbol{\theta},$$

with the dynamic matrix

$$\boldsymbol{A}_\theta = \begin{bmatrix} -21.61 & 21.2 & 0 & \dots & \dots & 0 \\ 21.14 & -42.3 & 21.14 & \ddots & & \vdots \\ 0 & 21.14 & -42.3 & 21.14 & \ddots & \vdots \\ \vdots & \ddots & \ddots & \ddots & \ddots & 0 \\ \vdots & & \ddots & 21.14 & -42.3 & 21.14 \\ 0 & \dots & \dots & 0 & 21.2 & -21.61 \end{bmatrix} \tag{8.26b}$$

the unknown-input matrix

$$\boldsymbol{D}_\theta = \boldsymbol{B}_\theta \begin{bmatrix} \boldsymbol{e}_3 & \boldsymbol{e}_{11} \end{bmatrix} \tag{8.26c}$$

and the output matrix

$$\boldsymbol{C}_\theta = \begin{bmatrix} \boldsymbol{e}_{27}^{\mathrm{T}} \\ \boldsymbol{e}_{93}^{\mathrm{T}} \\ \boldsymbol{e}_{142}^{\mathrm{T}} \end{bmatrix}. \tag{8.26d}$$

This LTI system of order $N = 156$ with $m = 2$ unknown inputs and $p = 3$ outputs serves as the basis for the subsequent observer design.

Original System
$$\frac{\mathrm{d}\boldsymbol{\theta}}{\mathrm{d}t} = \boldsymbol{A}_\theta\boldsymbol{\theta} + \boldsymbol{D}_\theta\boldsymbol{w}$$
$$\boldsymbol{y} = \boldsymbol{C}_\theta\boldsymbol{\theta}$$

Diagonalization
$$\boldsymbol{\xi} = \begin{bmatrix}\boldsymbol{\xi}_1 \\ \boldsymbol{\xi}_2\end{bmatrix} = \boldsymbol{T}_\xi\boldsymbol{\theta}$$

Diagonal System
$$\begin{bmatrix}\dot{\boldsymbol{\xi}}_1 \\ \dot{\boldsymbol{\xi}}_2\end{bmatrix} = \begin{bmatrix}\boldsymbol{A}_{\xi,11} & \boldsymbol{0} \\ \boldsymbol{0} & \boldsymbol{A}_{\xi,22}\end{bmatrix}\begin{bmatrix}\boldsymbol{\xi}_1 \\ \boldsymbol{\xi}_2\end{bmatrix} + \begin{bmatrix}\boldsymbol{D}_{\xi,1} \\ \boldsymbol{D}_{\xi,2}\end{bmatrix}\boldsymbol{w}$$
$$\boldsymbol{y} = \begin{bmatrix}\boldsymbol{C}_{\xi,1} & \boldsymbol{C}_{\xi,2}\end{bmatrix}\begin{bmatrix}\boldsymbol{\xi}_1 \\ \boldsymbol{\xi}_2\end{bmatrix}$$

Model Order Reduction
$$\dot{\boldsymbol{\xi}}_2 = \boldsymbol{0}$$

Reduced-order System
$$\dot{\boldsymbol{\xi}}_1 = \boldsymbol{A}_{\xi,11}\boldsymbol{\xi}_1 + \boldsymbol{D}_{\xi,1}\boldsymbol{w}$$
$$\boldsymbol{y} = \boldsymbol{C}_{\xi,1}\boldsymbol{\xi}_1 - \boldsymbol{C}_{\xi,2}\boldsymbol{A}_{\xi,22}^{-1}\boldsymbol{D}_{\xi,2}\boldsymbol{w}$$
$$\boldsymbol{\xi}_2 = -\boldsymbol{A}_{\xi,22}^{-1}\boldsymbol{D}_{\xi,2}\boldsymbol{w}$$

Augmentation of the State Vector
$$\boldsymbol{x} = \begin{bmatrix}\boldsymbol{\xi}_1 \\ \boldsymbol{w} \\ \dot{\boldsymbol{w}}\end{bmatrix}$$

Augmented System
$$\dot{\boldsymbol{x}} = \boldsymbol{A}\boldsymbol{x} + \boldsymbol{D}\ddot{\boldsymbol{w}}$$
$$\boldsymbol{y} = \boldsymbol{C}\boldsymbol{x}$$

Transformation to Observer Normalform
$$\bar{\boldsymbol{x}} = \boldsymbol{T}^{-1}\boldsymbol{x}$$
$$\bar{\boldsymbol{y}} = \boldsymbol{\Gamma}\boldsymbol{y}$$

System in Observer Normal Form
$$\dot{\bar{\boldsymbol{x}}} = \bar{\boldsymbol{A}}\bar{\boldsymbol{x}} + \bar{\boldsymbol{D}}\ddot{\boldsymbol{w}}$$
$$\bar{\boldsymbol{y}} = \bar{\boldsymbol{C}}\bar{\boldsymbol{x}}$$

Figure 8.5: *Transformation of the original system into a form suitable for the observer design. A modal model order reduction is applied first. The state vector of the reduced-order system is augmented by the unknown input $\boldsymbol{w}$ and its derivative. The resulting augmented system is transformed into the proposed observer normal form for LTI multivariable systems with unknown inputs, in which the observer is finally designed.*

8.3 Unknown Input Observer Design for the Estimation of the Temperature Profile

For the purpose of observer design, model (8.26) is first transformed into an appropriate form. Figure 8.5 depicts the transformations applied. The original system (8.26) exhibits a high order that causes numerical problems in calculating the transformation into observer normal form. For this reason, a modal model order reduction is applied. The system is transformed into diagonal form to identify the relevant system dynamics represented by $\boldsymbol{\xi}_1$. The negligible dynamics represented by $\boldsymbol{\xi}_2$ are substituted by a quasi-static approximation to reduce the system order. Then, the state vector is augmented by the unknown input $\boldsymbol{w}$ and its first derivative $\dot{\boldsymbol{w}}$. The augmented system is transformed into the proposed observer normal form, in which the observer design is done. An equivalent discrete-time observer is designed for the final implementation in a digital framework with periodically available measurements. In the following, the individual steps are motivated and described in detail.

8.3.1 Modal Model Order Reduction

The given system (8.26) has a order of $N = 156$. A numerically stable transformation into observer normal form is not possible with a realistic calculation accuracy. For this reason, a modal model order reduction is applied, such that the reduced-order system covers only the mainly relevant parts of the dynamics.

In order to identify the relevant dynamics, system (8.26) is transformed into diagonal form using the regular state transformation

$$\boldsymbol{\xi} = \boldsymbol{T}_\xi \boldsymbol{\theta} \qquad \text{with} \quad \boldsymbol{T}_\xi^{-1} = \begin{bmatrix} \boldsymbol{v}_1 & \boldsymbol{v}_2 & \dots & \boldsymbol{v}_N \end{bmatrix}, \tag{8.27}$$

where $\boldsymbol{v}_1, \boldsymbol{v}_2, \dots, \boldsymbol{v}_N$ are the right eigenvectors of $\boldsymbol{A}_\theta$, see [115, pp. 70–72] or [116, pp. 416–417]. The matrix $\boldsymbol{A}_\theta$ has purely real and distinct eigenvalues and, thus, there exist N linearly independent eigenvectors which ensure the state transformation (8.27) to be invertible. The transformed system in diagonal form is given by

$$\begin{aligned} \dot{\boldsymbol{\xi}} &= \boldsymbol{A}_\xi \boldsymbol{\xi} + \boldsymbol{D}_\xi w, \\ \boldsymbol{y} &= \boldsymbol{C}_\xi \boldsymbol{\xi}, \end{aligned} \tag{8.28}$$

where $\boldsymbol{A}_\xi = \boldsymbol{T}_\xi \boldsymbol{A}_\theta \boldsymbol{T}_\xi^{-1} = \mathrm{diag}(s_1, s_2, \dots, s_N)$ is a diagonal matrix containing the eigenvalues $s_1, s_2, \dots, s_N$, $\boldsymbol{D}_\xi = \boldsymbol{T}_\xi \boldsymbol{D}_\theta$ and $\boldsymbol{C}_\xi = \boldsymbol{C}_\theta \boldsymbol{T}_\xi^{-1}$. Without loss of generality, let the eigenvalues $s_1, s_2, \dots, s_N$ corresponding to the eigenvectors $\boldsymbol{v}_1, \boldsymbol{v}_2, \dots, \boldsymbol{v}_N$ be in descending order[9], i.e.,

$$s_1 > s_2 > \dots > s_N. \tag{8.29}$$

---

[9]As already mentioned, the system has purely real distinct eigenvalues only. In case of conjugate complex eigenvalues the real part could be considered as the measure for the eigenvalue ordering.

Then, the state vector can be partitioned into $\boldsymbol{\xi} = \begin{bmatrix} \boldsymbol{\xi}_1 & \boldsymbol{\xi}_2 \end{bmatrix}^{\mathrm{T}}$, where $\boldsymbol{\xi}_1 \in \mathbb{R}^{N_r}$ corresponds to N_r slow[10] or unstable[11] modes, whereas $\boldsymbol{\xi}_2 \in \mathbb{R}^{N-N_r}$ represents the remaining $N - N_r$ fast decaying modes. The dynamics (8.28) are rewritten in terms of the partitioned state vector, which yields

$$\begin{bmatrix} \dot{\boldsymbol{\xi}}_1 \\ \dot{\boldsymbol{\xi}}_2 \end{bmatrix} = \begin{bmatrix} \boldsymbol{A}_{\xi,11} & \boldsymbol{0} \\ \boldsymbol{0} & \boldsymbol{A}_{\xi,22} \end{bmatrix} \begin{bmatrix} \boldsymbol{\xi}_1 \\ \boldsymbol{\xi}_2 \end{bmatrix} + \begin{bmatrix} \boldsymbol{D}_{\xi,1} \\ \boldsymbol{D}_{\xi,2} \end{bmatrix} \boldsymbol{w},$$
$$\boldsymbol{y} = \begin{bmatrix} \boldsymbol{C}_{\xi,1} & \boldsymbol{C}_{\xi,2} \end{bmatrix} \begin{bmatrix} \boldsymbol{\xi}_1 \\ \boldsymbol{\xi}_2 \end{bmatrix}, \tag{8.30}$$

where $\boldsymbol{A}_{\xi,11} = \mathrm{diag}(s_1, \ldots, s_{N_r})$ and $\boldsymbol{A}_{\xi,22} = \mathrm{diag}(s_{N_r+1}, \ldots, s_N)$. The transients of $\boldsymbol{\xi}_2$ decay faster with respect to those related to $\boldsymbol{\xi}_1$ and, hence, a quasi-static approximation of its dynamics is applied. Therein, instead of the negligibly fast dynamics, it is assumed that the steady-state value is reached immediately, i.e., $\dot{\boldsymbol{\xi}}_2 = \boldsymbol{0}$. This allows for reducing the original system order N to the order N_r of the relevant dynamics $\boldsymbol{\xi}_1$. A detailed description of the quasi-static approximation is provided in Section 10.1 in the appendix. According to the appendix, the reduced-order system is given by[12]

$$\dot{\boldsymbol{\xi}}_1 = \boldsymbol{A}_{\xi,11} \boldsymbol{\xi}_1 + \boldsymbol{D}_{\xi,1} \boldsymbol{w},$$
$$\boldsymbol{y} = \boldsymbol{C}_{\xi,1} \boldsymbol{\xi}_1 - \boldsymbol{C}_{\xi,2} \boldsymbol{A}_{\xi,22}^{-1} \boldsymbol{D}_{\xi,2} \boldsymbol{w}, \tag{8.31a}$$

and the approximation of the remaining state variables yields

$$\boldsymbol{\xi}_2 = -\boldsymbol{A}_{\xi,22}^{-1} \boldsymbol{D}_{\xi,2} \boldsymbol{w}. \tag{8.31b}$$

It remains to choose the number of relevant modes N_r. Since a reasonable choice directly from the eigenvalues is not intuitive, their negative inverses $\tau_i = -\frac{1}{s_i}$, $i = 1, \ldots, N$, which can be interpreted as time constants of first-order linear dynamics[13], are considered instead. A glance at the set of time constants

$$\begin{aligned} &\tau_1 = 54.86 \text{ s}, \quad &\tau_2 = 32 \text{ s}, \quad &\tau_3 = 17.12 \text{ s}, \quad &\tau_4 = 9.83 \text{ s}, \\ &\tau_5 = 6.17 \text{ s}, \quad &\tau_6 = 4.18 \text{ s}, \quad &\ldots, \quad &\tau_{156} = 0.01 \text{ s}, \end{aligned} \tag{8.32}$$

suggests $N_r = 4$ as a reasonable choice, which takes into account all time constants larger than 10 s (including $\tau_4 \approx 10$ s).

8.3.2 Augmentation of the Model for Additional Estimation of the Unknown Inputs

In order to estimate the original system state, it is not sufficient to estimate $\boldsymbol{\xi}_1$ only as the inverse of the state transformation (8.27) requires an estimate of $\boldsymbol{\xi}_2$. According

---

[10]Eigenvalues with small negative real part are considered as slow modes.

[11]The considered system has eigenvalues with negative real part only, i.e., there are no unstable modes in this case.

[12]Note that $\boldsymbol{A}_{\xi,22}$ is invertible as all eigenvalues $s_i \neq 0$. Due to its diagonal structure, its inverse is simple to compute and numerically unproblematic.

[13]In diagonal form, the system consists of decoupled scalar differential equations. In the case of purely real negative eigenvalues s_i, these differential equations can be understood as a set of first-order dynamics with time constant $\tau_i = -\frac{1}{s_i}$ connected in parallel.

to (8.31b), the approximation of $\boldsymbol{\xi}_2$ requires the unknown input $\boldsymbol{w}$. Hence, $\boldsymbol{w}$ must be estimated from (8.31a) in addition to $\boldsymbol{\xi}_1$. For this purpose, the state vector is augmented with $\boldsymbol{w}$ and its derivative $\dot{\boldsymbol{w}}$, i.e.,

$$\boldsymbol{x} = \begin{bmatrix} \boldsymbol{\xi}_1 \\ \boldsymbol{w} \\ \dot{\boldsymbol{w}} \end{bmatrix}. \tag{8.33}$$

System (8.31a) is rewritten in terms of the augmented state vector $\boldsymbol{x}$ which yields

$$\begin{aligned} \dot{\boldsymbol{x}} &= \boldsymbol{A}\boldsymbol{x} + \boldsymbol{D}\ddot{\boldsymbol{w}}, \\ \boldsymbol{y} &= \boldsymbol{C}\boldsymbol{x}, \end{aligned} \tag{8.34}$$

where

$$\boldsymbol{A} = \begin{bmatrix} \boldsymbol{A}_{\xi,11} & \boldsymbol{D}_{\xi,1} & \boldsymbol{0}_{N_r \times m} \\ \boldsymbol{0}_{m \times N_r} & \boldsymbol{0}_{m \times m} & \boldsymbol{I}_m \\ \boldsymbol{0}_{m \times N_r} & \boldsymbol{0}_{m \times m} & \boldsymbol{0}_{m \times m} \end{bmatrix}, \qquad \boldsymbol{D} = \begin{bmatrix} \boldsymbol{0}_{N_r \times m} \\ \boldsymbol{0}_{m \times m} \\ \boldsymbol{I}_m \end{bmatrix}, \\ \boldsymbol{C} = \begin{bmatrix} \boldsymbol{C}_{\xi,1} & -\boldsymbol{C}_{\xi,2}\boldsymbol{A}_{\xi,22}^{-1}\boldsymbol{D}_{\xi,2} & \boldsymbol{0}_{p \times m} \end{bmatrix} \tag{8.35}$$

and $\ddot{\boldsymbol{w}}$ denotes the second derivative of $\boldsymbol{w}$. Note that the temperature profile estimation problem has been reduced to the estimation of the state vector $\boldsymbol{x}$ of system (8.34) in the presence of the unknown input $\ddot{\boldsymbol{w}}$.

8.3.3 Transformation to Observer Normal Form

In order to design an unknown input observer according to Section 6.2, system (8.34) is transformed into the proposed observer normal form (6.1). The application of the corresponding state transformation $\bar{\boldsymbol{x}} = \boldsymbol{T}^{-1}\boldsymbol{x}$ and output transformation $\bar{\boldsymbol{y}} = \boldsymbol{\Gamma}\boldsymbol{y}$ yields

$$\begin{aligned} \dot{\bar{\boldsymbol{x}}} &= \bar{\boldsymbol{A}}\bar{\boldsymbol{x}} + \bar{\boldsymbol{D}}\ddot{\boldsymbol{w}}, \\ \bar{\boldsymbol{y}} &= \bar{\boldsymbol{C}}\bar{\boldsymbol{x}}, \end{aligned} \tag{8.36a}$$

with the matrices

$$
\bar{A} = \left[
\begin{array}{cccc|cc|cc}
0.037 & 1 & 0 & 0 & -0.53 & 0 & 6.42 & 0 \\
0.011 & 0 & 1 & 0 & 0.0076 & 0 & 1.71 & 0 \\
-0.014 & 0 & 0 & 1 & 0.011 & 0 & 0.06 & 0 \\
-0.001 & 0 & 0 & 0 & 0.0004 & 0 & -0.0027 & 0 \\
\hline
0.1 & 0 & 0 & 0 & 0.16 & 1 & 0.23 & 0 \\
-0.025 & 0 & -0.45 & 2.23 & 0.017 & 0 & -0.6 & 0 \\
\hline
0.0063 & 0 & 0 & 0 & 0.028 & 0 & -0.41 & 1 \\
-0.0005 & 0 & -0.068 & 0.06 & -0.0003 & 0 & -0.11 & 0
\end{array}
\right] ,
$$

(8.36b)

$$
\bar{D} = 10^{-4} \cdot \left[
\begin{array}{cc}
0 & 0 \\
0 & 0 \\
0 & 0 \\
0 & 0 \\
\hline
0 & 0 \\
52.4 & -3 \\
\hline
0 & 0 \\
7.7 & 3.7
\end{array}
\right] , \quad
\bar{C} = \left[
\begin{array}{cccc|cc|cc}
1 & 0 & 0 & 0 & 0 & 0 & 0 & 0 \\
0 & 0 & 0 & 0 & 1 & 0 & 0 & 0 \\
0 & 0 & 0 & 0 & 0 & 0 & 1 & 0
\end{array}
\right] .
$$

The system in observer normal form (8.36a) has order $n = 8$, $m = 2$ unknown inputs and $p = 3$ outputs. It consists of $p = 3$ coupled subsystems, each with a single output. The second and the third subsystem of order $\mu_2 = \mu_3 = 2$ are directly affected by $\ddot{w}$, whereas the first subsystem of order $\mu_1 = 4$ is not.

8.3.4 Unknown Input Observer Design in Observer Normal Form

As proposed in Section 6.2, an observer of the form

$$
\dot{\hat{\bar{x}}} = \bar{A}\hat{\bar{x}} + \bar{\Pi}\sigma_{\bar{y}} + \bar{l}(\sigma_{\bar{y}}),
$$
$$
\hat{\bar{y}} = \bar{C}\hat{\bar{x}} = \begin{bmatrix} \hat{\bar{y}}_1 & \hat{\bar{y}}_2 & \hat{\bar{y}}_3 \end{bmatrix}^{\mathrm{T}} = \begin{bmatrix} \hat{\bar{x}}_1 & \hat{\bar{x}}_5 & \hat{\bar{x}}_7 \end{bmatrix}^{\mathrm{T}} ,
$$

(8.37a)

is designed, where

$$
\sigma_{\bar{y}} = \bar{y} - \hat{\bar{y}} = \begin{bmatrix} \sigma_1 & \sigma_5 & \sigma_7 \end{bmatrix}^{\mathrm{T}}
$$

(8.37b)

is the output error and the linear output-injection matrix compensating for the couplings is given by

$$
\bar{\Pi} = \left[
\begin{array}{ccc}
0.037 & -0.53 & 6.42 \\
0.011 & 0.0076 & 1.71 \\
-0.014 & 0.011 & 0.06 \\
-0.001 & 0.0004 & -0.0027 \\
\hline
0.10 & 0.16 & 0.23 \\
-0.025 & 0.017 & -0.6 \\
\hline
0.0063 & 0.028 & -0.41 \\
-0.0005 & -0.0003 & -0.11
\end{array}
\right] .
$$

(8.37c)

The remaining task deals with the choice of the nonlinear output injection $\bar{l}(\boldsymbol{\sigma}_{\bar{y}})$. As discussed in the previous section, the first subsystem is not directly affected by the unknown inputs. For this reason, the application of a linear observer for this subsystem is sufficient for asymptotic convergence[14]. For the second and the third subsystem, an RED-based output injection is used in order to compensate for the unknown inputs. In summary, the nonlinear output injection is given by

$$
\bar{l}(\boldsymbol{\sigma}_{\bar{y}}) =
\begin{bmatrix}
\kappa_{1,3}\sigma_1 \\
\kappa_{1,2}\sigma_1 \\
\kappa_{1,1}\sigma_1 \\
\kappa_{1,0}\sigma_1 \\
\hline
\kappa_{2,1}\lfloor\sigma_5\rceil^{\frac{1}{2}} \\
\kappa_{2,0}\lfloor\sigma_5\rceil^{0} \\
\hline
\kappa_{3,1}\lfloor\sigma_7\rceil^{\frac{1}{2}} \\
\kappa_{3,0}\lfloor\sigma_7\rceil^{0}
\end{bmatrix} .
\tag{8.37d}
$$

The particular choice of the tuning parameters $\kappa_{j,i}$ is given in Section 8.4, Table 8.3.

8.3.5 Discrete-Time Implementation of the Unknown Input Observer

The designed unknown input observer should be implemented in a digital framework in the laboratory. The thermal imaging camera serves as temperature sensor generating discrete-time measurements with a frame rate of 10 Hz. Hence, a discrete-time implementation of the continuous-time observer (8.37) with discretization time $t_{\mathrm{d}} = 0.1$ s is required. In the following, all functions of time are considered at discrete-time instances $t_k = k t_{\mathrm{d}}$ with $k = 0, 1, 2, \dots$ representing the discrete time variable[15]. Hereafter, all discrete-time functions are denoted by the corresponding continuous-time symbol expanded with the discrete time variable in the subscript, e.g. $\bar{\boldsymbol{x}}_k = \bar{\boldsymbol{x}}(k t_{\mathrm{d}})$ or $\bar{\boldsymbol{y}}_k = \bar{\boldsymbol{y}}(k t_{\mathrm{d}})$.

At first, the Forward Euler discretization of system (8.36) is considered, as it simple to use and sufficiently accurate in this case[16]. Furthermore, the Forward Euler discretization preserves the insightful structure of the coupled subsystems, which allows for directly applying established discretization schemes for the differentiator-based output injection $\bar{l}(\boldsymbol{\sigma}_{\bar{y}})$ such as [34–41]. The Forward Euler discretization of (8.36) is given by

$$
\begin{aligned}
\bar{\boldsymbol{x}}_{k+1} &= \bar{\boldsymbol{A}}_{\mathrm{d}}\bar{\boldsymbol{x}}_k + \bar{\boldsymbol{D}}_{\mathrm{d}}\ddot{\boldsymbol{w}}_k, \\
\bar{\boldsymbol{y}}_k &= \bar{\boldsymbol{C}}_{\mathrm{d}}\bar{\boldsymbol{x}}_k,
\end{aligned}
\tag{8.38}
$$

---

[14]Although an RED-based observer theoretically converges in finite time, a linear observer will in general converge faster into a certain error band from a practical point of view.

[15]Note that during the modelling, the thermal conductivity is also denoted by k. However, the thermal conductivity is not required any more and, from the usage, it is easy to distinguish.

[16]The discretization time $t_{\mathrm{d}} = 0.1$ s is small compared to the system dynamics. All remaining modes are comparatively slow because of the previously applied modal model order reduction.

where $\bar{\boldsymbol{A}}_{\mathrm{d}} = \boldsymbol{I} + t_{\mathrm{d}}\bar{\boldsymbol{A}}$, $\bar{\boldsymbol{D}}_{\mathrm{d}} = t_{\mathrm{d}}\bar{\boldsymbol{D}}$ and $\bar{\boldsymbol{C}}_{\mathrm{d}} = \bar{\boldsymbol{C}} = \begin{bmatrix} \bar{\boldsymbol{c}}_1 & \bar{\boldsymbol{c}}_2 & \bar{\boldsymbol{c}}_3 \end{bmatrix}^{\mathrm{T}}$. In accordance with the continuous-time observer (8.37), the discrete-time observer takes the form

$$
\begin{aligned}
\hat{\bar{\boldsymbol{x}}}_{k+1} &= \bar{\boldsymbol{A}}_{\mathrm{d}}\hat{\bar{\boldsymbol{x}}}_k + \bar{\boldsymbol{\Pi}}_{\mathrm{d}}\boldsymbol{\sigma}_{\bar{\boldsymbol{y}},k} + \bar{\boldsymbol{l}}_{\mathrm{d}}(\boldsymbol{\sigma}_{\bar{\boldsymbol{y}},k}), \\
\hat{\bar{\boldsymbol{y}}}_k &= \bar{\boldsymbol{C}}_{\mathrm{d}}\hat{\bar{\boldsymbol{x}}}_k = \begin{bmatrix} \hat{\bar{y}}_{1,k} & \hat{\bar{y}}_{2,k} & \hat{\bar{y}}_{3,k} \end{bmatrix}^{\mathrm{T}} = \begin{bmatrix} \hat{\bar{x}}_{1,k} & \hat{\bar{x}}_{5,k} & \hat{\bar{x}}_{7,k} \end{bmatrix}^{\mathrm{T}},
\end{aligned}
\tag{8.39}
$$

where the linear output-injection matrix $\bar{\boldsymbol{\Pi}}_{\mathrm{d}} = t_{\mathrm{d}}\bar{\boldsymbol{\Pi}}$ partially decouples[17] the subsystems and the nonlinear output injection $\bar{\boldsymbol{l}}_{\mathrm{d}}(\boldsymbol{\sigma}_{\bar{\boldsymbol{y}},k})$ needs to be chosen appropriately. The subsequently choice of $\bar{\boldsymbol{l}}_{\mathrm{d}}(\boldsymbol{\sigma}_{\bar{\boldsymbol{y}},k})$ follows the ideas of the so-called matching approach for the discretization of homogenous differentiators [40, 41], which allows for suppressing the discretization chattering phenomenon. Therein, the dynamics of the estimation error

$$
\boldsymbol{\sigma}_k = \bar{\boldsymbol{x}}_k - \hat{\bar{\boldsymbol{x}}}_k = \begin{bmatrix} \sigma_{1,k} & \ldots & \sigma_{8,k} \end{bmatrix}^{\mathrm{T}}
\tag{8.40}
$$

are given by

$$
\boldsymbol{\sigma}_{k+1} = (\bar{\boldsymbol{A}}_{\mathrm{d}} - \bar{\boldsymbol{\Pi}}_{\mathrm{d}}\bar{\boldsymbol{C}}_{\mathrm{d}})\boldsymbol{\sigma}_k - \bar{\boldsymbol{l}}_{\mathrm{d}}(\boldsymbol{\sigma}_{\bar{\boldsymbol{y}},k}) + \bar{\boldsymbol{D}}_{\mathrm{d}}\ddot{w}_k,
\tag{8.41}
$$

The matrix $\bar{\boldsymbol{A}}_{\mathrm{d}} - \bar{\boldsymbol{\Pi}}_{\mathrm{d}}\bar{\boldsymbol{C}}_{\mathrm{d}}$ has the block-triangular form

$$
\bar{\boldsymbol{A}}_{\mathrm{d}} - \bar{\boldsymbol{\Pi}}_{\mathrm{d}}\bar{\boldsymbol{C}}_{\mathrm{d}} = \begin{bmatrix} \bar{\boldsymbol{A}}_{\mathrm{d},11} & \boldsymbol{0}_{4\times 2} & \boldsymbol{0}_{4\times 2} \\ \bar{\boldsymbol{A}}_{\mathrm{d},12} & \bar{\boldsymbol{A}}_{\mathrm{d},22} & \boldsymbol{0}_{2\times 2} \\ \bar{\boldsymbol{A}}_{\mathrm{d},13} & \boldsymbol{0}_{2\times 2} & \bar{\boldsymbol{A}}_{\mathrm{d},33} \end{bmatrix}
\tag{8.42}
$$

where the diagonal blocks

$$
\bar{\boldsymbol{A}}_{\mathrm{d},11} = \begin{bmatrix} 1 & t_{\mathrm{d}} & 0 & 0 \\ 0 & 1 & t_{\mathrm{d}} & 0 \\ 0 & 0 & 1 & t_{\mathrm{d}} \\ 0 & 0 & 0 & 1 \end{bmatrix}, \qquad \bar{\boldsymbol{A}}_{\mathrm{d},22} = \bar{\boldsymbol{A}}_{\mathrm{d},33} = \begin{bmatrix} 1 & t_{\mathrm{d}} \\ 0 & 1 \end{bmatrix},
\tag{8.43}
$$

refer to Forward Euler discretized chains of integrators and $\bar{\boldsymbol{A}}_{\mathrm{d},12}$ and $\bar{\boldsymbol{A}}_{\mathrm{d},13}$ account for the remaining couplings $\beta_{j,k,l}$, see Section 6.1.1. Due to this block-diagonal form, it is reasonable to choose the $\bar{\boldsymbol{l}}_{\mathrm{d}}(\boldsymbol{\sigma}_{\bar{\boldsymbol{y}},k})$ such that the output injection into each subsystem depends on its particular output only, i.e.,

$$
\bar{\boldsymbol{l}}_{\mathrm{d}}(\boldsymbol{\sigma}_{\bar{\boldsymbol{y}},k}) = \begin{bmatrix} \bar{\psi}_1(\sigma_{1,k})\sigma_{1,k} \\ \bar{\psi}_2(\sigma_{5,k})\sigma_{5,k} \\ \bar{\psi}_3(\sigma_{7,k})\sigma_{7,k} \end{bmatrix}.
\tag{8.44a}
$$

The functions $\bar{\psi}(\sigma_{1,k})$, $\bar{\psi}_2(\sigma_{5,k})$, $\bar{\psi}_3(\sigma_{7,k})$ are chosen according to [40, eqn. (24)], such that the eigenvalues of $(\bar{\boldsymbol{A}}_{\mathrm{d},11} - \bar{\psi}_1(\sigma_{1,k})\bar{\boldsymbol{c}}_{1,\mathrm{d}}^{\mathrm{T}})$, $(\bar{\boldsymbol{A}}_{\mathrm{d},22} - \bar{\psi}_2(\sigma_{5,k})\bar{\boldsymbol{c}}_{2,\mathrm{d}}^{\mathrm{T}})$ and

---

[17]As in the continuous-time case, the linear output injection compensates for the couplings originating from the coefficients $\alpha_{j,k}$ of $\bar{\boldsymbol{A}}$ only. The couplings originating from the coefficients $\beta_{j,k,l}$ remain.

$(\bar{\boldsymbol{A}}_{\mathrm{d},33} - \bar{\boldsymbol{\psi}}_3(\sigma_{7,k})\bar{\boldsymbol{c}}_{3,\mathrm{d}}^{\mathrm{T}})$ are located at

$$z_{1,i} = \mathrm{e}^{t_{\mathrm{d}} p_{1,i}},$$

$$z_{2,i}(\sigma_{5,k}) = \mathrm{e}^{t_{\mathrm{d}} p_{2,i} \left| \sigma_{5,k} \right|^{-\frac{1}{2}}}, \tag{8.44b}$$

$$z_{3,i}(\sigma_{7,k}) = \mathrm{e}^{t_{\mathrm{d}} p_{3,i} \left| \sigma_{7,k} \right|^{-\frac{1}{2}}},$$

respectively, where the constants $p_{j,i}$, $j = 1, \ldots, 3$, $i = 0, \ldots, \mu_j$ are the zeros of

$$s^{\mu_j} + \kappa_{j,\mu_j-1} s^{\mu_j-1} + \ldots + \kappa_{j,1} s + \kappa_{j,0} = 0. \tag{8.44c}$$

It is pointed out that, since a linear observer has been designed for the first subsystem, the eigenvalues $z_{1,i}$ and also $\bar{\boldsymbol{\psi}}_1(\sigma_{1,k})$ are constant, i.e., independent of $\sigma_{1,k}$. The assignment of the state-dependent eigenvalues (8.44b), e.g. by applying Ackermann's formula [89], finally yields

$$\bar{\boldsymbol{\psi}}_1(\sigma_{1,k}) = \begin{bmatrix} \sum_{j=1}^{4}(1 - z_{1,j}) \\ \frac{1}{t_{\mathrm{d}}} \sum_{j_1=1}^{4} \sum_{\substack{j_2=1 \\ j_2 \neq j_1}}^{4} (1 - z_{1,j_1})(1 - z_{1,j_2}) \\ \frac{1}{t_{\mathrm{d}}^2} \sum_{j_1=1}^{4} \sum_{\substack{j_2=1 \\ j_2 \neq j_1}}^{4} \sum_{\substack{j_3=1 \\ j_3 \neq j_1 \\ j_3 \neq j_2}}^{4} (1 - z_{1,j_1})(1 - z_{1,j_2})(1 - z_{1,j_3}) \\ \frac{1}{t_{\mathrm{d}}^3}(1 - z_{1,1})(1 - z_{1,2})(1 - z_{1,3})(1 - z_{1,4}) \end{bmatrix},$$

$$\bar{\boldsymbol{\psi}}_2(\sigma_{5,k}) = \begin{bmatrix} \big(1 - z_{2,1}(\sigma_{5,k})\big) + \big(1 - z_{2,2}(\sigma_{5,k})\big) \\ \frac{1}{t_{\mathrm{d}}}\big(1 - z_{2,1}(\sigma_{5,k})\big)\big(1 - z_{2,2}(\sigma_{5,k})\big) \end{bmatrix}, \tag{8.44d}$$

$$\bar{\boldsymbol{\psi}}_3(\sigma_{7,k}) = \begin{bmatrix} \big(1 - z_{3,1}(\sigma_{7,k})\big)\big(1 - z_{3,2}(\sigma_{7,k})\big) \\ \frac{1}{t_{\mathrm{d}}}\big(1 - z_{3,1}(\sigma_{7,k})\big)\big(1 - z_{3,2}(\sigma_{7,k})\big) \end{bmatrix}.$$

It is pointed out that the discrete-time observer (8.39) with the choice (8.44) for $\bar{\boldsymbol{l}}_{\mathrm{d}}(\boldsymbol{\sigma}_{\bar{\boldsymbol{y}},k})$ formally approaches the continuous-time observer (8.37) as $t_{\mathrm{d}} \to 0$.

8.4 Experimental Results

The discrete-time observer is implemented in a digital framework in the laboratory. There, a desired electrical current can be applied to the TEMs and the temperature measurements are available in real-time.

8.4.1 Experimental Procedure

In this experiment, the electric currents (in Ampere) of TEM 3 and TEM 11 were chosen as

$$i_3(t) = -0.6 + 0.4 \sin\left(\frac{2\pi}{221}(t + t_0)\right),$$

$$i_{11}(t) = 0.6 + 0.15 \cos\left(\frac{2\pi}{100}(t + t_0)\right), \tag{8.45}$$

i	0	1	2	3
$\kappa_{1,i}$	0.0037	0.0611	0.3722	1
$p_{1,i+1}$	-0.3	-0.2667	-0.2333	-0.2
$\kappa_{2,i}$	0.44	0.9487	–	–
$p_{2,i+1}$	$-0.4743 + 0.4637j$	$-0.4743 - 0.4637j$	–	–
$\kappa_{3,i}$	0.22	0.6708	–	–
$p_{3,i+1}$	$-0.3354 + 0.3279j$	$-0.3354 - 0.3279$	–	–

Table 8.3: *Chosen observer parameters $\kappa_{j,i}$, $j = 1, \ldots, 3$, $i = 0, \ldots, \mu_j - 1$, see (8.37d). The coefficients $p_{j,i+1}$ are required for the discrete-time implementation of the observer, see (8.44b) and (8.44c). The parameters are represented rounded to four decimal places.*

respectively. The time shift t_0 is introduced because the electrical currents are switched on a while before the observer is launched. This causes an initial temperature profile different from the ambient temperature and, hence, yields a more interesting transient response of the observer. Since the respective electrical current i_3 is negative, TEM 3 is in cooling mode, whereas TEM 11 is in heating mode.

The observer requires the unknown inputs $\ddot{w}_1$ and $\ddot{w}_2$ to be bounded. As the electrical currents and their derivatives are bounded, also the unknown inputs are bounded, which follows from [109].

The chosen parameters of the observer are given in Table 8.3. For the linear observer of subsystem 1, purely real eigenvalues were assigned, which are uniformly distributed between -0.3 and -0.2. The RED-based observers for subsystems 2 and 3 were chosen according to [29, Section 6.7]. As the bounds for the unknown inputs $\ddot{w}_1$ and $\ddot{w}_2$ are unknown, the scaling parameter was increased until convergence of the respective output errors σ_5 and σ_7, see (8.37b), was achieved. The initial estimate of the temperature profile $\hat{T}_i$ is set to $\hat{T}_i(t = 0) = 18°C$, $i = 1, \ldots, 156$. The initial values for the unknown input estimate $\hat{\boldsymbol{w}}$ and the derivative estimate $\dot{\hat{\boldsymbol{w}}}$ are set to $\hat{\boldsymbol{w}}(t = 0) = \dot{\hat{\boldsymbol{w}}}(t = 0) = \boldsymbol{0}$. Individual pixels of the thermal camera, which are located in the centre of the rod, serve as measurements for the observer as well as for its validation.

8.4.2 Estimation Results

Figure 8.6 and Figure 8.7 depict the convergence of the observer estimates to the actually measured temperature profile. Since the thermal imaging camera provides two-dimensional pictures, the measured rod temperature is represented as surface, where the height indicates the local temperature. In order to comparably represent the observer estimates, which actually correspond to a line in longitudinal direction, they are stretched in transverse direction. The position of the measurements used by the observer are indicated by black lines.
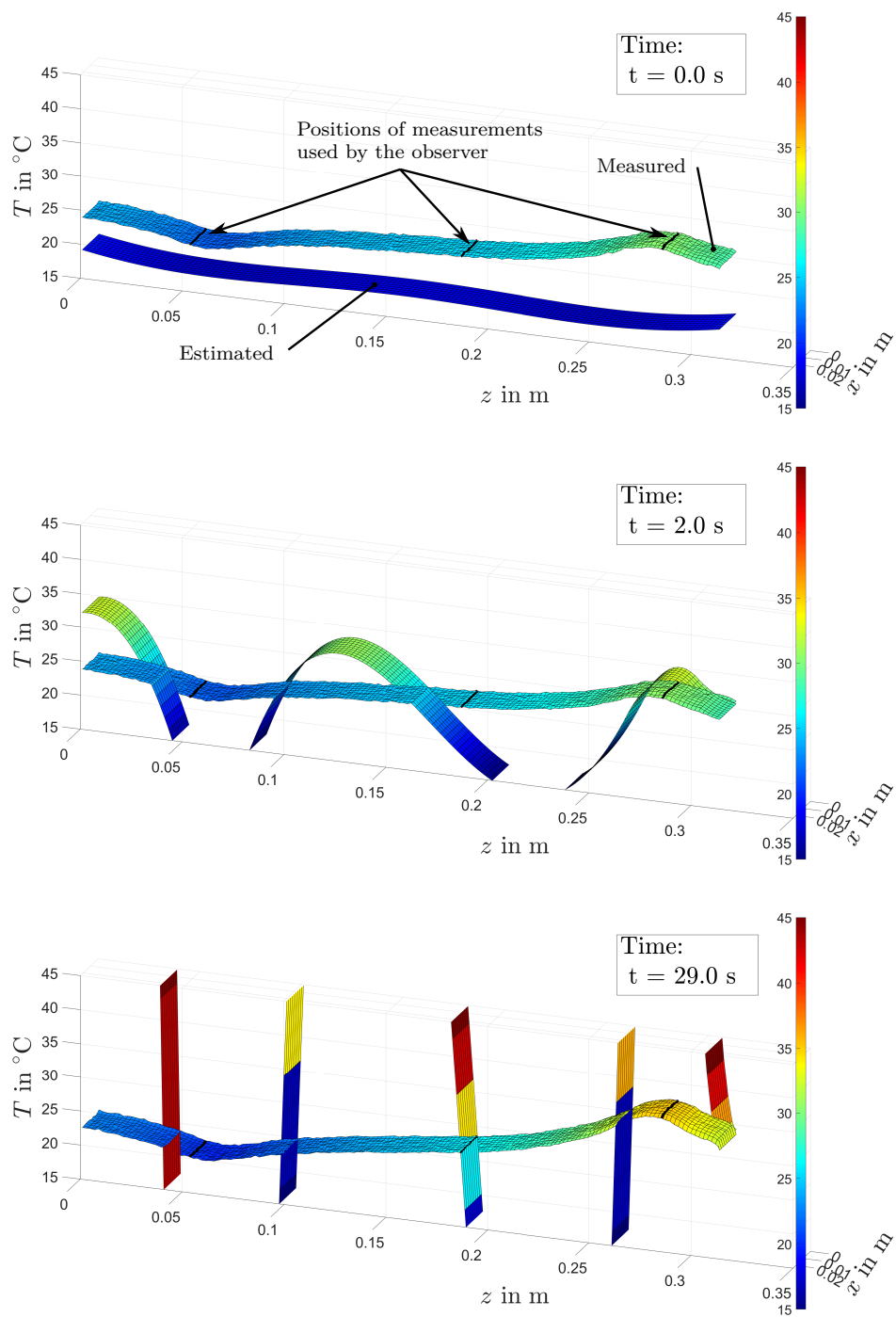
Figure 8.6: *Comparison of the measured and the estimated temperature profile along the aluminium rod at $t = 0$ s, $t = 2$ s and $t = 29$ s. The further evolution is depicted in Figure 8.7.*
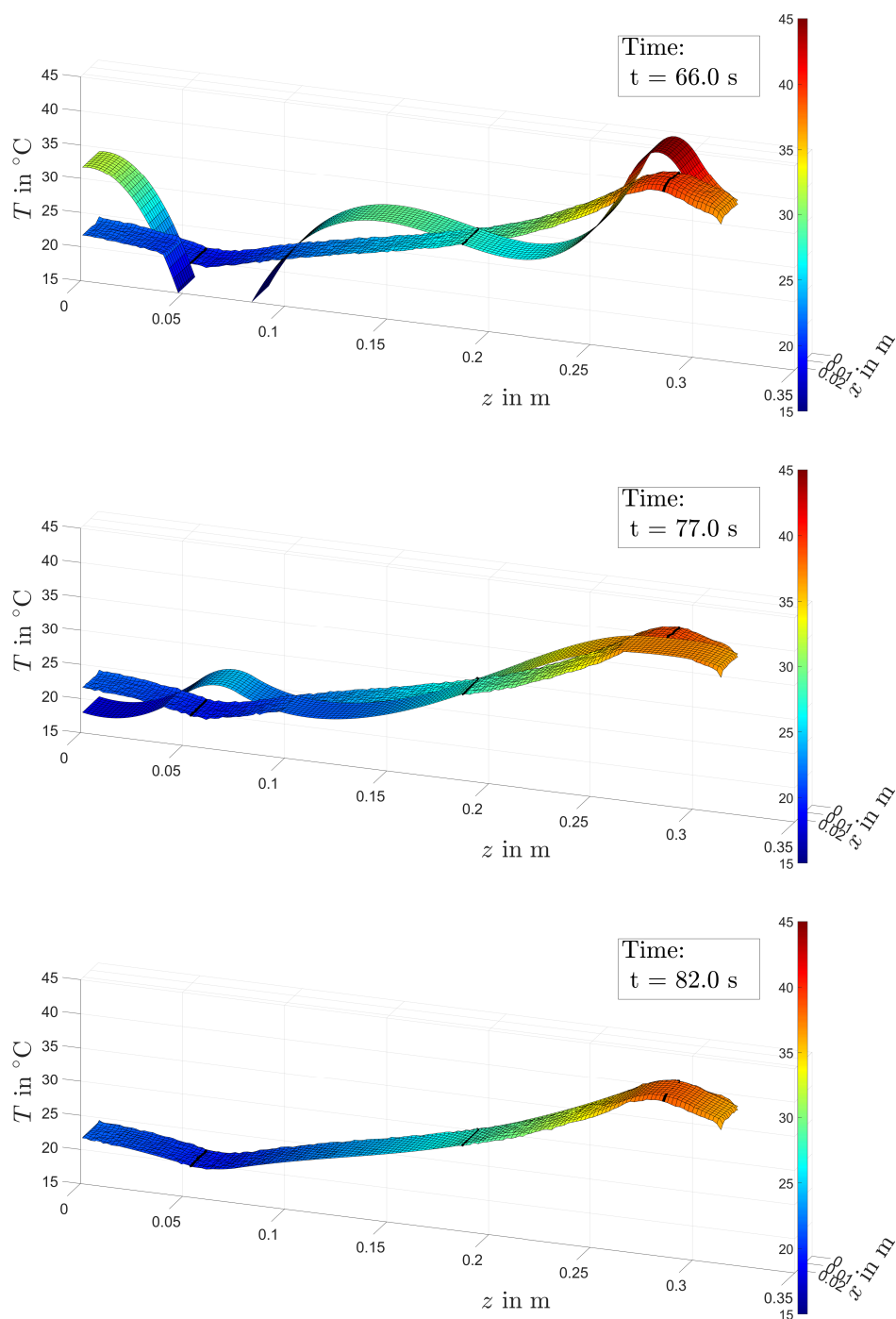
Figure 8.7: *Comparison of the measured and the estimated temperature profile along the aluminium rod at $t = 66$ s, $t = 77$ s and $t = 82$ s, see also Figure 8.6. After approximately 82 s the temperature profile estimate has converged to the actual temperature profile.*

Due to the applied model order reduction, the initial estimate can not be represented as a constant temperature of 18°C, but shows some small deviations. Furthermore, the initial estimation is far off the actual temperature profile, also on average, which leads to strong transients. After approximately 82 s it can be regarded that, practically, the observer has converged, i.e., it approximates the rod's temperature.

Figure 8.8 shows a comparison of the temperature measurements T_i and its respective estimates $\hat{T}_i$ at four exemplary positions distributed along the rod. Again, it becomes apparent that the estimates track the actual temperatures after the transients phase. It is noticeable that the estimates T_9 and T_{147} located close to the rod boundaries have lower accuracy than those located further inside the considered domain.
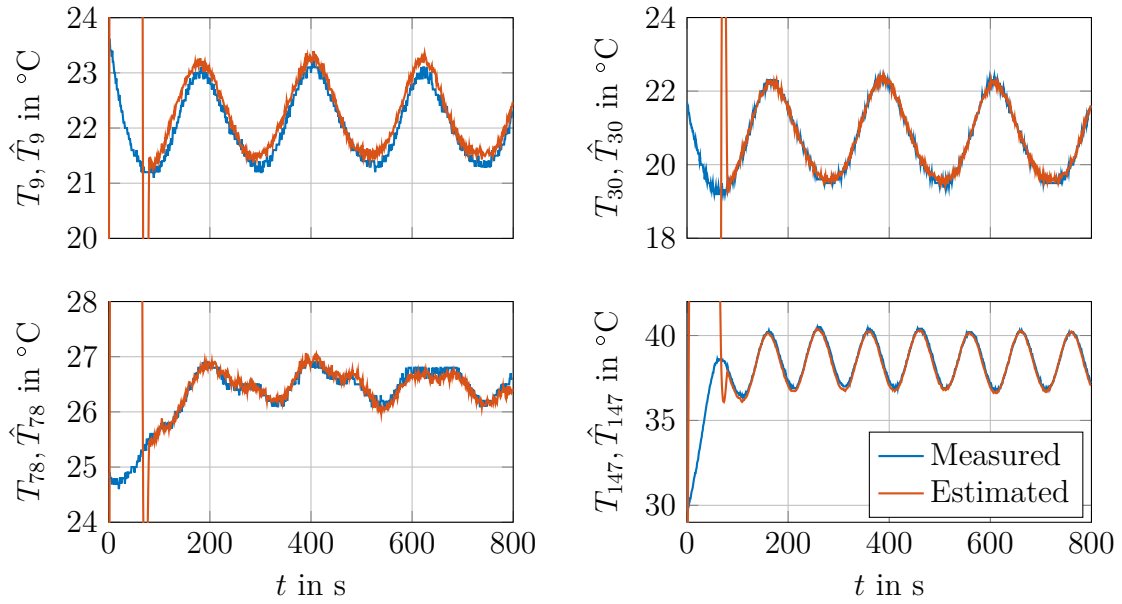
Figure 8.8: *Comparison of measurements T_i and estimates $\hat{T}_i$ at four exemplary positions (out of $N = 156$ node positions in total) along the rod.*

In order to illustrate the achieved estimation accuracy, all estimation errors $T_i - \hat{T}_i$ are shown in Figure 8.9. The majority of the estimation errors converges into a band with an accuracy of ± 0.5°C. A few estimates, which are located close to one of the boundaries, have a larger error band given by ± 0.7°C.

Figure 8.10 provides further insight in the statistics of the estimation error. Therein, the mean and the standard deviation in steady-state are depicted as a function of the position z. In addition to the positions of the measurements used by the observer, also the positions of the active TEMs are plotted. The standard deviation of the steady-state estimation error is almost constant along the rod, whereas the mean varies depending on the particular position. A possible reason is the uncertainty of the convective heat loss at the boundary, which explains the increasing error close to the boundaries. Furthermore, the TEMs entail some uncertainty regarding their position and the distribution of the generated heat flux, which might be not perfectly
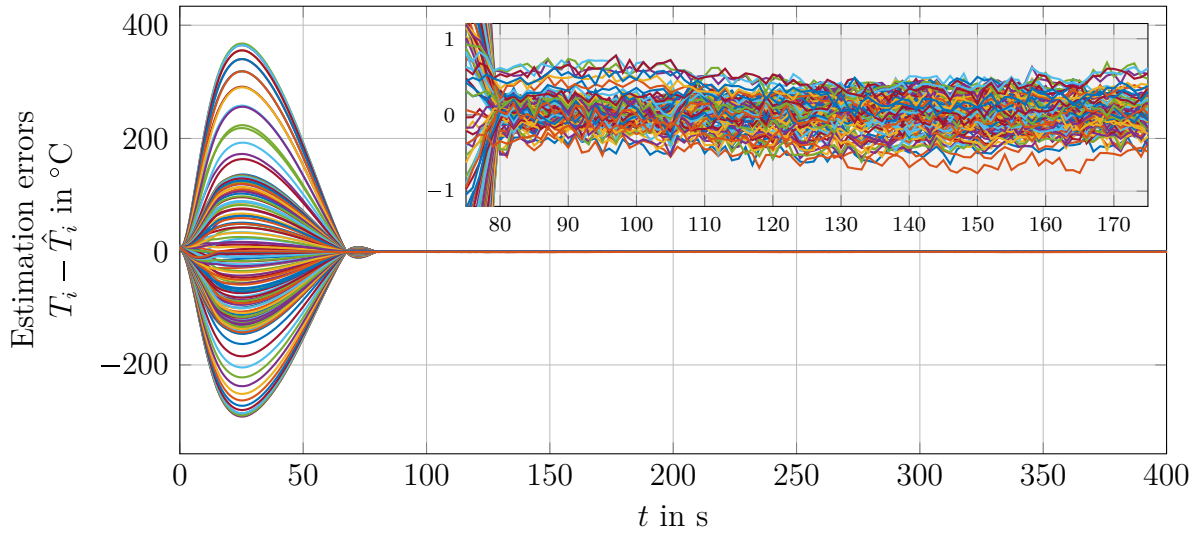
Figure 8.9: *Evolution of the errors $T_i - \hat{T}_i$ of the estimated temperature profile over time. Within approximately 82 s, the errors convergence into a small band around 0.*
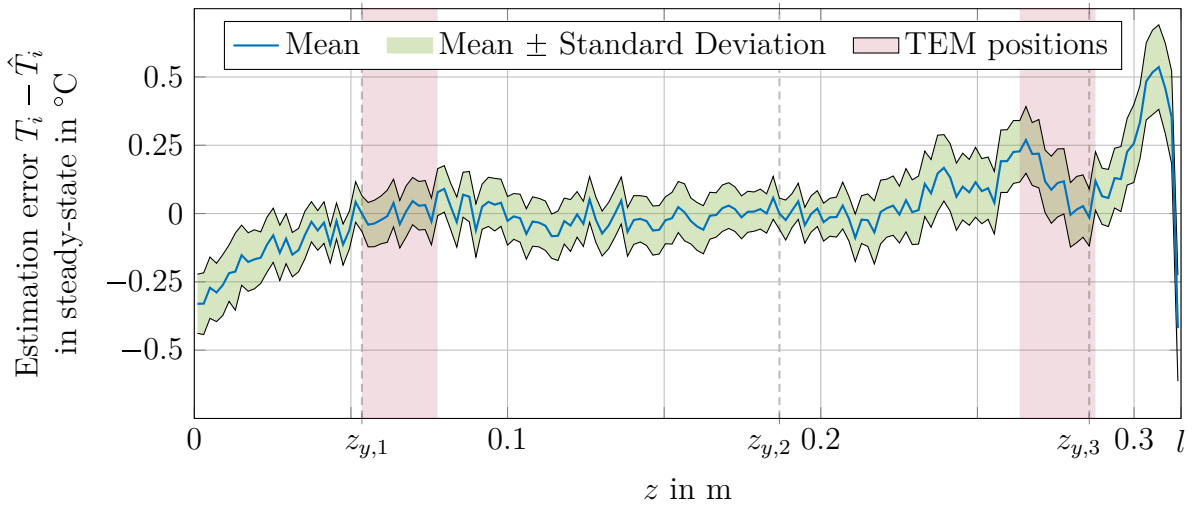

Figure 8.10: *Mean and standard deviation of the steady-state estimation error as a function of the position z along the rod. The positions $z_{y,1}$, $z_{y,2}$ and $z_{y,3}$ indicate the temperature measurements available to the observer. The red areas mark the contact surface of the TEMs that excite the rod with a heat flux unknown to the observer.*

uniformly distributed over the contact surface as assumed by the model, see (8.7). The steady-state estimation error around the position of TEM 11 indicates such an error.

Figure 8.11 shows the estimates $\hat{w}_1$ and $\hat{w}_2$ of the volumetric heat fluxes w_1 and w_2. Note that the actual values are unknown and, thus, not available for comparison. However, the result seems plausible, as it suggest TEM 3 cooling and TEM 11 heating the rod. Furthermore, the cycle durations of the estimated signals coincide with the ones of the applied electrical currents i_3 and i_{11}. In comparison to the temperature estimates, the estimates of the volumetric heat fluxes are quite noisy. This behaviour can be explained by the fact that the signals are generated by differentiating noisy temperature measurements with a quantization step size of $0.1°$C. The given estimates of the unknown heat fluxes can be used to identify proper models for the TEMs, see [109].
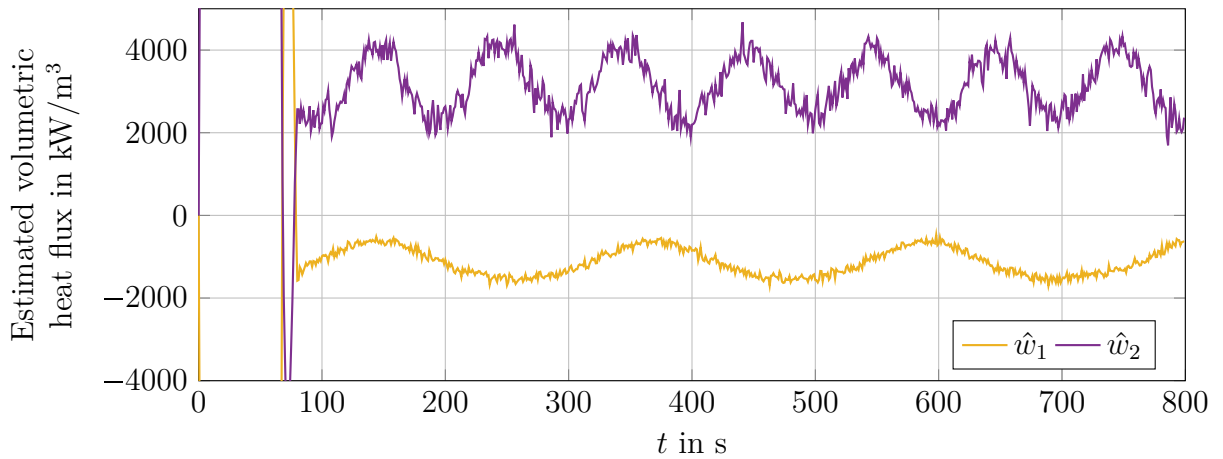

Figure 8.11: *Estimates $\hat{w}_1$ and $\hat{w}_2$ of the volumetric heat fluxes generated by TEM 3 and TEM 11, respectively.*

8.5 Summary, Conclusion and Outlook

The proposed observer design method for LTI multivariable systems with unknown inputs has been successfully applied for the temperature profile estimation of an aluminium rod which is exposed to unknown heat fluxes. The PDE model of the rod was spatially discretized and simplified by means of a modal model order reduction. The resulting LTI system of lower order was transformed into the proposed observer normal form. It was demonstrated that, due the advantageous structure of the observer normal form, the observer design is straightforward. The applied observer consists of a linear part for subsystem 1, which is not directly affect by the unknown inputs, and two RED-based parts for subsystem 2 and subsystem 3, whose dynamics are directly influenced by the unknown inputs. A discrete-time implementation of the observer was proposed for its implementation in a digital framework. The estimation results

illustrate that the given observer is suitable for estimating the rod's temperature profile with high accuracy. The experiment successfully demonstrates that the proposed observer design method constitutes an applicable solution to practical problems.

The discrete-time implementation of the observer uses the Forward Euler discretized plant in order to carry over the appreciated structure of coupled subsystems from the continuous-time model. Future work should deal with more accurate approaches using zero-order hold (ZOH) discretization of the plant which gets especially important for a large discretization time t_d. The available methods for homogeneous differentiators [34, 40] could serve as a basis for work in this research direction.

9

Conclusion and Outlook

In this final chapter of the thesis, conclusions are drawn on the research work presented and an outlook on possible new research topics in this field is given.

9.1 Conclusion

In this thesis, the problem of unknown input observation for LTI systems was considered. In particular, the class of strongly observable systems was investigated, since the error dynamics of these systems can be specified entirely by the observer. Once the unknown input observation problem is solved for the strongly observable case, the extension to the more general class of strongly detectable systems, which fulfil the minimum requirement for the design of stable unknown input observers with asymptotically decaying estimation error, is straightforward, see Section 7.2.

Although the considered system class is a very basic one, it was found that all existing unknown input observer concepts exhibit adverse properties. Their application either requires the system to satisfy restrictive structural conditions, relies on bounded state variables or yields an unnecessarily high observer order which results in a complex design and tuning procedure. For this reason, the aim was to develop new design approaches for unknown input observers to avoid those limitations and disadvantages of existing methods.

Like many other unknown input observers in the literature, the ones proposed in this thesis are based on existing numerical differentiation methods. The decisive difference to existing work is given by the underlying system representation in which these methods are applied. One of the main findings of this thesis is that it is not the respective differentiation method that is decisive, but rather the chosen representation of the system under consideration.

In the SISO case the classical observability canonical form proved to be the key for the unknown input observer design. Due to the beneficial system structure, numerical differentiators can be applied as unknown input observers in a straightforward manner without suffering from the aforementioned limitations and disadvantages of existing approaches. If the respective differentiator is selected from a particular family of

homogeneous differentiators, the observer design can even be carried out in original coordinates, i.e., without explicitly transforming the system. The proposed design formula for the calculation of the output error injection can be regarded as a nonlinear generalization of Ackermann's formula. A necessary condition on the choice of the observer parameters supports the tuning of the unknown input observer.

In contrast to the SISO case, the MIMO case turned out much more complex, especially due to the couplings between inputs and outputs. There were no suitable normal forms for the design of unknown input observers available in the literature, which motivated the development of a new observer normal form. At first glance, the proposed observer normal form is reminiscent of Luenberger's observability canonical form for multivariable systems. However, by permitting additional coupling terms between the subsystems, a specific structure of the unknown-input matrix is achieved which is advantageous in terms of the unknown input observer design. Once the system is represented in observer normal form, the application of different numerical differentiators is straightforward. Again, the resulting unknown input observer does not suffer from the limitations and disadvantages of existing approaches and a necessary condition on the choice of the observer parameters is provided.

One additional strength of the proposed observer concept is the great degree of versatility. The respective numerical differentiation scheme can be selected individually for each of the subsystems in observer normal form. For example, it can be chosen depending on the desired convergence properties of the estimation error. Extensions to systems with direct feed-through[1], strongly detectable systems and systems with unbounded unknown inputs with bounded derivative were presented. The exemplary application to state-feedback control for systems with matched disturbance inputs was demonstrated. Moreover, a method for minimizing the required observer parameters in the case of unknown inputs with asymmetric bounds was proposed.

Finally, the practical applicability of the proposed unknown input observer was successfully demonstrated by estimating the temperature profile along an aluminium rod subjected to unknown external heat fluxes. For the realization in a digital framework, a discrete-time implementation of the unknown input observer was developed and promising estimation results were obtained.

9.2 Outlook

Future research could deal with the following two important topics which emerge from the practical application presented in the Chapter 8.

Numerical stability of the proposed transformations: The spatial discretization of the PDE considered in Chapter 8 results in a system of high order. Due to numerical problems, it is not possible to transform this system into the proposed observer normal form and, hence, a model order reduction is applied. Future research could focus on a numerically stable implementation of proposed transformations into observer

---

[1]The observer normal form considers systems without direct feed-through only.

normal form. The work presented in [117, 118] may serve as a starting point for the development of numerically stable algorithms.

Discretization of the unknown input observer: In practical applications, a discrete-time version of the unknown input observer is typically required. In the application example presented in Chapter 8, the discretization of the unknown input observer is based on the Forward Euler discretization of the continuous-time plant. This type of discretization is advantageous in the sense that it maintains the beneficial structure of coupled subsystems from the continuous-time domain. However, if the discretization time is not sufficiently small, this discretization method exhibits a very poor approximation accuracy. Future work should involve more accurate approaches using e.g. zero-order hold discretization of the plant. The available approaches for homogeneous differentiators [34, 40] could serve as a basis for research in this direction.

10

Appendix

10.1 Model Order Reduction for High-Order LTI Systems Using Quasi-Static Approximation

Consider an LTI system partitioned into

$$
\begin{bmatrix} \dot{\boldsymbol{x}}_1 \\ \dot{\boldsymbol{x}}_2 \end{bmatrix} = \begin{bmatrix} \boldsymbol{A}_{11} & \boldsymbol{A}_{12} \\ \boldsymbol{A}_{21} & \boldsymbol{A}_{22} \end{bmatrix} \begin{bmatrix} \boldsymbol{x}_1 \\ \boldsymbol{x}_2 \end{bmatrix} + \begin{bmatrix} \boldsymbol{B}_1 \\ \boldsymbol{B}_2 \end{bmatrix} \boldsymbol{u},
$$
$$
\boldsymbol{y} = \begin{bmatrix} \boldsymbol{C}_1 & \boldsymbol{C}_2 \end{bmatrix} \begin{bmatrix} \boldsymbol{x}_1 \\ \boldsymbol{x}_2 \end{bmatrix} + \boldsymbol{E}\boldsymbol{u},
$$

$$(10.1)$$

where the state vector $\boldsymbol{x}_1$ covers the relevant directions of the system dynamics whereas the dynamics of $\boldsymbol{x}_2$ are neglected in order to reduce the overall system order. In a quasi-static approximation as discussed in [119, p. 285] and [120], it is assumed that $\boldsymbol{x}_2$ does not follow the dynamics any more, but that all changes happen instantaneously, i.e.,

$$
\dot{\boldsymbol{x}}_2 = 0. \tag{10.2}
$$

Thus, the dynamics of $\boldsymbol{x}_2$ turn into a system of algebraic equations, which is solved for

$$
\boldsymbol{x}_2 = -\boldsymbol{A}_{22}^{-1}\boldsymbol{A}_{21}\boldsymbol{x}_1 - \boldsymbol{A}_{22}^{-1}\boldsymbol{B}_2\boldsymbol{u} \tag{10.3}
$$

assuming that $\boldsymbol{A}_{22}$ is invertible. Insertion of (10.3) reduces the original system (10.1) to the reduced order system

$$
\dot{\boldsymbol{x}}_1 = \underbrace{\left(\boldsymbol{A}_{11} - \boldsymbol{A}_{12}\boldsymbol{A}_{22}^{-1}\boldsymbol{A}_{21}\right)}_{\boldsymbol{A}_{\mathrm{r}}}\boldsymbol{x}_1 + \underbrace{\left(\boldsymbol{B}_1 - \boldsymbol{A}_{12}\boldsymbol{A}_{22}^{-1}\boldsymbol{B}_2\right)}_{\boldsymbol{B}_{\mathrm{r}}}\boldsymbol{u},
$$
$$
\boldsymbol{y} = \underbrace{\left(\boldsymbol{C}_1 - \boldsymbol{C}_2\boldsymbol{A}_{22}^{-1}\boldsymbol{A}_{21}\right)}_{\boldsymbol{C}_{\mathrm{r}}}\boldsymbol{x}_1 + \underbrace{\left(\boldsymbol{E} - \boldsymbol{C}_2\boldsymbol{A}_{22}^{-1}\boldsymbol{B}_2\right)}_{\boldsymbol{E}_{\mathrm{r}}}\boldsymbol{u}.
$$

$$(10.4)$$

In steady-state, $\boldsymbol{x}_1$ and $\boldsymbol{x}_2$ approximated by the low-order system (10.4) and the algebraic relation (10.3), respectively, coincide with the states of the original system (10.1).

10.2 Proof of Lemma 6.3.1

In the following, the parts (a) to (f) of Lemma 6.3.1 are proven. The proofs are adopted from:

H. Niederwieser, M. Tranninger, R. Seeber, M. Reichhartinger, Unknown input observer design for linear time-invariant multivariable systems based on a new observer normal form, International Journal of Systems Science 53 (10) (2022) 2180–2206. `doi:10.1080/00207721.2022.2046201`

10.2.1 Proof of Lemma 6.3.1(a)

Since Step 1 relies on the steps SCB.1, SCB.2 and SCB.3 of the decomposition algorithm proposed in [25, Section 5.3, pages 119-127] this proof mainly refers to the results given in the cited book. Therein, a structural decomposition of a general LTI system of the form (6.2) into four parts is presented. Due to the considered system class only the strongly observable system parts (labelled as b and d in [25]) need to be considered. The regular output transformation (6.11) and the regular state transformation $\tilde{\boldsymbol{x}} = \begin{bmatrix} \tilde{\boldsymbol{x}}_1^{\mathrm{T}} & \ldots & \tilde{\boldsymbol{x}}_p^{\mathrm{T}} \end{bmatrix}^{\mathrm{T}} = \boldsymbol{Z}\boldsymbol{x}$ decompose the system into p coupled chains of integrators of the form

$$
\dot{\tilde{\boldsymbol{x}}}_j = \begin{bmatrix} 0 & 1 & 0 & \ldots & 0 \\ \vdots & \ddots & \ddots & \ddots & \vdots \\ \vdots & & \ddots & \ddots & 0 \\ 0 & \ldots & \ldots & 0 & 1 \\ 0 & \ldots & \ldots & \ldots & 0 \end{bmatrix} \tilde{\boldsymbol{x}}_j + \begin{bmatrix} \boldsymbol{0}^{\mathrm{T}} \\ \vdots \\ \vdots \\ \boldsymbol{0}^{\mathrm{T}} \\ \tilde{\boldsymbol{a}}_j^{\mathrm{T}} \end{bmatrix} \tilde{\boldsymbol{x}} - \tilde{\boldsymbol{\Xi}}_j \boldsymbol{y} + \begin{bmatrix} \boldsymbol{0}^{\mathrm{T}} \\ \vdots \\ \vdots \\ \boldsymbol{0}^{\mathrm{T}} \\ \tilde{\boldsymbol{d}}_j^{\mathrm{T}} \end{bmatrix} \boldsymbol{w},
$$

$$
\bar{y}_j = \begin{bmatrix} 1 & 0 & \ldots & 0 \end{bmatrix} \tilde{\boldsymbol{x}}_j, \tag{10.5}
$$

with one single output $\bar{y}_j$, some linear combination of $\boldsymbol{w}$ as unknown input and some couplings $\tilde{\boldsymbol{a}}_j^{\mathrm{T}} \tilde{\boldsymbol{x}}$ in the last differential equation. In this representation, $\boldsymbol{w}$ either occurs explicitly only in the μ_j-th derivative of $\bar{y}_j$ or does not explicitly act on the jth subsystem at all if $\tilde{\boldsymbol{d}}_j^{\mathrm{T}} = \boldsymbol{0}^{\mathrm{T}}$, i.e., under the output injection $\tilde{\boldsymbol{\Xi}}_j \boldsymbol{y}$ the relative degree of $\bar{y}_j$ with respect to $\boldsymbol{w}$, if it exists, is equal or larger than μ_j. Thus, by applying the output injection $\boldsymbol{\Xi}\boldsymbol{y} = \boldsymbol{Z}^{-1} \begin{bmatrix} \tilde{\boldsymbol{\Xi}}_1^{\mathrm{T}} & \ldots & \tilde{\boldsymbol{\Xi}}_p^{\mathrm{T}} \end{bmatrix}^{\mathrm{T}} \boldsymbol{y}$ and the output transformation (6.11) to the original system (6.2) one exactly obtains the auxiliary system (6.14) satisfying the conditions (6.17) and (6.18).

10.2.2 Proof of Lemma 6.3.1(b)

In order to show that the transformation matrix $\boldsymbol{T}$ given in (6.37) is non-singular, a procedure similar to the one in [80] is applied. Consider constants $\xi_{j,i}$ such that the linear combination of the column vectors of the transformation matrix $\boldsymbol{T}$ equals the

zero vector, i.e.,

$$\sum_{j=1}^{p} \sum_{i=0}^{\mu_j - 1} \xi_{j,i} \boldsymbol{t}_{\mu_1 + \cdots + \mu_j - i} = \boldsymbol{0}. \tag{10.6}$$

Substituting $\boldsymbol{t}_{\mu_1 + \cdots + \mu_j - i}$ according to (6.45) and multiplication of both sides with $\boldsymbol{c}_{\bar{j}}^{\mathrm{T}} \boldsymbol{\check{A}}^{\bar{i}}$ from the left-hand side yields

$$\sum_{j=1}^{p} \sum_{i=0}^{\mu_j - 1} \xi_{j,i} \left(\boldsymbol{\check{c}}_{\bar{j}}^{\mathrm{T}} \boldsymbol{\check{A}}^{i+\bar{i}} \boldsymbol{t}_{\mu_1 + \cdots + \mu_j} - \sum_{r=j+1}^{p} \sum_{q=1}^{i} \beta_{j,r,\mu_j - q} \boldsymbol{\check{c}}_{\bar{j}}^{\mathrm{T}} \boldsymbol{\check{A}}^{i-q+\bar{i}} \boldsymbol{t}_{\mu_1 + \cdots + \mu_r} \right) = 0. \tag{10.7}$$

Due to the choice of the vectors $\boldsymbol{t}_{\mu_1}, \boldsymbol{t}_{\mu_1 + \mu_2}, \ldots, \boldsymbol{t}_n$ in (6.38), they satisfy

$$\begin{bmatrix} \boldsymbol{\check{c}}_1^{\mathrm{T}} \\ \vdots \\ \boldsymbol{\check{c}}_1^{\mathrm{T}} \boldsymbol{\check{A}}^{\mu_1 - 1} \\ \boldsymbol{\check{c}}_2^{\mathrm{T}} \\ \vdots \\ \boldsymbol{\check{c}}_2^{\mathrm{T}} \boldsymbol{\check{A}}^{\mu_2 - 1} \\ \vdots \\ \boldsymbol{\check{c}}_p^{\mathrm{T}} \\ \vdots \\ \boldsymbol{\check{c}}_p^{\mathrm{T}} \boldsymbol{\check{A}}^{\mu_p - 1} \end{bmatrix} \begin{bmatrix} \boldsymbol{t}_{\mu_1} & \boldsymbol{t}_{\mu_1 + \mu_2} & \cdots & \boldsymbol{t}_n \end{bmatrix} = \begin{bmatrix} 0 & 0 & \cdots & 0 \\ \vdots & \vdots & & \vdots \\ 1 & 0 & \cdots & 0 \\ 0 & 0 & \cdots & 0 \\ \vdots & \vdots & & \vdots \\ 0 & 1 & \cdots & 0 \\ \vdots & \vdots & & \vdots \\ 0 & 0 & \cdots & 0 \\ \vdots & \vdots & & \vdots \\ 0 & 0 & \cdots & 1 \end{bmatrix}. \tag{10.8}$$

Consider equation (10.7) for $\bar{i} = 0$. Taking into account (10.8) reduces (10.7) to

$$\xi_{\bar{j},\mu_{\bar{j}} - 1} = 0 \qquad \text{for} \quad \bar{j} = 1, 2, \ldots, p. \tag{10.9}$$

Furthermore, consider equation (10.7) for $\bar{i} = 1$. Taking into account (10.8) and (10.9) reduces (10.7) to

$$\xi_{\bar{j},\mu_{\bar{j}} - 2} = 0 \qquad \text{for} \quad \bar{j} = 1, 2, \ldots, p. \tag{10.10}$$

Continuing in this way, $\xi_{j,i} = 0$ can be shown for $j = 1, 2, \ldots, p$, $i = 0, 1, \ldots, \mu_j - 1$. Hence, it can be concluded that the columns of the transformation matrix $\boldsymbol{T}$ are linearly independent and, thus, $\boldsymbol{T}$ is non-singular. Note that this proof does not require any restrictions regarding the coefficients $\beta_{j,k,l}$ and, thus, $\boldsymbol{T}$ is non-singular regardless of the values of $\beta_{j,k,l}$.

10.2.3 Proof of Lemma 6.3.1(c)

The existence of a unique solution $\boldsymbol{\beta}^{(j)}$ of the system of equations (6.42) is ensured, if and only if the matrices $\boldsymbol{H}^{(j)}$ are non-singular in any case for $j = 1, \ldots, p - 1$.

Consider the determinant

$$
\det \boldsymbol{H}^{(j)} \overset{(6.39)}{=}
\begin{vmatrix}
\boldsymbol{H}^{(j)}_{j+1,j+1} & \cdots & \boldsymbol{H}^{(j)}_{j+1,p-1} & \boldsymbol{H}^{(j)}_{j+1,p} \\
\vdots & \ddots & \vdots & \vdots \\
\boldsymbol{H}^{(j)}_{p-1,j+1} & \cdots & \boldsymbol{H}^{(j)}_{p-1,p-1} & \boldsymbol{H}^{(j)}_{p-1,p} \\
\boldsymbol{H}^{(j)}_{p,j+1} & \cdots & \boldsymbol{H}^{(j)}_{p,p-1} & \boldsymbol{H}^{(j)}_{p,p}
\end{vmatrix}.
\tag{10.11}
$$

Since the block $\boldsymbol{H}^{(j)}_{p,p}$ of size $(\mu_j - \mu_p) \times (\mu_j - \mu_p)$ is an upper unitriangular matrix, see (6.40), its determinant satisfies

$$
\det \boldsymbol{H}^{(j)}_{p,p} = 1.
\tag{10.12}
$$

Furthermore, its inverse always exists and is again upper unitriangular, i.e.,

$$
\boldsymbol{H}^{(j)^{-1}}_{p,p} =
\begin{bmatrix}
1 & * & \cdots & * \\
0 & \ddots & \ddots & \vdots \\
\vdots & \ddots & \ddots & * \\
0 & \cdots & 0 & 1
\end{bmatrix},
\tag{10.13}
$$

which allows to rewrite the determinant (10.11) in terms of the Schur complement of $\boldsymbol{H}^{(j)}_{p,p}$, i.e.,

$$
\det \boldsymbol{H}^{(j)} = \underbrace{\det \boldsymbol{H}^{(j)}_{p,p}}_{\overset{(10.12)}{=} 1} \cdot
\left| \begin{bmatrix}
\boldsymbol{H}^{(j)}_{j+1,j+1} & \cdots & \boldsymbol{H}^{(j)}_{j+1,p-1} \\
\vdots & \ddots & \vdots \\
\boldsymbol{H}^{(j)}_{p-1,j+1} & \cdots & \boldsymbol{H}^{(j)}_{p-1,p-1}
\end{bmatrix} -
\begin{bmatrix}
\boldsymbol{H}^{(j)}_{j+1,p} \\
\vdots \\
\boldsymbol{H}^{(j)}_{p-1,p}
\end{bmatrix} \boldsymbol{H}^{(j)^{-1}}_{p,p}
\begin{bmatrix}
\boldsymbol{H}^{(j)}_{p,j+1} & \cdots & \boldsymbol{H}^{(j)}_{p,p-1}
\end{bmatrix} \right| =
$$

$$
=
\begin{vmatrix}
\boldsymbol{H}^{(j)}_{j+1,j+1} - \boldsymbol{H}^{(j)}_{j+1,p}\boldsymbol{H}^{(j)^{-1}}_{p,p}\boldsymbol{H}^{(j)}_{p,j+1} & \cdots & \boldsymbol{H}^{(j)}_{j+1,p-1} - \boldsymbol{H}^{(j)}_{j+1,p}\boldsymbol{H}^{(j)^{-1}}_{p,p}\boldsymbol{H}^{(j)}_{p,p-1} \\
\vdots & \ddots & \vdots \\
\boldsymbol{H}^{(j)}_{p-1,j+1} - \boldsymbol{H}^{(j)}_{p-1,p}\boldsymbol{H}^{(j)^{-1}}_{p,p}\boldsymbol{H}^{(j)}_{p,j+1} & \cdots & \boldsymbol{H}^{(j)}_{p-1,p-1} - \boldsymbol{H}^{(j)}_{p-1,p}\boldsymbol{H}^{(j)^{-1}}_{p,p}\boldsymbol{H}^{(j)}_{p,p-1}
\end{vmatrix}.
\tag{10.14}
$$

Furthermore, due to the special structure of the blocks $\boldsymbol{H}^{(j)}_{r,p}$, $\boldsymbol{H}^{(j)}_{p,s}$ given in (6.40) and $\boldsymbol{H}^{(j)^{-1}}_{p,p}$ indicated in (10.13), the blocks

$$
\boldsymbol{H}^{(j,1)}_{r,s} = \boldsymbol{H}^{(j)}_{r,s} - \boldsymbol{H}^{(j)}_{r,p}\boldsymbol{H}^{(j)^{-1}}_{p,p}\boldsymbol{H}^{(j)}_{p,s}
\qquad \text{for} \quad
\begin{aligned}
r &= j+1,\ldots,p-1, \\
s &= j+1,\ldots,p-1,
\end{aligned}
\tag{10.15}
$$

of the matrix in (10.14) offer exactly the same structure as the original blocks $\boldsymbol{H}^{(j)}_{r,s}$, i.e., the zero elements and also the ones on the main diagonal for the case $r = s$ of the original matrix $\boldsymbol{H}^{(j)}$ are preserved. Thus, it is again possible to rewrite the determinant (10.14) in terms of the Schur complement of $\boldsymbol{H}^{(j,1)}_{p-1,p-1}$ which is again

upper unitriangular, i.e.,

$$\det \boldsymbol{H}^{(j)} = \underbrace{\det \boldsymbol{H}^{(j,1)}_{p-1,p-1}}_{=1}$$

$$\times \left| \begin{bmatrix} \boldsymbol{H}^{(j,1)}_{j+1,j+1} & \cdots & \boldsymbol{H}^{(j,1)}_{j+1,p-2} \\ \vdots & \ddots & \vdots \\ \boldsymbol{H}^{(j,1)}_{p-2,j+1} & \cdots & \boldsymbol{H}^{(j,1)}_{p-2,p-2} \end{bmatrix} - \begin{bmatrix} \boldsymbol{H}^{(j,1)}_{j+1,p-1} \\ \vdots \\ \boldsymbol{H}^{(j,1)}_{p-2,p-1} \end{bmatrix} \boldsymbol{H}^{(j,1)\,-1}_{p-1,p-1} \begin{bmatrix} \boldsymbol{H}^{(j,1)}_{p-1,j+1} & \cdots & \boldsymbol{H}^{(j,1)}_{p-1,p-2} \end{bmatrix} \right| =$$

$$= \left| \begin{matrix} \boldsymbol{H}^{(j,1)}_{j+1,j+1} - \boldsymbol{H}^{(j,1)}_{j+1,p-1}\boldsymbol{H}^{(j,1)\,-1}_{p-1,p-1}\boldsymbol{H}^{(j,1)}_{p-1,j+1} & \cdots & \boldsymbol{H}^{(j,1)}_{j+1,p-2} - \boldsymbol{H}^{(j,1)}_{j+1,p-1}\boldsymbol{H}^{(j,1)\,-1}_{p-1,p-1}\boldsymbol{H}^{(j,1)}_{p-1,p-2} \\ \vdots & \ddots & \vdots \\ \boldsymbol{H}^{(j,1)}_{p-2,j+1} - \boldsymbol{H}^{(j,1)}_{p-2,p-1}\boldsymbol{H}^{(j,1)\,-1}_{p-1,p-1}\boldsymbol{H}^{(j,1)}_{p-1,j+1} & \cdots & \boldsymbol{H}^{(j,1)}_{p-2,p-2} - \boldsymbol{H}^{(j,1)}_{p-2,p-1}\boldsymbol{H}^{(j,1)\,-1}_{p-1,p-1}\boldsymbol{H}^{(j,1)}_{p-1,p-2} \end{matrix} \right|.$$

$$(10.16)$$

Again, the blocks

$$\boldsymbol{H}^{(j,2)}_{r,s} = \boldsymbol{H}^{(j,1)}_{r,s} - \boldsymbol{H}^{(j,1)}_{r,p-1}\boldsymbol{H}^{(j,1)\,-1}_{p-1,p-1}\boldsymbol{H}^{(j,1)}_{p-1,s} \qquad \text{for} \quad r = j+1,\ldots,p-2,$$
$$s = j+1,\ldots,p-2,$$
$$(10.17)$$

of the matrix in (10.16) offer the same structure as $\boldsymbol{H}^{(j,1)}_{r,s}$ and, thus, also as the original blocks $\boldsymbol{H}^{(j)}_{r,s}$, which again allows to rewrite the determinant in (10.16) in terms of the Schur complement of the upper unitriangular matrix $\boldsymbol{H}^{(j,2)}_{p-2,p-2}$ and so on. Continuing this way until

$$\det \boldsymbol{H}^{(j)} = \underbrace{\det \boldsymbol{H}^{(j,p-j-2)}_{j+2,j+2}}_{=1} \cdot \left| \boldsymbol{H}^{(j,p-j-2)}_{j+1,j+1} - \boldsymbol{H}^{(j,p-j-2)}_{j+1,j+2}\boldsymbol{H}^{(j,p-j-2)\,-1}_{j+2,j+2}\boldsymbol{H}^{(j,p-j-2)}_{j+2,j+1} \right| =$$
$$= \det \boldsymbol{H}^{(j,p-j-1)}_{j+1,j+1} = 1 \neq 0,$$
$$(10.18)$$

it finally follows that $\boldsymbol{H}^{(j)}$ is non-singular and, thus, there always exists a unique solution of the system of equations (6.42).

10.2.4 Proof of Lemma 6.3.1(d)

Multiplication of (6.12a) with $\boldsymbol{T}$ from the left-hand side and substitution of $\boldsymbol{A}$ by the decomposition (6.13) yields

$$\boldsymbol{T}\bar{\boldsymbol{A}} = \check{\boldsymbol{A}}\boldsymbol{T} - \boldsymbol{\Xi}\boldsymbol{C}\boldsymbol{T}. \tag{10.19}$$

The results of Lemma 6.3.1(f) and the insertion of the identity matrix $\boldsymbol{\Gamma}^{-1}\boldsymbol{\Gamma}$ allow to simplify the term $\boldsymbol{\Xi}\boldsymbol{C}\boldsymbol{T}$ to

$$\boldsymbol{\Xi}\boldsymbol{C}\boldsymbol{T} = \boldsymbol{\Xi}\boldsymbol{\Gamma}^{-1}\underbrace{\boldsymbol{\Gamma}\boldsymbol{C}\boldsymbol{T}}_{\overset{(6.12c)}{=}\bar{C}} \overset{(6.1d)}{=} \boldsymbol{\Xi}\boldsymbol{\Gamma}^{-1} \begin{bmatrix} \boldsymbol{e}^{\mathrm{T}}_1 \\ \boldsymbol{e}^{\mathrm{T}}_{\mu_1+1} \\ \vdots \\ \boldsymbol{e}^{\mathrm{T}}_{\mu_1+\cdots+\mu_{p-1}+1} \end{bmatrix} = \tag{10.20}$$

$$= \begin{bmatrix} \tilde{\boldsymbol{\alpha}}_1 & \boldsymbol{0}_{n\times(\mu_1-1)} & | & \tilde{\boldsymbol{\alpha}}_2 & \boldsymbol{0}_{n\times(\mu_2-1)} & | & \ldots & | & \tilde{\boldsymbol{\alpha}}_p & \boldsymbol{0}_{n\times(\mu_p-1)} \end{bmatrix},$$

where $\tilde{\boldsymbol{\alpha}}_j \in \mathbb{R}^n$, $j = 1, \ldots, p$. Using (10.20) and the definitions of $\bar{\boldsymbol{A}}$ in (6.1b) and $\boldsymbol{T}$ in (6.37) allows to express equation (10.19) in terms of its column vectors, i.e.,

$$
\begin{bmatrix}
\boldsymbol{T}\boldsymbol{\alpha}_1 & \boldsymbol{t}_1 + \sum_{r=2}^{p} \beta_{1,r,1}\boldsymbol{t}_{\mu_1+\cdots+\mu_r} & \cdots & \boldsymbol{t}_{\mu_1-1} + \sum_{r=2}^{p} \beta_{1,r,\mu_1-1}\boldsymbol{t}_{\mu_1+\cdots+\mu_r} \\
\boldsymbol{T}\boldsymbol{\alpha}_2 & \boldsymbol{t}_{\mu_1+1} + \sum_{r=3}^{p} \beta_{2,r,1}\boldsymbol{t}_{\mu_1+\cdots+\mu_r} & \cdots & \boldsymbol{t}_{\mu_1+\mu_2-1} + \sum_{r=3}^{p} \beta_{2,r,\mu_2-1}\boldsymbol{t}_{\mu_1+\cdots+\mu_r} & \cdots \\
\boldsymbol{T}\boldsymbol{\alpha}_p & \boldsymbol{t}_{\mu_1+\cdots+\mu_{p-1}+1} & \cdots & \boldsymbol{t}_{n-1}
\end{bmatrix} =
$$

$$
= \begin{bmatrix}
\check{\boldsymbol{A}}\boldsymbol{t}_1 - \tilde{\boldsymbol{\alpha}}_1 & \check{\boldsymbol{A}}\boldsymbol{t}_2 & \cdots & \check{\boldsymbol{A}}\boldsymbol{t}_{\mu_1} \\
\check{\boldsymbol{A}}\boldsymbol{t}_{\mu_1+1} - \tilde{\boldsymbol{\alpha}}_2 & \check{\boldsymbol{A}}\boldsymbol{t}_{\mu_1+2} & \cdots & \check{\boldsymbol{A}}\boldsymbol{t}_{\mu_1+\mu_2} & \cdots & \check{\boldsymbol{A}}\boldsymbol{t}_{\mu_1+\cdots+\mu_{p-1}+1} - \tilde{\boldsymbol{\alpha}}_p & \check{\boldsymbol{A}}\boldsymbol{t}_{\mu_1+\cdots+\mu_{p-1}+2} & \cdots & \check{\boldsymbol{A}}\boldsymbol{t}_n
\end{bmatrix},
$$

$$\tag{10.21}$$

where $\boldsymbol{\alpha}_j = \begin{bmatrix} \alpha_{j,1} & \cdots & \alpha_{j,n} \end{bmatrix}^{\mathrm{T}}$, $j = 1, 2, \ldots, p$. It follows from (10.21) that the matrix $\bar{\boldsymbol{A}}$ offers the desired structure (6.1b) if

$$
\boldsymbol{t}_{\mu_1+\cdots+\mu_j-i} + \sum_{r=j+1}^{p} \beta_{j,r,\mu_j-i}\boldsymbol{t}_{\mu_1+\cdots+\mu_r} = \check{\boldsymbol{A}}\boldsymbol{t}_{\mu_1+\cdots+\mu_j-i+1} \tag{10.22}
$$

for $j = 1, 2, \ldots, p$, $i = 1, 2, \ldots, \mu_j - 1$, is satisfied. This is shown by finally substituting $\boldsymbol{t}_{\mu_1+\cdots+\mu_j-i}$ and $\boldsymbol{t}_{\mu_1+\cdots+\mu_j-i+1}$ into (10.22) according to (6.45), i.e.,

$$
\check{\boldsymbol{A}}^i \boldsymbol{t}_{\mu_1+\cdots+\mu_j} - \sum_{r=j+1}^{p} \sum_{q=1}^{i} \beta_{j,r,\mu_j-q}\check{\boldsymbol{A}}^{i-q}\boldsymbol{t}_{\mu_1+\cdots+\mu_r} + \sum_{r=j+1}^{p} \beta_{j,r,\mu_j-i}\boldsymbol{t}_{\mu_1+\cdots+\mu_r} =
$$

$$
= \check{\boldsymbol{A}}\left(\check{\boldsymbol{A}}^{i-1}\boldsymbol{t}_{\mu_1+\cdots+\mu_j} - \sum_{r=j+1}^{p} \sum_{q=1}^{i-1} \beta_{j,r,\mu_j-q}\check{\boldsymbol{A}}^{i-q-1}\boldsymbol{t}_{\mu_1+\cdots+\mu_r} \right),
$$

$$\tag{10.23}$$

which is true for all $j = 1, 2, \ldots, p$, $i = 1, \ldots, \mu_j - 1$.

10.2.5 Proof of Lemma 6.3.1(e)

Insertion of the identity matrix $\boldsymbol{\mathcal{O}}_{\mathrm{R}}^{-1}\boldsymbol{\mathcal{O}}_{\mathrm{R}}$ into the transformation rule (6.12b) for the unknown-input matrix $\bar{\boldsymbol{D}}$ of the transformed system yields

$$
\bar{\boldsymbol{D}} \overset{(6.12b)}{=} \boldsymbol{T}^{-1}\boldsymbol{D} = \boldsymbol{T}^{-1}\boldsymbol{\mathcal{O}}_{\mathrm{R}}^{-1}\boldsymbol{\mathcal{O}}_{\mathrm{R}}\boldsymbol{D}. \tag{10.24}
$$

Note that $\mathcal{O}_{\mathrm{R}}$ is invertible which directly follows from Lemma 6.3.1(a). Condition (6.18) allows to express the product $\mathcal{O}_{\mathrm{R}} D$ as

$$
\mathcal{O}_{\mathrm{R}} D \overset{(6.16)}{=}
\begin{bmatrix}
\check{c}_1^{\mathrm{T}} D \\
\vdots \\
\check{c}_1^{\mathrm{T}} \check{A}^{\mu_1-2} D \\
\check{c}_1^{\mathrm{T}} \check{A}^{\mu_1-1} D \\
\vdots \\
\check{c}_p^{\mathrm{T}} D \\
\vdots \\
\check{c}_p^{\mathrm{T}} \check{A}^{\mu_p-2} D \\
\check{c}_p^{\mathrm{T}} \check{A}^{\mu_p-1} D
\end{bmatrix}
\overset{(6.18)}{=}
\begin{bmatrix}
0^{\mathrm{T}} \\
\vdots \\
0^{\mathrm{T}} \\
\check{c}_1^{\mathrm{T}} \check{A}^{\mu_1-1} D \\
\vdots \\
0^{\mathrm{T}} \\
\vdots \\
0^{\mathrm{T}} \\
\check{c}_p^{\mathrm{T}} \check{A}^{\mu_p-1} D
\end{bmatrix}
= \sum_{j=1}^{p} e_{\mu_1+\cdots+\mu_j} \check{c}_j^{\mathrm{T}} \check{A}^{\mu_j-1} D.
$$
(10.25)

Substituting (10.25) into (10.24) and taking into account (6.38) yields

$$
\bar{D} \overset{(10.25)}{=} \sum_{j=1}^{p} T^{-1} \mathcal{O}_{\mathrm{R}}^{-1} e_{\mu_1+\cdots+\mu_j} \check{c}_j^{\mathrm{T}} \check{A}^{\mu_j-1} D =
$$
$$
\overset{(6.38)}{=} \sum_{j=1}^{p} T^{-1} t_{\mu_1+\cdots+\mu_j} \check{c}_j^{\mathrm{T}} \check{A}^{\mu_j-1} D.
$$
(10.26)

The vector $t_{\mu_1+\cdots+\mu_j}$ corresponds to the $(\mu_1 + \cdots + \mu_j)$-th column of T, i.e., $t_{\mu_1+\cdots+\mu_j} = T e_{\mu_1+\cdots+\mu_j}$, which allows to simplify (10.26) to

$$
\bar{D} = \sum_{j=1}^{p} T^{-1} T e_{\mu_1+\cdots+\mu_j} \check{c}_j^{\mathrm{T}} \check{A}^{\mu_j-1} D = \sum_{j=1}^{p} e_{\mu_1+\cdots+\mu_j} \check{c}_j^{\mathrm{T}} \check{A}^{\mu_j-1} D =
\begin{bmatrix}
0^{\mathrm{T}} \\
\vdots \\
0^{\mathrm{T}} \\
\check{c}_1^{\mathrm{T}} \check{A}^{\mu_1-1} D \\
\vdots \\
0^{\mathrm{T}} \\
\vdots \\
0^{\mathrm{T}} \\
\check{c}_p^{\mathrm{T}} \check{A}^{\mu_p-1} D
\end{bmatrix},
$$
(10.27)

which finally completes the proof.

10.2.6 Proof of Lemma 6.3.1(f)

The output matrix $\bar{C}$ of the transformed system can be expressed by its elements, i.e.,

$$
\bar{C} \overset{(6.12c)}{=} \Gamma C T \overset{(6.15)}{\underset{(6.37)}{=}}
\begin{bmatrix}
\check{c}_1^{\mathrm{T}} \\
\vdots \\
\check{c}_p^{\mathrm{T}}
\end{bmatrix}
\begin{bmatrix} t_1 & \ldots & t_n \end{bmatrix}
=
\begin{bmatrix}
\check{c}_1^{\mathrm{T}} t_1 & \ldots & \check{c}_1^{\mathrm{T}} t_n \\
\vdots & & \vdots \\
\check{c}_p^{\mathrm{T}} t_1 & \ldots & \check{c}_p^{\mathrm{T}} t_n
\end{bmatrix},
$$
(10.28)

where the single elements can be described as

$$\check{\boldsymbol{c}}_{\bar{j}}^{\mathrm{T}}\boldsymbol{t}_{\mu_1+\cdots+\mu_j-i} \overset{(6.45)}{=} \check{\boldsymbol{c}}_{\bar{j}}^{\mathrm{T}}\check{\boldsymbol{A}}^i\boldsymbol{t}_{\mu_1+\cdots+\mu_j} - \sum_{r=j+1}^{p}\sum_{q=1}^{i}\beta_{j,r,\mu_j-q}\check{\boldsymbol{c}}_{\bar{j}}^{\mathrm{T}}\check{\boldsymbol{A}}^{i-q}\boldsymbol{t}_{\mu_1+\cdots+\mu_r} \tag{10.29}$$

for $\bar{j}=1,\ldots,p$, $j=1,\ldots,p$ and $i=0,\ldots,\mu_j-1$. In the following, the scalar product $\check{\boldsymbol{c}}_{\bar{j}}^{\mathrm{T}}\boldsymbol{t}_{\mu_1+\cdots+\mu_j-i}$ given in (10.29) is considered for the cases (a) $\bar{j}<j$, (b) $\bar{j}=j$ and (c) $\bar{j}>j$:

(a) For $\bar{j}<j$, all the terms on the right-hand side of (10.29) vanish which follows directly from (10.8), i.e.,

$$\check{\boldsymbol{c}}_{\bar{j}}^{\mathrm{T}}\boldsymbol{t}_{\mu_1+\cdots+\mu_j-i} = \underbrace{\check{\boldsymbol{c}}_{\bar{j}}^{\mathrm{T}}\check{\boldsymbol{A}}^i\boldsymbol{t}_{\mu_1+\cdots+\mu_j}}_{\overset{(10.8)}{=}0} - \sum_{r=j+1}^{p}\sum_{q=1}^{i}\beta_{j,r,\mu_j-q}\underbrace{\check{\boldsymbol{c}}_{\bar{j}}^{\mathrm{T}}\check{\boldsymbol{A}}^{i-q}\boldsymbol{t}_{\mu_1+\cdots+\mu_r}}_{\overset{(10.8)}{=}0} = 0 \tag{10.30}$$

for $\bar{j}=1,\ldots,p-1$, $j=\bar{j}+1,\ldots,p$ and $i=0,\ldots,\mu_j-1$.

(b) For $\bar{j}=j$, (10.29) simplifies to

$$\check{\boldsymbol{c}}_{j}^{\mathrm{T}}\boldsymbol{t}_{\mu_1+\cdots+\mu_j-i} = \check{\boldsymbol{c}}_{j}^{\mathrm{T}}\check{\boldsymbol{A}}^i\boldsymbol{t}_{\mu_1+\cdots+\mu_j} - \sum_{r=j+1}^{p}\sum_{q=1}^{i}\beta_{j,r,\mu_j-q}\underbrace{\check{\boldsymbol{c}}_{j}^{\mathrm{T}}\check{\boldsymbol{A}}^{i-q}\boldsymbol{t}_{\mu_1+\cdots+\mu_r}}_{\overset{(10.8)}{=}0} =$$

$$= \check{\boldsymbol{c}}_{j}^{\mathrm{T}}\check{\boldsymbol{A}}^i\boldsymbol{t}_{\mu_1+\cdots+\mu_j} \overset{(10.8)}{=} \begin{cases} 1 & \text{if } i=\mu_j-1 \\ 0 & \text{else} \end{cases} \tag{10.31}$$

for $j=1,\ldots,p$, $i=0,\ldots,\mu_j-1$.

(c) In the case $\bar{j}>j$, only the coefficients β_{j,r,μ_j-q} whose indices satisfy $\mu_j-q\geqslant\mu_r$ are nonzero, see (6.44), and make a contribution to the sum in (10.29) which allows to change the upper limit of the summation with respect to the index q as

$$\check{\boldsymbol{c}}_{\bar{j}}^{\mathrm{T}}\boldsymbol{t}_{\mu_1+\cdots+\mu_j-i} = \check{\boldsymbol{c}}_{\bar{j}}^{\mathrm{T}}\check{\boldsymbol{A}}^i\boldsymbol{t}_{\mu_1+\cdots+\mu_j} - \sum_{r=j+1}^{p}\sum_{q=1}^{\mu_j-\mu_r}\beta_{j,r,\mu_j-q}\check{\boldsymbol{c}}_{\bar{j}}^{\mathrm{T}}\check{\boldsymbol{A}}^{i-q}\boldsymbol{t}_{\mu_1+\cdots+\mu_r} \tag{10.32}$$

for $\bar{j}=2,\ldots,p$, $j=1,\ldots,\bar{j}-1$, $i=0,\ldots,\mu_j-1$. Since the term $\sum_{r=j+1}^{p}\sum_{q=1}^{\mu_j-\mu_r}\beta_{j,r,\mu_j-q}\check{\boldsymbol{c}}_{\bar{j}}^{\mathrm{T}}\check{\boldsymbol{A}}^{i-q}\boldsymbol{t}_{\mu_1+\cdots+\mu_r}$ reassembles the left-hand side of the $\left((\bar{j}-j+1)\mu_j-(\mu_{j+1}+\cdots+\mu_{\bar{j}})-i\right)^{\text{th}}$ equation (6.42), it equals the corresponding right-hand side of (6.42), i.e.,

$$\sum_{r=j+1}^{p}\sum_{q=1}^{\mu_j-\mu_r}\beta_{j,r,\mu_j-q}\check{\boldsymbol{c}}_{\bar{j}}^{\mathrm{T}}\check{\boldsymbol{A}}^{i-q}\boldsymbol{t}_{\mu_1+\cdots+\mu_r} = \check{\boldsymbol{c}}_{\bar{j}}^{\mathrm{T}}\check{\boldsymbol{A}}^i\boldsymbol{t}_{\mu_1+\cdots+\mu_j} \tag{10.33}$$

for $\bar{j} = 2, \ldots, p$, $j = 1, \ldots, \bar{j} - 1$, $i = 0, \ldots, \mu_j - 1$. Substituting (10.33) into (10.32) yields

$$\check{c}_{\bar{j}}^{\mathrm{T}} t_{\mu_1 + \cdots + \mu_j - i} = \check{c}_{\bar{j}}^{\mathrm{T}} \check{A}^i t_{\mu_1 + \cdots + \mu_j} - \check{c}_{\bar{j}}^{\mathrm{T}} \check{A}^i t_{\mu_1 + \cdots + \mu_j} = 0 \tag{10.34}$$

for $\bar{j} = 2, \ldots, p$, $j = 1, \ldots, \bar{j} - 1$, $i = 0, \ldots, \mu_j - 1$.

Putting together the intermediate results (10.30), (10.31) and (10.34) yields

$$\check{c}_{\bar{j}}^{\mathrm{T}} t_{\mu_1 + \cdots + \mu_j - i} = \begin{cases} 1 & \text{if } \bar{j} = j \text{ and } i = \mu_j - 1 \\ 0 & \text{else} \end{cases} \tag{10.35}$$

for $\bar{j} = 1, \ldots, p$, $j = 1, \ldots, p$ $i = 0, \ldots, \mu_j - 1$. Substituting (10.35) into (10.28) finally proves that $\bar{C}$ has the desired form (6.1d).

List of Abbreviations

ISS   Input-To-State Stable

LTI   Linear Time-Invariant

MIMO   Multiple-Input Multiple-Ouput

ODE   Ordinary Differential Equation

PDE   Partial Differential Equation

RED   Robust Exact Differentiator

SISO   Single-Input Single-Ouput

TEM   Thermoelectric Module

ZOH   Zero-Order Hold

Bibliography

[1] P. Lynch, The origins of computer weather prediction and climate modeling, Journal of computational physics 227 (7) (2008) 3431–3444. `doi:10.1016/j.jcp.2007.02.034`. (cited on page 1.)

[2] P. Courtier, J.-F. Geleyn, A global numerical weather prediction model with variable resolution: Application to the shallow-water equations, Quarterly Journal of the Royal Meteorological Society 114 (483) (1988) 1321–1346. `doi:10.1002/qj.49711448309`. (cited on page 1.)

[3] R. Bauer, M. Gölles, T. Brunner, N. Dourdoumas, I. Obernberger, Modelling of grate combustion in a medium scale biomass furnace for control purposes, Biomass and Bioenergy 34 (4) (2010) 417–427. `doi:10.1016/j.biombioe.2009.12.005`. (cited on page 1.)

[4] R. E. Jonjo, S. T. Nyalloma, Modeling the effect of road excitation on vehicle suspension system, International Journal of Engineering Materials and Manufacture 5 (1) (2020) 19–28. `doi:10.26776/ijemm.05.01.2020.04`. (cited on page 1.)

[5] C. Kleinstreuer, T. Poweigha, Modeling and simulation of bioreactor process dynamics, in: Bioprocess Parameter Control, Springer, 2005, pp. 91–146. `doi:10.1007/BFb0006381`. (cited on page 1.)

[6] M. Chernov, A. R. Gallant, E. Ghysels, G. Tauchen, Alternative models for stock price dynamics, Journal of Econometrics 116 (1-2) (2003) 225–257. `doi:10.1016/S0304-4076(03)00108-8`. (cited on page 1.)

[7] D. G. Luenberger, Observing the state of a linear system, IEEE Transactions on Military Electronics 8 (2) (1964) 74–80. `doi:10.1109/TME.1964.4323124`. (cited on pages 1, 26 and 41.)

[8] R. J. Patton, P. M. Frank, R. N. Clarke, Fault Diagnosis in Dynamic Systems: Theory and Application, Prentice-Hall, Inc., USA, 1989. (cited on page 2.)

[9] B. Yang, Y. Hu, H. Huang, H. Shu, T. Yu, L. Jiang, Perturbation estimation based robust state feedback control for grid connected DFIG wind energy conversion system, International Journal of Hydrogen Energy 42 (33) (2017) 20994–21005. `doi:10.1016/j.ijhydene.2017.06.222`. (cited on page 2.)

[10] M. L. Hautus, Strong detectability and observers, Linear Algebra and its Applications 50 (1983) 353–368. `doi:10.1016/0024-3795(83)90061-7`. (cited on pages 2, 12, 13, 15, 16, 28 and 41.)

[11] A. F. Filippov, Differential equations with discontinuous righthand sides: control systems, Vol. 18, Springer Science & Business Media, 2013. `doi:10.1007/978-94-015-7793-9`. (cited on pages 5 and 19.)

[12] M. Hautus, Stabilization controllability and observability of linear autonomous systems, in: Indagationes mathematicae (proceedings), Vol. 73, North-Holland, 1970, pp. 448–455. `doi:10.1016/S1385-7258(70)80049-X`. (cited on pages 8 and 9.)

[13] R. E. Kalman, On the general theory of control systems, in: Proceedings First International Conference on Automatic Control, Moscow, USSR, 1960, pp. 481–492. `doi:10.1016/S1474-6670(17)70094-8`. (cited on page 9.)

[14] S. R. Kou, D. L. Elliott, T. J. Tarn, Observability of nonlinear systems, Information and Control 22 (1) (1973) 89–99. `doi:10.1016/S0019-9958(73)90508-1`. (cited on page 9.)

[15] F. R. Gantmacher, Matrizentheorie (Theory of Matrices), Springer-Verlag, 1986. `doi:10.1007/978-3-642-71243-2`. (cited on pages 10 and 49.)

[16] G. J. Olsder, J. W. van der Woude, Mathematical systems theory, Vol. 4, VSSD Delft, 2005. (cited on pages 9 and 13.)

[17] J. Gilbert, L. Gilbert, Linear algebra and matrix theory, Elsevier, 2014. `doi:10.1016/C2009-1-28539-X`. (cited on page 11.)

[18] L. Fridman, J. Davila, A. Levant, High-order sliding-mode observation for linear systems with unknown inputs, Nonlinear Analysis: Hybrid Systems 5 (2) (2011) 189–205. `doi:10.1016/j.nahs.2010.09.003`. (cited on pages 12, 32 and 41.)

[19] F. J. Bejarano, L. Fridman, A. Poznyak, Unknown input and state estimation for unobservable systems, SIAM Journal on Control and Optimization 48 (2) (2009) 1155–1178. `doi:10.1137/070700322`. (cited on pages 12, 32 and 41.)

[20] M. Tranninger, R. Seeber, M. Steinberger, M. Horn, Exact state reconstruction for LTI-systems with non-differentiable unknown inputs, in: 2019 18th European Control Conference (ECC), IEEE, 2019, pp. 3096–3102. `doi:10.23919/ECC.2019.8796142`. (cited on pages 12, 13, 30, 32, 33, 35 and 41.)

[21] W. Kratz, Characterization of strong observability and construction of an observer, Linear Algebra and its Applications 221 (1995) 31–40. `doi:10.1016/0024-3795(93)00221-K`. (cited on pages 13 and 16.)

[22] H. Rosenbrock, State-space and Multivariable Theory, Studies in dynamical systems, Wiley Interscience Division, 1970. (cited on page 15.)

[23] J. Zhang, F. Zhu, On the observer matching condition and unknown input observer design based on the system left-invertibility concept, Transactions of the Institute of Measurement and Control 40 (9) (2018) 2887–2900. `doi:10.1177/0142331217711494`. (cited on page 16.)

[24] H. L. Trentelman, A. A. Stoorvogel, M. Hautus, Control theory for linear systems, Springer Science & Business Media, 2012. `doi:10.1007/978-1-4471-0339-4`. (cited on page 16.)

[25] B. M. Chen, Z. Lin, Y. Shamash, Linear systems theory: a structural decomposition approach, Springer Science & Business Media, 2004. `doi:10.1007/978-1-4612-2046-6`. (cited on pages 16, 61, 66, 76, 78 and 120.)

[26] E. Cruz-Zavala, J. A. Moreno, Lyapunov functions for continuous and discontinuous differentiators, IFAC-PapersOnLine 49 (18) (2016) 660–665. `doi:10.1016/j.ifacol.2016.10.241`. (cited on pages 18, 19, 20, 59 and 73.)

[27] A. Levant, Robust exact differentiation via sliding mode technique, Automatica 34 (3) (1998) 379–384. `doi:10.1016/S0005-1098(97)00209-4`. (cited on page 19.)

[28] A. Levant, Higher-order sliding modes, differentiation and output-feedback control, International Journal of Control 76 (9-10) (2003) 924–941. `doi:10.1080/0020717031000099029`. (cited on pages 19 and 20.)

[29] Y. Shtessel, C. Edwards, L. Fridman, A. Levant, et al., Sliding mode control and observation, Vol. 10, Springer, 2014. `doi:10.1007/978-0-8176-4893-0`. (cited on pages 20, 30, 34, 39, 50, 73, 84 and 108.)

[30] M. Reichhartinger, S. Spurgeon, An arbitrary-order differentiator design paradigm with adaptive gains, International Journal of Control 91 (9) (2018) 2028–2042. `doi:10.1080/00207179.2018.1429671`. (cited on page 20.)

[31] V. I. Zubov, Systems of ordinary differential equations with generalized-homogeneous right-hand sides, Izvestiya Vysshikh Uchebnykh Zavedenii. Matematika (1) (1958) 80–88. (cited on page 20.)

[32] E. Bernuau, D. Efimov, W. Perruquetti, A. Polyakov, On homogeneity and its application in sliding mode control, Journal of the Franklin Institute 351 (4) (2014) 1866–1901. `doi:10.1016/j.jfranklin.2014.01.007`. (cited on page 20.)

[33] E. Cruz-Zavala, J. A. Moreno, Levant's arbitrary-order exact differentiator: a lyapunov approach, IEEE Transactions on Automatic Control 64 (7) (2018) 3034–3039. `doi:10.1109/TAC.2018.2874721`. (cited on page 20.)

[34] M. Livne, A. Levant, Proper discretization of homogeneous differentiators, Automatica 50 (8) (2014) 2007–2014. `doi:10.1016/j.automatica.2014.05.028`. (cited on pages 20, 105, 114 and 117.)

[35] S. Koch, M. Reichhartinger, M. Horn, L. Fridman, Discrete-time implementation of homogeneous differentiators, IEEE Transactions on Automatic Control 65 (2) (2019) 757–762. `doi:10.1109/TAC.2019.2919237`. (cited on pages 20 and 105.)

[36] J. E. Carvajal-Rubio, J. D. Sánchez-Torres, M. Defoort, M. Djemai, A. G. Loukianov, Implicit and explicit discrete-time realizations of homogeneous differentiators, International Journal of Robust and Nonlinear Control 31 (9) (2021) 3606–3630. `doi:10.1002/rnc.5505`. (cited on pages 20 and 105.)

[37] R. Seeber, S. Koch, Structural conditions for chattering avoidance in implicitly discretized sliding mode differentiators, IEEE Control Systems Letters (2023). `doi:10.1109/LCSYS.2023.3282886`. (cited on pages 20 and 105.)

[38] B. Andritsch, M. Horn, S. Koch, H. Niederwieser, M. Wetzlinger, M. Reichhartinger, The robust exact differentiator toolbox revisited: Filtering and discretization features, in: 2021 IEEE International Conference on Mechatronics (ICM), IEEE, 2021, pp. 01–06. `doi:10.1109/ICM46511.2021.9385675`. (cited on pages 20 and 105.)

[39] J.-P. Barbot, A. Levant, M. Livne, D. Lunz, Discrete sliding-mode-based differentiators, in: 2016 14th International Workshop on Variable Structure Systems (VSS), IEEE, 2016, pp. 166–171. `doi:10.1109/VSS.2016.7506910`. (cited on pages 20 and 105.)

[40] S. Koch, M. Reichhartinger, Discrete-time equivalent homogeneous differentiators, in: 2018 15th International Workshop on Variable Structure Systems (VSS), IEEE, 2018, pp. 354–359. `doi:10.1109/VSS.2018.8460284`. (cited on pages 20, 105, 106, 114 and 117.)

[41] M. Reichhartinger, S. Koch, H. Niederwieser, S. K. Spurgeon, The robust exact differentiator toolbox: Improved discrete-time realization, in: 2018 15th International Workshop on Variable Structure Systems (VSS), IEEE, 2018, pp. 1–6. `doi:10.1109/VSS.2018.8460388`. (cited on pages 20, 105 and 106.)

[42] A. Hanan, A. Levant, A. Jbara, Low-chattering discretization of homogeneous differentiators, IEEE Transactions on Automatic Control 67 (6) (2021) 2946–2956. `doi:10.1109/TAC.2021.3099446`. (cited on page 20.)

[43] M. R. Mojallizadeh, B. Brogliato, V. Acary, Time-discretizations of differentiators: Design of implicit algorithms and comparative analysis, International Journal of Robust and Nonlinear Control 31 (16) (2021) 7679–7723. `doi:10.1002/rnc.5710`. (cited on page 20.)

[44] J.-P. Barbot, A. Levant, M. Livne, D. Lunz, Discrete differentiators based on sliding modes, Automatica 112 (2020) 108633. `doi:10.1016/j.automatica.2019.108633`. (cited on page 20.)

[45] L. K. Vasiljevic, H. K. Khalil, Differentiation with high-gain observers the presence of measurement noise, in: Proceedings of the 45th IEEE Conference on

Decision and Control, IEEE, 2006, pp. 4717–4722. `doi:10.1109/CDC.2006.377230.` (cited on page 20.)

[46] L. K. Vasiljevic, H. K. Khalil, Error bounds in differentiation of noisy signals by high-gain observers, Systems & Control Letters 57 (10) (2008) 856–862. `doi:10.1016/j.sysconle.2008.03.018.` (cited on page 20.)

[47] J. A. Moreno, Arbitrary-order fixed-time differentiators, IEEE Transactions on Automatic Control 67 (3) (2021) 1543–1549. `doi:10.1109/TAC.2021.3071027.` (cited on pages 21 and 59.)

[48] J. A. Moreno, Bi-homogeneous differentiators, in: Sliding-Mode Control and Variable-Structure Systems: The State of the Art, Springer, 2023, pp. 71–96. `doi:10.1007/978-3-031-37089-2_4.` (cited on page 21.)

[49] S. Mudge, R. Patton, Analysis of the technique of robust eigenstructure assignment with application to aircraft control, in: IEE Proceedings D (Control Theory and Applications), Vol. 135, IET, 1988, pp. 275–281. `doi:10.1049/ip-d.1988.0038.` (cited on pages 25 and 66.)

[50] T. Floquet, J.-P. Barbot, An observability form for linear systems with unknown inputs, International Journal of Control 79 (2) (2006) 132–139. `doi:10.1080/00207170500472909.` (cited on pages 25, 32 and 41.)

[51] H. Niederwieser, M. Tranninger, R. Seeber, M. Reichhartinger, Unknown input observer design for linear time-invariant multivariable systems based on a new observer normal form, International Journal of Systems Science 53 (10) (2022) 2180–2206. `doi:10.1080/00207721.2022.2046201.` (cited on pages 25, 53, 75, 82 and 120.)

[52] J. Kautsky, N. K. Nichols, P. Van Dooren, Robust pole assignment in linear state feedback, International Journal of control 41 (5) (1985) 1129–1155. `doi:10.1080/0020718508961188.` (cited on pages 26, 27 and 33.)

[53] H. K. Khalil, L. Praly, High-gain observers in nonlinear feedback control, International Journal of Robust and Nonlinear Control 24 (6) (2014) 993–1015. `doi:10.1002/rnc.3051.` (cited on page 28.)

[54] A. Tornambè, High-gain observers for non-linear systems, International Journal of Systems Science 23 (9) (1992) 1475–1489. `doi:10.1080/00207729208949400.` (cited on page 28.)

[55] V. Andrieu, L. Praly, A. Astolfi, High gain observers with updated gain and homogeneous correction terms, Automatica 45 (2) (2009) 422–428. `doi:10.1016/j.automatica.2008.07.015.` (cited on page 28.)

[56] P. Kudva, N. Viswanadham, A. Ramakrishna, Observers for linear systems with unknown inputs, IEEE Transactions on Automatic Control 25 (1) (1980) 113–115. `doi:10.1109/TAC.1980.1102245.` (cited on pages 28 and 41.)

[57] F. Yang, R. W. Wilde, Observers for linear systems with unknown inputs, IEEE Transactions on Automatic Control 33 (7) (1988) 677–681. `doi:10.1109/9.1278`. (cited on pages 28 and 41.)

[58] Y. Guan, M. Saif, A novel approach to the design of unknown input observers, IEEE Transactions on Automatic Control 36 (5) (1991) 632–635. `doi:10.1109/9.76372`. (cited on pages 28 and 41.)

[59] M. Hou, P. C. Muller, Design of observers for linear systems with unknown inputs, IEEE Transactions on Automatic Control 37 (6) (1992) 871–875. `doi:10.1109/9.256351`. (cited on pages 28 and 41.)

[60] M. Darouach, M. Zasadzinski, S. J. Xu, Full-order observers for linear systems with unknown inputs, IEEE Transactions on Automatic Control 39 (3) (1994) 606–609. `doi:10.1109/9.280770`. (cited on pages 28 and 41.)

[61] D. Koenig, S. Nowakowski, A. Bourjij, Observers for linear systems with unknown inputs, IFAC Proceedings Volumes 30 (6) (1997) 479–484. `doi:10.1016/S1474-6670(17)43410-0`. (cited on pages 28 and 41.)

[62] M. Lungu, R. Lungu, Full-order observer design for linear systems with unknown inputs, International Journal of Control 85 (10) (2012) 1602–1615. `doi:10.1080/00207179.2012.695397`. (cited on page 28.)

[63] B. Walcott, S. Zak, State observation of nonlinear uncertain dynamical systems, IEEE Transactions on Automatic Control 32 (2) (1987) 166–170. `doi:10.1109/TAC.1987.1104530`. (cited on pages 28 and 41.)

[64] C. Edwards, S. Spurgeon, Sliding mode control: theory and applications, Crc Press, 1998. `doi:10.1201/9781498701822`. (cited on pages 28 and 41.)

[65] V. Utkin, J. Guldner, J. Shi, Sliding mode control in electro-mechanical systems, CRC press, 2009. `doi:10.1201/9781420065619`. (cited on pages 28 and 41.)

[66] F. Zhu, Y. Fu, T. N. Dinh, Asymptotic convergence unknown input observer design via interval observer, Automatica 147 (2023) 110744. `doi:10.1016/j.automatica.2022.110744`. (cited on page 28.)

[67] J. Davila, L. Fridman, A. Pisano, E. Usai, Finite-time state observation for nonlinear uncertain systems via higher-order sliding modes, International Journal of Control 82 (8) (2009) 1564–1574. `doi:10.1080/00207170802590531`. (cited on pages 29 and 41.)

[68] T. Sanchez, J. A. Moreno, Homogeneous output-feedback control with disturbance-observer for a class of nonlinear systems, International Journal of Robust and Nonlinear Control 31 (9) (2021) 3686–3707. `doi:10.1002/rnc.5207`. (cited on pages 29 and 41.)

[69] A. Ferreira de Loza, L. Fridman, L. T. Aguilar, R. Iriarte, High-order sliding-mode observer–based input-output linearization, International Journal of Robust and Nonlinear Control 29 (10) (2019) 3183–3199. `doi:10.1002/rnc.4556`. (cited on pages 29 and 41.)

[70] F. Zhu, State estimation and unknown input reconstruction via both reduced-order and high-order sliding mode observers, Journal of Process Control 22 (1) (2012) 296–302. `doi:10.1016/j.jprocont.2011.07.007`. (cited on pages 29 and 41.)

[71] R. Merzouki, J. Davila, L. Fridman, J. Cadiou, Backlash phenomenon observation and identification in electromechanical system, Control Engineering Practice 15 (4) (2007) 447–457. `doi:10.1016/j.conengprac.2006.09.001`. (cited on pages 31 and 41.)

[72] J.-P. Barbot, T. Boukhobza, M. Djemai, Sliding mode observer for triangular input form, in: Proceedings of 35th IEEE Conference on Decision and Control, Vol. 2, IEEE, 1996, pp. 1489–1490. `doi:10.1109/CDC.1996.572727`. (cited on pages 32 and 41.)

[73] T. Floquet, J.-P. Barbot, A sliding mode approach of unknown input observers for linear systems, in: 43rd IEEE Conference on Decision and Control (CDC), Vol. 2, IEEE, 2004, pp. 1724–1729. `doi:10.1109/CDC.2004.1430293`. (cited on pages 32 and 41.)

[74] T. Floquet, J.-P. Barbot, Super twisting algorithm-based step-by-step sliding mode observers for nonlinear systems with unknown inputs, International Journal of Systems Science 38 (10) (2007) 803–815. `doi:10.1080/00207720701409330`. (cited on pages 32 and 41.)

[75] T. Floquet, C. Edwards, S. K. Spurgeon, On sliding mode observers for systems with unknown inputs, International Journal of Adaptive Control and Signal Processing 21 (8-9) (2007) 638–656. `doi:10.1002/acs.958`. (cited on pages 32 and 41.)

[76] L. Fridman, A. Levant, J. Davila, High-order sliding-mode observation and identification for linear systems with unknown inputs, in: Proceedings of the 45th IEEE Conference on Decision and Control, IEEE, 2006, pp. 5567–5572. `doi:10.1109/CDC.2006.377385`. (cited on page 32.)

[77] L. Fridman, J. Davila, A. Levant, High-order sliding-mode observation of linear systems with unknown inputs, IFAC Proceedings Volumes 41 (2) (2008) 4779–4790. `doi:10.3182/20080706-5-KR-1001.00804`. (cited on pages 32 and 41.)

[78] M. Tranninger, S. Zhuk, M. Steinberger, L. M. Fridman, M. Horn, Sliding Mode Tangent Space Observer for LTV Systems with Unknown Inputs, in: 2018 IEEE Conference on Decision and Control (CDC), IEEE, 2018, pp. 6760–6765. `doi:10.1109/CDC.2018.8619848`. (cited on pages 32 and 41.)

[79] H. Ríos, State estimation for a class of uncertain nonlinear systems: a finite-time observer approach, International Journal of Control 95 (4) (2022) 1051–1059. `doi:10.1080/00207179.2020.1837961`. (cited on pages 32 and 41.)

[80] D. Luenberger, Canonical forms for linear multivariable systems, IEEE Transactions on Automatic Control 12 (3) (1967) 290–293. `doi:10.1109/TAC.1967.1098584`. (cited on pages 36, 55 and 120.)

[81] R. Gupta, F. Fairman, Luenberger's canonical form revisited, IEEE Transactions on Automatic Control 19 (4) (1974) 440–441. `doi:10.1109/TAC.1974.1100589`. (cited on page 36.)

[82] H. Ríos, M. Mera, D. Efimov, A. Polyakov, Robust output-control for uncertain linear systems: Homogeneous differentiator-based observer approach, International Journal of Robust and Nonlinear Control 27 (11) (2017) 1895–1914. `doi:10.1002/rnc.3643`. (cited on pages 37 and 41.)

[83] J. Dávila, M. Tranninger, L. Fridman, Finite-time state observer for a class of linear time-varying systems with unknown inputs, IEEE Transactions on Automatic Control 67 (6) (2021) 3149–3156. `doi:10.1109/TAC.2021.3096863`. (cited on pages 37 and 41.)

[84] J. Yang, F. Zhu, K. Yu, X. Bu, Observer-based state estimation and unknown input reconstruction for nonlinear complex dynamical systems, Communications in Nonlinear Science and Numerical Simulation 20 (3) (2015) 927–939. `doi:10.1016/j.cnsns.2014.05.016`. (cited on page 39.)

[85] M. Mueller, Normal form for linear systems with respect to its vector relative degree, Linear Algebra and its Applications 430 (4) (2009) 1292–1312. `doi:10.1016/j.laa.2008.10.014`. (cited on page 39.)

[86] H. Niederwieser, S. Koch, M. Reichhartinger, A generalization of Ackermann's formula for the design of continuous and discontinuous observers, in: 2019 IEEE 58th Conference on Decision and Control (CDC), IEEE, 2019, pp. 6930–6935. `doi:10.1109/CDC40024.2019.9030192`. (cited on page 43.)

[87] R. E. Kalman, Mathematical description of linear dynamical systems, Journal of the Society for Industrial and Applied Mathematics, Series A: Control 1 (2) (1963) 152–192. `doi:10.1137/0301010`. (cited on page 44.)

[88] S. Barnett, Introduction to Mathematical Control Theory, Oxford applied mathematics and computing science, Oxford University Press, 1975. (cited on page 44.)

[89] J. Ackermann, Der Entwurf linearer Regelungssysteme im Zustandsraum (Design of a Linear Control System Involving State-Space Vector Feedback), at-Automatisierungstechnik 20 (1-12) (1972) 297–300. `doi:10.1524/auto.1972.20.112.297`. (cited on pages 49 and 107.)

[90] H. Nakamura, Y. Yamashita, H. Nishitani, Homogeneous eigenvalue analysis of homogeneous systems, IFAC Proceedings Volumes 38 (1) (2005) 85–90. `doi:10.3182/20050703-6-CZ-1902.00668`. (cited on page 49.)

[91] H. Nakamura, Y. Yamashita, H. Nishitani, Asymptotic stability analysis for homogeneous systems using homogeneous eigenvalues, in: Proceedings of the 45th IEEE Conference on Decision and Control, IEEE, 2006, pp. 4230–4235. `doi:10.1109/CDC.2006.377542`. (cited on page 49.)

[92] H. Nakamura, G. Nishida, H. Nishitani, Y. Yamashita, Stabilization of nonlinear planer systems using homogeneous eigenvalues, in: 2006 SICE-ICASE International Joint Conference, IEEE, 2006, pp. 2390–2393. `doi:10.1109/SICE.2006.315106`. (cited on page 49.)

[93] W. Perruquetti, T. Floquet, E. Moulay, Finite-time observers: application to secure communication, IEEE Transactions on Automatic Control 53 (1) (2008) 356–360. `doi:10.1109/TAC.2007.914264`. (cited on page 59.)

[94] M. Tranninger, H. Niederwieser, R. Seeber, M. Horn, Unknown input observer design for linear time-invariant systems—a unifying framework, International Journal of Robust and Nonlinear Control 33 (15) (2023) 8911–8934. `doi:10.1002/rnc.6399`. (cited on page 78.)

[95] F. J. Bejarano, L. Fridman, High order sliding mode observer for linear systems with unbounded unknown inputs, International Journal of Control 83 (9) (2010) 1920–1929. `doi:10.1080/00207179.2010.501386`. (cited on page 80.)

[96] L. Fridman, A. Levant, J. Davila, High-order sliding modes observer for linear systems with unbounded unknown inputs, IFAC Proceedings Volumes 42 (17) (2009) 216–221. `doi:10.3182/20090916-3-ES-3003.00038`. (cited on page 80.)

[97] A. Chakrabarty, M. Corless, Estimating unbounded unknown inputs in nonlinear systems, Automatica 104 (2019) 57–66. `doi:10.1016/j.automatica.2019.02.050`. (cited on page 80.)

[98] K. Ogata, Y. Yang, Modern control engineering, Vol. 5, Prentice hall India, 2002. (cited on page 82.)

[99] R. W. Brockett, Finite dimensional linear systems, SIAM, 2015. `doi:10.1137/1.9781611973884`. (cited on page 82.)

[100] C.-T. Chen, Linear system theory and design, Oxford University Press, Inc., 1998. (cited on page 82.)

[101] H. Septanto, A. Syaichu-Rohman, D. Mahayana, Static anti-windup compensator design of linear sliding mode control for input saturated systems, in: Proceedings of the 2011 International Conference on Electrical Engineering and Informatics, IEEE, 2011, pp. 1–4. `doi:10.1109/ICEEI.2011.6021650`. (cited on page 86.)

[102] M. A. Golkani, S. Koch, R. Seeber, M. Reichhartinger, M. Horn, An anti-windup scheme for the super-twisting algorithm, in: 2019 IEEE 58th Conference on Decision and Control (CDC), IEEE, 2019, pp. 6947–6952. `doi: 10.1109/CDC40024.2019.9029793`. (cited on page 86.)

[103] C. M. Oliveira, M. L. Aguiar, J. R. Monteiro, W. C. Pereira, G. T. Paula, T. E. Almeida, Vector control of induction motor using an integral sliding mode controller with anti-windup, Journal of Control, Automation and Electrical Systems 27 (2016) 169–178. `doi:10.1007/s40313-016-0228-4`. (cited on page 86.)

[104] A. Levant, Chattering analysis, IEEE Transactions on Automatic Control 55 (6) (2010) 1380–1389. `doi:10.1109/TAC.2010.2041973`. (cited on page 86.)

[105] V. Utkin, H. Lee, Chattering problem in sliding mode control systems, in: International Workshop on Variable Structure Systems, 2006. VSS'06., IEEE, 2006, pp. 346–350. `doi:10.1109/VSS.2006.1644542`. (cited on page 86.)

[106] H. Niederwieser, S. Koch, M. Reichhartinger, Unknown Input Observer for Temperature Profile Estimation in Systems with Unknown Heat Fluxes, in: 2024 22nd European Control Conference (ECC), IEEE, 2024. (cited on page 89.)

[107] L. Pfaffeneder, A. Sauseng, Entwurf und Inbetriebnahme einer thermischen Regelstrecke (Design and comissioning of a thermal control system), Bachelor's Thesis (in German), Institute of Automation and Control, University of Technology Graz (Jan. 2021). (cited on pages 89 and 91.)

[108] A. Anabith, Late-Lumping Controller Synthesis for a Heated Rod with Boundary Actuation, Master's Thesis, Institute of Automation and Control, University of Technology Graz (May 2022). (cited on pages 89 and 91.)

[109] C. Alaoui, Peltier thermoelectric modules modeling and evaluation, International Journal of Engineering (IJE) 5 (2011) 114–121. (cited on pages 90, 108 and 113.)

[110] H. J. Goldsmid, Introduction to thermoelectricity, 2nd Edition, Springer, 2016. `doi:10.1007/978-3-642-00716-3`. (cited on page 90.)

[111] W. Brostow, G. Granowski, N. Hnatchuk, J. Sharp, J. B. White, Thermoelectric phenomena, Journal of Materials Education 36 (2014) 175–185. (cited on page 90.)

[112] H. D. Baehr, K. Stephan, Wärme-und Stoffübertragung, Vol. 5, Springer, 2006. (cited on pages 92, 93, 94 and 95.)

[113] Verein deutscher Ingenieure, VDI-Wärmeatlas, 11th Edition, Springer, Berlin Heidelberg, 2013. `doi:10.1007/978-3-642-19981-3`. (cited on page 98.)

[114] thyssenkrupp Materials (UK) Ltd, Aluminium 6060 (2023).
URL `https://www.thyssenkrupp-materials.co.uk/aluminium-6060.html`
(cited on page 98.)

[115] T. E. Fortmann, K. L. Hitz, An introduction to linear control systems, Vol. 5, Crc Press, 1977. (cited on page 101.)

[116] O. Föllinger, Regelungstechnik, 8th Edition, Hüthig Buch Verlag Heidelberg, 1994. (cited on page 101.)

[117] D. Chu, X. Liu, R. C. Tan, On the numerical computation of a structural decomposition in systems and control, IEEE Transactions on Automatic Control 47 (11) (2002) 1786–1799. `doi:10.1109/TAC.2002.804484`. (cited on page 117.)

[118] X. Liu, B. M. Chen, Z. Lin, Linear systems toolkit in Matlab: structural decompositions and their applications, Journal of Control Theory and Applications 3 (2005) 287–294. `doi:10.1007/s11768-005-0051-0`. (cited on page 117.)

[119] A. C. Antoulas, Approximation of large-scale dynamical systems, SIAM, 2005. `doi:10.1137/1.9780898718713`. (cited on page 119.)

[120] K. Fernando, H. Nicholson, Singular perturbational model reduction in the frequency domain, IEEE Transactions on Automatic Control 27 (4) (1982) 969–970. `doi:10.1109/TAC.1982.1103037`. (cited on page 119.)